

Cellular Senescence and Cardiac Surgery Associated – Acute Kidney Injury

Submitted for Degree of Doctor of Philosophy

Mr Damian Balmforth
MBBS BSc MRCS MRCP

Supervisors: Professor M M Yaqoob and Professor R
Uppal

William Harvey Research Institute,
Queen Mary University of London
Charterhouse Square,
London
EC1M 6BQ

Tel: 020 7882 8182

Email: d.balmforth@qmul.ac.uk

Statement of Originality

I, Damian Balmforth, confirm that the research included within this thesis is my own work or that where it has been carried out in collaboration with, or supported by others, that this is duly acknowledged below and my contribution indicated. Previously published material is also acknowledged below.

I attest that I have exercised reasonable care to ensure that the work is original, and does not to the best of my knowledge break any UK law, infringe any third party's copyright or other Intellectual Property Right, or contain any confidential material.

I accept that the College has the right to use plagiarism detection software to check the electronic version of the thesis.

I confirm that this thesis has not been previously submitted for the award of a degree by this or any other university.

The copyright of this thesis rests with the author and no quotation from it or information derived from it may be published without the prior written consent of the author.

Signature:

Date: 31 July 2019

Details of collaboration and publications:

Prof Duncan Baird

Professor of Cancer and Genetics

Division of Cancer and Genetics

Cardiff University

Declaration of individual contribution to work presented

In preparation of this thesis, I designed the study protocol and obtained all of the required approvals including peer review, research ethics approval, and sponsorship from the Joint Research Management Office of QMUL.

I recruited all of the study patients, collected their blood and urine samples and processed them prior to storage. I performed all DNA and RNA extraction and performed quality control of the extracted DNA by spectrophotometry and gel electrophoresis.

I optimised and validated the protocol of Telomere length measurement for our laboratory equipment and performed all of the telomere length analysis. I ran multiple experiments in an attempt to optimise the Telomerase Activity ELISA.

I developed the study database and collected all of the clinical data on the recruited patients. I performed all analyses including statistical analysis with the aid of SPSS version 22 statistical software.

Abstract

Introduction: Cardiac-surgery associated-acute kidney injury (CSA-AKI) is associated with increased morbidity and mortality. Furthermore, patients who develop CSA-AKI have higher incidences of progression to chronic renal impairment and reduced long-term mortality. The mechanism for this association is not fully understood. We hypothesized that increased cellular senescence and biological age might be linked to both the development of CSA-AKI and future reduced mortality.

Objectives: To investigate the relationship between markers of cellular senescence and aging and the development of CSA-AKI.

Methods: DNA was extracted from peripheral leukocytes pre-operatively. Telomere length was measured with quantitative polymerase chain reaction (qPCR) and DNA methylation-based models of biological age and senescence were developed using targeted sequencing.

Results: Between January 2016 and April 2017, 254 patients were recruited. Of these 54 (21.3%) developed AKI. No association was found between mean Telomere length (mTL) and CSA-AKI on univariate analysis ($p=0.304$), or on propensity matching ($p=0.833$). However, a subgroup analysis of South Asian patients showed a significant association between reduced mTL and CSA-AKI on both univariate ($p = 0.025$) and multivariate analysis ($p = 0.036$). Predicted methylation age (pMA) was significantly associated with CSA-AKI ($p=0.013$) whereas chronological age was not ($p=.0.106$). ROC curve analysis also demonstrated that pMA was a better predictor of CSA-AKI than chronological age ($p=0.012$ vs $p=0.047$). In subgroup analysis, South Asian patients again demonstrated a stronger association with CSA-AKI than other

ethnicities. On propensity matched analysis of the total population, the difference between chronological age and pMA (Delta age) was reduced in the AKI cohort, although this failed to reach statistical significance ($p=0.07$).

Conclusion: pMA was significantly associated with CSA-AKI with a predictive ability superior to that of chronological age. mTL was found to be significantly associated with CSA-AKI in the South Asian population but not in the study population as a whole.

Acknowledgements

I would like to thank my supervisors Professor Yaqoob and Professor Uppal for giving me the opportunity to complete this thesis and their endless support and advice throughout.

At the William Harvey Research Institute, I would like to thank Dr Steven Harwood for all of his help both in the laboratory and in guiding me through the steps of writing up. I would also like to thank Julius Keswiche for his technical advice as well as my fellow PhD candidates, Dr Vasantha Muthuppalaniappan and Dr Sai Duraisingham, who helped me in innumerable ways over the three years and made spending hours in the laboratory much more enjoyable.

I would like to thank the Barts BioResource for registering my project and allowing me to conduct it at the Barts Heart Centre. I am also extremely grateful to the HCA Research Fellowship and Barts Charity for providing funding to complete this work. I would also like to thank Dr Gabriella Captur for her invaluable advice on statistical analysis.

Finally, I must thank my family for all their love and support over the last 3 years. My father's own experience of completing his PhD has been of great support during the difficult times. Above all, I must thank my wonderful wife Hermione and my 2 daughters, Ophelia and Cecily, for the sacrifices that they have made to allow me to complete my studies.

Prizes

1. **The SCTS Ronald Edward Medal:** Best oral scientific presentation at the 2019 SCTS meeting.

Presentations to Learned Societies

1. Is reduced telomere length associated with an increased risk of acute kidney injury following cardiac surgery? Damian C. Balmforth, Vasantha M. Muthuppalaniappan, Sai Krishna Duraisingham, Steven M. Harwood, Julius E. Kieswich, Rakesh Uppal, Muhammad M. Yaqoob. American Society of Nephrology. New Orleans 2017
2. No gender difference in telomere length in patients undergoing coronary artery bypass surgery. Damian Balmforth, Steve Harwood, Magdi Yaqoob, Rakesh Uppal. SCTS Research Meeting. Leicester 2017
3. Reduced telomere length is not associated with an increased risk of acute kidney injury following cardiac surgery: A propensity matched analysis. Damian Balmforth, Vasantha Muthuppalaniappan, Sai Duraisingham, Steven Harwood, Julius Keiswich, Muhammad M Yaqoob, Rakesh Uppal. Society of Cardiothoracic Surgery 2019
4. Epigenetic markers of aging are associated with increased risk of acute kidney injury after cardiac surgery. Damian Balmforth, Vasantha Muthuppalaniappan, Sai Duraisingham, Steven Harwood, Julius Keiswich, Muhammad M Yaqoob, Rakesh Uppal. Society of Cardiothoracic Surgery, London 2019

Table of Contents

Statement of Originality	2
Declaration of individual contribution to work presented.....	3
Abstract	4
Acknowledgements.....	6
Prizes	7
Presentations to Learned Societies.....	7
List of Abbreviations	13
List of Figures	16
List of Tables	19
CHAPTER 1: General Introduction.....	24
1.1 Cardiac surgery associated Acute Kidney Injury	24
1.1.1 Definition of CSA-AKI	24
1.1.2 Pathophysiology of CSA-AKI	27
1.1.3 Risk factors for CSA-AKI.....	29
1.1.4 Genetic pre-disposition for CSA-AKI	31
1.1.5 Existing models for predicting CSA-AKI.....	33
1.1.6 Predictive risk calculators for mortality following cardiac surgery	35
1.1.7 Clinical significance of CSA-AKI.....	36
1.1.7.1 Association with long-term mortality	36
1.1.7.2 Association with long-term renal dysfunction.....	37
1.2 Developing the hypothesis – linking CSA-AKI with decreased long-term mortality and risk of CKD.....	37
1.3 Cell senescence	39
1.3.1 Markers of cellular senescence	40
1.4 The role of Telomeres and Telomerase in Cell Senescence.....	41
1.4.1 The structure and function of Telomeres	41
1.4.2 The structure and function of telomerase	44
1.4.3 How does TL induce senescence?	47
1.4.4 Non-telomere dependent mechanisms of cell senescence	50
1.5 The role of DNA methylation in cell senescence.....	50
1.5.1 Introduction to DNA methylation.....	50
1.5.2 DNA methylation, gene expression and disease	51
1.5.3 DNA methylation and cellular senescence.....	52
1.6 Cell senescence, aging and disease	53

1.6.1	Telomere biology and cardiovascular disease.....	53
1.6.3	Telomere biology and AKI	56
1.6.4	DNA Methylation and cardiovascular disease.....	57
1.6.5	DNA Methylation studies and AKI	59
1.7	Summary of Hypothesis.....	60
CHAPTER 2:	Aims	61
2.1	Aims of Mean Telomere Length analysis experiment	61
2.2	Aims of STELA experiment	61
2.3	Aims of DNA methylation experiment.....	61
CHAPTER 3:	Methods: Clinical study.....	62
3.1	Study Overview	62
3.2	Study Objectives.....	62
3.3	Sample size.....	62
3.4	Study duration.....	63
3.5	Patient Recruitment	63
3.5.1	Inclusion criteria:	63
3.5.2	Exclusion criteria.....	63
3.5.3	Timing of Recruitment	64
3.6	Informed Consent.....	64
3.7	Criteria for discontinuation.....	65
3.8	Data Collection	65
3.8.1	Protocol for data collection.....	65
3.9	Specimen Sample Collection	67
3.9.1	Blood sampling	67
3.9.2	Urine sampling.....	68
3.10	Ethical Approval and Trial Registration.....	68
3.11	Study Populations and Statistical Analyses.....	69
CHAPTER 4:	Methods: Laboratory	71
4.1	Rationale of chosen methodology for Telomere length measurement	71
4.1.1	Introduction.....	71
4.1.3	Quantitative polymerase chain reaction (qPCR)	72
4.1.4	Short Telomere Length Analysis (STELA).....	74
4.1.5	Quantitative fluorescence in-situ hybridisation (Q-FISH)	76
4.1.6	Rationale for selecting qPCR as the primary method of TL measurement	77
4.2	Measuring DNA methylation signatures of aging and cellular senescence	79
4.3	Sample processing.....	81

4.3.1 Immediate sample processing.....	81
4.3.2 Sample storage	81
4.3.3 DNA extraction	82
4.3.4 DNA Quantification and Quality Control.....	82
4.3.5 RNA extraction.....	84
4.3.6 RNA quantification and Quality Control.....	85
4.4 Telomere Length Analysis by Quantitative PCR	85
4.4.1 DNA Thawing.....	85
4.4.2 Thermocycling equipment	86
4.4.3 Principals of PCR set-up	86
4.4.4 Final PCR protocol.....	86
4.4.5 Calculation of T/S ratio.....	90
4.4.6 Optimisation and rationale of chosen protocol	90
4.4.7 Standard curve method Vs delta-delta CT method for relative quantitation of TL	93
4.4.8 Confirmation of valid PCR for Telomere length	94
4.5 Measurement of Single Telomere Length Analysis (STELA).....	98
4.6 DNA Methylation Methods.....	99
CHAPTER 5: Mean Telomere Length and Cardiac Surgery Associated -Acute Kidney Injury	102
5.1 Results of Validation experiments.....	102
5.1.1 Intra-assay variability.....	102
5.1.2 Inter-assay variability.....	102
5.2 The study population.....	103
5.3 Tests of Normality	104
5.4 Univariate associations of Telomere Length with main outcomes.	106
5.5 Propensity matched analysis of mTL and CSA-AKI	110
5.6 Whole population associations with mean Telomere Length	111
5.7 Analysis of significant predictors of CSA-AKI	116
5.7.1: Univariate analysis.....	116
5.7.2: Multivariate analysis.....	120
5.7.2.1 Variable selection.....	120
5.8 Analysis of mTL as a predictor of 1-year mortality.....	122
5.9 Potential over-fitting of multivariate model.....	127
5.10 Receiver Operating Characteristic curve analyses	128
5.11. Additional Analyses on Mean Telomere Length and CSA-AKI.....	132

5.11.1 Analysis of effects of fall in serum creatinine level	132
5.11.2 mTL and CSA-AKI: Investigating the effect of removing patients of South Asian Origin	134
5.11.2.1: Univariate analysis of mTL and CSA-AKI in South Asians	137
5.11.2.2. Multivariate analysis of mTL and CSA-AKI in South Asians	137
5.11.3 Analysis of mTL as a predictor of 1-year mortality in South Asian population	140
5.12 Results of STELA Experiment.....	141
5.13 Correlation between qPCR and STELA measurements of mean TL.....	144
5.14 Discussion of mTL Telomere Length and CSA-AKI	145
5.14.1 Discussion of main findings	145
5.14.2 Comparison of results with previous studies	151
5.14.3 Discussion of additional analysis of mTL in CSA-AKI.....	153
5.14.4 Discussion of STELA Pilot experiment.....	154
5.14.5 Strengths and limitations of mTL experiments	156
5.14.6 Conclusion	160
CHAPTER 6: DNA Methylation Aging Signatures and Cardiac Surgery Associated- Acute Kidney Injury.....	161
6.1 Building a Methylation signature for aging.....	161
6.2 Measures of aging in DNA methylation study.....	164
6.3 The study population.....	164
6.4 Univariate associations of methylation aging with main outcomes.	165
6.5 Propensity matched analysis of methylation aging and CSA-AKI.....	167
6.6 Whole population Associations with chronological age, predicted methylation age, AMAR, and Delta age.....	168
6.7 Analysis of methylation aging as a predictor of CSA-AKI	178
6.7.1 Univariate analysis.....	178
6.7.2 Multivariate analysis.....	181
6.8 Analysis of methylation age as a predictor of 1-year mortality.....	182
6.9 Adjustment for over fitting	186
6.10 Receiver Operating Characteristic curve analyses of DNA methylation aging measures	187
6.10.1. Predictors of AKI	187
6.10.2 Predictors of 1-year mortality	189
6.11 Additional Analyses of DNA methylation aging.....	191
6.11.1 Analysis of effects of fall in serum creatinine level	191
6.11.2 Investigating the effect of removing patients of South Asian Origin.....	192
6.11.2.1: Univariate analysis of pMA and CSA-AKI in South Asians	195

6.11.3 Analysis of DNA methylation aging as a predictor of 1-year mortality in the South Asian population	195
6.12 DNA methylation markers of senescence and outcomes after cardiac surgery	197
6.12.1 DNA Methylation senescence markers: Methodology	197
6.12.2 DNA Methylation senescence markers: Results	200
6.13 Logistical regression analysis of individual CpG sites and CSA-AKI	202
6.14 General Discussion of DNA methylation data	203
6.14.1 Discussion of significant findings in aging model of DNA Methylation	203
6.14.2 Discussion of significant findings in senescence models of DNA Methylation.	211
6.14.3 Comparison of results with previous studies	212
6.14.4 Discussion of additional analysis of pMA in CSA-AKI	215
6.14.5 Strengths and limitations DNA methylation experiments	216
CHAPTER 7: Telomerase Activity and outcome after cardiac surgery: Summary of failed optimisation experiments	220
7.1 Introduction	220
7.2 Isolation of Peripheral Blood Mononuclear Cells.....	220
7.2.1 Harvest of Peripheral Blood Mononuclear Cells	220
7.2.2 Quantifying starting amount of PBMC.....	222
7.3 Measuring Telomerase activity: Validation experiments	223
7.3.1 Telomerase activity: validation experiments 1	223
7.3.2 Conclusions from validation experiment 1	225
7.3.3: Telomerase activity: Validation experiments 2	226
7.3.4 Conclusions from validation experiment 2	228
7.4 Measuring TERT expression	228
7.4.1 Introduction.....	228
7.4.2 Methodology	229
7.4.3 Results.....	231
7.4.4 Conclusions.....	233
7.5 Overall Conclusion of Telomerase Experiments.....	234
CHAPTER 8. Conclusions and Future Work.....	235
8.1 Summary of Key Findings.....	235
8.2 Clinical impact of these findings.....	236
8.3 Potential future analyses	237
References	239
Appendices.....	261

List of Abbreviations

AF	Atrial fibrillation
AKI	Acute kidney injury
APOE	Apolipoprotein E
APOL	Apolipoprotein L
AUC	Area under curve
AKIN	Acute kidney injury network
CABG	Coronary artery bypass grafting
CAD	Coronary artery disease
CI	Confidence interval
CSA-AKI	Cardiac surgery associated acute kidney injury
CVD	Cardiovascular disease
CV	Coefficient of variance
CT	Cycle threshold
DDR	DNA damage response
DMSO	Dimethyl sulphoxide
DNA	Deoxyribonucleic acid
DNAm	DNA methylation
DSB	DNA double strand breaks
ESRD	End stage renal disease
EWAS	Epigenome wide association study
FISH	Fluorescence in-situ hybridisation
GFR	Glomerular filtration rate

GWAS	Genome wide association study
Hb	Haemoglobin
IRI	Ischaemia-reperfusion injury
MACCE	Major adverse cardiovascular and cerebrovascular events
MAE	Mean average error
MMqPCR reaction	Monochrome multiplex quantitative polymerase chain reaction
mTL	Mean telomere length
NYHA	New York heart association
NFW	Nuclease free water
OR	Odds Ratio
PCR	Polymerase chain reaction
RCF	Relative centrifugal force
RCT	Randomised control trial
RIFLE	Risk, injury, failure, loss, end-stage
RMSE	Root mean squared error
RNA	Ribonucleic acid
RPM	Revolutions per minute
RRT	Renal replacement therapy
RR	Relative Risk
SCG	Single copy gene
sCr	Serum creatinine
SD	Standard deviation
SNP	Single nucleotide polymorphism

STELA	Single telomere length analysis
STS	Society of thoracic surgeons
TERC	Telomerase RNA component
TERT	Telomerase reverse transcriptase
TIA	Transient ischaemic attack
TL	Telomere length
TRF	Terminal restriction fragment
WHRI	William Harvey Research Institute
WOSCOPS	West of Scotland Primary Prevention Study

List of Figures

Figure 1: Schematic representation of the structure of the mammalian telomere	43
Figure 2: Schematic representation of telomere elongation by telomerase..	45
Figure 3: Flow chart demonstrating the procedure for study data collection	65
Figure 4: PCR output showing successful quantification of a 5-point standard curve for the Telomere Reaction run in duplicate.....	74
Figure 5: XpYp STELA.....	75
Figure 6: Gel electrophoresis for DNA integrity.....	84
Figure 7: Typical amplification plots and standard curves for Telomere run (A, C) and SCG run (B, D).....	96
Figure 8: Melt curve analysis for Telomere run (A) and SCG run (B).	97
Figure 9: Results of validation experiment.	103
Figure 10: Schematic outlining patient recruitment and sampling.	105
Figure 11: Box plots for mTL in the AKI and No-AKI groups.	108
Figure 12: Box plots for mTL and development of the Composite outcome	109
Figure 13: Boxplot of mTL in Cases Vs Controls in 51 propensity matched patient pairings.	111
Figure 14: Relationship between age and mTL.....	115
Figure 15: Combined ROC curve of mTL (T/S Ratio), age and Logistic EuroSCORE for predicting CSA-AKI	130
Figure 16: Combined ROC curve of mTL (T/S Ratio), age and Logistic EuroSCORE for predicting 1-year mortality.....	131
Figure 17: Boxplots for mTL and the development of CSA-AKI in the whole population excluding patients whose serum Cr fell by >26 $\mu\text{mol/l}$	133

Figure 18: Boxplots for mTL and the development of CSA-AKI in the whole population excluding patients of South Asian descent.....	135
Figure 19: Boxplots for mTL and the development of CSA-AKI in patients of South Asian descent.	136
Figure 20: Boxplots for mTL and 1-year mortality in patients of South Asian descent.....	140
Figure 21: STELA Gels of the 12 matched AKI-control pairs.	142
Figure 22: Scatter plot showing the distribution of telomere lengths for each sample.	143
Figure 23: Correlation between Mean TL as measured by STELA and T/S Ratio measured by qPCR.	144
Figure 24: Telomere length as a function of age in controls and cases.	148
Figure 25: Predicted age in years based on methylation status against actual age in years for the training group of 24 healthy controls.	163
Figure 26: Correlation of Predicated methylation age with chronological age for all subjects (AKI and non-AKI).	175
Figure 27: Correlation between predicted methylation age and length of post-operative stay.	176
Figure 28: Relationship between smoking history and mean chronological age and predicted age.....	177
Figure 29: Receiver Operator characteristic (ROC) Curve demonstrating the diagnostic ability for the 4 measured aging measures in predicting CSA-AKI.....	188
Figure 30: Receiver Operator characteristic (ROC) Curve demonstrating the diagnostic ability for the 4 measured aging measures in predicting 1-year mortality.	190
Figure 31: Boxplot of pMA and development of CSA-AKI in the whole population excluding patients of South Asian descent..	193
Figure 32: Boxplot of pMA and development of CSA-AKI in the patients of South Asian descent.....	194

Figure 33: Methylation level of the 6 CpG sites plotted against passage number.	199
Figure 34: Box plots for age for the study cohort and the Model derivation cohort.....	209
Figure 35: Figure demonstrating the separation of blood in a BD Vacutainer CPT tube after centrifugation.	221
Figure 36: Method of cell counting using a haemocytometer.	223
Figure 37: Results of gel electrophoresis of 11 samples of extracted RNA plus 1 control sample (GC-Ctrl).....	232
Figure 38: Electrogram for sample S1.....	233

List of Tables

Table 1: Comparison of the RIFLE, AKIN and KDIGO classification criteria for defining AKI..	26
Table 2: Primer sequence for the Telomere reaction (Tel1/Tel2) and the single copy gene (36b4).	87
Table 3: Components of PCR Mastermixes for TL measurement.	89
Table 4: PCR cycling conditions for TL measurement.	89
Table 5: Association between TL and the main study outcomes. *Composite outcome includes New AF, Stroke, Reoperation, and AKI.	107
Table 6: Association of rates of AKI, In-hospital mortality, 1-year mortality, and composite outcome in patients in the top and bottom quintiles of mTL.	110
Table 7: Comparison of mTL in Cases Vs Controls in 51 propensity matched patient pairings.	110
Table 8: Summary table of Spearman correlations between mTL and all continuous independent variables. P-values <0.05 shown in bold.	112
Table 9: Summary of associations of mTL with independent categorical variables.	115
Table 10: Univariate analysis of the association of all pre-operative and intra-operative variables with the development of CSA-AKI.	118
Table 11: Summary of predictors of CSA-AKI on univariate analysis listed by strength of association.	118
Table 12: Differences in pre-operative and intra-operative variables between patients who developed CSA-AKI and those who did not.	119
Table 13: Multivariate model of independent predictors of CSA-AKI.	121
Table 14: Univariate analysis of the association of all pre-operative and intra-operative variables with 1-year mortality.	124

Table 15: Summary of predictors of 1-year mortality on univariate analysis listed by strength of association	125
Table 16: Multivariate model of independent predictors of 1-year mortality.....	126
Table 17: Multivariate model of independent predictors of CSA-AKI limited to 5 predictors.	128
Table 18: Multivariate model of independent predictors of 1-year mortality limited to 2 predictors.	128
Table 19: Diagnostic ability of mTL (T/S Ratio), age, and Logistic EuroSCORE for predicting CSA-AKI with cut-off points shown.	130
Table 20: Diagnostic ability of mTL (T/S Ratio), age, and Logistic EuroSCORE for predicting 1-year mortality with cut-off points shown.....	131
Table 21: Association between mTL and development of CSA-AKI in the whole population excluding patients whose serum Cr fell by >26 µmol/l.....	133
Table 22: Association between mTL and development of CSA-AKI in the whole population excluding patients of South Asian descent.....	135
Table 23: Association between mTL and development of CSA-AKI in patients of South Asian descent.....	136
Table 24: Univariate analysis of the association of all pre-operative and intra-operative variables with CSA-AKI for the South Asian population.	138
Table 25: Summary of univariate analysis of predictors of CSA-AKI in the South Asian population listed by strength of association.	139
Table 26: Results of a Multivariate analysis of mTL and CSA-AKI in the South Asian population	139
Table 27: Results of the multivariate analysis when age is added as a variable in the model. mTL remained an independent predictor of CSA-AKI in the South Asian population.	139

Table 28: Association between mTL and 1-year mortality in patients of South Asian descent	140
Table 29: Comparison of mean TL, median TL and 25 th percentile TL between the 11 propensity matched sample pairs.....	143
Table 30: Association between Age, Predicted methylation age, AMAR and Delta age with the main study outcomes.....	166
Table 31: Association of rates of AKI, In-hospital mortality, 1-year mortality, and composite outcome in patients in the top and bottom quintiles of Age, pMA, AMAR, and Delta Age.	167
Table 32: Comparison of Age, pMA, AMAR, and Delta Age in Cases Vs Controls in 43 propensity patched patient pairings.....	168
Table 33: Summary table of Spearman correlations between Age, Predicted age, AMAR, and Delta age and all continuous independent variables.....	169
Table 34: Summary of associations of Age, Predicted age, AMAR, and Delta age with independent categorical variables.....	173
Table 35: Univariate analysis of the association of all pre-operative and intra-operative variables with the development of CSA-AKI in the DNA methylation population.....	180
Table 36: Summary of predictors of CSA-AKI on univariate analysis listed by strength of association.....	181
Table 37: Multivariate model of independent predictors of CSA-AKI.....	182
Table 38: Univariate analysis of the association of all pre-operative and intra-operative variables with the development of 1-year mortality in the DNA methylation population.	184
Table 39: Summary of predictors of 1-year mortality on univariate analysis listed by strength of association.....	185
Table 40: Multivariate model of independent predictors of 1-year mortality.....	186

Table 41: Multivariate model of independent predictors of CSA-AKI limited to 5 predictors.	187
Table 42: Multivariate model of independent predictors of 1-year mortality limited to 2 predictors.	187
Table 43: Diagnostic ability of age, predicted methylation age, AMAR, and Delta age for predicting cardiac surgery associated AKI.....	189
Table 44: Diagnostic ability of age, predicted methylation age, AMAR, and Delta age for predicting 1-year mortality.....	190
Table 45: Association between the 4 measures of aging and development of CSA-AKI in the whole population excluding patients whose serum Cr fell by >26 µmol/l.....	191
Table 46: Association between the 4 measures of aging and development of CSA-AKI in the whole population excluding patients of South Asian descent.....	192
Table 47: Association between the 4 measures of aging and development of CSA-AKI in the patients of South Asian descent..	194
Table 48: Association between the 4 measures of aging and 1-year mortality in the whole population excluding patients of South Asian descent.	196
Table 49: Association between the 4 measures of aging and 1-year mortality in patients of South Asian descent.	196
Table 50: The 6 CpG sites in the senescence panel and their corresponding genetic sequences.	197
Table 51: Results of Binary logistical regression for each of the CpG sites with development of CSA-AKI.....	200
Table 52: Analysis of CpG sites coded into senescent/Non-senescent based on cut-off values of % methylation approximating to passage numbers of 5, 10 and 15.....	200
Table 53: Multivariate model of independent predictors of CSA-AKI including KRTAP133- Sen.....	201

Table 54: Summary of TA experiments using TeloTAGGG Telomerase PCR ELISA kit.	225
Table 55: Summary of TA experiments using TeloTAGGG Telomerase PCR ELISA PLUS kit.	227
Table 56: Measures of reproducibility in AS and RTA for samples D and J	227

CHAPTER 1: General Introduction

1.1 Cardiac surgery associated Acute Kidney Injury

Cardiac surgery associated acute kidney injury (CSA-AKI) is an acute decline in kidney function that occurs following a cardiac surgical procedure. The incidence of CSA-AKI is approximately 0.3% to 30% depending on the definition of acute kidney injury (AKI) (1). Its underlying cause is thought to be multifactorial including the patient's pre-morbid condition, and the insults that they sustained intra-operatively and in the early post-operative period. CSA-AKI is clinically significant as it has been found to be associated with increased morbidity and reduced short and long term-mortality.

1.1.1 Definition of CSA-AKI

The study of AKI was initially complicated by a lack of consensus as to how to define this clinical entity. In 2004, the Acute Dialysis Quality Initiative Group introduced the Risk-Injury-Failure-Loss-End-Stage (RIFLE) classification; a consensus definition by which to grade AKI (2). The criteria that they developed is shown in *Table 1* and can be met by changes in either serum creatinine (sCr) or glomerular filtration rate (GFR) or by changes in urine output. The RIFLE criteria measures changes from baseline over a seven-day period and has been validated in the setting of cardiac surgery (3).

In 2007, the Adult Kidney Injury Network (AKIN) modified the RIFLE criteria in response to findings that even minimal changes in sCr were associated with adverse

outcomes after cardiac surgery (4, 5). The AKIN criteria differ from the RIFLE criteria in 5 ways;

1. Risk, injury, and failure categories were replaced with stages 1, 2, and 3. Loss and ESRF were lost as categories.
2. An absolute increase in creatinine of 0.3mg/dl ($>26.4 \mu\text{mol/l}$) or more was added to stage 1.
3. The use of eGFR was abandoned
4. All patients with Renal Replacement Therapy (RRT) classified as stage 3
5. Changes in serum Creatinine or urine output are measured over any 48-hour period within the first 7 days post-operatively rather than as a change from baseline within a 7-day period.

The change in time periods between AKIN and RIFLE has the advantage of eliminating the need for a baseline creatinine. However, the AKIN criteria have been criticised for the over-diagnosis of AKI if the patient's serum creatinine is not corrected for fluid status. This is because an initial drop in sCr due to fluid overload in the first 24 hours post-operatively can lower the threshold for stage 1 AKI for any subsequent rise in creatinine. Engelberger *et al* argue that this effect leads to the over-diagnosis of CSA-AKI due to a state of fluid overload following cardiac surgery (6). However, several other studies suggest no significant difference in peri-operative predictive power of RIFLE and AKIN (7, 8), whilst Bastin *et al* found that the AKIN criteria correlate better with mortality post-cardiac surgery (9).

A third attempt was made to standardise the definition of AKI with the Kidney Disease: Improving Global Outcomes (KDIGO) classification (10). This classification effectively combines the RIFLE and AKIN by classifying AKI as either an increase in sCr of $>26.4 \mu\text{mol/l}$ over 48 hours or an increase of 1.5 times baseline over a rolling 7-day period (*Table 1*). The definition of AKI by urine output classified in the RIFLE criteria is common to all three classification systems. However, whilst the KDIGO classification has been validated in cardiac surgery, it has not been found to be superior to the AKIN criteria for the prediction of AKI (9) or mortality (11). As such, in this thesis the more established AKIN criteria will be used for the definition of CSA-AKI.

RIFLE Stages	Definition (over 7 days)	AKIN stages	Definition (over 48hrs)	KDIGO stages	Definition
Risk	sCr >1.5 x baseline/ reduced GFR $>25\%$	Stage 1	sCr >1.5 x baseline/ $>0.3\text{mg/dl}$ ($>26.4 \mu\text{mol/l}$) increase	Stage 1	sCr > 1.5 x baseline over 7 days or $>0.3\text{mg/dl}$ ($>26.4 \mu\text{mol/l}$) increase over 48 hours
Injury	sCr >2 x baseline/ reduced GFR $>50\%$	Stage 2	sCr >2 x baseline	Stage 2	sCr > 2 x baseline
Failure	sCr >3 x baseline/ reduced GFR $>75\%$	Stage 3	sCr >3 x baseline or increased to 4.0mg/dl [$\geq 354 \mu\text{mol/l}$] with an acute increase of at least 0.5mg/dl [$44 \mu\text{mol/l}$]	Stage 3	sCr > 3 x baseline or increase to 4mg/dl or any RRT
Loss	Persistent AKI with complete loss of function > 4 weeks				
End stage	RRT for > 3 months				

Table 1: Comparison of the RIFLE, AKIN and KDIGO classification criteria for defining AKI.

1.1.2 Pathophysiology of CSA-AKI

The pathogenesis of CSA-AKI is not fully understood but is thought to be multifactorial. Multiple processes including ischaemia-reperfusion injury (IRI), nephrotoxic agents, venous congestion, systemic inflammation, microembolisation, neurohormonal activation, oxidative stress, and haemodynamic factors may all contribute to the development of AKI in a synergistic manner (12). Cardiopulmonary bypass (CPB) has been cited as the cause for several of these mechanisms. Due to their high metabolic activity, the kidneys are susceptible to ischemia-reperfusion injury associated with CPB. A reduced cardiac output state activates the renin-angiotensin system, the sympathetic nervous system and the release of vasopressin (13). This results in vasoconstriction with reduced renal blood flow and glomerular filtration. The renal medulla has a PaO₂ of approximately 10-20mmHg and is highly metabolically active (14). As such it is susceptible to regional hypoxia. Sgouralis *et al* recently developed a mathematical model of renal blood flow and oxygen transport in rats during CPB. They conclude that the rewarming phase of CPB is when the kidney is most likely to suffer hypoxic injury due to the combination of low medullary blood flow and high medullary oxygen consumption (15).

Renal micro-emboli released at the time of cardiac surgery are thought to contribute to the development of CSA-AKI. Blauth *et al* demonstrated renal atheroembolic disease in 10.4% of patients undergoing CPB for coronary revascularisation or valve disease (16). Furthermore, CPB is itself known to be a source of micro-emboli (17). However, no studies have demonstrated a direct association between embolic load and CSA-AKI.

The use of CPB has been associated with an increased systemic inflammatory response and induction of oxidative stress. CPB has been shown to result in elevated levels of pro-inflammatory cytokines and complement activation (18, 19) due to the interface between the blood and the artificial membrane of the bypass circuit. It is associated with increased haemolysis and the release of intravascular free haemoglobin (Hb), resulting in increased renal tubular cell exposure to free iron which may result in renal injury (20).

It is important to consider that the above mechanisms of renal injury are not confined to cardiopulmonary bypass. Renal ischaemia, micro-emboli, systemic inflammation and oxidative stress are also thought to be factors in cardiac surgery without cardiopulmonary bypass ('off pump surgery') but to a lesser degree. However, objective comparative evidence between the two techniques is lacking and clinical studies comparing renal outcomes in cardiac surgery with and without the use of cardiopulmonary bypass have failed to consistently demonstrate a benefit to performing surgery 'off-pump'. A 2010 meta-analysis of 22 randomised controlled trials comparing the incidence of AKI in on-pump and off-pump cardiac surgery found a significant reduction in AKI in the off-pump group but no significant difference in the rate of RRT (21). It should be noted that this trial is limited by the lack of consensus definition for AKI used in the included studies. In two more recent randomised controlled trials (RCTs), AKIN criteria were used to define AKI. Reents *et al* (22) found no significant difference in AKI between on-pump and off-pump in 1612 elderly coronary artery bypass graft (CABG) patients. However, the CORONARY trial

(23) randomised patients between on and off-pump CABG and found a significant reduction in CSA-AKI at 30 days in the off-pump group. These mixed findings suggest that additional factors may play more of a role in the development of CSA-AKI than the use of cardiopulmonary bypass. Such factors include nephrotoxic agents, blood transfusion and pre-operative predispositions (e.g. genetic variation)

1.1.3 Risk factors for CSA-AKI

Numerous studies have investigated associations and risk factors of CSA-AKI. In a recent meta-analysis of 14 case control studies, pre-operative, intra-operative and post-operative risk factors for AKI were studied (24). All studies defined AKI using the RIFLE criteria. Age, NYHA class III/IV, hypertension, preoperative creatinine, peripheral vascular disease, respiratory system disease, diabetes mellitus, and cerebrovascular disease were identified as pre-operative factors associated with AKI. Intra-operative factors were cardiopulmonary bypass time, aortic clamping time, use of intra-aortic balloon pump, and type of surgery, whilst postoperative factors were infection, need for re-sternotomy, and low cardiac output. All of these factors are non-modifiable and are therefore clinically useful only in terms of early identification of at-risk patients. Several studies that have focused on modifiable risk factors of CSA-AKI identified the use of nephrotoxic agents, pre-operative anaemia and intra/post-operative transfusion.

Nephrotoxic Agents

Potential nephrotoxic agents associated with CSA-AKI include Angiotensin Converting Enzyme (ACE) Inhibitors, Angiotensin receptor blockers (ARBs), Non-steroidal anti-inflammatory drugs (NSAIDs), diuretics, metformin and intravenous contrast from pre-operative angiography. However, evidence to date is mostly limited to the pre-operative use of Renin inhibitors, ACE Inhibitors and ARB's. Coca *et al* (25) demonstrated a graded increase in CSA-AKI across three levels of pre-operative ACE Inhibitor use (none, held, and continued), whilst a meta-analysis of predominantly non-randomised retrospective trials found pre-operative ACE Inhibitor use to be associated with both increased rates of AKI and mortality following cardiac surgery (26). A significant number of patients undergo angiography with contrast in the pre-operative period. A limited number of single center, retrospective studies have evaluated the time period between angiogram and cardiac surgery as a risk factor for CSA-AKI with conflicting results. Ranucci *et al* (27) and Medallion *et al* (28) both found angiography to be independently associated with CSA-AKI if performed within 24 hours of surgery. The latter study also demonstrated an association with angiography up to 5 days from surgery if high contrast doses were used. However, Ozkaynak *et al* (29) demonstrated no such association in 573 consecutive patients. As such, a common practice is to delay surgery until at least 5 days from angiogram if the patient's condition is stable enough to allow such a wait.

Pre-operative anaemia and blood transfusion

Pre-operative anaemia, major post-operative bleeding and the need for allogenic blood transfusion are interdependent in terms of their effect on outcomes after

cardiac surgery. Many studies have demonstrated that pre-operative anaemia is associated with poor outcomes and AKI post cardiac surgery. Loo *et al* (30) demonstrated that pre-operative anaemia and blood transfusion had a combined effect on post-operative eGFR with an incremental decline in renal function across the groups: - anaemia/ - transfusion; + anaemia/ - transfusion; - anaemia/ + transfusion; and + anaemia/ + transfusion. This study suggests that transfusion plays a greater role in CSA-AKI than pre-operative anaemia. This finding is supported by Goldberg *et al* (31), who investigated nadir haematocrit and transfusion during CPB and concluded that transfusion has a more profound effect on post-operative outcomes than anaemia. Rannucci *et al* (32), showed that major bleeding was also an independent risk factor of CSA-AKI and, together with pre-operative anaemia and transfusion, had a cumulatively detrimental effect on in-hospital death, stroke and AKI. Interestingly, a recent study that corrected for the detrimental effects of perioperative bleeding and transfusion as well as patient co-morbidity, found no relationship between pre-operative anaemia and rates of CSA-AKI (33). As such a balance must be found between correcting anaemia and avoiding blood transfusion.

1.1.4 Genetic pre-disposition for CSA-AKI

The current evidence for a genetic predisposition to CSA-AKI is sparse and has focused on demonstrating the associations with various single nucleotide polymorphisms (SNP's). In 2003, Gaudino *et al* (34) quantified the -174G/C polymorphism of the promotor region of the Interleukin (IL) -6 gene in 111 patients undergoing cardiac surgery and found that G homozygotes had worse post-operative renal and pulmonary function. A single-center study of 130 coronary artery bypass

patients found a relationship between Apolipoprotein E (APOE) status and CSA-AKI with patients who lack the APOE E4 allele being at increased risk (35). APOE is a mediator of cholesterol metabolism. Stafford-Smith *et al* (36) performed pre-operative genetic testing of 12 candidate polymorphisms in 1671 patients undergoing cardiac surgery. When combined with clinical risk factors certain polymorphisms improved the predictability of CSA-AKI 4-fold in Caucasians and 2-fold in African-Americans. Most of the polymorphisms were associated with increased renal inflammatory or vasoconstrictor responses. Similar work by Isbir *et al* (37) confirmed the association of the ACE I/D and APOE gene polymorphisms with the development of CSA-AKI.

More recently, Jouan *et al* (38) failed to find any such association with CSA-AKI and single nucleotide polymorphisms (SNP's) of APOE (Cys112Arg, Arg158Cys), Tumour necrosis factor (TNF-308G>A), or Lymphotoxin- α (Cys13Arg, +252 A>G), but did find that IL6-572G>C and IL10-592C polymorphisms predicted the combined clinical endpoint of death, myocardial infarction, stroke, low cardiac output state, AKI, and sepsis. In 2015, a genome wide association study (GWAS) of CSA-AKI was performed to identify predisposing genetic loci (39). 9 SNP's were found to meet significance in the discovery set, with 2 replicated with significance in the validation set; rs13317787 at 3p21.6 and rs10262995 at 7p14.3. For both SNP's, AKI incidence increased with each copy of the minor allele. The 3p21.6 locus is an intergenic region bounded by GRM7 (glutamate receptor, metabotropic 7) and LMCD1 (LIM and cysteine rich domains protein 1, dyxin) genes. No direct functional roles are currently attributed to this region. The 7p14.3 locus involves a region in the BBS9 gene, named for its

association with Bardet-Biedl syndrome (BBS). Kidney disease is a key feature and major source of early mortality with BBS and a BBS9 translocation is associated with Wilm's Tumour.

The limited number of studies done to date demonstrate that there does appear to be a genetic predisposition to CSA-AKI, primarily through the mediation of the post-operative inflammatory response (34). The majority of studies conclude that the addition of genetic polymorphisms significantly improves predictive risk compared to models based solely on clinical parameters. However, to date, such tests have not been routinely implemented in clinical practice. Moreover, receiver operative characteristic (ROC) curve analysis has not been performed to assess additional incremental predictive value of these genetic variations over clinical parameters.

1.1.5 Existing models for predicting CSA-AKI

Several risk stratification models have been developed to predict the risk of a patient developing AKI following cardiac surgery (40). Early models primarily focused on AKI requiring post-operative renal replacement therapy (RRT) but more recent models have also been developed for milder forms of AKI. To date, only the RRT scoring systems have been externally validated. In 1997, Chertow *et al* (41) first published a risk stratification algorithm for predicting AKI following cardiac surgery in the Continuous Improvement in Cardiac Surgery Study (CICSS). AKI was defined as a patient requiring RRT within 30 days of their index operation. In their prospectively collected data of 42,773 patients, 1.1% were defined as having AKI. The Area under

Curve (AUC) was 0.76 for the multivariate analysis of 10 variables. The score was internally validated in a smaller cohort of 3795 patients. In several external validation studies, the AUC was only modest (42-44). This is thought to be due to the CICSS population not being representative of the normal cohort of cardiac surgical patients as it included a very high proportion of males 99.1%, and excluded patients with pre-existing renal failure. Several other scoring systems have since been developed to predict CSA-AKI requiring RRT (45-47). Thakar *et al* (47), developed the Cleveland Clinic Score to predict post-operative RRT in a retrospective analysis of 33,217 patients. It has been extensively validated externally and has also been tested in less severe forms of CSA-AKI not requiring RRT. Wong *et al* (48) found that the Cleveland Clinic Score was a good predictor of more severe degrees of CSA-AKI (AUC of 0.78 for AKIN stage 3) but less so for the milder degrees of AKI (AKIN 1 and 2). Mehta *et al* (45) developed a bed-side tool scoring system for post-op AKI requiring RRT using data from the Society of Thoracic Surgeons (STS) database. The STS database has subsequently been used to develop an online scoring calculator to predict a range of post-operative morbidities of which one is renal failure as defined by the RIFLE criteria. Wijesundera *et al* (46) developed a simple 8-point scoring system, which predicted post-op RRT with similar accuracy compared to the more complex systems developed by Thakar and Mehta. An external comparison of the predictive powers of these three main scoring systems found that whilst all three tended to underestimate the true risk of RRT post cardiac surgery, the Cleveland Clinic score performed best with an AUC of 0.82 (49).

More recent studies have tried to apply scoring tools to less severe forms of CSA-AKI. Palomba *et al* (50) derived the Acute Kidney Injury in Cardiac Surgery (AKICS) Score in ARF defined as Cr >2mg/dl or a rise of >50% above baseline (corresponding to AKIN 1 or RIFLE R). The AKICS score was based on 8 variables with 5 categories developed to predict risk and differs from previous scores in that it includes intra-operative variables such as cardiopulmonary bypass time and central venous pressure. It demonstrated good discrimination in both the development and validation cohorts with AUC values of 0.843 and 0.847 respectively. Brown *et al* (51) developed the Northern New England Cardiovascular Disease Study Group (NNECDSG) score prospectively on 8363 patients with an endpoint of severe renal failure (Defined as an eGFR of <30) or RRT. Pre-operative patients with moderate (eGFR<60) or severe renal insufficiency (eGFR<30) were excluded from analysis. The NNECDSG score included 11 peri-operative variables and performed reasonably well in the derivation cohort with an AUC of 0.72. However, no further external validation has been performed of this scoring system.

1.1.6 Predictive risk calculators for mortality following cardiac surgery

Predictive risk calculators are routinely used in cardiac surgery to estimate patient mortality risk prior to undertaking a procedure. The two most widely used scoring systems currently in practice are the Society of Thoracic Surgeons (STS) online calculator (52) and the European System for Cardiac Operative Risk Evaluation (EuroSCORE) (53). Of the two, the STS score is more in depth containing 65 fields compared to 17 in the EuroSCORE. The EuroSCORE also only provides a prediction on in-hospital mortality whilst the STS score also provides risk scores for Renal failure,

stroke, prolonged ventilation, deep sternal wound infection, reoperation, and long length of stay. Despite these differences, a comparison between the two scores by Ad *et al* (54) showed gross equivalence between the two in terms of predicting in-hospital mortality following cardiac surgery. As EuroSCORE is the primary risk score used in Europe and is the score used for risk adjusted mortality in the UK, it will be used in the current study to provide an indicator of the risk of specific patient groups

1.1.7 Clinical significance of CSA-AKI

1.1.7.1 Association with long-term mortality

CSA-AKI is more prevalent in patients with high levels of co-morbidity. As such, it is not surprising that the development of AKI post-cardiac surgery is associated with increased in-hospital mortality (55). Several studies have also demonstrated an association between post-operative AKI and reduced long-term survival (56). Interestingly, this association persists even when the degree of kidney injury is mild (57), and where there is complete resolution of the injury prior to discharge (58). Gallagher *et al* (59) demonstrated that CSA-AKI was an independent predictor of mortality at a median follow-up of 5.6 years in a propensity matched analysis of 1124 patients undergoing first time CABG. Previous studies have also demonstrated a link with CSA-AKI and increased long-term rates of cardiovascular events including myocardial infarction, heart failure and stroke. Hansen *et al* (60) studied 4752 patients undergoing cardiac surgery of which 1457 (30.7%) developed AKI within 30 days. Of those with AKI, the weighted hazard ratio (HR) was 1.37 (95% CI: 1.05-1.80) for all-cause mortality and 1.41 (95% CI: 1.11-1.80) for the 5-year risk of the composite cardiovascular endpoint of heart failure, myocardial infarction and stroke.

However, the mechanism by which CSA-AKI is related to increased long-term mortality is not currently understood.

1.1.7.2 Association with long-term renal dysfunction

Recent studies have shown that AKI post cardiac surgery is also associated with an increased rate of developing subsequent Chronic Kidney Disease (CKD) (61-63). Ryden *et al* (62) demonstrated a hazard ratio for end-stage renal disease of 2.92 (95% CI, 1.87–4.55) for mild kidney injury (AKIN stage 1) and 3.81 (95% CI, 2.14–6.79) for moderate kidney injury (AKIN stage 2 to 3). As with the effect of AKI on long-term mortality, Xu *et al* (61) demonstrated that the relationship between AKI and subsequent CKD persisted even if complete resolution of AKI occurred prior to discharge.

1.2 Developing the hypothesis – linking CSA-AKI with decreased long-term mortality and risk of CKD

The underlying mechanism by which CSA-AKI predisposes to reduced long-term mortality and renal function has not yet been elicited. Animal studies have demonstrated that episodes of severe ischaemic renal injury result in morphological changes at the renal tubule level that predispose to reduced long term renal function (64). There is also evidence that ischaemic renal injury in rats results in persistent alterations in gene expression (65). These results suggest that episodes of AKI result in physical changes in the kidney that predispose to a decline in long-term function. With this in mind it is interesting to note the results of a sub-group analysis of the

CORONARY trial (66) that looked at the development of post-operative AKI in patients randomised to coronary artery bypass grafting with (on-pump) or without (off-pump) cardiopulmonary bypass. On-pump surgery has been shown to be associated with increased rates of AKI in comparison to off-pump cardiac surgery (21). This is thought to be due to renal ischaemic injury and an increased systemic inflammatory response associated with cardiopulmonary bypass. As such we would expect that off-pump surgery results in less CSA-AKI and subsequently reduced rates of long-term renal dysfunction. However, although the CORONARY trial did show that off-pump coronary surgery reduced the risk of CSA-AKI by 17%, there was no difference between the two groups in terms of loss of kidney function at 1 year (expressed as patients with a new requirement for RRT). Nor was there any difference seen in mortality at one year between the groups. If AKI was acting as a direct causal factor for further renal decline then the difference between the two groups would be expected to continue beyond a year. Also, a mortality difference might also be expected as the development of CSA-AKI has consistently been demonstrated as being associated with increased long-term mortality. Possible explanations for the lack of such findings are;

1. The follow up period of 1 year was too short to detect a change in development of CKD/mortality.
2. The number of patients with AKI was too low to affect the overall outcome of long-term CKD/mortality.
3. The development of CSA-AKI is not a direct causal link to the subsequent development of CKD/mortality.

We suggest that patients who develop AKI post-cardiac surgery are already at an increased risk of CKD and increased long-term mortality due to some underlying predisposition. In 'on-pump' surgery this predisposition is more likely to result in AKI due to the larger associated inflammatory response, without altering the progression to long-term CKD and death. We hypothesise that this predisposition lies in a patient's capacity for cellular regeneration, with those patients with increased senescence being more susceptible to ischaemia induced AKI, the long-term development of CKD, and reduced long-term survival.

1.3 Cell senescence

Cell senescence is defined as the process whereby normal diploid cells cease to divide. As cells continue to divide the risk of them accumulating oncogenic mutations increases. Mechanisms of inducing cellular senescence exist to limit the number of cell divisions that can occur physiologically and prevent damaged cells from taking part in further replication. As such senescence has an anti-oncogenic effect. It should be noted that senescence does not in itself cause aging. Rather it is the failure to clear senescent cells and the reduced capacity of progenitor cells to replace them that decreases tissue regeneration and produces an aged phenotype (67). Increased senescence may contribute to aging by changes in the secretome profile of senescent cells to favour proinflammatory cytokines and matrix metalloproteinases (68).

Cell senescence appears to be triggered as a response to DNA damage. It has been postulated that these DNA damage response (DDR) signals can be generated either

by progressive telomere shortening and dysfunction (the telomere theory of senescence), or by mitochondrial induced reactive oxidative species causing damage to DNA (the mitochondrial theory of senescence) (69).

1.3.1 Markers of cellular senescence

Several markers have been used in attempts to develop a signature of cellular senescence and aging. Telomere biology has been extensively used as a marker of cellular senescence and biological aging. Studies have primarily focused on Telomere length (TL) as a marker of senescence. Different markers of telomere induced senescence include mean telomere length, measurement of the shortest telomere length in a cell, and the rate of telomere attrition.

Several other markers have been commonly used to measure senescence. Levels of proteins such as Senescence-associated β -galactosidase (SA β G) are associated with senescence but have been found not to trigger it (70). Other markers used to measure senescence such as senescence-associated heterochromatin foci (SAHF), phosphorylated H2AX histone (γ H2AX), p16, p53, and Promyelocytic leukemia nuclear bodies (PML-NBs) are all involved in the senescence inducing pathways resulting from DNA damage or telomere shortening (71).

Numerous microarray studies have demonstrated altered gene expression in aging with a 2009 meta-analysis identifying 56 genes that are consistently overexpressed with increasing age and 17 that are consistently under-expressed (72). Evidence for

altered gene expression in cell senescence is less well studied but evidence exists of genes that are candidate markers of senescence (73).

Finally, it has been proposed that epigenetic modifications play a role in aging and cell senescence by acting as molecular switches, switching off or activating senescence related genes (the gene-silencing theory of aging) (74). In particular, DNA methylation of gene promotor regions has been found to be well associated with chronological age (75) and more recently DNA methylation signatures for both aging and cellular senescence have been developed (76, 77).

In this thesis we will focus on genetic and epigenetic markers of cell senescence by studying Telomere biology and DNA methylation status and their association with CSA-AKI.

1.4 The role of Telomeres and Telomerase in Cell Senescence

1.4.1 The structure and function of Telomeres

Telomeres are repetitive, non-coding DNA sequences located at the end of chromosomes that control when a dividing cell undergoes senescence (78). Their primary function is to provide a protective cap to the chromosome so that coding genetic material is not lost during cell division. During cell division, the replicating DNA polymerase is not able to completely copy the lagging strand of DNA all the way to its end, resulting in the loss of a portion of DNA at the 5' end with each division.

This has been termed the 'end replication problem' (79). The presence of the telomere cap ensures that it is telomeric DNA and not coding DNA that is lost during DNA replication, maintaining the integrity of the genome. With each subsequent cell division, the telomere length is progressively shortened until a critical length is reached at which point the cell is no longer able to divide and is rendered senescent, undergoing apoptosis (80). As such, telomere length has been postulated as a biomarker for biological age.

Telomeres not only protect genomic material during DNA replication, their structure also prevents free DNA ends from degradation by DNA repair mechanisms. These mechanisms are designed to recognise single stranded DNA at chromosomal breaks and trigger either degradation by nucleases or end-joining reactions that fuse two free DNA ends. Mammalian telomeres are comprised of double stranded tandem TTAGGG hexameric repeats followed by 3' G-rich single stranded overhangs (78) (Figure 1). This 3' single stranded free end folds back on itself and binds to the double stranded telomeric DNA forming a 't-loop'. At the point where this binding occurs, the duplex DNA is displaced forming a triple stranded structure (d-loop) that is stabilised by telomere binding proteins (81). Telomeres are coated with a complex of 6 binding proteins collectively termed the Shelterin proteins (82). It is this T-loop-Shelterin protein complex that prevents the free DNA end from degradation.

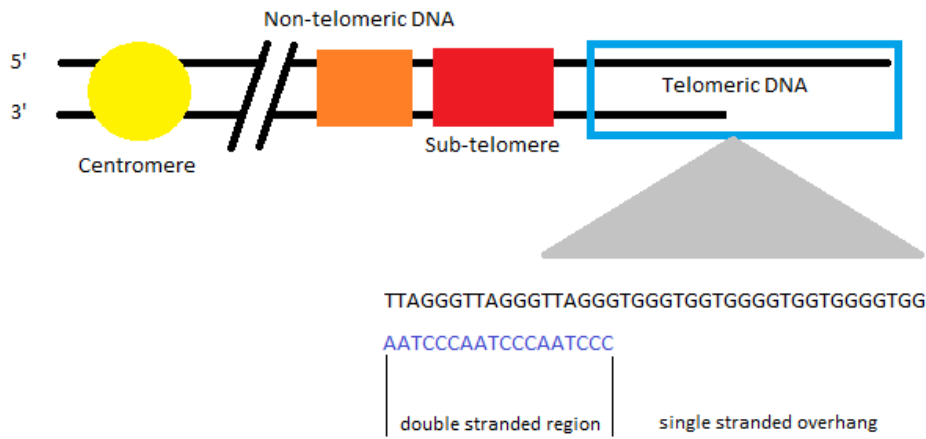


Figure 1: Schematic representation of the structure of the mammalian telomere

1.4.2 The structure and function of telomerase

The process by which telomere length (TL) changes with each cell division is non-linear. Several processes are involved in telomere homeostasis, principally the action of the enzyme complex telomerase. The primary function of telomerase is to maintain telomere length by adding TTAGGG repeats to the 3' end of the chromosome (83). It is a ribonuclear protein consisting of two main subunits; Telomerase RNA Component (TERC) and Telomerase reverse transcriptase (TERT). TERC contains an 11-bp sequence complimentary to the telomeric overhang which TERT, a DNA polymerase, uses as a template to synthesise telomeric DNA to the ends of chromosomes (*Figure 2*). Telomerase thereby acts to counter the Telomere attrition that occurs during cell replication. As such, telomerase activity is tissue dependent with higher levels seen in tissues with increased cell replication such as germ cells, stem cells, haematopoietic cells, and activated lymphocytes. Most cancerous cells also show increased telomerase activity, allowing prolonged cell division. In contrast, terminally differentiated somatic cells usually express low or absent levels of telomerase activity.

leukocytes. Janic *et al*, (87) demonstrated that TERT expression was upregulated in circulating leukocytes of patients treated with low dose statin therapy and that this upregulation correlated with an improvement of endothelial function and a decrease of inflammation/oxidative stress.

TERT expression and subsequently Telomerase activity can be modulated in response to certain stimuli in both health and disease. Gizard *et al* (88) demonstrated that TERT expression was inducible by certain inflammatory stimuli resulting in high levels of TERT expression in macrophages of human atherosclerotic lesions. Furthermore, Cheng *et al* (89) demonstrated that TERT knock out (KO) mice show telomere shortening and reduced regenerative capacity following renal ischaemic injury. Similar murine models were found to cause progressive cardiac myocyte death and hypertrophy suggesting that telomere shortening may contribute to age related heart failure in humans (90). Conversely, when heart failure was induced mechanically, telomerase activity was upregulated as part of a compensatory mechanism to promote cell regeneration. The increased telomerase activity was found to co-localise with the proliferation marker Ki67 in the nuclei of dividing myocytes, and was associated with prolonged telomere length (TL) (91). Richardson *et al* (92) demonstrated a 6.45-fold increase in cells expressing TERT in response to myocardial cryoinjury. As well as upregulation in response to pathological stimuli, increased physical activity via voluntary wheel running in mice is found to upregulate telomerase activity with subsequent reduction in vascular apoptosis regulators (93). A similar finding is found in humans where significant changes in lifestyle are associated with increased telomerase activity and telomere length (94). Aberrant

expression of human TERT can effectively immortalise cells by maintaining TL and thus preventing triggering of cell senescence.

1.4.3 How does TL induce senescence?

There appear to be two mechanisms that can induce cell senescence. The first, termed Mortality stage 1 (M1) senescence is triggered by critical telomere shortening and is irreversible in the sense that it cannot be overcome by physiological mechanisms. It represents replicative exhaustion on the part of the dividing cell and has thus been termed replicative senescence. However, mutations in the cell cycle inhibitors p53, p16 /Retinoblastoma (Rb) protein can allow cells to bypass M1 senescence and continue to divide with further telomere attrition. This process eventually results in crisis where non-telomere dependent mechanisms trigger a truly irreversible cell cycle arrest (termed M2 senescence) (95). Despite their inability to proliferate both M1 and M2 senescent cells remain viable.

Direct evidence that telomere shortening results in cell senescence can be demonstrated by inducing TERT expression in Telomerase negative cells. Such cells aberrantly expressing transfected TERT demonstrate increased Telomere length and are able to divide indefinitely (96). Furthermore, inducing a transient expression of telomerase increases a cell's lifespan in accordance with its increased telomere length rather than for the duration of telomerase expression (97). This indicates that it is telomere length that directly controls senescence rather than telomerase activity.

Although there is a considerable body of evidence suggesting that it is telomere shortening that is responsible for triggering M1 senescence, the exact mechanism behind this trigger is not fully understood. Current mechanisms proposed include DNA damage induced by short telomeres, telomere position effects and the loss of 3' G-rich telomere single-strand overhangs.

The preferred theory of telomere induced cell senescence proposes that shortened, dysfunctional telomeres trigger events that are usually triggered by DNA double strand breaks (DSBs). Cells react to DSBs by triggering the DNA damage checkpoint response (DDR) which halts cell proliferation until the damaged DNA has been removed. Telomeres function to protect chromosomal ends and stop them being recognized as double strand DNA breaks. However, progressive shortening leads to loss of the protective functions of the telomere associated proteins Telomeric repeat binding factor 2 (TRF-2) and Protection-of-Telomeres – 1 (POT-1), allowing critically short telomeres to be recognized as DNA breaks and trigger a DDR (98). If this DDR response is prolonged, cells are triggered to enter M1 senescence. D'Adda *et al* (99) showed that senescent human fibroblasts express phosphorylated H2AX (γ H2AX), a robust marker of cellular DSBs. Using Chromatin Immunoprecipitation (ChIP) the authors demonstrated that these γ H2AX foci localized to a sub-telomeric region on specific chromosomes of senescent cells known to have short telomeres. H2AX foci signal through ataxia-telangiectasia mutated serine/threonine kinase (ATM) to p53, resulting in the upregulation of p21 and G2 phase growth arrest (100). For any given cell, it is only one or two of the shortest telomeres that produce such γ H2AX repair foci. This suggests that the proportion of critically short telomeres may be a more

relevant marker of cell senescence than average telomere length. This theory is supported by the findings of Hemann *et al* (101) who crossed mTR^{-/-} G6 mice that have short telomeres with mice heterozygous for telomerase (mTR^{+/-}) that have long telomeres. The resulting offspring had an equal mix of short and long-telomeres but their phenotype mimicked that of the mTR^{-/-} mice. Further analysis showed that it was these shortened telomeres that were associated with telomere dysfunction.

Telomere position effects (TPE) refers to the reversible inactivation of genes near a telomere by mechanisms that depend both on the length of the telomere and its distance to the gene. Initial experiments on the chromosomal end of yeast *S. Cerevisiae* demonstrated that genes placed immediately adjacent to the telomeric repeats were repressed in terms of both phenotype and mRNA analysis (102). The frequency of gene silencing is decreased by increasing the distance between the gene promoter and the telomere (103). Baur *et al* (104) demonstrated that this silencing of peri-telomeric genes also occurs in Mammalian cells and that it is potentiated by increasing telomere length. This suggests that the expression of genes near telomeric DNA may alter as the telomere shortens, providing a potential mechanism as to how cell senescence may be triggered by telomere attrition. However, to date, no culprit genes have been identified to support this theory.

A final proposed mechanism for telomere induced senescence is the erosion of 3'G rich single stranded overhangs. Whereas telomere length decreases progressively with population doubling, the 3'G rich single stranded overhang remains relatively conserved until declining rapidly as the cell approaches senescence (105). Further

evidence that cell senescence is governed by mechanisms other than critically short telomere length is the finding that upregulation of certain telomere binding proteins (such as TRF) can delay the onset of senescence by lowering the TL setpoint at which senescence is induced (106).

1.4.4 Non-telomere dependent mechanisms of cell senescence

In addition to replicative senescence induced by telomere attrition, it is accepted that senescence can also be triggered by non-telomeric pathways. Processes that cause DNA damage or activate proliferative pathways can also induce senescence by triggering a DDR. Such induction of senescence acts as a tumour suppressor mechanism. Oncogene activation is a hallmark of cancer but in normal cells, oncogene activation triggers cell senescence (107). As with replicative senescence, oncogene induced senescence is triggered via the formation of a DDR. However, the mechanisms by which this occurs are not yet understood.

1.5 The role of DNA methylation in cell senescence

1.5.1 Introduction to DNA methylation

DNA methylation (DNAm) is one of several epigenetic phenomena. Epigenetics refers to functional modifications to the genetic code that do not alter the base nucleotide sequence. Such modifications can switch genes on or off and thus determine which proteins are transcribed and include DNA methylation, histone modification, non-coding RNA and RNA splicing variants. DNAm is a post-translational process in which

a methyl group is covalently added to fifth position of the cytosine pyrimidine ring within DNA. In mammalian cells, DNAm almost exclusively occurs in the context of CG dinucleotides, referred to as CpG sites (i.e. where a cytosine is followed by a guanine). CpG sites are concentrated in large clusters, termed CpG islands, and are often found in gene promoter regions (108). Whilst the majority of CpG sites in non-promotor regions are methylated, CpG islands are usually hypomethylated (109).

1.5.2 DNA methylation, gene expression and disease

The effect of DNA methylation is to inhibit transcription either directly via methyl groups projecting into the major groove of the DNA helix or indirectly by the recruitment of DNA binding proteins (110, 111). Changes in DNA methylation have been shown to alter gene expression by several mechanisms. Hypermethylation at CpG island promotor sites may result in gene silencing. This mechanism has been well documented in the setting of carcinogenesis due to the silencing of tumour-suppressor genes, allelic loss or genetic mutation (112). The role of DNA methylation at non-CpG island promoters is less well understood, with methylation still able to alter gene expression even in genes without CpG islands in their promotor region (113). Global hypomethylation at non-gene promotor sites can result in the loss of transcriptional inhibition, resulting in the aberrant and potentially harmful expression of normally silenced genes. As such, methylation status has the potential to alter gene expression independently of the underlying genetic code.

Several processes can influence DNA methylation including environmental factors. Fraga *et al* (114) studied monozygotic twins with identical genotypes and found that although they are epigenetically indistinguishable when young, as they aged, they displayed increasing variability in their epigenetic signatures both in terms of DNAm and histone acetylation. Methylation driven alterations in gene expression as a result of environmental stimuli provide a possible explanation for the link between genotype and phenotype. Furthermore, if such alterations occur within the germline then they have the potential to be passed directly onto the subsequent generations. As such, epigenetic modifications such as DNA methylation provide a potential mechanism for environmental risk factors to alter gene expressions and contribute to the pathogenesis of disease. Disease processes that are triggered by such mechanisms include cancer and cardiovascular disease (115, 116). DNA methylation is also thought to play a role in the aging process and the development of cellular senescence.

1.5.3 DNA methylation and cellular senescence

DNAm is heavily implicated in cellular senescence (117). Studies have identified patterns of methylation that correlate with cell senescence. Koch *et al* (77) demonstrated 6 specific CpG sites that correlated closely with cellular senescence in regard to the number of passages, population doublings, or days of in-vitro culture. Whilst these epigenetic patterns for senescence correlate well with those of aging, they are not identical (118). This suggests that cell senescence is not just a hallmark of the aging process but that it can be altered by underlying molecular processes,

including DNA methylation. In this thesis, the DNA methylation status of patients undergoing cardiac surgery in the context of both cardiovascular disease and renal ischaemic injury will be investigated.

1.6 Cell senescence, aging and disease

Since the turn of the century, cardiovascular disease (CVD) has topped the World Health Organisation list as the single biggest cause of death in the world. A number of established risk factors exist for the development of CVD. These are traditionally classified as modifiable such as hypertension, hypercholesterolaemia, smoking, diabetes and obesity, or non-modifiable such as age, sex and ethnicity. However, the high prevalence of CVD cannot always be attributed to these risk factors. As a result, the search for novel predictors of cardiovascular disease is ongoing. As CVD is an age-related condition, mechanisms of aging and cell senescence have been postulated as having key roles in its pathogenesis.

1.6.1 Telomere biology and cardiovascular disease

Ever since 1990 when Harley *et al* proposed that reduced telomere length is related to the aging process, telomere shortening has been linked to age related disease processes (119). Cawthon *et al* (120) showed that overall mortality was associated with short telomere lengths in people over the age of 60 and there is a growing body of evidence linking telomere attrition with cardiovascular disease, neurodegenerative disease, and cancer (121),(122),(123). Since telomerase functions

to maintain telomere length, reduced telomerase activity is also thought to be implicated in the development of age-related diseases. In this thesis, we will focus on the role of cellular senescence and Telomere biology in cardiovascular disease, and CSA-AKI.

Telomere biology has been associated with several age related cardiovascular disease processes including atherosclerosis (124), ventricular diastolic dysfunction (125), coronary artery calcification (126), calcific aortic stenosis (127) and prognosis following acute coronary syndrome (128). Several theories have been postulated for mechanisms underlying these associations. The 'Telomere hypothesis' states that short telomeres are the primary abnormality responsible for the subsequent development of disease. This hypothesis is supported by the findings of Brouillette *et al* (129) that the offspring of patients with coronary artery disease have shorter telomeres than matched controls prior to the onset of any disease. This theory states that genetically determined short telomere length (TL) predisposes to the development of atherosclerosis and such an association has been found in several studies (124). This theory is further supported by the finding of reduced TL in vascular smooth muscle cells taken from atherosclerotic plaques of patients with coronary artery disease (CAD) (130). However, there is conflicting evidence as to the causal role of short telomeres in CAD with de Meyer *et al* (131) demonstrating no association between TL and pre-clinical atherosclerosis in carotid and femoral vessels. Furthermore, in a second study De Meyer *et al* (132) found no association between TL and the development of atherosclerosis in a repeat of Brouillette's

experiment. These findings cast doubts over the validity of the telomere hypothesis of cardiovascular disease.

An alternative 'modulating effects' hypothesis suggests that rather than inherited TL predisposing to cardiovascular disease it is the effect of modulating environmental factors on telomere attrition that is responsible (133). Several cardiovascular risk factors have been found to be associated with short TL including smoking, diabetes, hypercholesterolaemia, hypertension, physical inactivity and obesity (134-137). TL is thought to be associated with these risk factors due to increased inflammation, oxidative stress, and factors that modulate the activity of telomerase. Inflammation is associated with increased cell proliferation and hence increased telomere attrition in somatic cells due to their low telomerase activity. Oxidative stress results in the formation of single stranded breaks, preferentially at the telomeres, causing accelerated telomere attrition at the next cell division (134, 138).

A competing hypothesis for a telomeric predisposition for cardiovascular disease is the immunosenescence theory. This theory states that in patients with either inherited reduced TL or environmentally accelerated telomere attrition, critical telomere shortening causes haematopoietic progenitors to become senescent. Early senescence of endothelial progenitor cells (EPC's) results in reduced vascular endothelial repair mechanisms and increased atherosclerosis (133). Hammadah *et al* (139) set to test this hypothesis by measuring the effect of TL and number of circulating progenitor cells (CD34+ cells) on outcomes in patients with coronary artery disease. They found both TL and CD34+ cell number to be independent and

additive risk factors for cardiovascular events. The same mechanism of increased haematopoietic senescence has been attributed to the association of anaemia with short telomeres in setting of chronic heart failure (140).

In summary, no single theory has yet been able to fully explain all aspects of the associations so far demonstrated between telomere length and the development of cardiovascular disease. Whilst there may be a predisposition to cardiovascular disease due to inherited short telomere length, this mechanism does not appear to be via the development of atherosclerosis. There is convincing evidence that environmental factors modulating the rate of telomere shortening play a crucial role in disease, and a growing body of evidence that the early senescence of haematopoietic and endothelial progenitor cells might also have an important role to play.

1.6.3 Telomere biology and AKI

Westhoff *et al* (141) performed a detailed analysis of the potential mechanisms by which increased cell senescence might cause renal impairment in mice. Using a TERC knock out mice model the authors simulate the short telomere lengths seen in the aging kidney due to the loss of functional telomerase activity. They demonstrated that critical telomere shortening is associated with reduced structural and functional integrity of the kidney in response to ischaemia reperfusion injury (IRI). TERC negative mice developed more marked reduction in Creatinine Clearance, increased interstitial fibrosis at 30 days and a lack of compensatory hypertrophy of the non-

injured kidney. In addition, they identify several markers of cell senescence that are upregulated in response to critically short telomeres and IRI including p21, p53 and p16 with downregulation of the proliferation marker Ki67. Cheng *et al* (89) demonstrated similar findings in both TERC and TERT knock out mice, demonstrating that the knock outs displayed delayed recovery following IRI compared to wild type mice. They also showed a similar upregulation of P16 and delayed expression of Ki67 in response to IRI.

To date, no clinical studies have examined telomere biology and the development of AKI in humans. The animal studies outlined above are based on ischaemic models of AKI.

1.6.4 DNA Methylation and cardiovascular disease

The role of DNA methylation in the pathophysiology of cardiovascular disease (CVD) is not yet well understood. Altered DNA methylation in CVD could be due to changes in methylation associated with the classical cardiovascular risk factors such as age, sex, smoking and diabetes or with the underlying disease mechanisms such as atherosclerosis. Zhang *et al* (116) reviewed the topic in 2016 and concluded that the relationship between DNAm, cardiovascular disease and its associated risk factors is complicated with different studies reporting conflicting results. For example, the development of atherosclerosis, the underlying pathology in the majority of CVD, has been shown to be associated with both global hypo- and hypermethylation. Early studies demonstrated global DNA hypomethylation associated with atheroma

formation in APOE $-/-$ mice both in PBMC and aortic tissue prior to the onset of atheroma (142). Similar findings of global DNA hypomethylation were described by Hiltunen *et al* (143) both in advanced human atherosclerotic lesions and in APOE $-/-$ mice. They also described genomic hypomethylation in rabbits following intimal hyperplasia induced by balloon denudation of the aorta. Global hypomethylation was also demonstrated in a rabbit model of atherosclerotic aortas (144) as well as in peripheral leukocytes in patients with vascular disease compared to normal controls (145). However, more recent papers by Stenvinkel *et al* (146) and Kim *et al* (147) have demonstrated that global DNA hypermethylation in peripheral blood leukocytes is associated with the development of CVD. Even Lund's earlier work, although reporting global DNA hypomethylation in APOE $-/-$ mice, demonstrated hypermethylation of the human monocytic-macrophage cell line in response to Atherogenic lipoprotein profiles. Such cells were found to be present in the aorta prior to the onset of atherosclerosis suggesting that changes in DNA methylation may be a causal factor in the development of atheroma.

Zhang *et al* (116) suggest that a potential cause of these conflicting results lies in the fact that the studies measured different markers of global methylation status and did so using a variety of techniques. Furthermore, analyses were performed in different tissues. An alternative explanation is that the effect of DNA methylation may be variable overtime and a state of global hypomethylation does not preclude the later development of hypermethylation in CVD.

In addition to atherosclerosis, differential DNAm has been demonstrated in diabetes, hyperlipidemia, homocysteinuria, female gender, BMI, and smoking. For example, Tsaprounis *et al* (148) demonstrated lower DNA methylation levels in smokers compared to non-smokers, which may contribute to their predisposition to CVD. Interestingly, this effect was partially reversible on cessation of smoking for 3 months or more.

1.6.5 DNA Methylation studies and AKI

Several studies have demonstrated that DNA methylation status can be altered in response to AKI. In 2006, Pratt *et al* (149) reported altered DNAm status in rats following ischaemia/reperfusion injury (I/RP injury). However, it should be noted that this study only investigated methylation status at a single CpG site within the promoter region of the C3 gene, and the degree of I/RP injury was severe with 24 hours of cold ischaemia followed by 2 hours reperfusion in an ex-vivo circuit. Subsequently, both hypo- and hypermethylation of several promoter site CpG's have been proposed as biomarkers of AKI. Endo *et al* (150) report an association between increased levels of unmethylated DNA in the promoter region of Slc22a12, a urate transporter in proximal tubule cells, and acute kidney cortical necrosis. Furthermore, Huang *et al* (151) showed that there was a global reduction in DNA hydroxymethylation in the kidneys of mice with I/RP injury. Conversely, hypermethylation of CpG's of the promoter region of Kallikrein (KLK1) was seen in patients with established AKI versus healthy controls (152).

Whilst the above studies demonstrate that DNA methylation is altered in response to AKI or renal I/RP injury, they tell us little about the nature or mechanism of the association and further study is needed. Furthermore, whilst such changes may be useful in the early detection of AKI once the insult has occurred it does not allow us to predict a person's susceptibility to AKI prior to its onset. The current study aims to establish whether DNA methylation changes indicative of increased biological age and cellular senescence can predict the onset of CSA-AKI.

1.7 Summary of Hypothesis

We propose that patients with increased cellular senescence and a reduced ability for tissue regeneration are more susceptible to ischaemia-induced AKI and predisposed to reduced long-term survival. To test this hypothesis, we will study telomere biology and DNA methylation in patients undergoing cardiac surgery and compare those who develop AKI with those who do not. This population will also be followed up for the development of the primary endpoints of CKD and death.

CHAPTER 2: Aims

2.1 Aims of Mean Telomere Length analysis experiment

1. To determine if mean telomere length is associated with the development of cardiac surgery associated-acute kidney injury (CSA-AKI)

2.2 Aims of STELA experiment

The aims of this pilot study were 2-fold;

1. To determine if an alternative method of telomere length measurement was associated with the development of CSA-AKI.
2. To investigate the correlation in mean Telomere length measurement between STELA and qPCR performed on the same samples.

2.3 Aims of DNA methylation experiment

1. To correlate predetermined methylation signatures for aging and cellular senescence with the development of CSA-AKI.

CHAPTER 3: Methods: Clinical study

3.1 Study Overview

A single-center prospective cohort study was performed at Barts Heart Centre, London. Pre-operative blood tests were taken and processed to acquire DNA and RNA for subsequent analysis. Pre-operative baseline plasma, serum and urine were also collected. In a subset of patients, serum and urine samples were collected on the first post-operative day to allow for testing of novel renal biomarkers and markers of inflammation.

3.2 Study Objectives

The primary objective of this study was to investigate whether pre-operative markers of cell senescence could be used to predict the development of CSA-AKI.

3.3 Sample size

We aimed to recruit 50 cases of CSA-AKI for the primary analysis. From a review of the literature, the prevalence of AKI following cardiac surgery was estimated to be approximately 10-20%. As such it was estimated that 250 and 500 patients would need to be recruited to provide the required number of 50 in the AKI cohort. As the protocol requires minimal patient intervention/participation, a high drop-out rate was not envisaged. Accordingly, no correction in study numbers has been made for this.

3.4 Study duration

It was expected that the study would take between 12 and 18 months to recruit. In reality 254 patients (55 AKI cohort) were recruited between 27/1/16 and 28/9/16. Unfortunately, due to a sample processing error, 35 samples were found to have insufficient DNA for downstream processing. In 8 of these cases, DNA was successfully obtained after re-extraction. However, between 30/1/17 and 7/4/17 a further 27 patients had to be recruited to replace the inadequate samples.

3.5 Patient Recruitment

The study aimed to enroll the majority of patients undergoing cardiac surgery at Barts Health. As such the exclusion criteria were minimal. This was to allow the recruitment of a large number of patients and improve our ability to find trends in a heterogenous population of patients and surgical procedures.

3.5.1 Inclusion criteria:

- Patients undergoing cardiac surgery at Barts Heart Centre

3.5.2 Exclusion criteria

- Patients with renal transplant
- Patients on renal dialysis
- Patients unable to give informed consent.
- Patients already recruited into other trials

3.5.3 Timing of Recruitment

Elective patients were recruited on the evening prior to their surgery. If patients were to be operated in the afternoon they were sometimes consented on the day of surgery if there was sufficient time to allow the patient to consider their participation. We set this time period at no less than 2 hours. Potentially suitable patients were identified by review of the operating theatre schedule.

Urgent and emergency patients were recruited either on the evening prior to surgery or the morning of their surgery. However, all patients were given a minimum of 2 hours to consider their participation.

3.6 Informed Consent

All patients recruited to the study were given a typed Patient Information Sheet (PIS) outlining what their participation involved and the potential risks and the benefits. The PIS and consent form are shown in *Appendix A*. A patient's capacity to give informed consent was based on the clinical team's judgement when consenting the patient for surgery. If a patient was deemed to have capacity to consent for their cardiac surgical procedure, they were also assumed to have capacity to give informed consent for trial participation.

3.7 Criteria for discontinuation

A patient's involvement in the current study ended if either of the following criteria were met;

1. At 7 days post- operatively.
2. The patient was discharged from the hospital during the study period
3. The patient died
4. The patient withdrew consent for further participation

3.8 Data Collection

3.8.1 Protocol for data collection

The protocol for data collection is show in *Figure 3*.

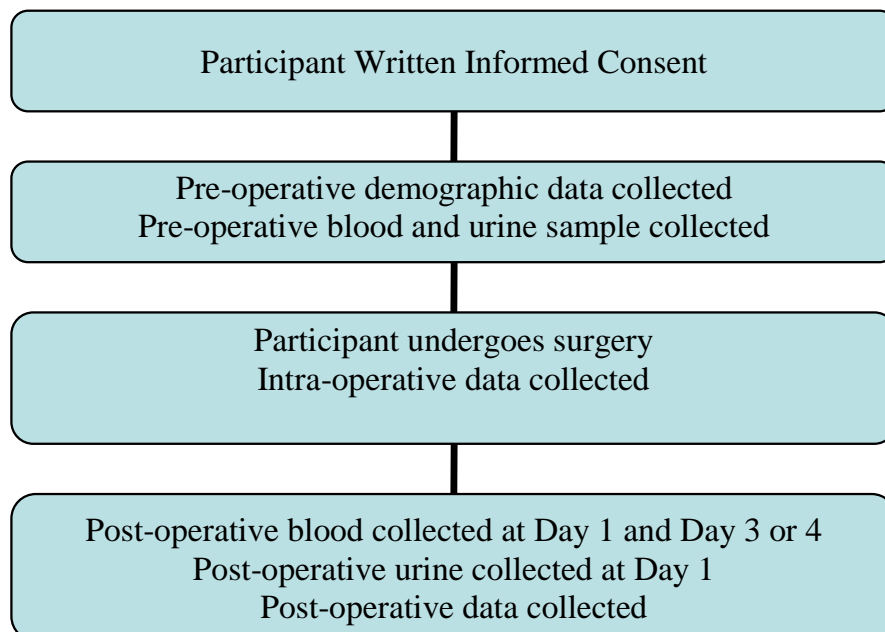


Figure 3: Flow chart demonstrating the procedure for study data collection

• **Pre-operatively:** Venous blood and urine sample were taken for baseline values of renal biomarkers and markers of inflammation. Pre-operative demographic and clinical data was recorded. The included fields were: Admission date; Recruitment date; Procedure Date; Age; Gender; Ethnicity; Height; Weight; Pre-operative angina status; Number of previous MI; Previous PCI; Previous cardiac surgery; History of malignancy; Diabetes; Hypertension; Hypercholesterolaemia; Smoking history; Renal disease; Pulmonary disease; Neurological impairment; Extracardiac arteriopathy; Pre-operative heart rhythm; extent of coronary artery disease; Left main stem disease; Pre-operative Angiotensin Converting Enzyme (ACE) inhibitor use; Pre-operative statin use; Pre-operative Diuretic use; Left ventricular function. Pre-operative white blood cell count (WCC); Preoperative Haemoglobin; Pre-operative International normalised ratio (INR); Activated Partial Thromboplastin Time (APTT)

• **Intra-operatively:** Routine intra-operative clinical data was recorded. The included fields were: Operative urgency; Operation type; Procedure Date; Cardiopulmonary bypass time; Aortic cross-clamp time

• **Post-operatively:** Blood and urine samples were collated on day 1 post-operatively. This blood was taken at 0900 hours regardless of the patient's time of surgery. This means that this day 1 sample is taken at approximately 15 – 20 hours post-operatively depending on whether the patient was operated in the morning or afternoon. However, it was decided that morning blood sampling represents real world practice and a useful biomarker would need to be able to

distinguish between risk of AKI and no risk of AKI for samples taken anywhere from 12-24 hours post-operatively. Further blood samples were taken on day 3 or 4 post-operatively for renal function. If any additional bloods were performed by the clinical team in the first 7 days, the renal function results were also noted. Post-operatively, clinical data was recorded including; Extubation date; Vasopressor discontinued date; Inotropes discontinued date; 1st haemoglobin in intensive care unit (ITU); Urine output in 1st 12 hours; Reoperation; Blood transfusion in ITU; Clotting products given; New Atrial Fibrillation (AF); Day of onset of AF; Pharmacology for treatment of AF; AF resolved prior to discharge; Post-operative Ileus; Respiratory tract infection; Sternal wound infection; Harvest site wound infection; Neurological dysfunction; New Stroke; Myocardial Ischaemia; repeat revascularisation; Date of discharge; length of stay; CRP on post-operative days 1, 2, and 3; Mortality at discharge; Mortality at 1 year follow up.

3.9 Specimen Sample Collection

3.9.1 Blood sampling

A total of 14.5 millilitres (mls) of blood was taken from the patient pre-operatively.

This was stored as;

- 2x Full blood count = 8 mls
- 1x Serum-separating tube (SST) = 4 mls
- 1x PAXgene RNA tubes = 2.5 mls

A further SST was taken on the first post-operative day. The results were documented of all renal function tests taken in the early post-operative period (1-7 days) as part of the patient's routine post-operative care. These were done at a minimum frequency of every 2 days and processed by the hospital laboratory.

3.9.2 Urine sampling

8mls of urine were taken from each patient pre-operatively via a mid-stream urine sample or directly from the catheter port at time of catheter insertion in surgery. A further 8mls were taken on the first post-operative day directly from the catheter bag. No urine was sampled from the urine collection bag.

3.10 Ethical Approval and Trial Registration

The study was sponsored by Queen Mary University of London (QMUL). Final Research and Development (R&D) approval was provided by the Joint Research Management Office of QMUL and Barts Health NHS Trust (Reference: 010706). Research Ethics Committee (REC) board approval was granted by London-Queen Square Research Ethics Committee. (REC Number: 15/LO/1741). The trial was registered with clinicaltrials.gov (Registration number: NCT02692833). The relevant documentation for sponsorship and R&D and ethical approvals is listed in *Appendix A*.

3.11 Study Populations and Statistical Analyses

The current studies were performed as case control studies with cases being defined by the outcome of CSA-AKI or mortality. As such associated risk factors were defined with Odd's ratio's and 95% confidence intervals generated by binary logistical regression. Univariate and multivariate analyses were performed with binary logistical regression with mTL and DNA methylation age as independent variables and development of AKI as the binary dependent variable. Further analyses were performed in which mTL and DNA methylation age were treated as an interval, non-normally distributed dependent variables and clinical parameters used as independent variables. For continuous independent variables Spearman's rho correlation was used. For categorical independent variables, the Mann-Whitney U test was used for variables with 2 levels and the Kruskal-Wallis test for variables with more than 2 levels.

A propensity score analysis was performed to match cases and controls for all significant determinants of AKI other than mTL. The propensity matching was performed by Dr Gabriella Captur (Cardiology Registrar, St Bartholomew's Hospital; using 'R' statistical software). Multiple logistical regression with 1:1 nearest neighbour matching was used to develop the propensity score with the development of CSA-AKI as the dependent variable. Factors entered into the model were based on well documented predictors of AKI from the literature and included age, gender, ethnicity, BMI, type of operation, diabetes; pre-op LV function, Pre-operative AF, Pre-op creatinine; Bypass time and Logistic EuroSCORE.

All continuous variables were tested for normality with the Shapiro-Wilks test. P-values of <0.05 were considered as significant. Analyses were performed using SPSS Version 22 and R version 3.0.1 for propensity matching.

CHAPTER 4: Methods: Laboratory

4.1 Rationale of chosen methodology for Telomere length measurement

4.1.1 Introduction

Telomere length (TL) can be measured by several different methods. The suitability of any one method is dependent on a number of factors including the raw material available, the accuracy of the measurements required, and the resources available (153). Different methods that have been utilised to measure TL include terminal restriction fragment (TRF) length analysis, polymerase chain reaction (PCR) based techniques, and fluorescent in-situ hybridisation (FISH) techniques.

4.1.2 Terminal restriction fragment (TRF) analysis

The first method used to quantify TL was TRF analysis by Southern blotting. As such, it has been used to validate subsequent methods of TL measurement that have been developed and is therefore considered the gold standard technique. In brief, the technique uses restriction enzymes to digest genomic DNA in a way that excludes the telomeric sequences, resulting in short fragments of genomic DNA and the longer uncut telomeres. The digestion products are then visualised using Southern blotting or by in-gel hybridisation using a probe specific for telomeric DNA (154). The resulting DNA is seen as a smear due to the variable telomere lengths between chromosomes and between different cells of the same individual. The length of this smear as well as the signal intensity are used to calculate an average telomere length for the sample. The advantages of this technique are that it has good reliability and provides

an absolute rather than a relative measure of TL. Despite this, comparisons of TL measured by TRF analysis are not necessarily comparable across different studies due to differences in restriction enzymes used. Different restriction enzymes differ in the average distance from the last available restriction site to the start of the true telomeric repeats. This means that both the length of the telomeric region and a variable portion of the sub-telomeric region are included in the measure for mean TL (mTL). The degree of variation cannot be measured and is an inherent source of error in measuring TL length by TRF analysis. Other drawbacks of the TRF technique is that it requires large amounts of input DNA and is relatively expensive and time consuming to perform in comparison to other techniques such as qPCR.

4.1.3 Quantitative polymerase chain reaction (qPCR)

Q-PCR involves labelling the target DNA of interest with a fluorescent probe and then amplifying it by PCR. A standard curve generated by serial dilution of a standard of known concentration is run in the same reaction allowing for quantification of the unknown samples (*Figure 4*). Initial attempts to measure TL by qPCR using oligonucleotide primers designed to hybridise to the TTAGGG and CCCTTA repeats failed due to the formation of only primer dimer products. In 2002, Cawthon *et al's* (155) landmark paper described a method of measuring relative mean telomere length using a primer pair that anneal to both the 3' and 5' ends of the Telomere but have mismatches along their length preventing primer-dimer formation. This method determines relative mean telomere length by calculating the factor by which each experimental DNA sample differs from a reference DNA sample in its ratio of

telomere repeat copy number to single copy gene (SCG) copy number. This ratio, termed the Telomere/SCG (T/S) ratio, should be proportional to the mean telomere length of the experimental samples. This original 2002 protocol is the method most frequently used by investigators to measure mTL. The reasons for this are that it allows high throughput of samples as PCR cyclers commonly measure 96 samples or 384 samples in a single run. It is also relatively cheap to run but does require expensive PCR cycling equipment. However, qPCR is limited in terms of its tendency to produce variation between 'batches' of samples and therefore experimenters must ensure that appropriate measures are taken to account for inter-and intra-assay variability. Similar to TRF analysis, qPCR is limited in that it only measures mean TL and gives no information about individual short telomeres or chromosomal ends lacking a telomere (156). One of the main sources of variation in Cawthon's original 2002 protocol was variation due to pipetting errors in loading the reactions in separate Telomere (T) and Standards (S) wells/tubes. Cawthon later modified his own technique to allow both the telomere and SCG reactions to be run in the same reaction tube, thus eliminating this particular source of error. This technique is termed monochrome multiplex quantitative PCR reaction (MMqPCR)(157).

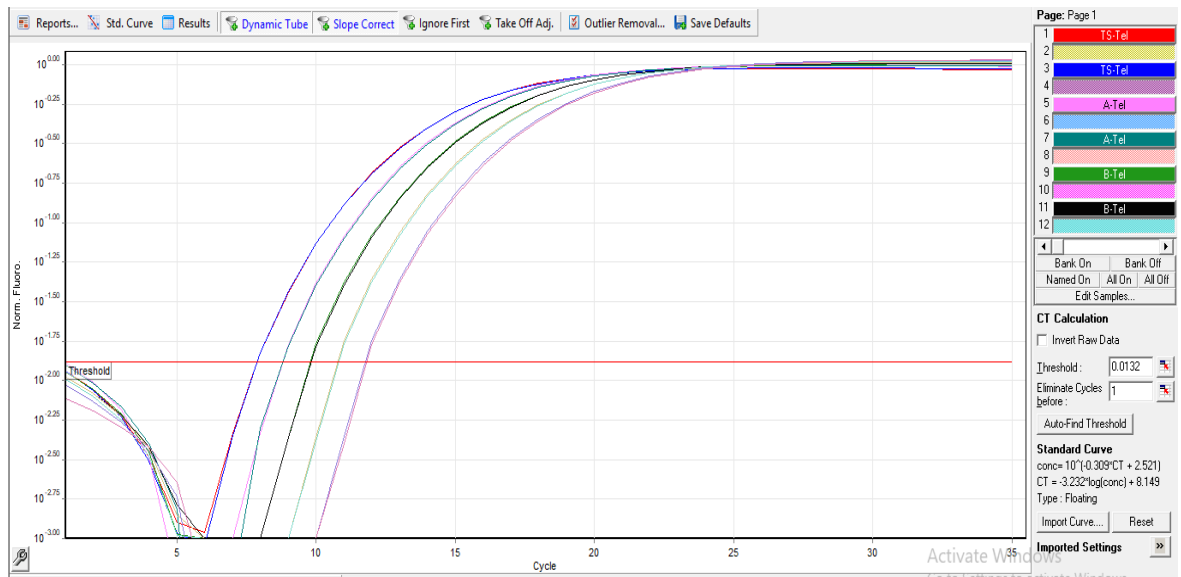


Figure 4: PCR output showing successful quantification of a 5-point standard curve for the Telomere Reaction run in duplicate.

A further modification to the qPCR method of Telomere length analysis was developed by O'Callaghan *et al* (158) aimed at allowing absolute rather than relative quantification of TL. To do this the original qPCR TL protocol was modified to use reference samples of known lengths. These lengths were 84 base pairs for the telomere reaction and 75 base pairs for the single copy gene with the telomere standard comprising 14 copies of the TTAGGG repeat.

4.1.4 Short Telomere Length Analysis (STELA)

A common limitation of both TRF analysis and qPCR is that they are only able to provide a measure of mean telomere length and provide no information of the length of the shortest telomeres, a factor that is thought to be central to the induction of senescence (101). To address this problem, Baird *et al* (159) modified the qPCR singleplex protocol to allow single telomere length analysis (STELA) from a subset of chromosomes. The technique relies on annealing a 6-base-pair 'telorette' (TTAGGG)

with a 20-nucleotide non-complementary tail to the G-rich 3' overhang. In a second step, the telorette is ligated to the 5' end of the complementary C-rich strand of the chromosome, which effectively tags the end of the telomere with the non-complementary telorette tail. PCR is then performed with a primer that matches this tail together with a chromosome specific upstream primer located in the sub-telomeric region. The main problem with this method is that not all chromosomes have sub-telomeric sequences suitable for primer design. As such, traditional STELA is limited to a small number of chromosomes only and STELA is primarily performed on the XpYp telomere (160). Following PCR, the reaction products are serially diluted and resolved by Southern blotting to determine individual telomere lengths (*Figure 5*).

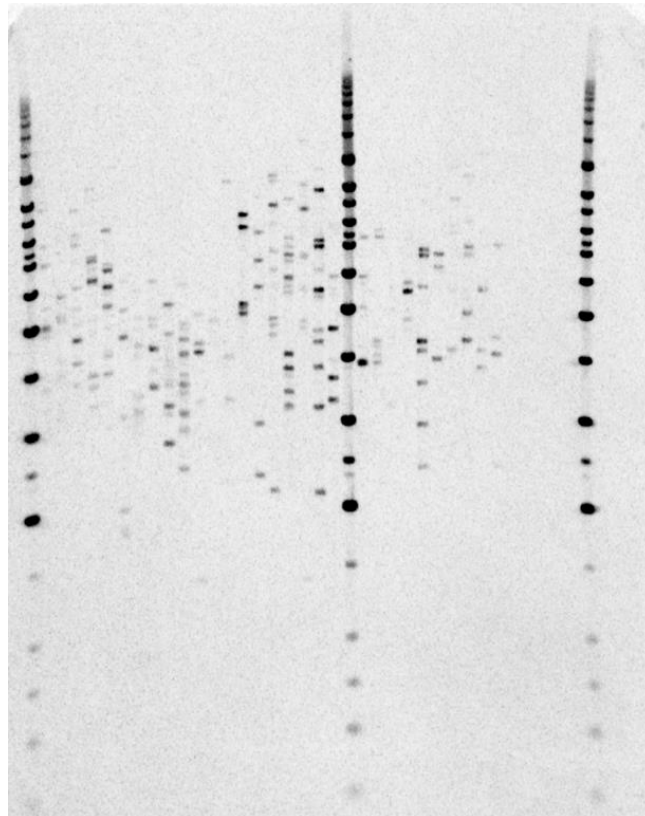


Figure 5: XpYp STELA. Following telomere specific PCR, the products are separated by Southern Blotting. On serial dilution, the TRF-like smear resolves to individual Telomeres from which the shortest telomere length can be derived.

Finally, a novel method termed universal-STELA (U-STELA) was developed by Bendix *et al* (161) and allows the length of individual telomeres to be measured regardless of position. This is achieved using restriction enzymes to cleave the DNA into short genomic fragments and intact telomeres as in TRF analysis. PCR is then performed using specialised oligonucleotides that are annealed to either end of both the genomic fragments and the telomeric DNA. In brief, the oligonucleotides annealed to the genomic fragments are designed in such a way as to bind to themselves once the double stranded fragments dissociate at the start of PCR. Meanwhile the oligonucleotide sequences annealed to either end of the telomeric DNA are designed to promote the binding of telomere specific primers and facilitate amplification. Therefore, the individual telomeres are selectively amplified. Finally, the PCR products are visualised by Southern blotting. The disadvantages of STELA are that it is highly labour intensive and technically challenging to perform and is less able to measure long telomere lengths.

4.1.5 Quantitative fluorescence in-situ hybridisation (Q-FISH)

Q-FISH for TL measurement was first described by Landorp *et al* (162) in 1996, and visualises telomeres by hybridisation using a probe for the telomeric repeat sequence (CCCTAA)₃. It therefore allows an estimation of the size of all 92 telomeres within the genome, unlike TRF or qPCR analysis. It is also able to identify telomere free chromosome ends. A crucial difference between Q-FISH and the methods of TL measurement outlined above is that it requires intact cells rather than DNA for the substrate of the reaction, in order to visualise the chromosomes in metaphase. A

limitation of the technique is that it cannot be used to measure TL in cells that are no longer dividing. This limits its use in large clinical studies where such cells are rarely available. It is also time consuming, labour intensive, and requires specialist equipment and knowledge of chromosomal banding patterns (156).

Flow-FISH is an adaptation of q-FISH which combines flow-cytometry with the hybridisation of telomere binding probes in solution. The use of flow cytometry allows for high throughput analysis and can also allow specific subpopulations of cells to be identified. As such it is particularly useful in measuring TL in hemopoietic cells (153). However, there are several disadvantages associated with its use. Non-fixed cells are difficult to work with due to issues such as fragility and clumping, and the technique is sensitive to reagents used to preserve cells. Also, as with qPCR and TRF analysis, only a measure of mean TL is produced with no data provided on individual telomere lengths.

4.1.6 Rationale for selecting qPCR as the primary method of TL measurement

In the current study, we elected to perform TL measurement by singleplex qPCR. As the substrate for our experiments is stored frozen DNA we are unable to perform FISH, which requires intact dividing cells. Whilst the TRF method is often considered the gold-standard for TL measurement, the numbers of patients in the current study (~250) would have made using this technique extremely time consuming. There is also the issue that the TRF method may lack precision as it measures an undefined portion of the sub-telomeric region in addition to the telomeric DNA. As such, qPCR

was chosen as the method of TL measurement as it is relatively cheap, easier to perform on large numbers of samples, and well established in the literature. Cawthon's original singleplex protocol was chosen over MMqPCR as it was felt that the additional complexity of this technique did not merit the improved precision reported with the singleplex and multiplex qPCR showing strong correlation in the measurement of mean TL (163). However, several modifications were made to this original protocol to optimise the results to our specific samples and laboratory equipment (See section 4.4.6).

4.2 Measuring DNA methylation signatures of aging and cellular senescence

Alterations in DNA methylation have been implicated in both aging and cellular senescence. Several studies have developed epigenetic clocks to predict chronological age based on the methylation status of age-linked CpG probes (76, 164). Furthermore, deviation of this predicted methylation age (pMA) away from the true chronological age has been used as a measure of 'biological age' to predict all-cause mortality (165). The first study to attempt to develop an epigenetic signature for aging was published by Koch *et al* in 2011 (166). This model was based on just 5 CpG sites and achieved a correlation between predicted and chronological age of 0.64 with an average precision of +/- 12.7 years.

In 2013, both Horvath and Hannum published their epigenetic clocks. Horvath (164) obtained DNA methylation data from several publicly available databases. This model was based on methylation at 353 CpG sites and was highly accurate across a range of tissues. Correlation with predicted age was 0.96 across all tissues with a mean absolute error (MAE) of 3.6 years when tested against a validation subset. In the same year, Hannum *et al* (76) published their genetic clock based on 71 CpG sites. This signature was developed from a derivation population of 656 individuals based on DNA derived from peripheral blood. This signature predicted chronological age in a validation cohort of 174 subjects with an R value of 0.91 and root mean squared error (RMSE) of 4.9 years. Interestingly, only 5 CpG sites overlapped between the epigenetic clocks of Horvath and Hannum.

In 2016, Weidner *et al* (167) produced an alternative epigenetic clock based on just 3 CpG sites. 102 age-associated CpG sites were identified from pooled DNA methylation data from 4 studies which used the Human-Methylation27 BeadChip platform (Illumina, San Diego, CA, USA). An epigenetic clock based on all 102 sites predicted chronological age with an R value of 0.98 and an RMSE of 4.26 years. When just the top 3 CpG sites were measured in a second independent population of 82 blood samples, chronological age was predicted with an RMSE of 7.3 years.

Finally, in 2018, Levine *et al* (168) published the PhenoAge clock. This clock combined DNA methylation data from 513 individuals together with clinical data to generate a measure of 'phenotypic age'. DNA PhenoAge was then correlated with chronological age ($R = 0.71$) and a range of clinical outcomes. PhenoAge was able to predict the onset of several age-related disease processes including all-cause mortality, cancers, health span, physical functioning, and Alzheimer's disease.

Of the 5 epigenetic clocks described above, Horvath's and Hannum's are the most accurate. Hannum's also has the advantage of being derived solely from DNA harvested from peripheral blood and from only 71 CpG sites rather than 353. As such, Hannum *et al*'s 71 CpG epigenetic clock was chosen as a marker of in the current experiment.

Koch *et al* (77) demonstrated an epigenetic signature for cellular senescence based on alterations in methylation at 6 CpG sites. This signature was derived from 51 samples of known passage number using the Human-Methylation27 BeadChip. These

51 samples were derived from a range of tissues. Combination of the 6 CpG sites enabled reliable estimations of passage numbers in fibroblasts and mesenchymal stem cells (MSC) ($R^2 = 0.90$; MAE = 3).

This thesis aims to correlate the methylation signature for aging described by Hannum and the methylation signature for senescence described by Koch, with outcomes after cardiac surgery. The primary outcome is the development of CSA-AKI, and secondary outcomes are in-hospital and 1-year mortality.

4.3 Sample processing

4.3.1 Immediate sample processing

All blood samples were processed at 30 minutes from time of collection. The PAXgene tubes were mixed by inversion and then frozen at $-20\text{ }^{\circ}\text{C}$ for long term storage. The technical information provided with the PAXgene system quotes that samples can be stored for 8 years in this state (169). The remaining samples were centrifuged at 4000 revolutions per minute (rpm) for 10 minutes and aliquoted into plasma, buffy coat and serum. These aliquots were then stored at $-80\text{ }^{\circ}\text{C}$ for subsequent analysis. Urine samples were aliquoted into 2ml cryovials and stored at $-80\text{ }^{\circ}\text{C}$.

4.3.2 Sample storage

PAXgene RNA tubes were stored in $-20\text{ }^{\circ}\text{C}$ freezers in the department of Translational Medicine at the William Harvey Research Institute (WHRI). The aliquoted samples of

urine, plasma, serum, and buffy coat were stored in -80 °C freezers at the Heart Centre, WHRI.

4.3.3 DNA extraction

DNA was extracted from frozen buffy coat using the EZ1 DNA blood 350µl kit and the Biorobot EZ1 containing a buffy coat card (Qiagen, Germany). The Biorobot is able to process 6 samples per run over a 20-minute time period. The automated process extracts DNA using magnetic particle technology. Cells are lysed allowing DNA to bind to the silica surface of magnetic particles. The particles are then separated from the lysates using a magnet, and finally the DNA is washed off the surface of the beads and eluted in a volume of 200µl. In brief, frozen buffy coat was thawed and mixed by retro-pipetting several times. For each sample, 300 µl of buffy coat was placed in a 1.5ml reaction tube and placed in the Biorobot together with a cartridge from the EZ1 DNA kit, a specialised pipette tip and holder, and a 1.5ml elution tube. The final eluted volume of 200µl was aliquoted into 1x120µl and 4x20µl aliquots and stored at -20 °C for subsequent analysis. Prior to aliquoting, a magnet was applied to the tube to draw residual magnetic beads from the extraction process to the bottom of the sample. The 120µl aliquot was stored at 4 °C until the purity and quantity of the DNA had been measured by Spectrophotometry (within 48 hours of extraction).

4.3.4 DNA Quantification and Quality Control

DNA concentration was measured on a Nanodrop 2000 Spectrophotometer (ThermoFischer Scientific, Germany) using 1µl of non-diluted eluted DNA. The

nanodrop was blanked with nuclease free, PCR-grade water as per the EZ1 handbook instructions (170). The Nanodrop spectrophotometer measures DNA concentrations by measuring the absorbance of light at a wavelength of 260nm, using a modification of the Beer-Lambert equation. Whilst Thermofischer quote a working detection range of 0.4 – 15000 ng/ μ l, expert opinion is that readings of less than 10ng/ μ l may be unreliable. As such, any samples with a concentration of <10ng/ μ l were not deemed suitable for downstream processing and were earmarked for DNA re-extraction.

DNA Purity was indicated using the ratio of absorbance at 260nm and 280nm (the 260/280 ratio). Pure DNA has a 260/280 ratio of approximately 1.8. Any sample with a ratio of <1.7 or > 2 was re-extracted. The 260/230 ratio is a secondary measure of DNA purity, and if low can represent the presence of contamination products absorbing at 230nm. Automated DNA extraction processes using magnetic bead separation are known to produce low 260/230 ratios due to the presence of residual magnetic beads in the eluted samples (171). However, this has not been found to interfere with downstream PCR experiments. Anslinger *et al* tested DNA extracted using the EZ1 Biorobot from a range of initial samples including blood, hair, sperm, teeth, and saliva. In downstream PCR experiments they found no evidence of any PCR inhibition (172). As such, we used the 260/280 ratio as the sole determinant of DNA purity.

Finally, DNA integrity was measured using gel electrophoresis. High DNA integrity is important for successful DNA methylation status experiments. In initial experiments

80ug of genomic DNA was found to produce a visible band on a 2% Agarose gel run at 70mV for 90 minutes. I subsequently found that adding 2µl of the undiluted DNA sample was universally sufficient to produce a visible band. An example gel electrophoresis result for DNA integrity is shown in *Figure 6*.

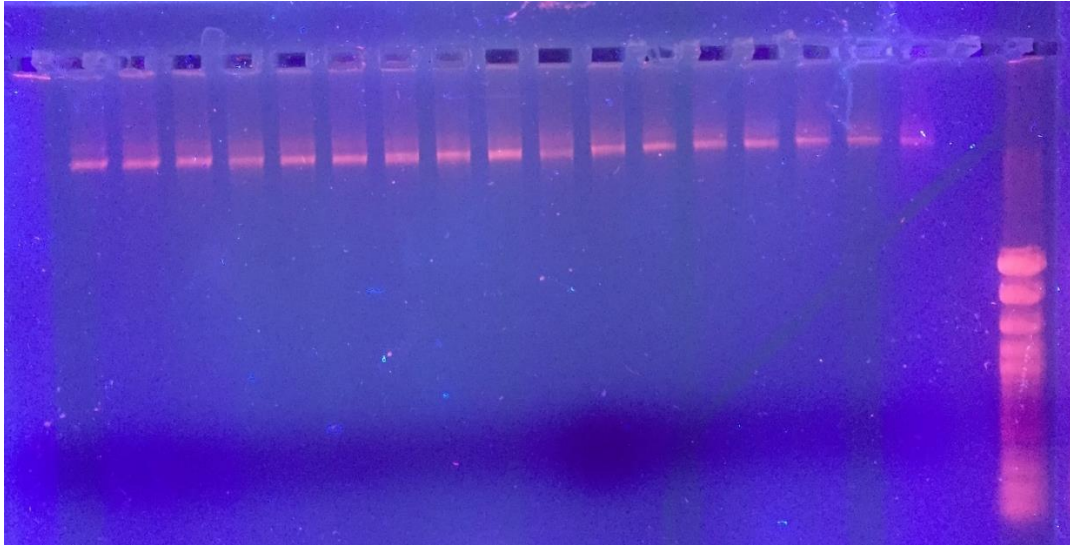


Figure 6: Gel electrophoresis for DNA integrity. 2% Agarose gel run for 90 minutes. Single band seen on gel at high molecular weight and no smear indicating good DNA integrity

4.3.5 RNA extraction

RNA extraction was performed manually using the PAXgene blood RNA system (Qiagen, Manchester, UK) consisting of a blood collection tube (PAXgene Blood RNA Tube) and a nucleic acid purification kit (PAXgene Blood RNA Kit) as per the manufacturer's instructions. In brief, 2.5mls of blood was collected in a PAXgene bottle and stored at -80 °C for subsequent analysis. Once defrosted samples were left to stand upright at room temperature for 2 hours to allow for full lysis of cells. The PAXgene tubes were centrifuged at 4000rpm for 10 minutes and the pellet washed

with RNase free water before repeat centrifuging. The washed pellet was suspended in ethanol before being lysed with a kit binding buffer and Protease K whilst shaking at 700 rpm for 10 minutes at 55 °C. The resulting lysate was then placed in a PAXgene shredder spin column and centrifuged to remove debris before undergoing a series of washes using PAXgene RNA spin columns. Next, the spin columns were incubated with a DNase incubation mix to remove genomic DNA contamination. After 3 further washing steps, RNA was eluted from the spin column membrane with a total of 80µl of elution buffer. Finally, the eluate was incubated for 5 minutes at 65 °C before being stored in aliquots at -20 °C.

4.3.6 RNA quantification and Quality Control

RNA was quantified using the same methodology as for DNA (see section 4.3.4). RNA purity was again indicated by the 260/280 ratio with pure RNA known to have a ratio of approximately 2.

4.4 Telomere Length Analysis by Quantitative PCR

4.4.1 DNA Thawing

All DNA samples were prepared as previously described in section 4.3. At the time of analysis, DNA samples were removed from storage at -20 °C and defrosted slowly on ice. After briefly centrifuging for 2-3 seconds to collect all the sample in the bottom of the reaction tubes, samples were mixed gently by retro-pipetting.

Spectrophotometry was then performed to ensure that the defrosted samples demonstrated similar traces, concentrations and ratios to their pre-frozen levels.

4.4.2 Thermocycling equipment

Real time PCR was performed with the Corbett Research Rotorgene 6000 Thermocycler (Qiagen, Manchester, UK). In the early optimisation stages of assay development individual reaction tubes were used in a 72 well carousel. For the study analysis, a 100 well, heat sealed rota-disc was used.

4.4.3 Principals of PCR set-up

PCR must be performed under strict conditions to prevent cross-contamination between samples and controls. All steps of the PCR set up were performed on a separate work-bench that was pre-treated with ethanol and RNase Away decontamination reagent (Fischer scientific, Loughborough, UK). All pipettes and reaction tubes were treated with Ultra-violet (UV) cross-linkage (Spectrolinker XL-1000, Spectroline,) which prevents PCR contamination by forming pyrimidine dimers in contaminant DNA which function as termination sites (173). All pre-amplification steps were performed using sterile, filter-pipette tips. All components of the PCR mix were stored in aliquots and used in a single PCR reaction only.

4.4.4 Final PCR protocol

The protocol for the TL analysis was based on that by Brouillette *et al* in the West of Scotland Primary Prevention Study (WOSCOPS) (174). In this study, the authors

measured TL in over 1500 patients, by a method modified from Cawthon's original 2002 protocol (155). This method was chosen over Cawthon's original protocol as it uses smaller reaction volumes of 20µl instead of 50uL and thus allows the use of a 100 well rotor-disc (15-25 µl reaction volumes).

The primers used were as described in the WOSCOPS protocol and are listed in *Table 2*. The reference gene 36b4 was used to provide a ratio for telomere repeat sequence copy number to single-copy gene copy number. All primers were ordered from Sigma Aldrich Co LLC (Poole UK). The desalted oligonucleotide primers were reconstituted with sterile nuclease free water (NFW) and stored in 20µl aliquots of 100µM concentrations at -20°C. At the time of use, aliquots were defrosted and mixed with 180µl of NFW to produce a working solution of 10µM concentration.

Primer	Sequence
Tel 1 (Forward)	5'CGGTTTGGTTGGGTTTGGGTTTGGGTTTGGGTTTGGGTT3'
Tel 2 (Reverse)	5'GGCTTGCCTTACCCTTACCCTTACCCTTACCCTTACCCT3'
36b4 Forward	5'CAGCAAGTGGGAAGGTGTAATCC3'
36b4 Reverse	5'CCCATTCTATCATCAACGGGTACAA3'

Table 2: Primer sequence for the Telomere reaction (Tel1/Tel2) and the single copy gene (36b4).

The components of the PCR Mastermixes are shown

Table 3. Two different master mixes were produced with a final volume of 15µl, one for the Telomere reaction and the other for the SCG. 5µl of sample DNA (concentration 1ng/µl) were added to the Mastermix to produce a final reaction

volume of 20 μ l. For each 100 well rotor disc both the Telomere and the SCG reactions for a single sample were run in parallel in the same PCR run. This was to minimise any difference in T/S ratio due to slight variations in individual run conditions. For each rotor disc, 50 wells were dedicated to Telomere reactions and 50 to the corresponding 36b4 SCG reactions. Each 50 wells included 19 samples, a 5-point standard curve and a negative control, all run in duplicate. The standard curve was produced from serial dilutions (5ng-0.156ng DNA; 2-fold dilution, 5 points) of stock human mixed genomic DNA (Promega, UK). The negative control was nuclease free water. After loading each well of the Rotor disc by manually pipetting, the disc was sealed with Rotor-disc heat sealer as per the manufacturer's instructions. Conditions were as described in the WOSCOPS protocol. The specificity of all amplifications was confirmed with melt curve analysis. The cycling conditions and settings of the melt curve analysis are given in *Table 4*.

Component	Concentration	Volume
Telomere run		
KiCqStart SYBR Green qPCR Readymix	-	10µl
Tel 1 Primer	300nmol/L	0.6µl
Tel 2 Primer	300nmol/L	0.6µl
Nuclease free water	-	3.8µl
Final Volume		15µl
Single copy gene run		
KiCqStart SYBR Green qPCR Readymix	-	10µl
36b4 F	300nmol/L	0.6µl
36b4 R	500nmol/L	1µl
Nuclease free water	-	3.4µl
Final Volume		15µl

Table 3: Components of PCR Mastermixes for TL measurement.

PCR Cycle	Settings
Annealing	95°C for 10 minutes
Amplification	35 cycles of 95°C for 15 seconds 58°C for 60 seconds
Melt	Ramp from 50 °C to 95 °C rising by 1 °C with each step Wait 90 seconds of pre-melt conditioning on first step Wait 5 seconds for each step afterwards Optimise gain before melt on all tubes The gain giving the highest fluorescence less than 90 will be selected

Table 4: PCR cycling conditions for TL measurement.

4.4.5 Calculation of T/S ratio

Standard curves were included in each run allowing concentrations to be measured for the samples for both the Telomere reaction (T) and the SCG reaction (S). The 'Automated Threshold' function was used to generate best fit standard curves. The duplicate runs produced two concentrations per sample which were then averaged to produce a mean concentration for both T and S. The mean relative telomere length was then calculated as a ratio of T/S.

4.4.6 Optimisation and rationale of chosen protocol

The following features characterise a well optimised PCR experiment;

1. **A high R² value:** The R² value, otherwise termed the coefficient of determination, is a measure of how well the standard curve fits with the data points that form it. Optimal PCR amplifications should have an R² value of >0.99. As such, this value was set as the minimum acceptable value for a PCR to be considered successful in this experiment.

2. **A reaction efficiency close to 100% (or 1):** The reaction efficiency is a measure of how much the DNA target is amplified in each PCR cycle. In a 100% efficient reaction, the amount of amplification product doubles with each PCR cycle. Whilst it is not theoretically possible for a single amplification product to amplify at >100% efficiency, a PCR amplification can yield an overall efficiency of >100% if the efficiency is measured from a standard curve gradient or if non-specific amplification occurs. It

is thought that PCR efficiencies should lie within the range of 0.90 and 1.10 (or 90 to 110%). efficiencies

3. Demonstration of reproducibility: both between duplicate samples in the same run (intra-assay variability) and across different runs (inter-assay variability). In PCR experiments the Coefficient of Variation (CV) is usually used as a measure of variation between repeat results. The CV is calculated as;

$$CV = \frac{\text{Standard deviation of series}}{\text{Mean of series}}$$

In this study, both the mean intra-assay and inter-assay variability were measured for both the validation and study cohorts (see section 5.1).

4. A single peak on melt-curve analysis: This implies that a single PCR product has been amplified.

As previously mentioned, the WOSCOPS protocol was chosen due to its smaller reaction volume allowing the use of the 100 well rotor-disc. Accordingly, the primers and PCR amplification conditions used were taken from same protocol. However, during our initial experiments to ensure the applicability of this protocol to our laboratory and thermocycling equipment we encountered several difficulties that required changes to be made to the standard protocol. These difficulties included;

1. Over efficiency of PCR amplification
2. Differences in reaction efficiencies between the telomere and SCG runs

3. Inconsistencies in the PCR runs with some runs demonstrating poor R^2 values and efficiencies despite no apparent changes in set-up.

In initial optimisation experiments, the WOSCOPS protocol was used without modification. However, increased reaction efficiencies of 1.15-1.6. were consistently demonstrated. As such, different amplification temperatures were used (54°C, 58°C, 62°C) to try to optimise the PCR efficiency to closer to 1. However, these changes did not affect the reactions. To minimise for the presence of PCR inhibitors, a more dilute serial dilution was performed with the concentration of the top standard reduced from 20mg/μl to 5ng/μl. This change had the effect of improving the reaction efficiency to 1.08 and 1.09 for the telomere and SCG runs respectively. Therefore, a 5-point, 2-fold dilution series ranging from 5ng-0.156ng of DNA was used for all subsequent runs. As a consequence of the change in the standard curve from that of the WOSCOPS protocol, the amount of input DNA was reduced to 5ng per reaction to ensure that the samples remained clustered around the middle of the standard curve.

The above changes to the protocol were performed using individual wells held in a 72 well carousel. For the validation and study runs, the 100 well rotor-disc was used. The PCR was found to run equally well in this format. In a further modification to the original protocol it was decided to run both the telomere and SCG reactions in adjacent wells of the same run to minimise errors resulting from slight differences in conditions between runs. To do this the telomere run was extended from 25 to 35 cycles.

The second two issues listed above were nullified by the method chosen for determining relative quantitation of telomere length. This will be described further in the following section.

4.4.7 Standard curve method Vs delta-delta CT method for relative quantitation of TL

In relative quantitation PCR, the amplification of the gene of interest is normalised to that of an endogenous reference or housekeeper gene that is ubiquitously expressed. Relative quantitation can be performed by one of two main methods; the standard curve method or the delta-delta cycle threshold (delta-delta CT) method. The first method involves running a standard curve comprised of serial dilutions of stock DNA of known concentration. The standard curve is produced by plotting concentration against cycle threshold (CT) level. The CT value of a sample is the amplification cycle at which the samples fluorescence signal exceeds an arbitrary threshold value above baseline and within the exponential amplification phase of the PCR. With the fluorescence threshold set for both the standards and samples within a run, the concentrations of the unknown samples can be measured by plotting their position on the standard curve according to their CT value. Separate standard curves are used to quantify expression of the gene of interest (X) and SCGs (Y) within the unknown samples and the relative gene expression recorded as a ratio of X/Y.

In contrast, the delta-delta CT method does not rely on standard curves and uses a single calibrator sample present in all runs to ensure comparison across runs. For

each sample, the CT value is normalised against that of the reference gene and then further normalised against that of a calibrator sample present in all runs

The standard curve method was chosen for this thesis as it has two main advantages over the delta-delta CT method. Firstly, the delta-delta CT method requires that the reaction efficiencies for the gene of interest (GOI) and the single copy reference gene be approximately the same. This is because raw CT data is compared directly with no correction made for differing reaction efficiencies. The standard curve method can correct for differences in reaction efficiency between the GOI and reference genes, as relative quantification is calculated separately using different standard curves. Secondly, running standard curves in each run provides an in-built form of quality control that ensures that the PCR has amplified effectively (i.e. a value for R^2 and a reaction efficiency is given for each run). The only disadvantage of the standard curve method is that it is more time consuming as the need for a set of standards in each run reduces the number of samples that can be processed within that run.

4.4.8 Confirmation of valid PCR for Telomere length

A typical appearance of the amplification plots and standard curves generated for both the Telomere and SCG runs are shown in *Figure 7*. Extending the telomere run from 25 to 35 cycles has the effect of producing a late amplification in the negative control. This is likely due to trace DNA contamination being amplified due to the ubiquitous expression of telomere DNA. However, the CT values of these negative controls were approximately 10 cycles more than those of the samples/standards

representing a DNA concentrations 1000-fold less than the most dilute standard. Such trace contamination will not affect the final results. When the Telomere run is run for 25 cycles, this amplification in the negative control is not seen. In addition, melt curve analysis of telomere amplification run over 25 cycles demonstrates no product formation in the negative controls (*Figure 8*).

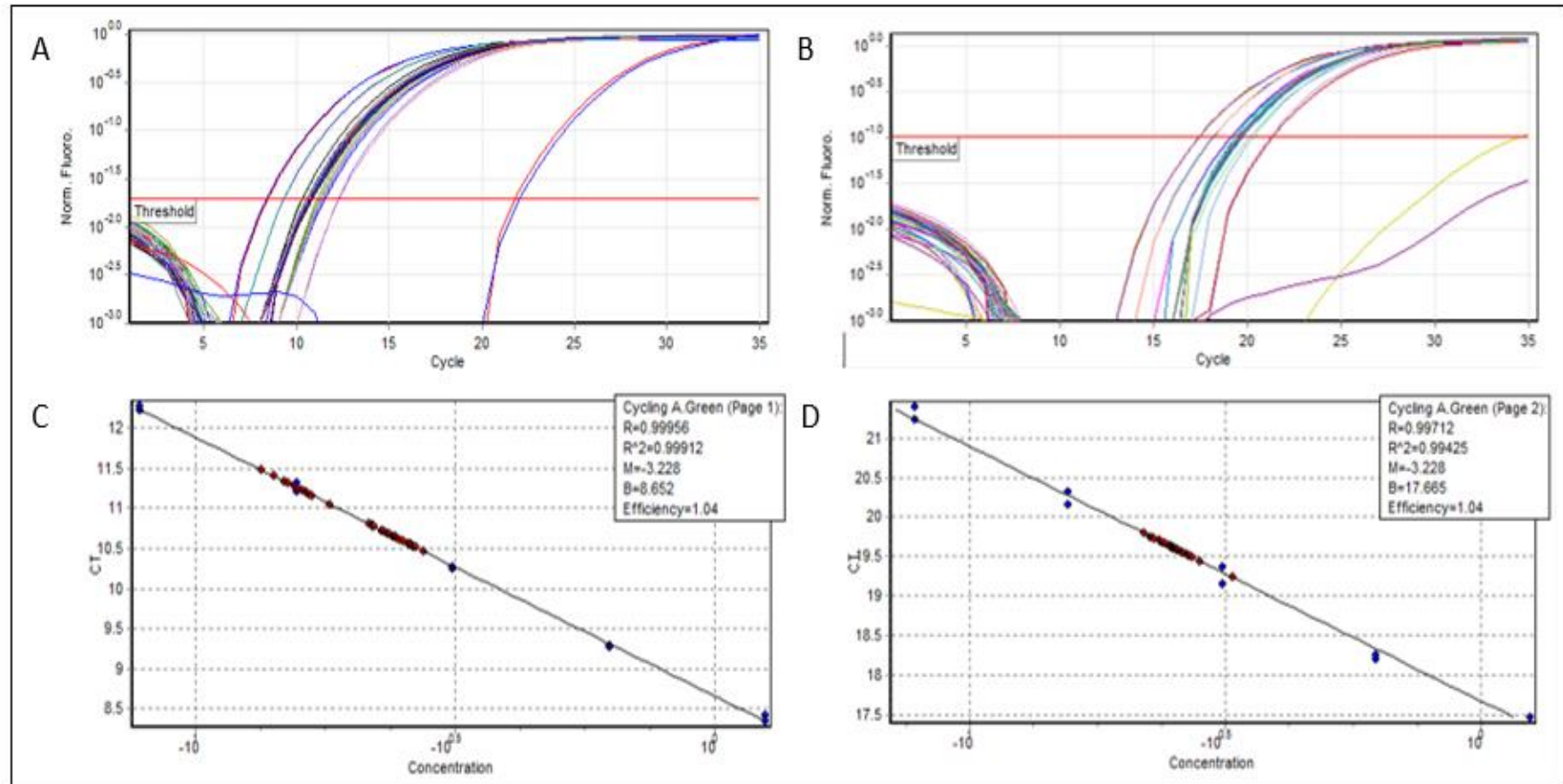


Figure 7: Typical amplification plots and standard curves for Telomere run (A, C) and SCG run (B, D). A: Amplification plot for Telomere run (CT value for negative controls > 10 cycles higher than samples/standards). B: Amplification plot for SCG run (Negative control does not reach threshold). C: Standard curve for telomere run. D: Standard curve for SCG. All samples (Red) lie within the points of the standard curve (Blue) for both telomere and SCG runs.

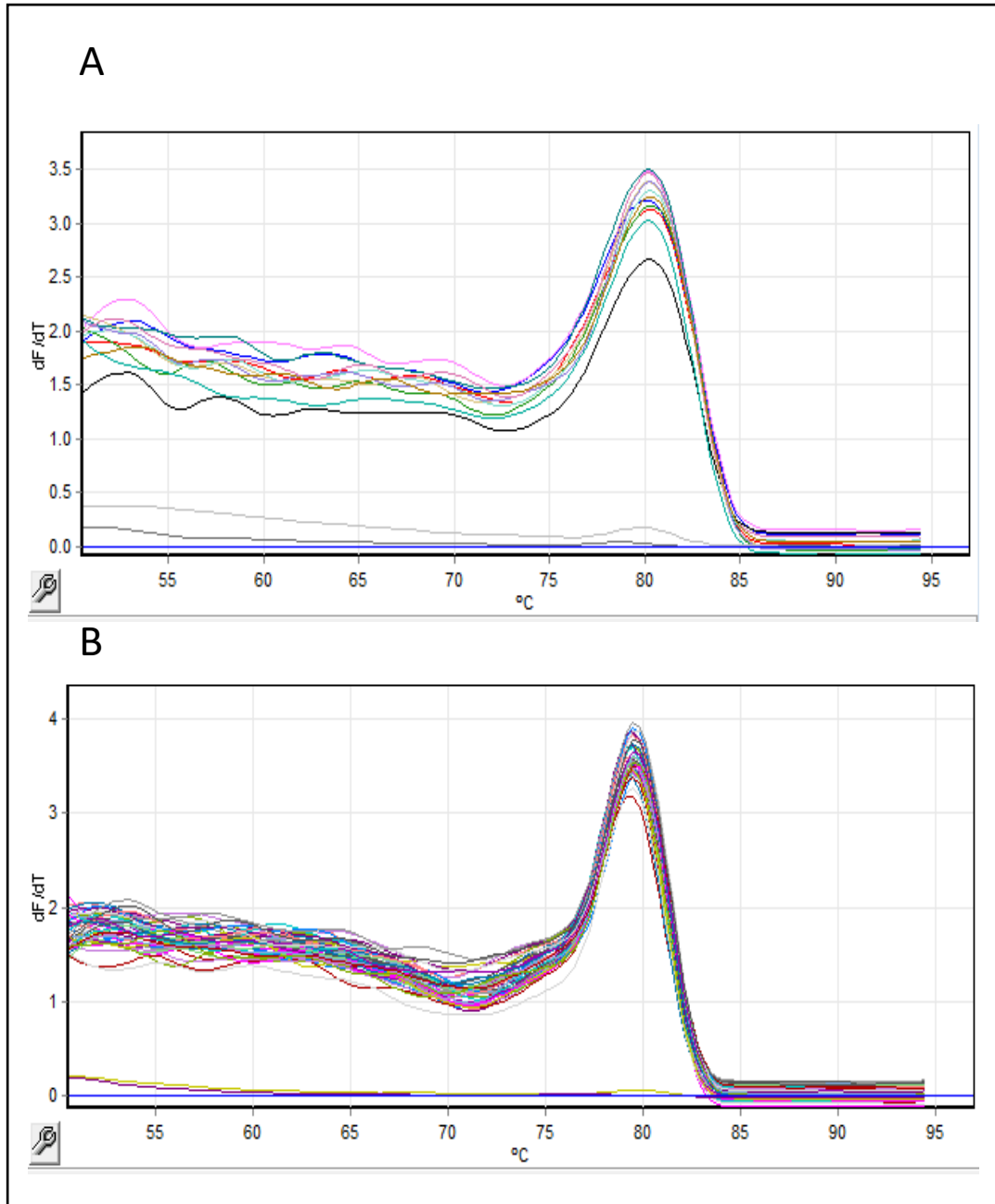


Figure 8: Melt curve analysis for Telomere run (A) and SCG run (B). A single peak is seen in each curve confirming the presence of a single amplification product. The negative controls are seen as flat lines at the bottom of each melt curve.

4.5 Measurement of Single Telomere Length Analysis (STELA)

As part of the main study analysis propensity matching was performed between patients with and without CSA-AKI. This resulted in 51 matched pairs (see section 5.5). Of these, 12 pairs were selected; 6 with AKIN stage 1 AKI patients and 6 with AKIN stage 2 AKI patients. In each case, the 6 pairs with the closest matched propensity scores were selected for analysis.

DNA was extracted as previously described in section 4.3.3. For STELA analysis at the XpYp telomere we used the single telomere length analysis (STELA) assay previously described (159). This analysis was performed for us by Professor Duncan Baird who first described the technique (Division of Cancer and Genetics, Cardiff University). Briefly, genomic DNA was solubilised by dilution in 10mM Tris-HCl (pH 7.5), quantified by Hoechst 33258 fluorometry (BioRad, Hercules, USA) and diluted to 10ng/ μ l in 10mM Tris-HCl (pH 7.5). 10ng of DNA was further diluted to 250 pg/ μ l in a volume of 40 μ l containing 1 μ M Telorette2 linker and 1 mM Tris-HCl pH 7.5. Multiple PCRs (typically 6 reactions per sample) were carried out for each test DNA in 10 μ l volumes 250pg of DNA, 0.5 μ M of the telomere-adjacent and Teltail primers, 75mM Tris-HCl pH8.8, 20mM (NH₄)₂SO₄, 0.01% Tween-20, 1.5mM MgCl₂, and 0.05 U of a 10:1 mixture of Taq (ABGene, Epsom, UK) and Pwo polymerase (Roche Molecular Biochemicals, Lewes, UK). The reactions were cycled with a Tetrad2 thermocycler (BioRad, USA) under the following conditions: 22 cycles of 94°C for 15 seconds, 65°C for 30 seconds and 68°C for 8mins. The DNA fragments were resolved by 0.5% TAE agarose gel electrophoresis, and detected by Southern hybridisations

with a random-primed α -³²P labelled (Ready-To-Go DNA Labeling Beads, GE Healthcare) TTAGGG repeat probe, together with a probe to detect the 1 Kb (Stratagene, La Jolla, USA) and 2.5 kb (BioRad) molecular weight marker. The hybridised fragments were detected by phosphorimaging with a Typhoon phosphorimager (GE Healthcare, USA). The molecular weights of the DNA fragments were calculated using the Phoretix 1D quantifier (Nonlinear Dynamics, Newcastle-upon-Tyne, UK).

The Wilcoxon rank log test was used for comparison of mTL and 25th centile Telomere length between the matched groups

4.6 DNA Methylation Methods

DNA was extracted and quality control performed as detailed in sections 4.3. In addition, sample concentration was determined by Fluorometric quantification (Qubit). The DNA then underwent bisulphite conversion. This process converts unmethylated cytosine (C) to thymine (T) whilst leaving methylated cytosine (Cm) unconverted. Sequencing of the bisulphite converted DNA can therefore determine the methylation status of every individual cytosine residue (175, 176).

A list of the desired CpG sites for study were sent to a third party (Dr Robert Lowe, Blizzard Institute, QMUL) for assistance with Primer Design. Unfortunately, only 44 out of 77 passed the design tests, meaning that the algorithms used in primer design were not able to find a pair of primers that would amplify the desired portion of the

genome within a prespecified range of stringency. By reducing the design stringency, we were able design primers for all the CpG sites but had to accept that in doing so we increased the likelihood that a proportion of the PCR reactions might fail. Primer pairs usually amplified portions of DNA containing multiple CpG sites. By overlapping the PCR products of the primer pairs, we were able to deduce the methylation status at individual sites.

Region specific PCR was performed with the Fluidigm 48:48 Access Array (Fluidigm, San Francisco, US), which allows target enrichment of 48 samples at one time. A detailed description of this methodology is given in *Appendix B*. This work was performed by Dr Charles Mein's team (the Genome Center, QMUL). In brief, the primer inlets of the Access Array were loaded with pooled primer pairs (forward and reverse) diluted to a final concentration of 1 μ M per primer. Fluidigm CS1 and CS2 custom sequences were added to the 5' end of each primer (CS1 is added to the forward, and CS2 is added to the reverse), allowing for the later addition of unique barcodes to each sample. Each of the 48 Sample inlets were loaded with 4 μ L of bisulphite converted DNA and mastermix solution. Once prepared, the Access Array was placed in the primed Pre-PCR IFC Controller AX for the samples and primers to be automatically combined (1.5 hours duration). The Array was then transferred to the Fluidigm FC1™ Cyclor for target amplification by PCR. Following amplification, the PCR products were harvested. Quality control was performed on a random selection of the harvested PCR products using an Aligent 2200 TapeStation System and D1000 ScreenTape (Aligent technologies) to determine the quantity and integrity of the PCR product.

The PCR products were then barcoded using a second PCR reaction. The function of this step was to label all amplicons from a given sample with a common sequence to allow subsequent identification once all of the PCR products had been pooled for sequencing. In addition, the barcode contains an Illumina sequencing adaptor (p5 or p7) that allows the final library of PCR products to bind to the oligo lawn of the Illumina Flow cell. Once the PCR products had been successfully barcoded they were pooled for sequencing using the Illumina MiSeq platform (Illumina, California, USA).

The sequencing process generates millions of reads in total representing all of the DNA fragments. Sequences within the pooled DNA library are separated into individual samples based on the unique sample specific barcodes attached to each fragment during preparation of the library. Within fragments from the sample, reads with similar base sequences are clustered and grouped by forward and reverse reads. Any discrepancies are resolved by comparison within these grouped reads. Finally, the percentage of methylated cytosine residues is calculated for each CpG site for all fragments generated from a single sample.

CHAPTER 5: Mean Telomere Length and Cardiac Surgery Associated -Acute Kidney Injury

5.1 Results of Validation experiments

Prior to performing the study runs, a validation experiment was performed to confirm the reproducibility of the telomere length assay. Three separate runs were performed on the first 19 samples in the cohort. Sample 10 was excluded as it had a low concentration of DNA to conserve it for the main study runs.

5.1.1 Intra-assay variability

All samples were run in duplicate. Intra-assay variability, defined as the coefficient of variability (CV) of duplicates, was calculated by averaging the CV values across all three runs separately for the Telomere and single copy gene (SCG) amplifications. This method gave an intra-assay variability of 4.99 and 2.85 for the Telomere and SCG amplifications respectively. However, a handful of samples showed a large variation in CV value which skewed the results and was thought to arise from pipetting loading variation. When duplicate samples with a CV value of greater than 10 were excluded from the analysis (7 out of 114 samples, 6.1%) the respective average CV values improved to 2.50 (Telomere) and 2.44 (SCG). As such, in our main cohort any duplicates with CV of greater than 10 were repeated.

5.1.2 Inter-assay variability

Inter-assay variability was measured as the average CV of the Telomere/SCG (T/S) ratio of all 19 samples across the 3 runs. A graphical representation of the variation

across the three runs is shown in *Figure 9*. The average CV for all samples was 8.03. This improved to 6.43 when the samples with large intra-assay variability were excluded from the analysis.

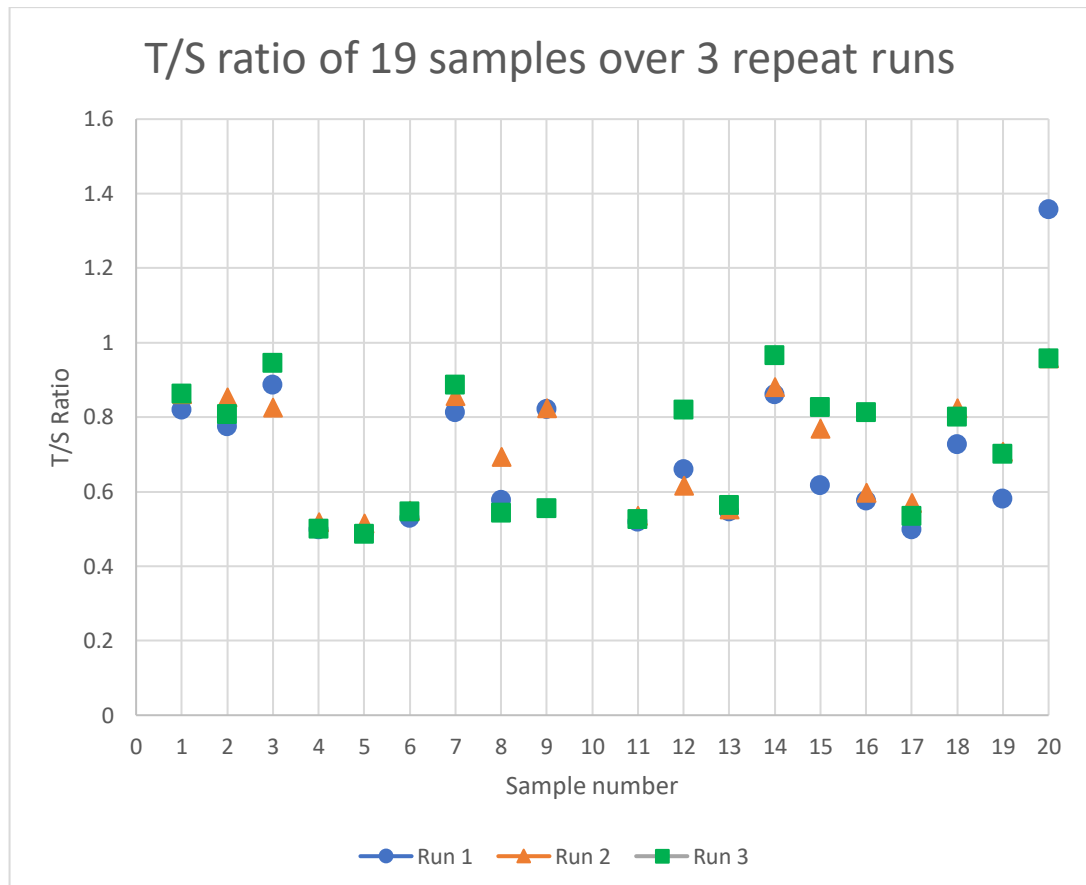


Figure 9: Results of validation experiment. Three separate runs were performed on 19 patient samples.

5.2 The study population

The current study is a prospective case control study. Cases were defined as patients who developed Cardiac Surgery Associated- Acute Kidney Injury (CSA-AKI) in accordance with AKIN criteria and controls were defined as patients with no AKI. The final number of patients tested for mean telomere length (mTL) was 254.

Figure 10 shows a graphical representation of the recruitment process. Of the 281 patients recruited 254 had valid DNA samples processed. Of the remaining 27, 5 had no blood collected. 1 patient withdrew consent prior to blood sampling, 3 patients had their operation cancelled and were rescheduled at times that precluded sampling and 1 patient was cancelled and was never rescheduled. The remaining 22 patients had blood samples taken but incorrectly processed for buffy coat resulting in DNA yields that were too low for downstream processing. Of the 254 patients who had valid DNA samples for mean telomere length analysis 54 developed CSA-AKI (cases) and 200 did not (controls). A sample log of the 254 patients tested for mTL is given in *Appendix C*. A summary of the raw data for mTL measurement is given in *Appendix D* together with a summary of the inter-assay variability between the standards measured in each PCR run (Coefficient of variation of standards = 2.9%)

5.3 Tests of Normality

Each continuous variable was tested for normality using the Shapiro Wilks test. P-values of less than 0.05 were regarded as differing significantly from a normal distribution. A summary of these normality tests is shown in *Appendix E*. These tests were used to determine which statistical tests were appropriate to run for each variable; e.g. Students t test for normally distributed continuous variables and Mann-Whitney U test for non-normally distributed continuous variables.

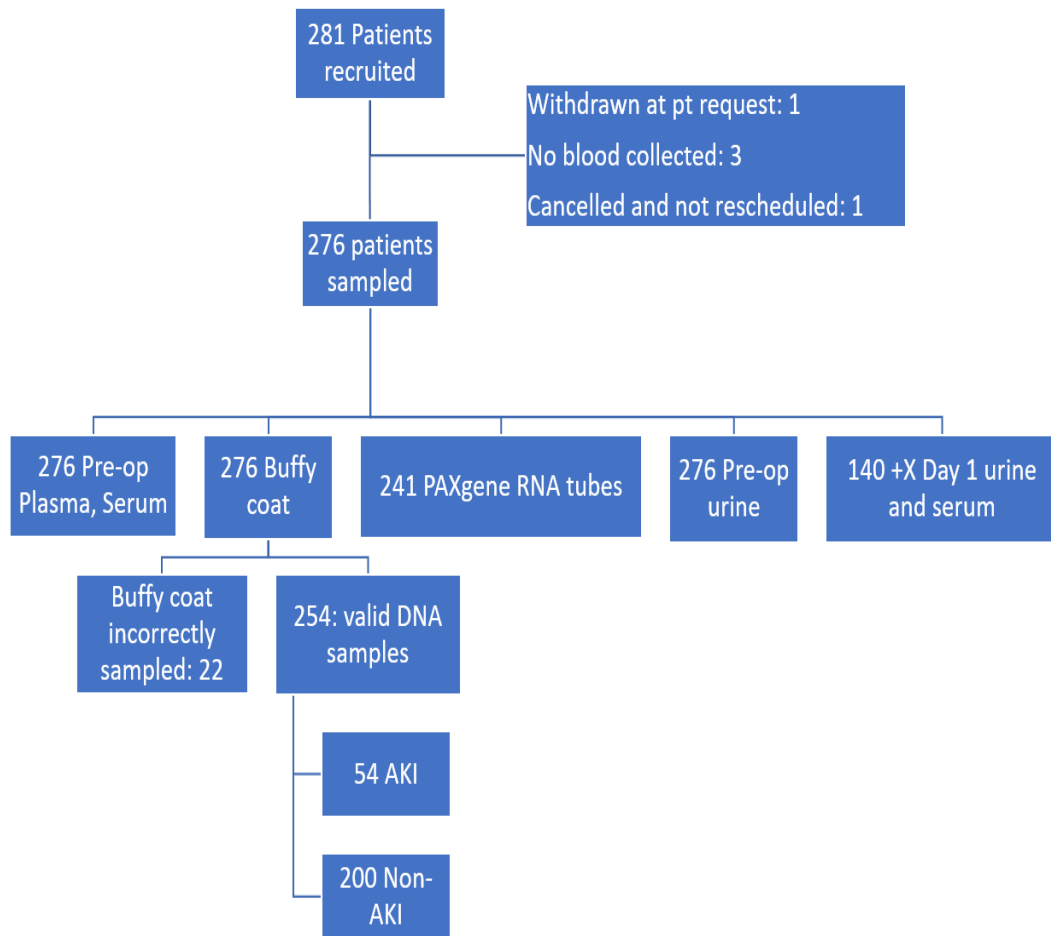


Figure 10: Schematic outlining patient recruitment and sampling. Of the 281 patients recruited, 254 patients had valid DNA samples processed. Of these, 54 experienced post-operative AKI.

5.4 Univariate associations of Telomere Length with main outcomes.

Binary logistic regression was used to determine associations between Telomere length and the primary outcome of development of CSA-AKI as well as the secondary endpoints of in-hospital mortality, 1-year mortality, and a composite outcome combining stroke, new AF, reoperation, and CSA-AKI.

No significant association was seen between mTL and the primary outcome of development of CSA-AKI as defined by the AKIN criteria (*Table 5*). Neither were any significant associations seen between the secondary endpoints of in-hospital mortality or 1-year mortality. To increase the number of events, a composite endpoint was created combining the following outcomes; New AF, Stroke, AKI, and return to theatre. However, no association was found between mTL and the presence of this composite endpoint. Box plots for mTL and AKI and mTL and composite endpoint are shown in *Figure 11* and *Figure 12*.

To further investigate the relationship between Telomere length and our primary and secondary outcomes, the study population was divided into quintiles of mean Telomere length. Differences in outcomes between patients in the top and bottom quintiles of mTL were then investigated. The rationale for doing this was to attempt to unmask any subtle associations between mTL and the outcome measures. Comparison of the rates of each of the endpoints between the top and bottom quintiles was performed using Fischer's exact test. Again, no significant associations

were found between Telomere length and any of the previous outcome measures; AKI, in-hospital mortality, 1-year mortality or composite outcome (*Table 6*).

Outcome measure	N	Mean T/S Ratio	SD	OR	95% CI	p-value
AKI						
No	200	0.760	0.162	0.375	0.058-2.436	0.304
Yes	54	0.735	0.163			
In-hospital mortality						
No	249	0.755	0.162	0.985	0.004-232.624	0.996
Yes	5	0.754	0.184			
1-year mortality						
No	205	0.755	0.162	0.315	0.013-7.787	0.481
Yes	16	0.726	0.162			
Composite outcome*						
No	133	0.766	0.161	0.409	0.089-1.886	0.252
Yes	121	0.742	0.164			

*Table 5: Association between TL and the main study outcomes. *Composite outcome includes New AF, Stroke, Reoperation, and AKI.*

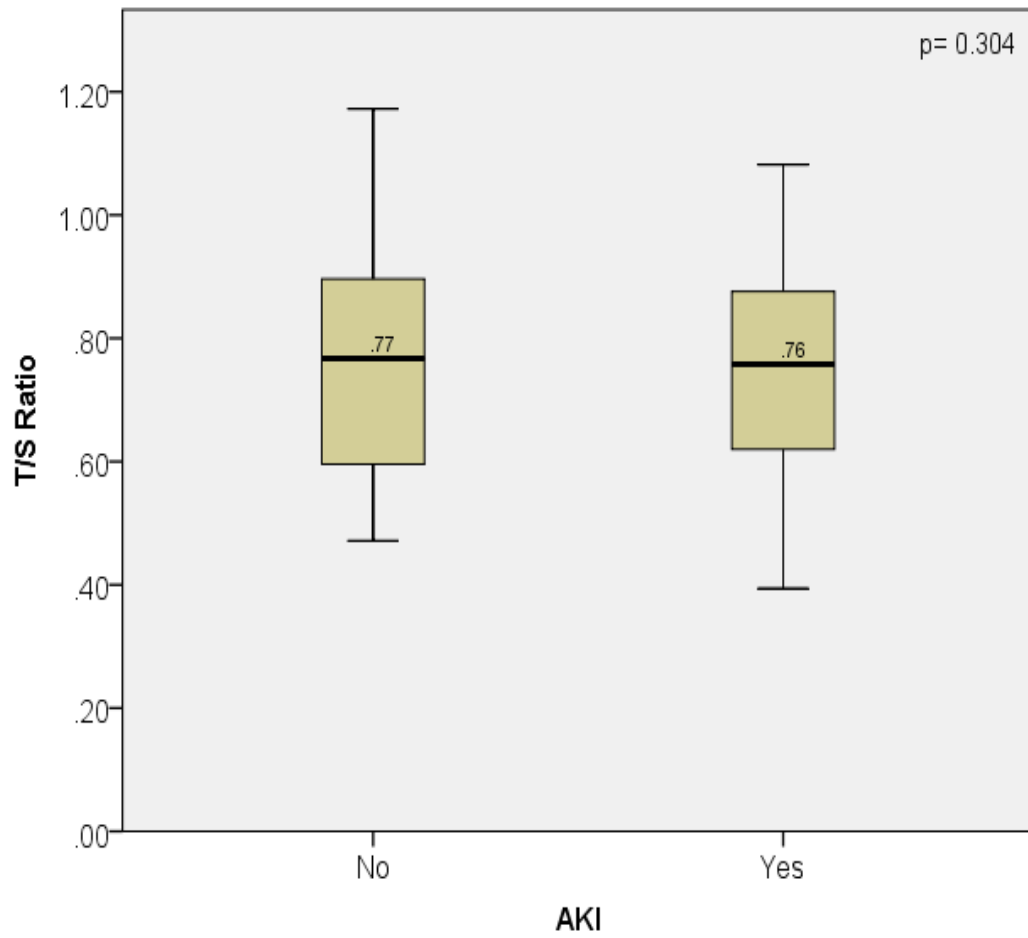


Figure 11: Box plots for mTL (black line) in the AKI and No-AKI groups: $p=0.304$. Black horizontal line represents median value, box represents interquartile range and vertical line indicates range.

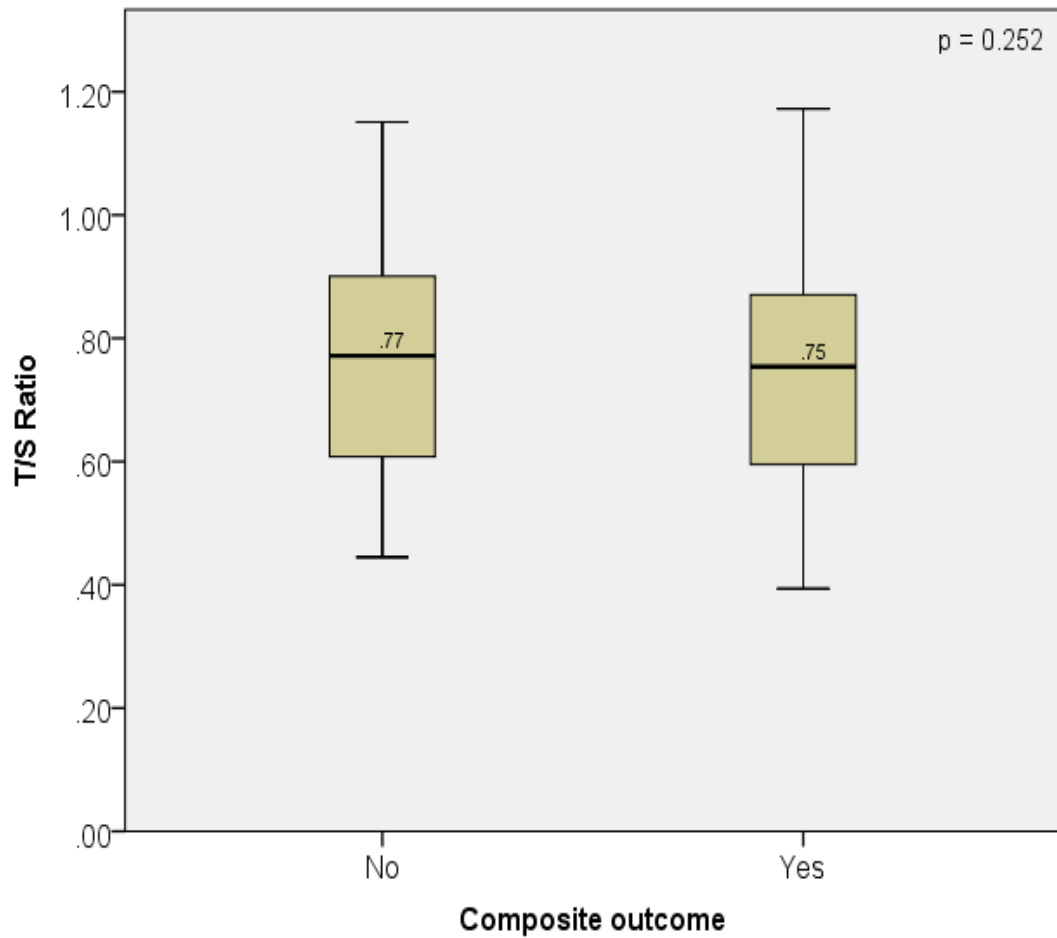


Figure 12: Box plots for mTL (black line) and development of the Composite outcome. $p=0.252$. Black horizontal line represents median value, box represents interquartile range and vertical line indicates range.

Association	Top Quintile TL n= 50	Bottom Quintile TL n = 51	p-value
AKI			0.323
Yes	8 (16.0%)	11 (21.6%)	
No	42 (84.0%)	40 (78.4%)	
In-hospital mortality			0.748
Yes	1 (2%)	1 (2%)	
No	49 (98%)	50 (98%)	
1-year mortality			0.308
Yes	1 (2.4%)	3 (7.3%)	
No	40 (97.6%)	38 (92.7%)	
Composite outcome			0.184
Yes	21 (42.0%)	27 (52.9%)	
No	29 (58.0%)	24 (47.1%)	

Table 6: Association of rates of AKI, In-hospital mortality, 1-year mortality, and composite outcome in patients in the top and bottom quintiles of mTL.

5.5 Propensity matched analysis of mTL and CSA-AKI

51 matched pairs were obtained from a possible maximum of 54. Details of the matched populations are given in *Appendix F*. Shapiro-Wilk's test of normality run on the matched cohort showed that mTL was normally distributed for both cases and controls. As such, comparison of mTL in the matched populations was performed using a Student t-test. No significant association was observed in mTL between cases and controls in the matched populations (*Table 7*). A boxplot of median mTL in the propensity matched groups is shown in *Figure 13*.

	Mean of differences	CI of difference	p- value
TS/ ratio No – T/S ratio Yes	0.00617	-0.0523 – 0.0646	0.833

Table 7: Comparison of mTL in Cases Vs Controls in 51 propensity matched patient pairings.

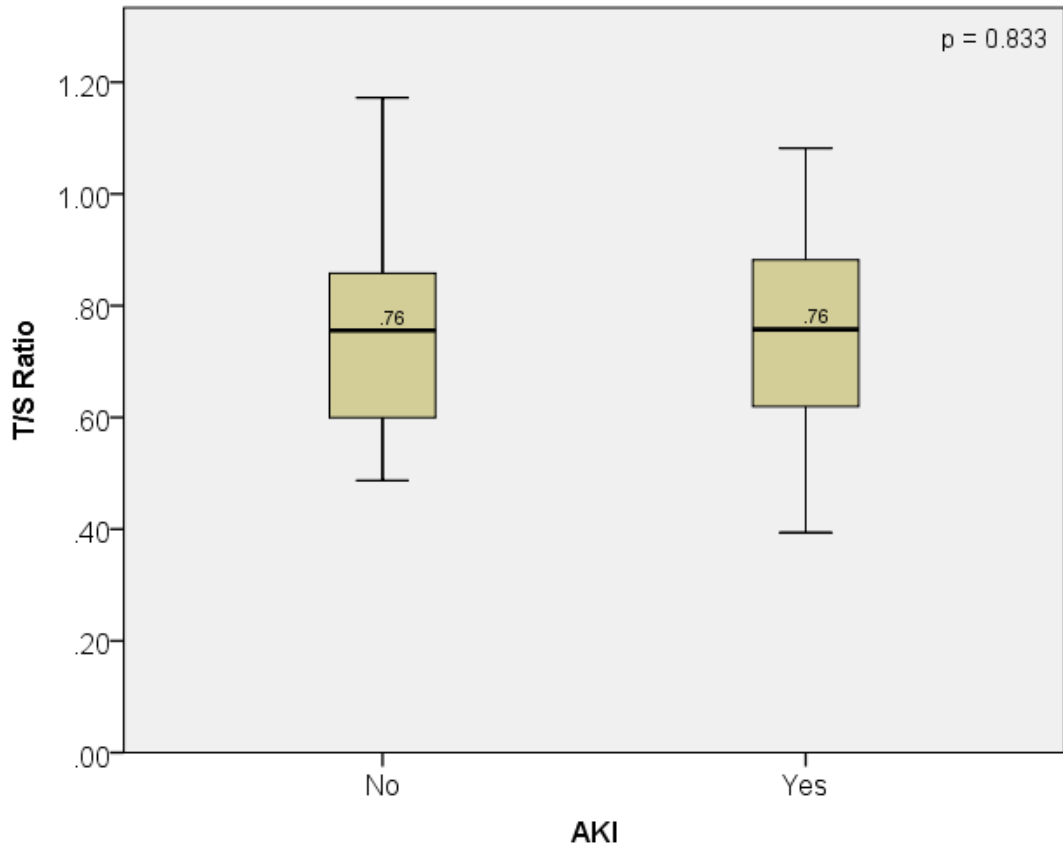


Figure 13: Boxplot of mTL in Cases Vs Controls in 51 propensity matched patient pairings.

5.6 Whole population associations with mean Telomere Length

The raw data for the measurement of mTL for all 254 study patients is given in *Appendix D*. A summary of the associations between mTL and all continuous independent pre-operative and intra-operative variables is shown in *Table 8*. A similar summary for categorical independent variables is shown in *Table 9*. Significant associations were seen between mTL and age, use of post-operative vasopressors, operation type (CABG Vs No CABG), and hypercholesterolaemia. A graphical representation of the variation of mTL with age is shown in *Figure 14*.

T/S ratio with	Correlation Coefficient	p-value
Age	-0.213	0.001
Length of Stay	-0.008	0.903
BMI	-0.079	0.208
Vasopressor duration	0.159	0.011
Inotropic duration	-0.059	0.355
Ventilation duration	-0.008	0.903
First Hb in ITU	0.05	0.446
UO in first 12 hours	0.101	0.125
CPB time	0.057	0.375
X-clamp time	0.000	0.994
Pre WCC	-0.032	0.611
Pre INR	-0.037	0.558
Pre-APTT	-0.005	0.936
Pre-CRP	0.155	0.245
Pre-Hb	0.043	0.491
Pre-op Cr	0.005	0.938
Pre-op eGFR	0.046	0.502
Day 3 CRP	-0.035	0.635
Day 1 Hb	0.094	0.139
Hb Diff	-0.12	0.851

Table 8: Summary table of Spearman correlations between mTL and all continuous independent variables. P-values <0.05 shown in bold.

	N	Mean T/S Ratio	SD	Median	p-value
Gender					
Male	183	0.754	0.163	0.757	0.817
Female	71	0.756	0.162	0.775	
Ethnicity					0.245
White	182	0.751	0.163	0.767	
South Asian	49	0.737	0.145	0.753	
Black	12	0.855	0.193	0.924	
Mixed	2	0.829	0.226	0.829	
Asian	3	0.853	0.206	0.924	
Middle Eastern	2	0.646	0.286	0.647	
Other	4	0.773	0.116	0.773	
CABG					0.02
No	104	0.783	0.171	0.821	
Yes	150	0.735	0.154	0.751	
Angina Status					0.106
CCS0	54	0.787	0.166	0.782	
CCS1	43	0.787	0.175	0.834	
CCS2	116	0.739	0.156	0.755	
CCS3	26	0.703	0.153	0.671	
CCS4	11	0.758	0.144	0.783	
Dyspnoea					0.654
NYHA 1	42	0.753	0.150	0.753	
NYHA 2	130	0.747	0.172	0.753	
NYHA 3	68	0.773	0.154	0.800	
NYHA 4	9	0.747	0.133	0.775	
Previous Cardiac Surgery					0.126
No	237	0.751	0.162	0.759	
Yes	17	0.805	0.161	0.778	
History of Malignancy					0.947
No	236	0.755	0.162	0.759	
Yes	18	0.755	0.170	0.778	
Diabetes					0.190
No	189	0.765	0.164	0.792	
Diet	4	0.777	0.112	0.817	
Oral	50	0.710	0.156	0.679	
Insulin	11	0.770	0.164	0.758	
Diabetes					0.076
No	189	0.765	0.164	0.792	
Yes	65	0.724	0.156	0.727	
Hypertension					0.162
No	64	0.781	0.178	0.835	
Yes	190	0.746	0.156	0.755	
Hypercholesterolaemia					0.042
No	132	0.774	0.168	0.821	

Yes	122	0.734	0.154	0.746	
Smoker					
Non-smoker	114	0.743	0.174	0.743	0.524
Ex-smoker	115	0.768	0.156	0.777	
Current smoker	25	0.745	0.133	0.760	
Pre-op Renal Disease					
No	209	0.757	0.162	0.760	0.633
Yes	45	0.743	0.163	0.767	
Pulmonary Disease					
No	225	0.757	0.160	0.768	0.936
COPD	17	0.738	0.197	0.647	
Asthma	12	0.734	0.164	0.656	
Neurological disease					
No	226	0.756	0.163	0.768	0.693
TIA/RIND	16	0.767	0.145	0.756	
CVA	12	0.717	0.185	0.647	
PVD					
No	241	0.758	0.163	0.769	0.130
Yes	13	0.689	0.137	0.644	
Previous PCI					
No	216	0.754	0.164	0.767	0.979
Yes	38	0.760	0.157	0.758	
Previous MI					
No	188	0.757	0.168	0.769	0.647
Yes	66	0.749	0.146	0.757	
Previous ACE					
No	151	0.763	0.164	0.775	0.322
Yes	103	0.742	0.159	0.753	
Previous Statin					
No	93	0.779	0.168	0.820	0.088
Yes	161	0.741	0.158	0.748	
Pre-op diuretic					
Yes	223	0.756	0.162	0.758	0.704
No	31	0.746	0.171	0.768	
LV Ejection Fraction					
Good	198	0.748	0.166	0.759	0.339
Fair	47	0.783	0.147	0.777	
Poor	9	0.745	0.168	0.758	
Operative Urgency					
Elective	217	0.760	0.166	0.769	0.382
Urgent	35	0.725	0.142	0.727	
Emergency	2	0.720	0.018	0.720	
Reoperation					
No	241	0.754	0.160	0.763	0.788
Yes	13	0.759	0.204	0.707	
Transfused in ITU					

No	160	0.758	0.164	0.759	0.501
Yes	94	0.748	0.161	0.768	
Clotting products in ITU					
No	200	0.759	0.162	0.775	0.333
Yes	54	0.740	0.166	0.753	
New AF					
No	181	0.754	0.163	0.758	0.914
Yes	73	0.756	0.163	0.772	
Post-op LRTI					
No	197	0.756	0.162	0.769	0.967
Yes	57	0.751	0.163	0.753	

Table 9: Summary of associations of mTL with independent categorical variables. P-values <0.05 shown in bold.

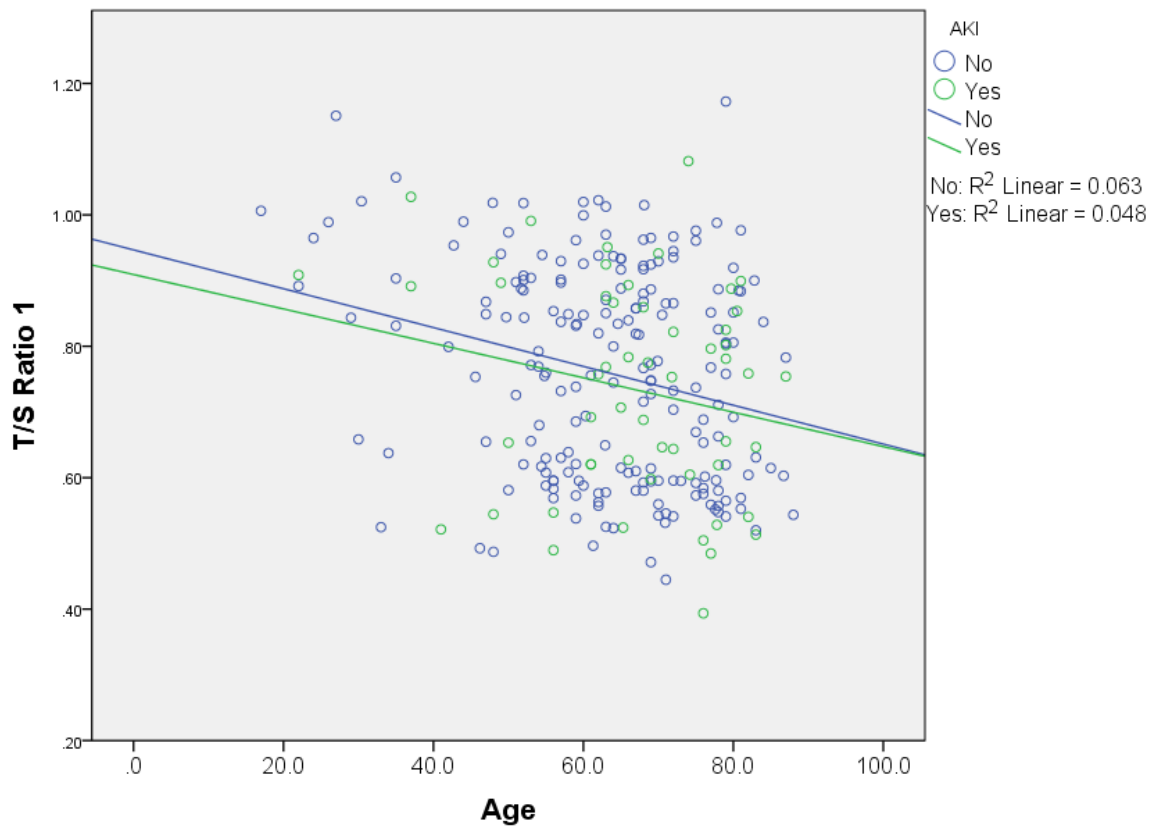


Figure 14: Relationship between age and mTL. The strength of the linear correlation is given by the R² value of 0.061 (p=0.001).

5.7 Analysis of significant predictors of CSA-AKI

5.7.1: Univariate analysis

A separate analysis to determine the significant predictors of CSA-AKI was performed using a range of pre-operative and intra-operative variables and AKI as a categorical dependant variable. Post-operative variables were excluded from analysis because although they may associate with AKI, they are not predictors of its development. The first haemoglobin measured in the intensive care unit (1st Hb in ITU) was included as a predictor as it is a measure of intra-operative blood loss/transfusion which is a known risk factor for CSA-AKI. Univariate analysis was performed using binary logistic regression with odds ratio's (OR) and 95% confidence intervals quoted (*Table 10*). Factors that were significant on univariate analysis were entered into a multivariate model to determine independent predictors of CSA-AKI. Significant factors ($p < 0.05$) on univariate analysis are summarised in *Table 11* and listed in order of strength of association.

A separate univariate analysis using AKI as the independent variable is given in *Table 12*. This table shows the differences in baseline demographics between those patients who developed CSA-AKI and those who did not.

Predictor	OR	95% CI	p-value
Age	1.019	0.995-1.044	0.118
Female Gender	1.11	0.573-2.151	0.757
Ethnicity (compared to white)			
South Asian	1.622	0.790-3.330	0.187
Black	1.352	0.348-5.249	0.663
Mixed	0.000	NA	0.999
Asian	0.000	NA	0.999
Middle Eastern	0.000	NA	0.999
Other	1.352	0.137-13.381	0.797
BMI	1.041	0.979-1.106	0.199
Cardiac Procedure (compared to CABG)			
CABG + valve	1.168	0.423-3.223	0.765
CABG + valve +other	4.087	0.246-67.82	0.326
CABG + other	1.362	0.135-13.71	0.793
Valve alone	1.202	0.577-2.505	0.623
Valve + other	0.876	0.232-3.304	0.845
Other	1.277	0.424-3.848	0.664
CABG (Yes Vs No)	0.917	0.499-1.686	0.781
Pre-op Angina (compared to stage 0)			
CCS 1	1.742	0.621-4.889	0.291
CCS 2	1.744	0.734-4.145	0.208
CCS 3	1.725	0.529-5.622	0.366
CCS 4	1.278	0.232-7.038	0.778
Pre-op NYHA stage			
NYHA 2	1.250	0.499-3.131	0.634
NYHA 3	1.538	0.574-4.124	0.392
NYHA 4	4.000	0.853-18.75	0.079
Previous Cardiac Surgery	1.599	0.538-4.753	0.399
Previous Malignancy	1.958	0.699-5.485	0.201
Diabetes Yes/No	2.026	1.064-3.859	0.032
Hypertension	1.230	0.601-2.514	0.571
Hypercholesterolaemia	2.164	1.165-4.018	0.015
Previous Smoking			
Ex-smoker	1.442	0.755-2.755	0.268
Current	1.828	0.674-4.956	0.236
Pre-op renal dysfunction (eGFR<60)	1.665	0.803-3.452	0.171
Pre op COPD	1.266	0.394-4.070	0.692

Pre-op Asthma	4.114	1.266-13.368	0.019
Pre-op Neuro disease			
TIA or RIND	0.503	0.111-2.287	0.374
CVA	0.704	0.149-3.318	0.657
Previous PVD	1.698	0.502-5.741	0.394
Pre-op ACEI	0.899	0.489-1.652	0.731
Pre-op Statin	0.977	0.524-1.822	0.942
Pre-op LV Function			
Fair	1.730	0.845-3.541	0.134
Poor	0.510	0.062-4.196	0.531
Pre-op Urgency			
Urgent	0.442	0.149-1.314	0.142
Emergency	3.429	0.211-55.82	0.387
1st Hb in ITU	0.981	0.964-0.999	0.036
Pre-op WCC	1.063	0.939-1.205	0.335
Pre-op INR	3.873	0.378-39.61	0.254
Pre-op APTT	1.039	0.968-1.115	0.287
Pre-op CRP	1.007	0.988-1.026	0.480
Pre-op Hb	0.776	0.649-0.928	0.005
Pre-op Cr	1.009	0.997-1.022	0.123
Pre-eGFR	0.992	0.979-1.005	0.234
Bypass time	1.013	1.006-1.020	<0.001
X-Clamp time	1.012	1.004-1.021	0.003
Logistic EuroSCORE	0.513	0.101-2.608	0.421
T/S Ratio	0.375	0.058-2.436	0.304

Table 10: Univariate analysis of the association of all pre-operative and intra-operative variables with the development of CSA-AKI.

Variable	OR	p-value
Bypass time	1.013	<0.001
X-Clamp time	1.012	0.003
Pre-op Hb	0.776	0.005
Hypercholesterolaemia	2.164	0.0145
Pre-op Asthma	4.114	0.019
Diabetes Yes/No	2.026	0.032
1st Hb in ITU	0.981	0.036

Table 11: Summary of predictors of CSA-AKI on univariate analysis listed by strength of association.

	Non-AKI (n=200)	AKI (n=54)	p-value
Age (median + IQR)	65 (20)	68 (16.8)	0.065
Male Gender	145 (72.5%)	38 (70.4%)	0.439
BMI	27.1 (6.4)	30.0 (6.3)	0.103
Ethnicity			0.502
White	146 (73%)	36 (66.7%)	
South Asian	35 (17.5%)	14 (25.9%)	
Black/Mixed	11 (5.5%)	3 (5.6%)	
Other	8 (4%)	1 (1.9%)	
Operation			0.944
CABG	97 (48.5%)	24 (44.4%)	
Valve	65 (32.5%)	18 (33.3%)	
CABG + Valve	22 (11%)	7 (13%)	
Other	16 (8%)	5 (9.3%)	
NYHA IV	5 (2.6%)	4 (7.5%)	0.290
CCS IV	9 (4.6%)	2 (3.8%)	0.765
Diabetes	45 (22.5%)	20 (37.0%)	0.025
Hypertension	148 (74%)	42 (77.8%)	0.354
Hypercholesterolaemia	88 (44%)	34 (63%)	0.010
Smoking History			0.376
Non-smoker	94 (47%)	20 (37%)	
Ex-smoker	88 (44%)	27 (50%)	
Current Smoker	18 (9%)	7 (13%)	
Pre-op eGFR <60	32 (16%)	13 (24.1%)	0.121
Previous COPD/Asthma	19 (9.5%)	10 (18.5%)	0.059
Previous TIA/CVA	24 (12%)	4 (7.4%)	0.245
LV Function			0.236
Good (>50%)	159 (79.5%)	39 (72.2%)	
Fair (39-49%)	33 (16.5%)	14 (25.9%)	
Poor (<39%)	8 (4%)	1 (1.9%)	
Operative Urgency			0.199
Elective	168 (84%)	49 (90.7%)	
Urgent	31 (15.5%)	4 (7.4%)	
Emergency	1 (0.5%)	1 (1.9%)	
Pre-op Haemoglobin	13.7 (2.3)	13.1 (1.9)	0.007
Pre-op Creatinine	82 (29)	86 (31)	0.083
Cross-Clamp Time	64 (43)	77 (59)	0.003
Cardiopulmonary Bypass Time	95 (39)	103 (65)	0.004

Table 12: Differences in pre-operative and intra-operative variables between patients who developed CSA-AKI and those who did not. Significant associations (p-value < 0.05) are shown in bold. IQR = interquartile range.

5.7.2: Multivariate analysis

5.7.2.1 Variable selection

There is no universally accepted method of variable selection in multivariate analysis and different studies use different methodology. A widely used practice in medical research is to perform variable selection by only including significant predictors on univariate analysis in a multivariate model. However, this method can risk masking of significant associations that are not significant on univariate analysis but that become significant once confounding factors are controlled for. Heinze *et al* (177) argue that non-significant variables should not be excluded from the multivariate model, particularly if they are the variable of interest. Furthermore, they argue that the most valid method of performing multivariate analysis is to include all variables without any selection. This however, is impractical for all but the largest of studies due to the problem of over-fitting the model.

Overfitting occurs when too many independent variables are applied to the multivariate model. The 'rule of 10 events' is a statistical standard that states that for logistic and Cox regression, models should be built with a minimum of 10 outcome events per predictor variable (EPV). Applying this rule means that we can only really correct for 5 variables for AKI and 2 variables for 1-year mortality. As such some method of variable selection is required. In the analysis below we have included all predictors with a significance level of $p < 0.05$ together with age and mTL in a multivariate model to find which were independent predictors for the development of CSA-AKI. Cross-clamp time was not included as it was not thought to be sufficiently independent from cardiopulmonary bypass time. The two variables are directly

related as bypass time incorporates cross-clamp time within it. Similarly, Pre-operative Haemoglobin (Pre-op Hb) and 1st Hb in ITU are also inter-dependant and so only the most significant variable, Pre-op Hb, was used. Results of this analysis are shown in *Table 13*.

This model improves the accuracy of predicting AKI from 78.7% to 81.2% (Nagelkerke R square value = 0.234). Increasing cardiopulmonary bypass time, pre-operative history of asthma, hypercholesterolaemia, and pre-operative haemoglobin level were found to be significant independent predictors of CSA-AKI. Neither mTL nor age were significant independent predictors of CSA-AKI.

Variable	Odds Ratio	95% CI	p-value
T/S Ratio	0.627	0.071-5.508	0.674
Age	1.008	0.980-1.037`	0.563
Hypercholesterolaemia	2.170	1.041-4.524	0.039
Hx of COPD	0.986	0.251-3.868	0.984
Hx of Asthma	6.240	1.584-24.584	0.009
Bypass Time	1.016	1.008-1.024	<0.001
Diabetes Yes/No	1.696	0.783-3.673	0.180
Pre-op Hb	0.771	0.625-0.953	0.016

Table 13: Multivariate model of independent predictors of CSA-AKI. Significant p-values <0.05 shown in bold.

5.8 Analysis of mTL as a predictor of 1-year mortality

The above analysis of section 5.7 was repeated to identify independent predictors of 1-year mortality following cardiac surgery. In this analysis post-operative factors that might be predictors of 1-year mortality were included in the analysis. Results of the univariate analyses are shown in *Table 14*, with significant predictors summarised by strength of association in *Table 15*.

Variable	OR	95% CI	p-value
LOS (increasing LOS a/w AKI)	1.04	1.014 - 1.075	0.004
Age	1.022	0.978 – 1.067	0.329
Female Gender	1.15	0.350 – 3.317	0.801
Ethnicity (compared to white)			
South Asian			
Black	1.007	0.270-3.751	0.992
Mixed	0	NA	0.999
Asian	0	NA	0.999
Middle Eastern	0	NA	0.999
Other	0	NA	0.999
	4.139	0.399-42.90	0.234
BMI	0.975	0.874-1.088	0.652
Cardiac Procedure (compared to CABG)			
CABG + valve	0.591	0.069-5.055	0.631
CABG + valve +other	0.000	NA	0.993
CABG + other	4.333	0.397-47.30	0.229
Valve alone	1.204	0.364-3.980	0.761
Valve + other	0.929	0.106-8.129	0.947
Other	0.684	0.079-5.890	0.730
CABG (Yes Vs No)	0.948	0.340-2.644	0.919
Pre-op Angina (compared to stage 0)			
CCS 1	1.667	0.350-7.930	0.521
CCS 2	1.348	0.341-5.330	0.670
CCS 3	0.625	0.062-6.339	0.691
CCS 4	0.000	NA	0.999
Pre-op NYHA stage			
NYHA 2	2.846	0.344-25.533	0.332
NYHA 3	2.741	0.294-25.51	0.376
NYHA 4	22.20	1.919-256.82	0.013
Previous Cardiac Surgery	0.910	0.112-7.396	0.929
Previous Malignancy	2.786	0.556-13.97	0.213
Pre-op Diabetes			
Diet	0.000	NA	0.995
Oral	2.600	0.887-7.618	0.082
Insulin	0.000	NA	0.991
Diabetes Yes/No	1.910	0.661-5.523	0.232
Hypertension	0.807	0.268-2.427	0.702
Hypercholesterolaemia	0.350	0.109-1.121	0.077
Smoking History			
Ex-smoker	2.480	0.738-8.339	0.142
Current	3.638	0.755-17.53	0.107
Pre-op renal dysfunction (eGFR<60)	2.652	0.860-8.174	0.09

Pre-op COPD	1.846	0.381-8.951	0.446
Pre-op Asthma	0.000	NA	0.999
Pre-op Neuro disease			
TIA	4.650	1.128-19.16	0.033
CVA	1.722	0.201-14.74	0.620
Previous PVD	1.176	0.142-9.731	0.881
Pre-op ACEI	2.041	0.636-6.546	0.230
Pre-op Statin	0.241	0.081-0.720	0.011
Pre-op LV Function			
Fair	0.571	0.087-2.175	0.473
Poor	1.714	0.088-10.74	0.626
Pre-op Urgency			
Urgent	1.639	0.434-6.187	0.466
Emergency	14.75	0.868-250.6	0.063
Extubation Date	1.610	1.149-2.256	0.006
Vasopressor Date	1.098	1.005-1.200	0.039
No. of Inotrope days	1.072	0.985-1.167	0.108
1st Hb in ITU	0.998	0.968-1.028	0.871
UO 1 st 12 hours	0.999	0.998-1.000	0.165
Reoperation	12.79	3.492-46.86	<0.001
Pt transfused in ITU	4.243	1.418-12.69	0.010
Clotting products	2.475	0.849-7.212	0.097
Post-op AF	0.787	0.244-2.537	0.688
Pre-op WCC	1.166	0.960-1.416	0.12
Pre-op INR	11.58	0.655-204.7	0.095
Pre-op APTT	1.036	0.866-1.239	0.699
Pre-op CRP	1.102	1.023-1.187	0.011
Pre-op Hb	0.555	0.404-0.762	<0.001
Pre-op Cr	1.031	1.012-1.051	0.002
Pre-eGFR	0.958	0.928-0.989	0.009
Bypass time	1.009	1.001-1.018	0.036
X-Clamp time	1.009	0.997-1.022	0.142
Logistic EuroSCORE	0.819	0.240-2.790	0.749
T/S Ratio	0.315	0.013-7.787	0.481

Table 14: Univariate analysis of the association of all pre-operative and intra-operative variables with 1-year mortality.

Variable	OR	p-value
Reoperation	12.79	<0.001
Pre-op Hb	0.555	<0.001
Pre-op Cr	0.974	0.002
LOS (increasing LOS a/w AKI)	1.04	0.004
Extubation Date	1.610	0.005
Pre-eGFR	0.958	0.009
Pt transfused in ITU	4.243	0.010
Pre-op CRP	1.102	0.011
Pre-op Statin	0.241	0.011
NYHA 4	22.20	0.013
TIA/RIND	4.65	0.033
Bypass time	1.009	0.036
Vasopressor Date	1.098	0.039

Table 15: Summary of predictors of 1-year mortality on univariate analysis listed by strength of association

Again, all of the factors in *Table 15* were entered into a multivariate logistic regression together with mTL and age, to find which were independent predictors for 1-year mortality (*Table 16*). Pre-CRP was excluded as more than 80% of cases were missing. The estimated GFR was also excluded. This was because the exact value for eGFR was not reported if more than 90. In such cases the results were reported as '>90' and therefore skewed the subsequent analyses. This model improves the accuracy of predicting 1-year mortality from 93.5% to 97% (Nagelkerke R square value = 0.760). Pre-operative history of stroke and pre-operative haemoglobin level were found to be significant predictors of 1-year mortality.

Mean TL was not found to be associated with 1-year mortality on multivariate modelling.

Variable	Adjusted Odds Ratio	95% CI	p-value
T/S Ratio	0.000	0.000-8.397	0.108
Age	1.015	0.909-1.133	0.793
LOS	0.933	0.788-1.104	0.418
NYHA 1	0.000	0.000-NA	0.997
NYHA 2	2.210	0.016-307.07	0.753
NYHA 3	9.660	0.052-1779.8	0.394
TIA	95.48	1.550-5881.9	0.030
CVA	76.71	1.173-5014.9	0.042
Pre-op Statin	0.455	0.041-5.056	0.522
Extubation days	2.120	0.518-8.671	0.296
Vasopressor days	1.131	0.963-1.329	0.133
Reoperation	6.462	0.006-6841.0	0.600
Blood Transfusion in ITU	14.62	0.525-406.5	0.114
Pre-op Hb	0.183	0.048-0.693	0.012
Pre-op Cr	1.030	0.995-1.065	0.092
Bypass Time	1.013	0.979-1.048	1.048

Table 16: Multivariate model of independent predictors of 1-year mortality. Significant p-values <0.05 shown in bold.

5.9 Potential over-fitting of multivariate model

As previously outlined in section 5.7.2.1, there is a potential problem of overfitting in the two multivariate analyses reported above due to relatively few outcome events; 54 in the case of AKI, and just 16 for 1-year mortality. Applying the 'rule-of-10' means that we can only really correct for 5 variables for AKI and 2 variables for 1-year mortality. The multivariate analysis for both CSA-AKI and 1-year mortality were repeated with the number of included variables limited to 5 and 2 respectively. For CSA-AKI, mTL and age were combined with the 3 most significant predictors on univariate analysis. For 1-year mortality mTL and pre-operative Hb were included in the model, as this variable was consistently strongly associated both on univariate and full multivariate analysis. The results of the multivariate analyses are shown in *Table 17* and *Table 18*. Again, mTL was neither associated with the development of CSA- AKI nor 1-year mortality. Both of these revised models had lower accuracy for predicting AKI and 1-year mortality than those including all significant predictors from the univariate analyses. In fact, Vittinghoff *et al* report that the rule-of-10-events can be relaxed, particularly for analyses undertaken to show adequate control of confounding (178).

Variable	Adjusted Odds Ratio	95% CI	p-value
T/S Ratio	0.567	0.068-4.712	0.599
Age	1.008	0.981-1.036	0.564
Bypass time	1.015	1.008-1.022	<0.001
Pre-op Hb	0.758	0.619-0.927	0.007
Hypercholesterolaemia	2.355	1.161-4.779	0.018

Table 17: Multivariate model of independent predictors of CSA-AKI limited to 5 predictors. Significant p-values <0.05 shown in bold

Variable	Adjusted Odds Ratio	95% CI	p-value
T/S Ratio	0.395	0.058-2.689	0.342
Pre-op Hb	0.778	0.650-0.930	0.006

Table 18: Multivariate model of independent predictors of 1-year mortality limited to 2 predictors. Significant p-values <0.05 shown in bold.

5.10 Receiver Operating Characteristic curve analyses

Receiver operating characteristic (ROC) curve analysis was performed for mTL against the development of CSA-AKI. This graphical plot determines the diagnostic ability of a variable to predict a binary outcome (e.g. AKI Vs No-AKI). Using every value of the variable as a cut-off point, the sensitivity (true positive rate) of a variable is plotted against the corresponding 1-specificity (false positive rate). The greater the area

under the resulting curve, the more useful the test is at predicting the outcome. An area under the curve (AUC) of 1 represents a test that perfectly predicts the correct outcome 100% of the time whilst an AUC of 0.5 indicates that the measurement of interest cannot distinguish between the two groups. An AUC significantly below 0.5 indicates that the test predicts a negative test outcome (e.g. if a patient does not have a disease). For our analysis, a p-value of <0.05 was used to indicate that the AUC was significantly different from 0.5.

ROC curves were calculated for mTL, age and Logistic EuroSCORE. The combined ROC curves for these three variables are shown in *Figure 15* with the accompanying AUC values, 95% confidence intervals and significance values shown in *Table 19*.

Whilst none of the variables are significant predictors of CSA-AKI, Age is the best predictor of the three with the highest AUC value. The AUC of 0.459 for mTL indicates that it is unable to predict CSA-AKI. The fact that this value is slightly less than 0.5 is consistent with the fact that a higher value of mTL would be expected to be associated with a lower biological age and thus a reduced risk of AKI; i.e. mTL would be expected to predict a negative disease state.

The same analyses were run for 1-year mortality as an outcome. The combined ROC curves for 1-year mortality for the same three variables are shown *Figure 16* with the accompanying Area under curve (AUC) values, 95% confidence intervals and significance values shown in *Table 20*. mTL was again not able to predict 1-year mortality with an AUC of 0.459. Age just missed significance (AUC 0.629, $p = 0.095$)

and EuroSCORE was seen to be able to predict 1-year mortality with an AUC of 0.741 (p=0.002).

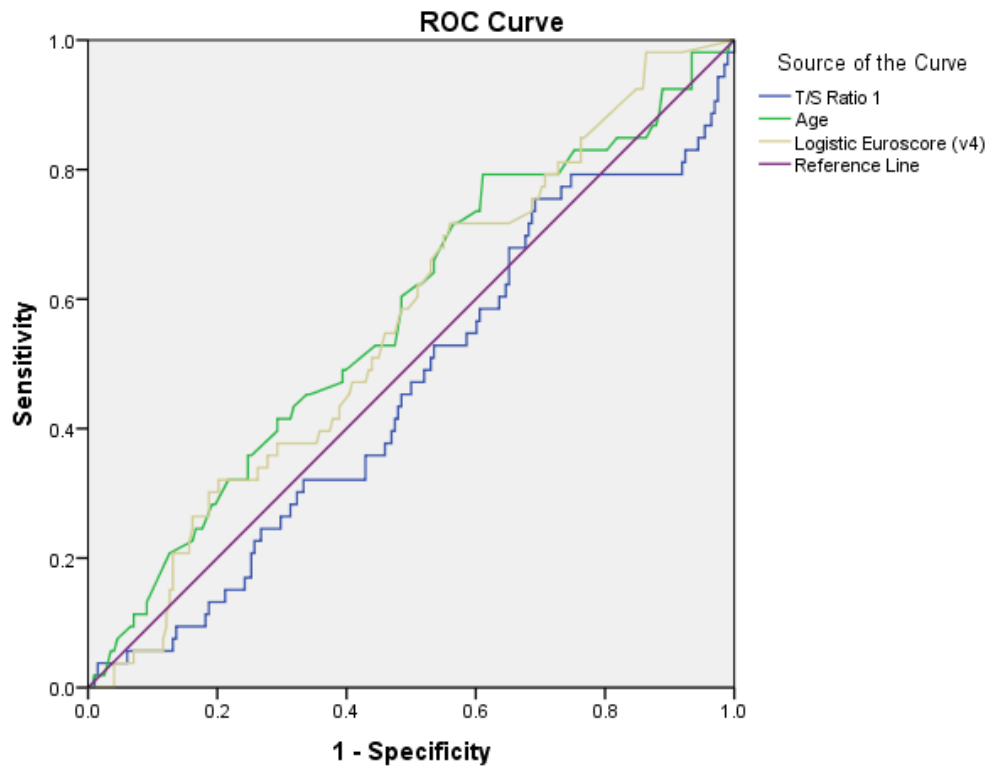


Figure 15: Combined ROC curve of mTL (T/S Ratio), age and Logistic EuroSCORE for predicting CSA-AKI

	AUC	95% CI	p-value	Cut-off	Sensitivity	Specificity
T/S ratio	0.459	0.373-0.545	0.357	0.618	0.759	0.305
Age	0.574	0.486-0.661	0.099	61.15	0.741	0.397
EuroSCORE	0.562	0.479-0.646	0.165	0.025 (2.5%)	0.717	0.419

Table 19: Diagnostic ability of mTL (T/S Ratio), age, and Logistic EuroSCORE for predicting CSA-AKI with cut-off points shown. None of the three variables are significant predictors of CSA-AKI.

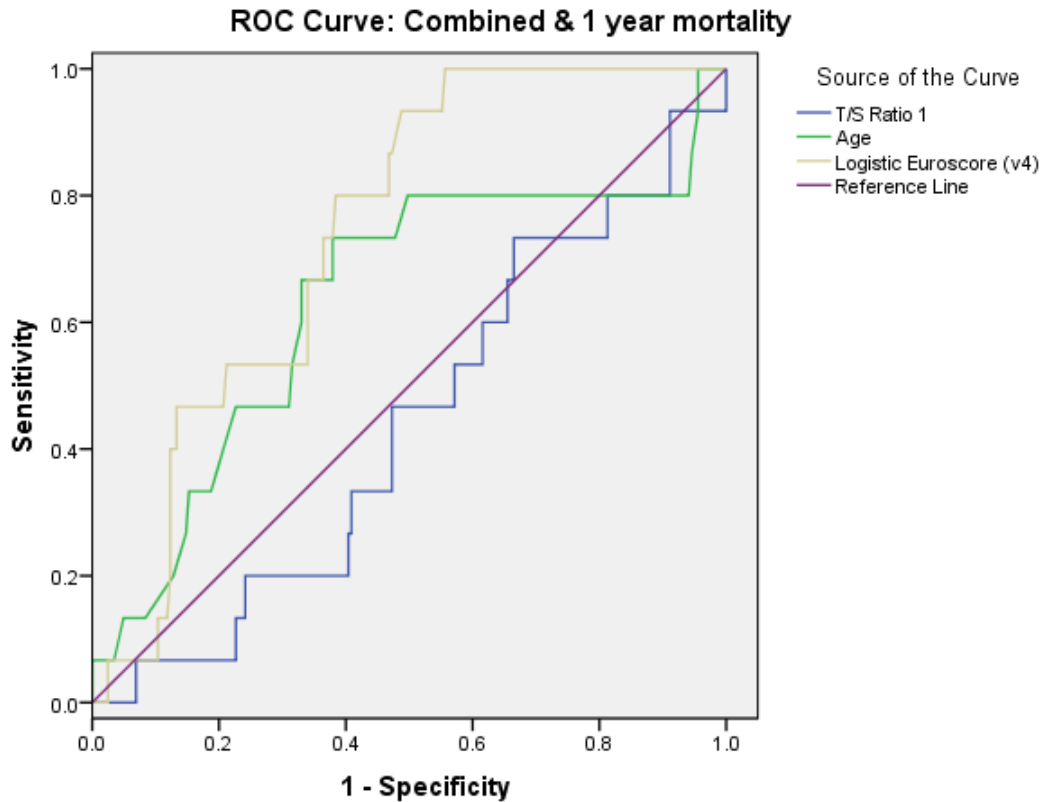


Figure 16: Combined ROC curve of mTL (T/S Ratio), age and Logistic EuroSCORE for predicting 1-year mortality

	AUC	95% CI	p-value	Cut-off	Sensitivity	Specificity
T/S ratio	0.459	0.320-0.597	0.581	0.634	0.75	0.332
Age	0.629	0.466-0.793	0.095	68.35	0.733	0.62
EuroSCORE	0.741	0.647-0.834	0.002	0.040 (4%)	0.733	0.635

Table 20: Diagnostic ability of mTL (T/S Ratio), age, and Logistic EuroSCORE for predicting 1-year mortality with cut-off points shown. P-values for statistically significant predictors are shown in bold.

5.11. Additional Analyses on Mean Telomere Length and CSA-AKI

5.11.1 Analysis of effects of fall in serum creatinine level

Studies have shown that the effect of an acute fall in serum creatinine is also associated with poor outcome similar to AKI (4). As such we identified all patients with an acute fall in serum creatinine $>26 \mu\text{mol/l}$ in keeping with the equivalent rise in creatinine defined as AKI in the AKIN criteria (*Table 1*). Only patients with a fall in the first 48 hours were identified to avoid classifying patients with recovery of previously elevated creatinine. Nine such patients were identified. Of note, 1 of the 9 patients was already classified as AKI due to a subsequent rise in serum creatinine after an initial fall. These nine patients were excluded from the data set completely and the analysis of mTL and AKI repeated. However, no significant association was found between mTL and the development of CSA-AKI (*Table 21, Figure 17*). The analysis was also repeated with the 9 patients added to the AKI group with no significant change in the association between mTL and CSA-AKI (results not shown).

Outcome measure	N	Mean T/S Ratio	SD	OR	95% CI	p-value
AKI						
No	192	0.761	0.163	0.363	0.055-2.400	0.293
Yes	53	0.734	0.164			

Table 21: Association between mTL and development of CSA-AKI in the whole population excluding patients whose serum Cr fell by >26 $\mu\text{mol/l}$.

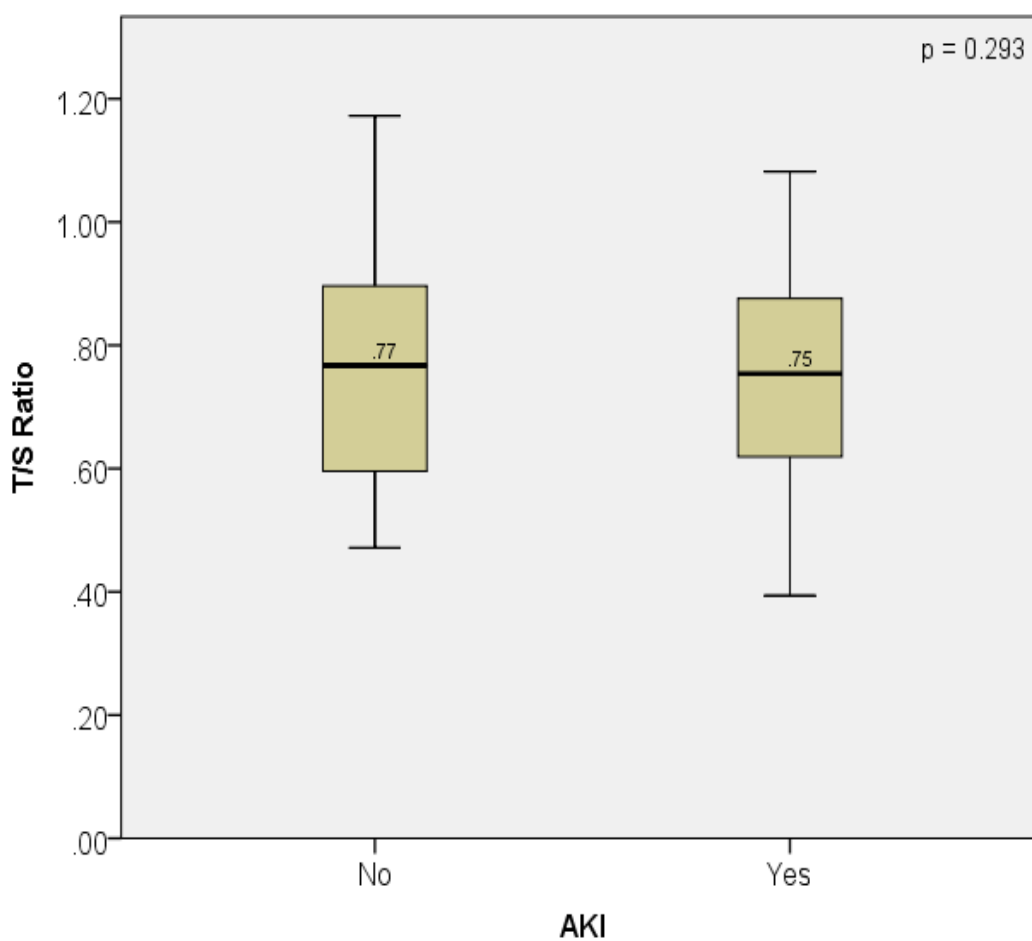


Figure 17: Boxplots for mTL and the development of CSA-AKI in the whole population excluding patients whose serum Cr fell by >26 $\mu\text{mol/l}$. Black bars represent median.

5.11.2 mTL and CSA-AKI: Investigating the effect of removing patients of South Asian Origin

The effect of ethnicity on Telomere length was investigated. We hypothesised that unreliability in the recorded birth dates of the South Asian immigrant population in East London might have affected our results. To test this theory, all patients of South Asian descent were excluded from the population and the association between mTL and CSA-AKI was rerun. The results are shown in *Table 22* and *Figure 18* and show that the trend towards shorter telomeres in the patients who developed CSA-AKI has been lost completely. As a result, we looked closer at just the South Asian population and found that in this population reduced mTL in patients was significantly associated with the development of CSA-AKI ($p=0.028$) (*Table 23, Figure 19*).

Outcome measure	N	Mean T/S Ratio	SD	OR	95% CI	p-value
AKI						
No	165	0.759	0.167	1.083	0.135-8.697	0.940
Yes	40	0.761	0.167			

Table 22: Association between mTL and development of CSA-AKI in the whole population excluding patients of South Asian descent.

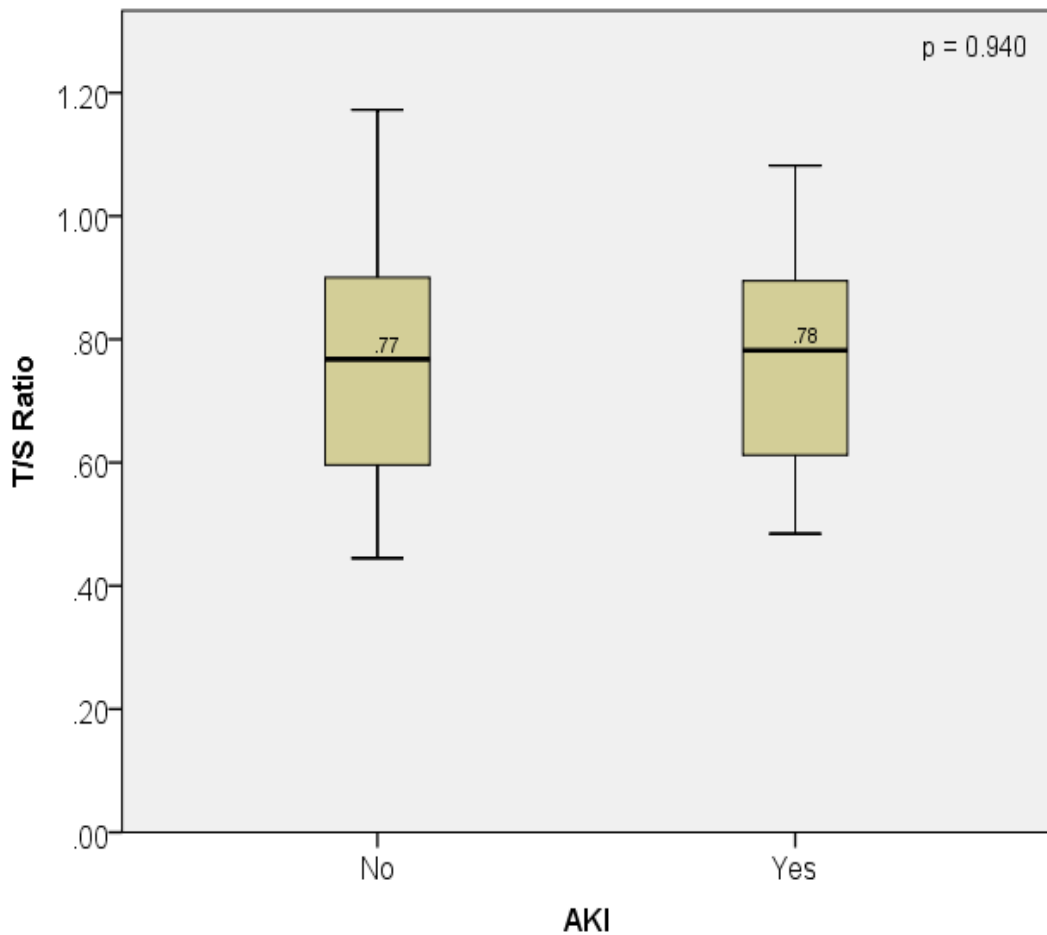


Figure 18: Boxplots for mTL and the development of CSA-AKI in the whole population excluding patients of South Asian descent. Black bars represent Median values.

Outcome measure	N	Mean T/S Ratio	SD	OR	95% CI	p-value
AKI						
No	35	0.767	0.142	0.003	0.000-0.489	0.025
Yes	14	0.660	0.127			

Table 23: Association between mTL and development of CSA-AKI in patients of South Asian descent

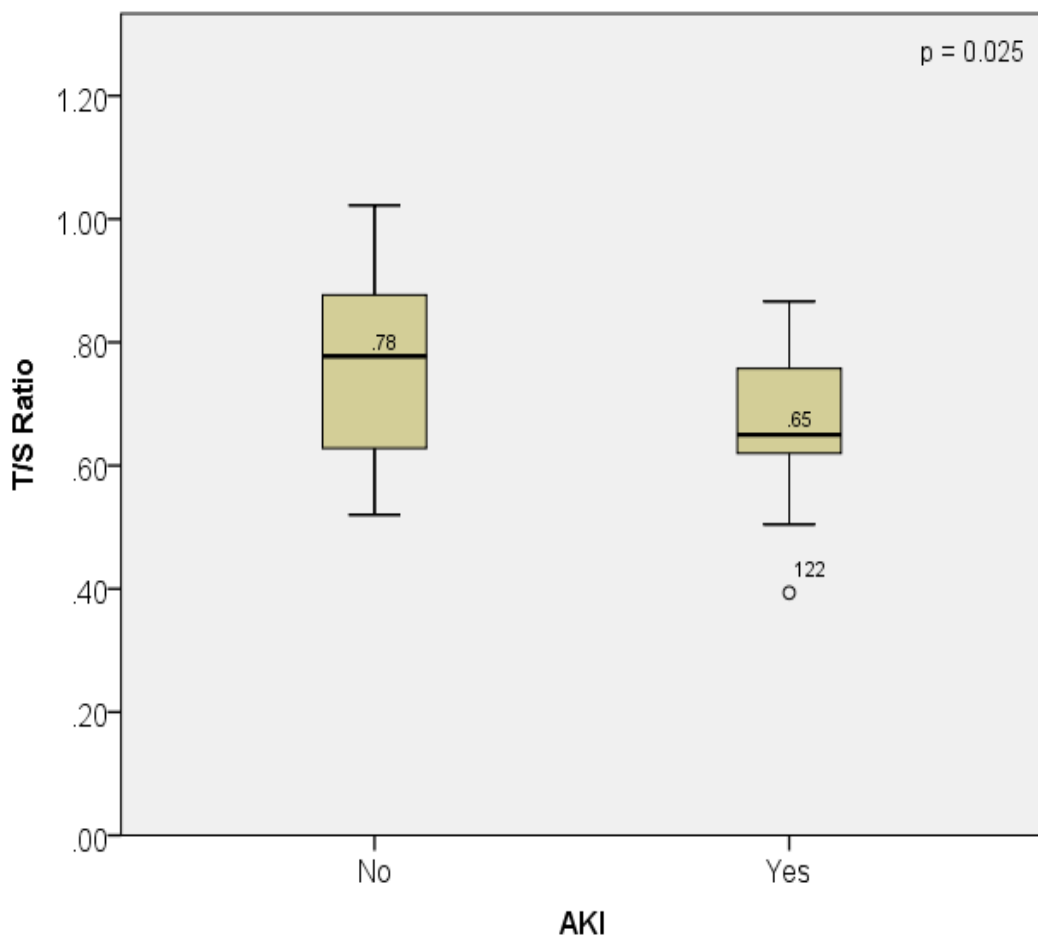


Figure 19: Boxplots for mTL and the development of CSA-AKI in patients of South Asian descent. Black bars represent median.

5.11.2.1: Univariate analysis of mTL and CSA-AKI in South Asians

A repeat of the univariate and multivariate analyses outlined in sections 5.7.1 and 5.7.2 were performed but limited to the South Asian population. Results of the Univariate analysis are shown in *Table 24*. Some categories are listed as Non-applicable (N/A) as the reduced sample size removed any events from one of the coding categories. Significant associations ($p < 0.1$) on univariate analysis are summarised in *Table 25*.

5.11.2.2. Multivariate analysis of mTL and CSA-AKI in South Asians

Of the significant predictors of CSA-AKI given in *Table 25*, Pre-op Hb and Pre-op eGFR were excluded for reasons described previously. The remaining two variables were run as a multivariate analysis thus avoiding the problem of overfitting with just 14 outcomes in the AKI group. The result shows that mTL remains an independent predictor of CSA-AKI (*Table 26*). Even when age was added to the model, mTL remained as a significant independent predictor of CSA-AKI in the South Asian population (*Table 27*).

Predictor	OR	95% CI	p-value
Age	1.042	0.976-1.112	0.218
Female Gender	0.682	0.156-2.972	0.610
BMI	0.997	0.881-1.136	0.997
CABG (Yes Vs No)	1.500	0.271-8.300	0.642
Pre-op Angina			
CCS 1	0.000	n/a	0.999
CCS 2	0.857	0..55-13.479	0.913
CCS 3	1.667	0.152-18.217	0.675
CCS 4	1.000	0.041-24.547	1.000
Pre-op NYHA stage			
NYHA 2	1.000	0.053-18.915	1.000
NYHA 3	0.947	0.076-11.870	0.967
NYHA 4	0.400	0.023-6.848	0.527
Previous Cardiac Surgery	2.615	0.152-44.968	0.508
Previous Malignancy	N/A		
Diabetes Yes/No	2.969	0.780-11.301	0.111
Hypertension	1.000	0.170-5.878	1.000
Hypercholesterolaemia	3.088	0.732-13.025	0.125
Previous Smoking	N/A		
Pre-op renal dysfunction (eGFR<60)	0.788	0.179-3.477	0.753
Pre op COPD	N/A		
Pre-op Asthma	N/A		
Pre-op Neuro disease	N/A		
Previous PVD	1.698	0.502-5.741	0.394
Pre-op ACEI	1.000	0.286-3.499	1.000
Pre-op Statin	3.852	0.435-34.130	0.226
Pre-op LV Function	N/A		
Pre-op Urgency	1.500	0.271-8.300	0.642
1st Hb in ITU	0.947	0.894-1.002	0.059
Pre-op WCC	1.192	0.872-1.629	0.271
Pre-op INR	17.792	0.198-1600.967	0.210
Pre-op APTT	1.141	0.915-1.423	0.241
Pre-op CRP	1.018	0.882-1.176	0.805
Pre-op Hb	0.674	0.437-1.041	0.075
Pre-op Cr	1.012	0.989-1.036	0.295
Pre-eGFR	0.969	0.940-0.999	0.045
Bypass time	1.007	0.982-1.032	0.576
X-Clamp time	0.995	0.967-1.023	0.703
Logistic EuroSCORE	0.147	0.000-46.472	0.514
T/S Ratio	0.003	0.000-0.489	0.025

Table 24: Univariate analysis of the association of all pre-operative and intra-operative variables with CSA-AKI for the South Asian population.

Predictor	OR	95% CI	p-value
T/S Ratio	0.003	0.000-0.489	0.025
Pre-eGFR	0.969	0.940-0.999	0.045
1st Hb in ITU	0.947	0.894-1.002	0.059
Pre-op Hb	0.674	0.437-1.041	0.075

Table 25: Summary of univariate analysis of predictors of CSA-AKI in the South Asian population listed by strength of association.

Predictor	OR	95% CI	p-value
T/S Ratio	0.002	0.000-0.521	0.028
1st Hb in ITU	0.941	0.882-1.003	0.061

Table 26: Results of a Multivariate analysis of mTL and CSA-AKI in the South Asian population

Predictor	OR	95% CI	p-value
T/S Ratio	0.002	0.000-0.665	0.036
Age	1.019	0.945-1.098	0.627
1st Hb in ITU	0.940	0.882-1.002	0.058

Table 27: Results of the multivariate analysis when age is added as a variable in the model. mTL remained an independent predictor of CSA-AKI in the South Asian population.

5.11.3 Analysis of mTL as a predictor of 1-year mortality in South Asian population

The analysis of mTL as a predictor of 1-year mortality was repeated for the South Asian population. The results are shown in *Table 28* and graphically in *Figure 20*. Of the 40 patients with complete 1-year mortality data, only 3 had died within 12 months of their index operation. (7.5%). Whilst these patients did have reduced telomere length the trend did not reach statistical significance ($p=0.118$). However, 1-year mortality was also associated with a trend towards increased age ($p=0.085$). When the association between mTL and age was corrected for age its significance was reduced ($p=0.236$).

Outcome measure	N	Mean T/S Ratio	SD	OR	95% CI	p-value
Alive at 1 year				0.000	0.000-7581	0.118
Yes	37	0.751	0.132			
No	3	0.611	0.197			

Table 28: Association between mTL and 1-year mortality in patients of South Asian descent

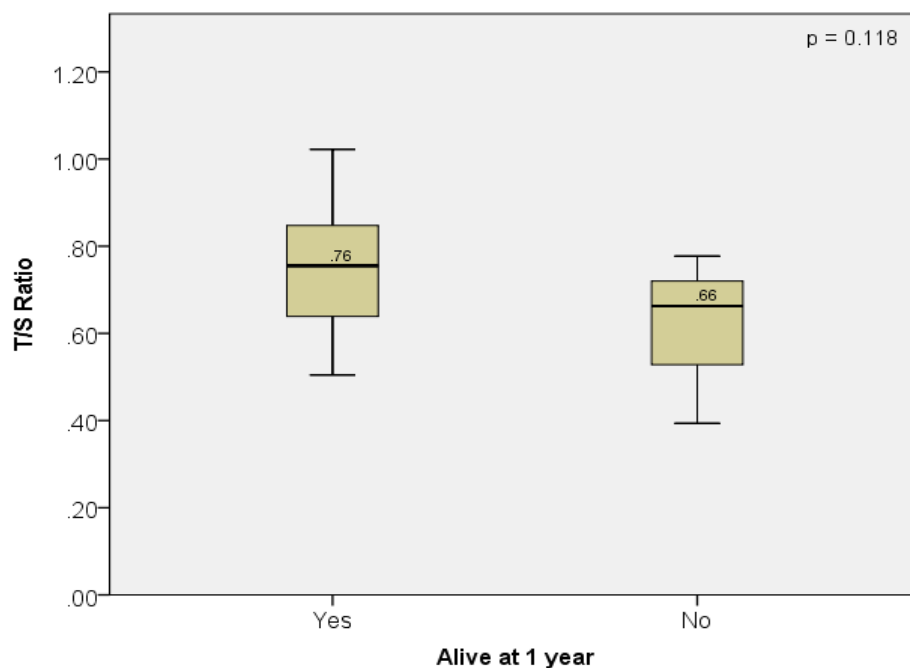


Figure 20: Boxplots for mTL and 1-year mortality in patients of South Asian descent. Black bars represent median

5.12 Results of STELA Experiment

The STELA gels of the 24 samples showing the telomere length distribution are shown in *Figure 21*. Due to one sample in the control population (sample 103) having a borderline DNA concentration an additional sample was run (sample 175) as an alternative match. Sample 103 was successfully run, negating the need for sample 175 in subsequent analysis. Unfortunately sample 244 (AKI cohort) failed. STELA analysis was repeated for this sample using an increased amount of input DNA but again failed. As such this sample and its matched control had to be excluded from subsequent analysis.

The raw data listing all telomere lengths for each sample is given in *Appendix G*. *Figure 22* is the graphical representation of this data and shows the distribution of the individual XpYp telomere lengths from each sample. From a visual inspection there does not appear to be an obvious trend in mean telomere length between the AKI cohort and their controls with many of the 95% CI's overlapping. *Table 29* shows a summary of the data for each sample including mean, median, and 25th percentiles of TL. No significant differences were found between the matched AKI and Non-AKI groups for either mTL (5.037 Vs 5.346; $p = 0.657$), median TL (4.920 Vs 5.134; $p = 0.859$) or 25th percentile TL (3.725 Vs 3.698; $p = 0.790$) using a related samples Wilcoxon signed rank test.

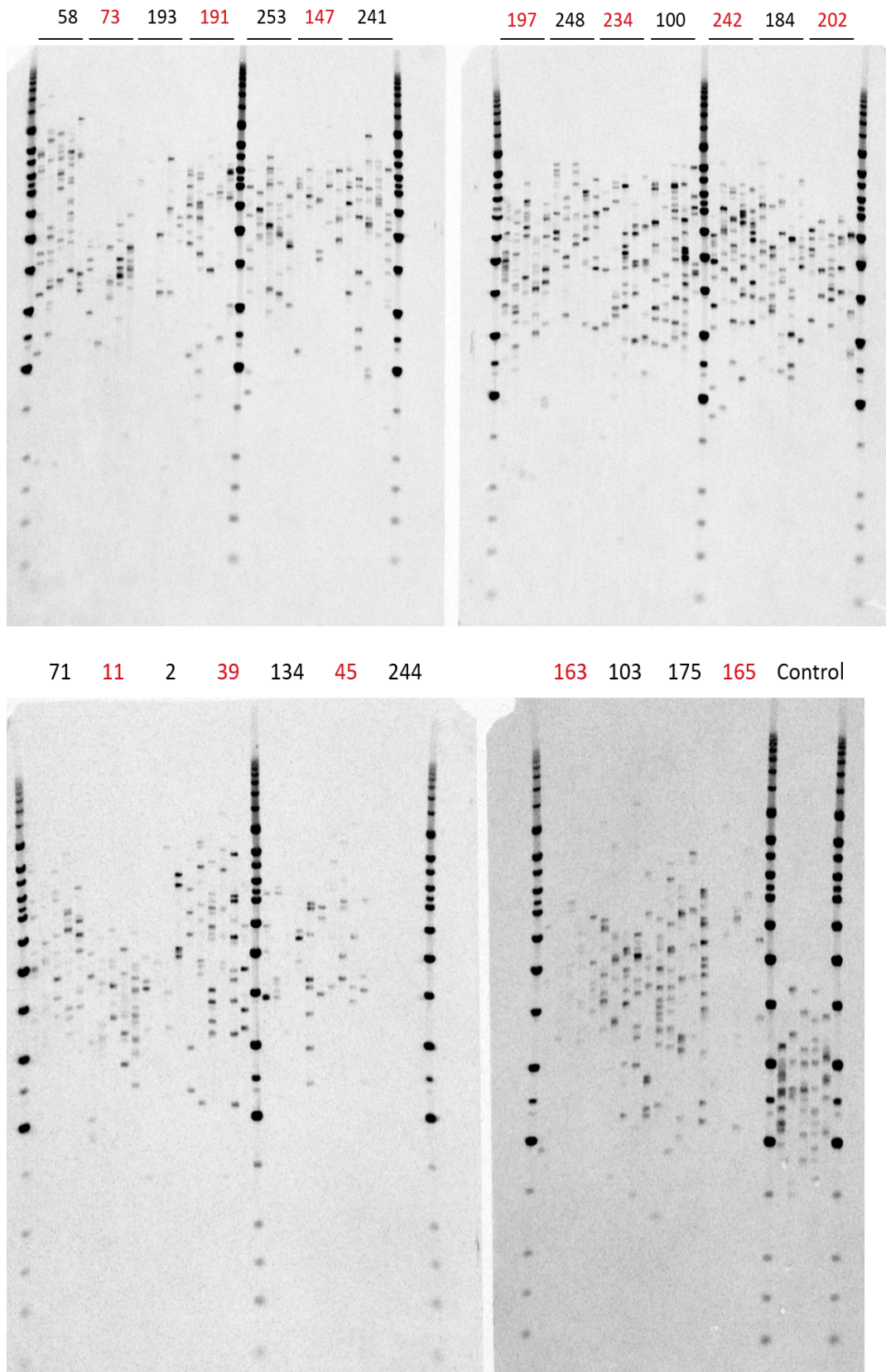


Figure 21: STELA Gels of the 12 matched AKI-control pairs. Red samples = AKI cohort. Note, no fragments seen for sample 244.

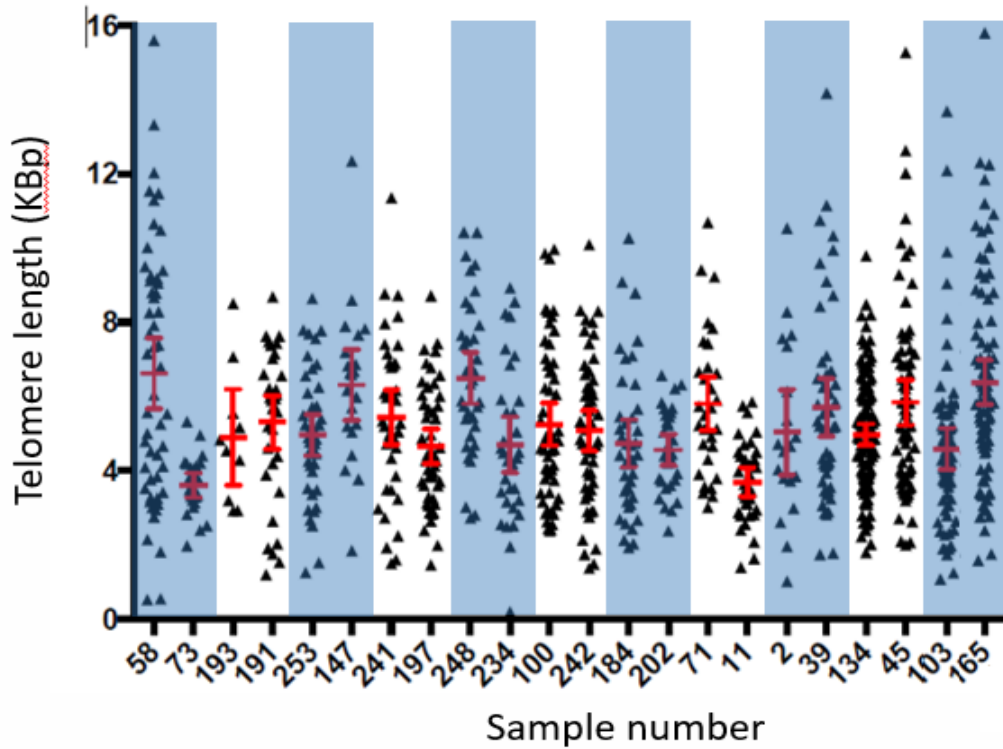


Figure 22: Scatter plot showing the distribution of telomere lengths for each sample. Red bars show the mean and 95% confidence intervals. Light blue and white bands indicate paired samples (11 total). Within each pair the first sample is the control, and the second from the AKI cohort.

Pair	25 th Percentile		Mean		Median	
	AKI	Non-AKI	AKI	Non-AKI	AKI	Non-AKI
1	3.151	3.586	3.605	6.62	3.539	6.421
2	4.048	3.126	5.303	4.899	5.89	4.687
3	5.123	3.761	6.311	4.959	6.594	4.858
4	3.371	3.679	4.644	5.445	4.284	5.341
5	3.174	5.011	4.701	6.497	4.408	6.402
6	3.517	3.409	5.075	5.247	5.104	4.811
7	3.696	3.198	4.555	4.734	4.429	4.421
8	2.864	4.208	3.693	5.808	3.538	5.595
9	3.707	3.733	5.708	5.037	5.207	4.664
10	3.800	3.767	5.837	4.975	5.220	4.902
11	4.529	3.205	6.375	4.589	5.902	4.370
Mean	3.725	3.698	5.073	5.346	4.920	5.134
p=value	0.790		0.657		0.859	

Table 29: Comparison of mean TL, median TL and 25th percentile TL between the 11 propensity matched sample pairs. Mean values for the combined AKI/Non-AKI cohorts are shown in dark grey.

5.13 Correlation between qPCR and STELA measurements of mean TL

23 samples were successfully analysed for mean TL by both qPCR and STELA. For these samples, the result of mTL obtained by each method were compared using Spearman's Correlation. The correlation is shown in *Figure 23*. The Spearman Correlation Coefficient between the two variables was 0.199 ($p= 0.374$).

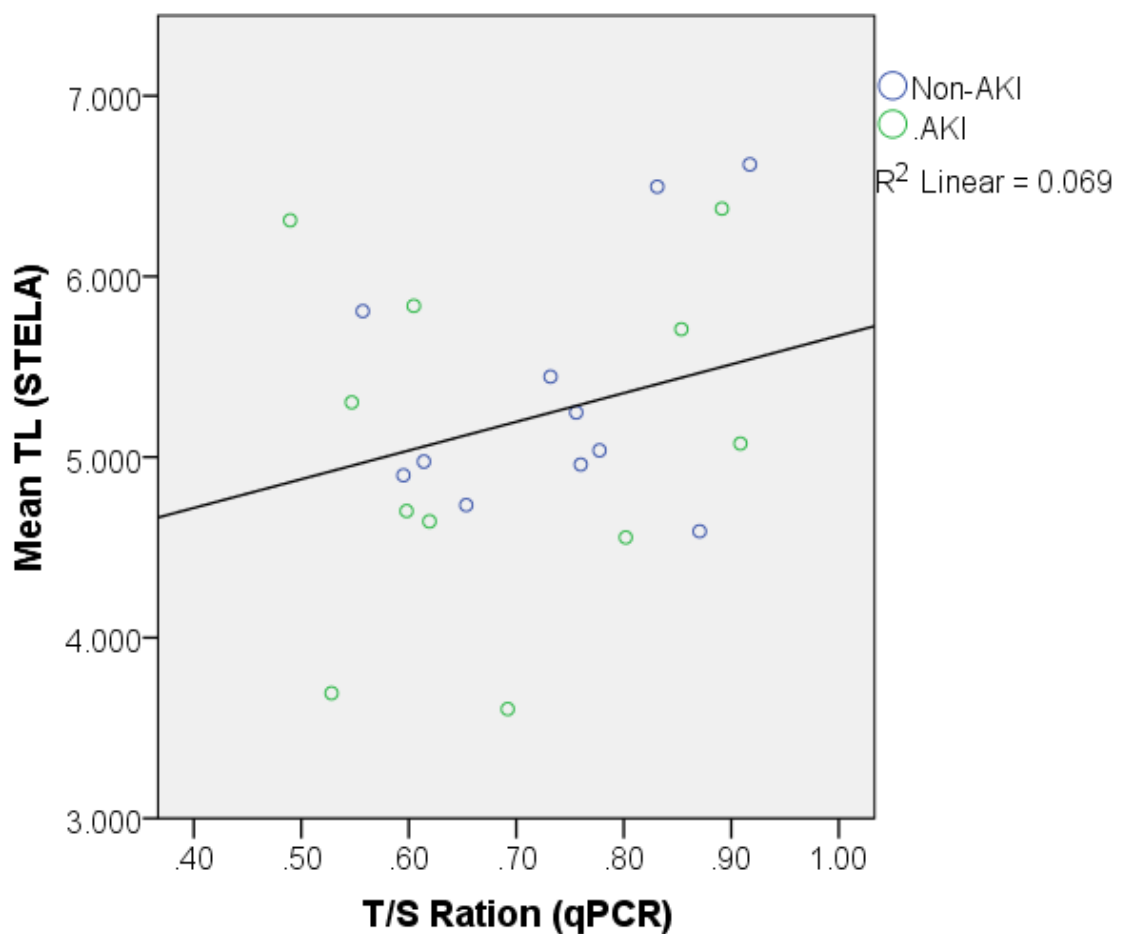


Figure 23: Correlation between Mean TL as measured by STELA and T/S Ratio measured by qPCR. Green dots = AKI cohort. Blue dots = Non-AKI cohort.

5.14 Discussion of mTL Telomere Length and CSA-AKI

5.14.1 Discussion of main findings

Primary outcome

This study attempts to determine if a well-recognised and studied marker of senescence such as Telomere length can predict the development of CSA-AKI. The main finding of this study is that, in our overall population, Telomere length is not associated with the development of CSA-AKI [OR 0.375 (0.058-2.436); $p=0.304$]. The trend of the non-significant association is in the expected direction with the $OR < 1$ signifying a negative correlation between Telomere length and AKI; i.e. as mTL decreases the risk of developing AKI increases. ROC curve analysis showed that mTL is a worse predictor of CSA-AKI and 1-year mortality than a patient's age.

The fact that mTL was not significantly associated with CSA-AKI in >250 patients means that it is unlikely to ever play a significant role in the risk stratification of patients undergoing cardiac surgery. It also implies that even if patients with reduced telomere length have higher levels of cellular senescence, this does not confer significantly increased risk of developing AKI when compared to the already recognised risk factors such as length of cardiopulmonary bypass and pre-operative anaemia.

Secondary endpoints

No significant association was found between mTL and any of the secondary outcomes of in-hospital mortality, 1-year mortality and the composite outcome. Due to the low numbers of endpoints in In-hospital mortality (n=5) and 1-year mortality (n=16), this is not surprising. The study is underpowered to detect all but the largest of effect sizes with these low number of endpoints. To try to address this, a composite outcome was created consisting of CSA-AKI, new AF, stroke, and reoperation. This endpoint was created to provide a measure of post-operative morbidity. The more commonly used composite outcome in studies of patients post-cardiac surgery is 'Major Adverse Cardiac and Cerebrovascular Events' (MACCE) (179). This endpoint encompasses 30-day mortality together with, stroke, myocardial infarction, and need for repeat revascularisation. This measure was not used in the current study due to the absence of patients with post-operative MI or repeat revascularisation. As such the use of MACCE would only have yielded 9 endpoints (5 deaths; 4 stroke).

Other significant findings

Mean Telomere length was found to be significantly associated with several other variables. The strongest association that we see is the correlation with age (Spearman correlation coefficient of -0.213; p=0.001). The spread of the values of mTL (T/S Ratio) are similar to that published by Qiagen in a validation experiment performed on the same PCR platform as used in the present study (Corbett Research Rotorgene 6000, Qiagen, Manchester, UK). (180). The abstract of this experiment is shown in *Appendix H* with the relationship between mTL and age shown in *figure 6*.

Qiagen's experiment serves as a measure of validation that the results that we have obtained for mTL in the current studies are accurate. However, it is also notable that the association found between mTL and age is not as strong in the current study as that found by Qiagen. This may be a result of the population being studied and reflect the fact that these are patients rather than healthy controls. Support for this can be found in the results of a large study of the West of Scotland Primary Prevention Study (WOSCOPS) cohort (174). Brouillette *et al* found that whilst the matched control population showed a significant correlation with age (n=1058; R=0.01; p<0.001) the cases with coronary artery disease did not (n=464; R =0.06; p=0.190)(Figure 24). The authors performed telomere length measurement in >1500 patients using broadly the same methodology for Telomere measurement as that used in the current study. In comparison, our study results show a stronger correlation between T/S ratio and age over a reduced number of similar patients (n=254; R=0.247; p=0.001).

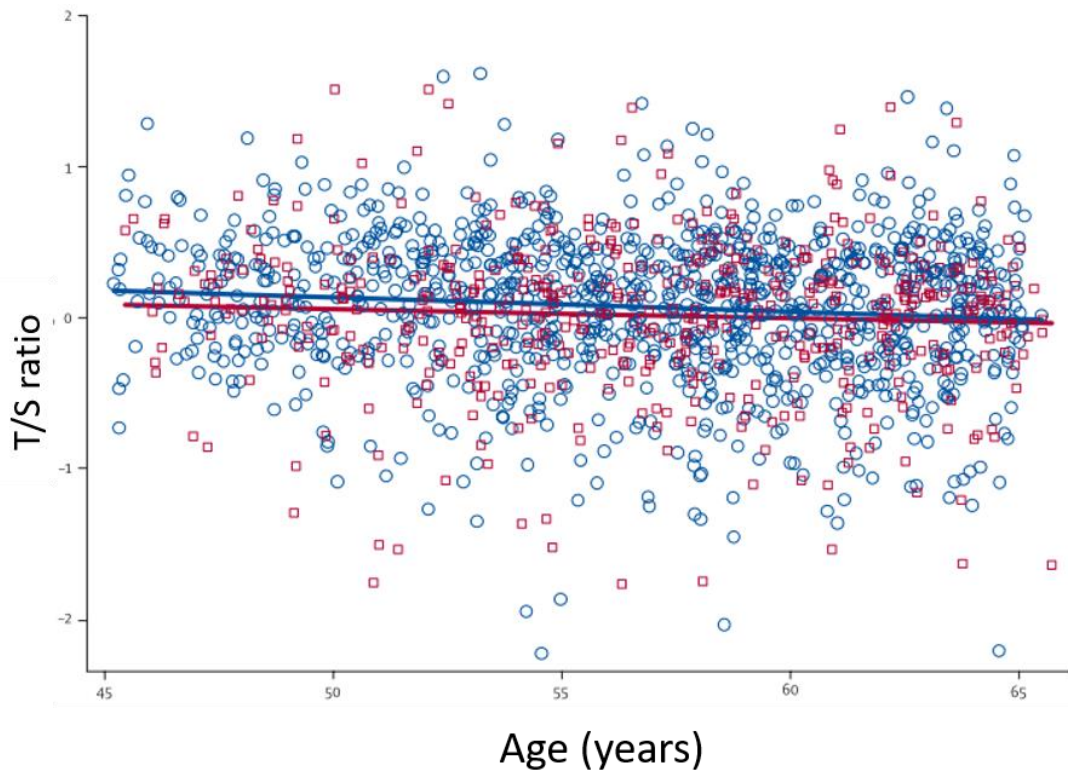


Figure 24: Telomere length as a function of age in controls and cases. Controls are shown as blue circles ($n=1058$), cases as red squares ($n=484$). Telomere length is plotted as log T/S ratio. R values were 0.01 ($p=0.001$) for controls and 0.06 ($p = 0.1902$) for cases. Reprinted from *The Lancet*, Vol 369, Telomere length, risk of coronary heart disease, and statin treatment in the West of Scotland Primary Prevention Study: a nested case-control study, Pages No 109, Copyright (2007), with permission from Elsevier.

The other significant associations that were found with Telomere length include duration of vasopressor therapy, history of hypercholesterolaemia and type of cardiac surgery (CABG Vs Non-CABG). Mean Telomere length was found to have a significant positive association with duration of post-operative vasopressor therapy (OR 0.159; $p=0.011$). The reason for this association is not clear and is the reverse of the relationship that we would have expected to observe. If we assume that more elderly or frail individuals are more likely to need blood pressure support following surgery, we would have expected a negative relationship between telomere length and vasopressor duration. However, this assumption may be incorrect. There is

evidence to suggest that the inflammatory response to cardiac surgery is reduced in elderly patients. Dieleman *et al* performed a retrospective analysis of 28,513 patients and investigated the link between age and the development of Systemic Inflammatory Response Syndrome (SIRS) following cardiac surgery (181). They found that increased patient age was strongly associated with reduced postoperative SIRS prevalence in the first 24 hours post-operatively with a relative risk value of 1.38 in patients aged less than 43 years compared to patients aged 72-83. As such, younger patients might on average be expected to require a greater duration of vasopressor support and would also be expected to have increased telomere length in comparison to older patients, although this hypothesis is purely speculative. If this were the case, we would expect to see a correlation between age and vasopressor support also. Our results do show a negative correlation between age and duration of vasopressor therapy but this does not reach statistical significance (Spearman correlation – 0.063; $p= 0.318$).

Mean Telomere length was found to have a statistically significant association with patients undergoing coronary artery bypass grafting (CABG) compared to those having other types of cardiac surgery (Non-CABG). The average mTL in the CABG group was 0.735 compared to 0.783 in the non-CABG group ($p=0.02$). This finding is in line with previous studies that report associations between telomere length, atherosclerosis and coronary artery calcification. Samini *et al* were the first to discover the association between reduced telomere length and CAD in a pilot study of 30 patients (124). The 10 patients with CAD had mean terminal restriction fragment (TRF) lengths of 303 (SD 90) base pairs shorter than those of the 20 control

patients ($p=0.002$). Weischer *et al* performed a large population study that measured mTL by PCR in >19000 patients who were followed up for the endpoints of MI, IHD and death over a 19-year period. Reduced mTL was found to be associated with increased risk of all three primary endpoints [adjusted HR= 1.10 (95% CI 1.01–1.19) for MI, 1.06 (1.00–1.11) for IHD, and 1.09 (1.05–1.13) for early death per 1000–base pair decrease in telomere length].

The potential underlying mechanisms for this well-established association has been previously discussed in section 1.6.1. The Telomere hypothesis states that it is the attrition of telomeres that is directly responsible for the development of subsequent disease. Alternatively, the modulating hypothesis states that it is the association of short telomere length with atherosclerotic risk factors such as smoking, diabetes, hypercholesterolaemia, hypertension, physical inactivity and obesity that is responsible for the observed association between mTL and CAD. If this second hypothesis is correct then mTL would be expected to be associated with the traditional atherosclerotic risk factors in this cohort. This is in line with our own observations. Hypercholesterolaemia was associated with a significant reduction in mTL with an average mTL of 0.734 and 0.744 in patients with and without hypercholesterolaemia respectively ($p=0.042$). A similar trend was seen in patients taking statin therapy although this did not reach statistical significance (0.081). This may reflect previous findings that statin therapy attenuates the risk of premature telomere shortening (174). In terms of other recognized atherosclerotic risk factors, we found trends towards reduced mTL in diabetes ($p=0.07$), hypertension ($p=0.162$)

and increased BMI ($p=0.2$), although none of these trends reached statistical significance.

5.14.2 Comparison of results with previous studies

The main outcome of this study is the lack of an association between mTL and CSA-AKI. This specific area has not been studied before and as such there is no body of evidence for direct comparison. To date, this study remains the sole study of the association between mTL and AKI in humans, with the animal models of AKI produced by Westhoff *et al* previously discussed in section 1.6.3. However, there are a few previous studies into Telomere length and outcomes after cardiac surgery.

Brault *et al* studied the relationship between Telomere length and frailty in elderly patients undergoing cardiac surgery (182). In 59 patients over the age of 70 there was an unexpected positive association between mTL and increasing number of clinical frailty criteria. Although the authors mention that one of the primary outcomes of the study was renal failure, the relationship between mTL and this outcome is not described. Since the study only included 59 patients, there were likely too few patients with post-operative renal failure to draw meaningful conclusions.

D'Amario *et al* studied the relationship between the growth properties of cardiac stem cells (CSCs) and several markers of cardiac function following cardiac surgery including ventricular wall thickness, chamber diameter and volume, ventricular mass and ejection fraction (183). In 55 patients, telomere length of CSC's harvested from

right atrial tissue was included as one of the studied growth properties. Statistically significant positive associations were described between mTL and ventricular wall thickness, ventricular mass, ventricular mass/chamber volume ratio, and post-operative ejection fraction, whilst a significant negative association was found with end-diastolic and end-systolic volumes. However, how these findings of reduced mTL and markers of reduced cardiac function related to clinical endpoints was not investigated.

Roberts *et al* investigated the relationship between mean peripheral leukocytes telomere length (LTL) and right atrial telomere length (ATL) with the incidence of post-operative AF in 35 patients undergoing cardiac surgery (184). The authors found no association between either LTL or ATL and the development of AF. They also demonstrated consistently higher LTL than ATL within patients, with a consistent relationship across both the AF and Non-AF cohort. Limitations of this study include its small patient numbers and the fact that patients with new onset of AF post-op were not differentiated from patients with a history of chronic or paroxysmal AF, two very distinct conditions in terms of pathophysiology. In the current study, no association was found with mTL and the incidence of new post-operative AF (OR 1.045; $p=0.959$) which is consistent with Roberts *et al's* findings. The current study remains one of the few of telomere length and clinical outcomes following cardiac surgery, and the largest to date.

5.14.3 Discussion of additional analysis of mTL in CSA-AKI.

Additional analyses showed that excluding patients with acute falls in serum creatinine did not alter the finding of a lack of association between mTL and CSA-AKI. However, a subgroup analysis based on ethnicity revealed an interesting finding of a significant association between mTL and CSA-AKI only in South Asian patients. The population as a whole are primarily either white (n=182) or South Asian (n=49) with just 14 black/mixed race patients and 9 patients with other ethnicities. When comparing the South Asian population with the rest of the cohort, there was no significant difference in mean TL (0.737 Vs 0.759; $p = 0.473$), incidence of AKI (28.6% Vs 19.5%; $p = 0.164$), or 1-year mortality (7.5% Vs 7.2%; $p = 0.944$). However, within the South Asian population, reduced mTL was significantly associated with the subsequent development of CSA-AKI on both univariate (OR = 0.003; $p = 0.025$) and multivariate analysis (OR 0.002; $p = 0.036$). At present the reason for the finding of reduced mTL in CSA-AKI for South Asians only is not clear and cannot be elicited further from the current findings. It may be that a second factor is predisposing South Asian patients with short Telomere's and increased cell senescence to CSA-AKI as part of a two-hit phenomenon. As a clinically based outcome study, the aim of the present study was to identify whether or not an association between mTL and the development of CSA-AKI existed, not to determine the mechanism underlying it. This will now form the focus of future investigation.

In this cohort, there was a trend towards reduced mTL in patients who were deceased at 1 year compared with those who were alive (0.611 Vs 0.751) but this failed to reach statistical significance ($p=0.118$). This was likely due to the extremely

low number of endpoints, with just 3 deaths at 1 year out of the 40 patients for which 1-year mortality data was available (7.5%). This makes the analysis underpowered and limits the validity of drawing any conclusions based on this small population. In addition, it is worth noting that at least part of the cause of this association was increased age in the deceased patients. When we corrected for age the strength of the association between mTL and 1-year mortality was reduced ($p=0.236$). It may be that with further follow up out to 5 years the number of endpoints increases sufficiently to allow any true association between long term survival and mTL to become apparent, both in the South Asian subgroup and in the study population as a whole.

5.14.4 Discussion of STELA Pilot experiment

The aims of this pilot study were to investigate whether an alternative method of TL measurement would reveal an association with CSA-AKI and to determine the correlation between TL measurements made by different methods in the same samples. The first finding of this pilot study was that, as with the main study, there was no significant difference between mTL between the AKI cohort and their matched controls. The STELA method measures the range of lengths of the XpYp telomeres within a sample. Lin *et al* (185) and Williams *et al* (186) have used STELA derived telomere length to determine prognosis in Chronic Lymphocytic Leukaemia (CLL), Acute Myeloid Leukaemia (AML) and Myelodysplastic Syndrome (MDS). Lin *et al* determined the fusogenic threshold of the XpYp chromosomes in CLL, defined as the value of mean TL in a sample below which telomere end-to-end fusion events

were seen to occur. For the XpYp telomere this fusogenic threshold was a mean TL of <3.81KBp. Williams *et al* found that using this same fusogenic threshold provided high prognostic resolution in MDS [HR = 5.0, P < 0.0001] but not AML [HR = 0.68, P = 0.2]. Unfortunately, this method of stratifying patients could not be used in this pilot study as only 2 of the 22 paired samples demonstrated a mTL level below this fusogenic threshold of 3.81. Interestingly both of these samples formed part of the AKI cohort. As such, mean TL, median TL and 25th Percentile TL were used to compare the two cohorts with none of these measures showing any significant difference between the matched cohorts (*Table 29*).

The second aim of this pilot study was to determine the intra-sample correlation between mTL measured by qPCR and STELA. Baird *et al* (187) demonstrated excellent correlation between mTL measured with XpYp STELA and with TRF analysis ($r=0.91$, $P<0.001$; $n=10$), suggesting that XpYp telomere length reflects genome-wide telomere length. In our analysis of 23 samples we found little correlation in mTL measurement between the two methods. This finding calls in to doubt the reliability of telomere length measurement on an individual level. The fact that the findings of our main study closely echo findings from previous studies such as correlation with age suggests that the distribution of telomere lengths within the population as a whole is accurate. However, there may be inter-individual differences in XpYp mTL and qPCR genome wide mTL that have resulted in our findings of poor mTL correlation within this relatively small subgroup.

In summary, the use of an alternative method of measurement did not alter the finding that mTL was not significantly associated with the development of CSA-AKI.

5.14.5 Strengths and limitations of mTL experiments

There are several strengths to the current study. Firstly, it is prospective in nature and therefore does not suffer from collection bias associated with retrospective studies. Secondly, the current study includes a larger population than the studies described previously that have investigated telomere length in the setting of cardiac surgery. A further strength of the current study is its ambition. It attempts what many studies into telomere length have not, which is to investigate if telomere length correlates with a disease process before the onset of that process. Several studies have associated reduced mTL with various disease states and have therefore suggested that, due to the link between telomere shortening and reduced cellular regeneration, mTL might act as a biomarker of age-related degenerative disease (188). In practice, this hypothesis is difficult to test as such a study would involve a long latency between mTL measurement and the development of the disease process. We have attempted to simulate this situation in a more acute setting with the use of an inducible disease process in the form of CSA-AKI. Mean telomere length was measured before the onset of the disease process (the ischaemic insult of cardiac surgery), and correlated with outcome (the development of CSA-AKI).

There are, however, limitations to the current study. The most obvious limitation is that the population's size may still be too small to detect weak associations between telomere length and surgical outcomes. As such, it may be that telomere length is a

contributing factor in the development of CSA-AKI but that the size of the effect is too small to be seen in a sample of 254 patients; i.e. the current study might be underpowered to detect a weak association between mTL and CSA-AKI. This primarily results from the fact that the outcomes studied are relatively infrequent in terms of the total population studied. In this cohort, the incidence of AKI, in-hospital mortality and 1-year mortality were 21%, 2%, and 7% respectively. As such, large numbers of patients need to be tested in order to generate sufficient endpoints to detect even moderate associations. However, the primary aim of this study was not to determine if a weak association exists between mTL and CSA-AKI. The aim was to determine whether a measure of biological age such Telomere length could predict CSA-AKI, and other post-operative outcomes, better than the patients chronological age or other recognised risk factors for AKI. As previously discussed in Chapter 1, the aetiology of CSA-AKI is multifactorial and numerous factors have been shown to be associated with its development previously. Hence, merely adding another factor to the list that is weakly associated with its development may not be clinically beneficial. From the results of our univariate analysis we identified several factors associated with the development of CSA-AKI in our cohort, such as cardiopulmonary bypass time, pre-operative haemoglobin, and hypercholesterolaemia. This suggests that the traditional risk factors are better predictors of CSA-AKI. Although age was also not significantly associated with CSA-AKI [OR 1.019 (0.995-1.044; $p = 0.118$), on ROC curve analysis it was a better predictor of AKI than mTL with an AUC of 0.574 compared to 0.479 for mTL. Hence, this study can conclude that, for the population as a whole, TL is not a clinically useful parameter in terms of predicting CSA-AKI.

A second potential limitation of the study is the possibility that the measured mean leukocyte telomere length is not representative of the mean telomere length in renal tissue. This could result in cellular senescence at a renal level being different to that measured in peripheral blood and masking any relationship between reduced telomere length and CSA-AKI. As it is not ethically or practically viable to perform a renal biopsy on every patient undergoing cardiac surgery in order to obtain renal tissue, peripheral blood was chosen as an alternative. There is conflicting evidence as to whether telomere length remains constant across different tissues within an individual. Dlouha *et al* (189) examined the relationship between mTL in leukocytes compared with mTL from 11 different body tissues including the kidney, liver, brain, muscle, skin, spleen, heart and fat. They found no significant correlations between mTL in leukocytes and any other tissue with the exception of skeletal smooth muscle. However, their analysis only included samples from 12 patients. This paper also highlighted that relative TL can be markedly affected by DNA degradation. As all of our samples were tested for integrity on gel electrophoresis prior to their analysis, this should not have introduced error into this study. In studies with larger sample sizes, mTL was seen to be more consistent across tissue types. Takubo *et al* (190) measured mTL across 5 different tissues (heart, liver, kidney, brain and spleen) and found that TL was relatively consistent across tissues of the same individual. Furthermore, they demonstrated that mTL in renal cortex showed a significant negative correlation with age. Friedrich *et al* (191) measured telomere length by Southern Blot in three tissues of different proliferation rates (peripheral blood leukocytes, skin, and synovial tissue). Although the authors found significantly shorter mTL in leukocytes than skin or synovial fluid, mTL was highly correlated

between all tissue types of the same individuals regardless of age. This led the authors to conclude that telomere length measurement in easily accessible tissues such as blood could serve as a surrogate parameter for the relative mTL in other tissues. As such, the majority of the studies into telomere length and associated disease have used peripheral leukocyte telomere length. Furthermore, for a test to be clinically useful it must be possible to obtain samples from patients in a way that is acceptable to them. With the above in mind, the decision to focus our area of study on leukocyte telomere length from peripheral blood seems justified.

A final limitation of the current study is that mTL may not be a true indicator of telomere induced cellular senescence. Despite the considerable body of work that has repeatedly demonstrated the relationship between mTL and age-related disease, Hemann *et al* (101) present evidence that it is the length of the shortest telomere within a cell rather than the mean length that triggers the cell to enter senescence. To address this potential issue, we performed STELA of the XpYp telomere in a subset of the study patients. However, as previously discussed this analysis was not able to address the issue of a single chromosome with short telomeres being able to trigger senescence of a whole cell because STELA is only able to be performed on a limited number of chromosomes (160). Although a single research group has reported their experience of Universal-STELA (U-STELA) which allows the length of individual telomeres to be measured regardless of position (161), this technique is not well established nor widely reported. As we have not been able to measure the burden of short telomere lengths for each sample, we have not been able to test Hemann *et al*'s hypothesis in this study. Rather we have assumed that given the large number of

peripheral leukocytes within each sample, the mTL across all chromosomes will correlate with the burden of short chromosomes capable of triggering senescence. This seems a fair assumption to make given that many previous studies have established the validity of mTL as a biomarker of senescence. However, it remains a potential source of error in our study findings.

5.14.6 Conclusion

The main finding of this experiment is that mTL is not a clinically useful predictor of the development of AKI for the majority of patients who undergo cardiac surgery. It is inferior in this respect to an individual's age or to the already recognized risk factors such as duration of cardiopulmonary bypass or pre-operative anaemia. However, more in-depth analysis has revealed an interesting finding that patients of South Asian descent do exhibit a significant association between reduced mTL and CSA-AKI. The underlying mechanism for this is not clear and its determination should form the basis of future investigation.

CHAPTER 6: DNA Methylation Aging Signatures and Cardiac Surgery Associated- Acute Kidney Injury.

6.1 Building a Methylation signature for aging.

The source data from the DNA methylation experiments was in the form of Beta values which give a percentage methylation for each CpG site. Therefore, for each sample up to 77 Beta values were generated (71 for the aging array and 6 for senescence). In order to study the associations of these values with clinical outcomes it was necessary to build a model that would combine the 71 aging associated beta values into a single measure of methylation predicted age. This model and the resulting values of predicted methylation age (pMA) was generated by Dr Robert Lowe (Blizzard Institute, QMUL)

To define an aging methylation signature a similar approach was used to that of both Hannum *et al.* [1] and Horvath [2]. The source data from the aging and senescence methylation CpG's generated a total of 526 CpG's. This is because our primers amplified fragments containing CpG's clustered around the target CpG. Analysis was restricted to those CpGs which were covered by more than 100 reads to reduce the effect of highly noisy methylation values, leaving a total of 316 CpGs. The initial aim was to build a model from the data provided by using 27 "healthy" control samples with known ages that were run in the same sequencing run as the study cohort. These healthy control samples were provided by Dr Vasantha Muthuppalaniappan and obtained from healthy kidney donors. Three samples were removed due to low

amount of sequencing leaving 24 samples to build a model on. Ages in years were transformed using the following function as suggested by Horvath [2].

$$f(A) = \begin{cases} \log(A + 1) - \log (A + 1), & A \leq 20 \\ \frac{A - 20}{A + 1}, & A > 20 \end{cases}$$

Where A is the age of a sample in years. The rationale for this transformation is that it is;

- a) continuous
- b) logarithmic up till 20 years old and then linear from that point onwards,
- c) defined for prenatal samples e.g. A can be -1.

Following this conversion, an elastic net regression model was used to regress the 316 CpGs and then a prediction based on the methylation levels of each of these 316 CpGs can be made. As part of the elastic net regression a single hyper-parameter was fitted using a 5-fold cross validation. To test the model, a leave one out cross validation was used. Specifically, a single sample was removed and the model trained as above and then the age of the missing sample predicted. This was done for each sample and the root mean squared error (RMSE) of the prediction calculated. This initial analysis resulted in a RMSE of 11.59 years.

To see if this prediction could be improved, the existing Illumina 450K data provided by Hannum *et al.* was used [1] (n=656). First, the 316 CpGs were overlapped with probes contained on the array leaving a total of 48 CpGs in common between the

two experiments. The CpG ID of these is provided in the *Appendix I*. Following the same approach as above an elastic net regression model was used to regress the 48 CpGs. The hyper-parameter was fitted using a 10-fold cross validation (due to the larger number of samples available) and the model was trained on the Hannum *et al* data and tested on the 24 “healthy” control samples. This resulted in a reduced RMSE of 6.89 years and a spearman correlation of 0.75 (*Figure 25*). The same model was then run on the remaining samples to predict the ages of each sample. These predicted ages were used in subsequent analyses for association with outcome after cardiac surgery.

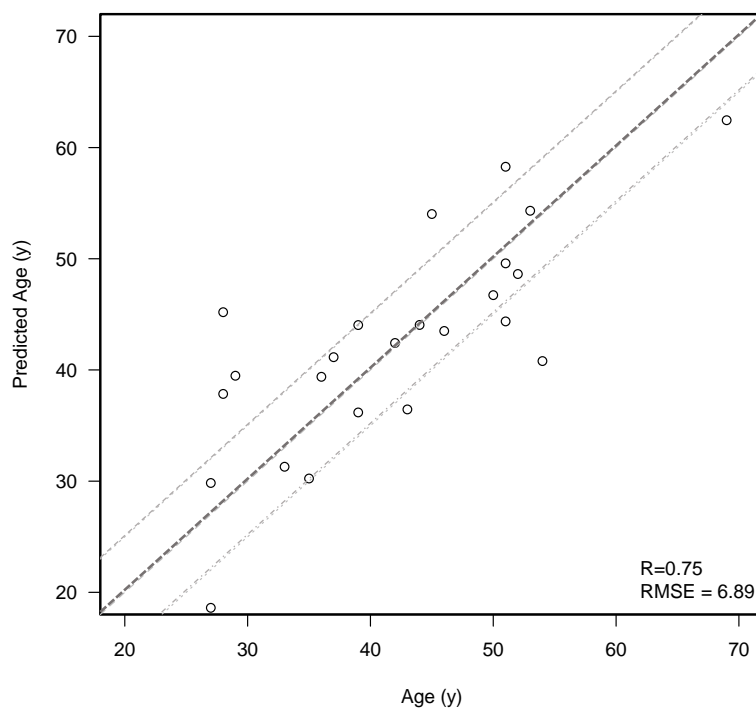


Figure 25: Predicted age in years based on methylation status against actual age in years for the training group of 24 healthy controls. The central dark grey dashed line represents a perfect prediction. Light grey dashed lines are +/- 5 years. Figure provided by Dr Robert Lowe.

6.2 Measures of aging in DNA methylation study

As a result of the aging model that we constructed built on the Hannum aging signature, each study participant had a single measure of predicted age. Previous papers have used varying methodologies to relate this predicted age with clinical outcomes. Hannum *et al* describe a measure of aging rate termed the Apparent Methylation Aging Rate (AMAR) which is the ratio of the methylation derived predicted age to the true chronological age. Therefore, a higher value of AMAR means a higher predicted age (76). Other studies use the difference between the chronological age and the predicted methylation age (Delta age) as a biomarker for aging and used this measure in subsequent analyses (164). For completeness, analyses have been run using the raw values of pMA together with both AMAR and Delta age to see if any significant associations exist with any of the measured outcomes.

6.3 The study population

Of the 254 patients that were sequenced (see section 5.2), 14 failed the sequencing process. The reason for this was thought to be a loss of DNA integrity. Sequencing of DNA methylation status requires DNA of high structural integrity as outlined previously in section 4.3.4. Although all DNA samples were tested for integrity using gel electrophoresis, after extraction it is possible that the storage of the DNA at -20°C and subsequent thawing may have led to degradation of a small proportion of the samples. Of the 240 samples successfully sequenced 50 developed cardiac surgery

associated-acute kidney injury (CSA-AKI) (20.8%; 50/240). This is a similar proportion as in the original study population (21.2%; 54/254).

Repeats of the normality tests for this reduced population were the same as those shown in *Appendix E*. Additional normality tests were performed for the 4 measures of aging and are also shown in *Appendix E*.

6.4 Univariate associations of methylation aging with main outcomes.

Univariate associations between the 4 markers of age (Age, pMA, AMAR, and Delta age) and the primary outcome of CSA-AKI is shown in *Table 30*, together with the secondary outcomes of in-hospital mortality, 1-year mortality, and composite endpoint (New AF, Stroke, Reoperation, and AKI). Of the 4 markers of age, only pMA was significantly associated with the development of CSA-AKI with a mean pMA of 65.62 in the AKI group and 59.7 in the non-AKI group ($p=0.013$).

No significant differences were seen for any of the other outcomes apart from the composite outcome of new AF, stroke, reoperation or AKI. Both Age and pMA were significantly increased in the patients reaching one of these endpoints; 66.19 years Vs 62.36 years for Age ($p=0.034$) and 63.47 years Vs 58.74 years for pMA ($p= 0.014$).

		AKI		In-hospital mortality		1-year mortality		Composite outcome	
		Yes n = 50	No n= 190	Yes n = 5	No n =235	Yes n = 16	No n =192	Yes n =113	No n =127
Age	Mean	66.99	63.41	65.18	64.13	66.62	63.54	66.19	62.36
	OR (95% CI)	1.021 (0.996-1.046)		1.006 (0.941-1.075)		1.018 (0.977-1.061)		1.021 (1.002-1.041)	
	p-value	0.106		0.868		0.385		0.034	
Predicted age	Mean	65.62	59.74	64.67	60.89	64.99	60.57	63.47	58.74
	OR (95% CI)	1.030 (1.006 - 1.053)		1.018 (0.957-1.084)		1.022 (0.986-1.060)		1.023 (1.005-1.042)	
	p-value	0.013		0.567		0.239		0.014	
AMAR	Mean	0.994	0.949	0.959	0.958	0.988	0.962	0.969	0.948
	OR (95% CI)	5.404 (0.812- 35.969)		1.045 (0.004- 254.80)		2.611 (0.126-54.185)		2.209 (0.453-10.78)	
	p-value	0.081		0.988		0.535		0.327	
Delta Age	Mean	1.38	3.67	0.51	3.25	1.63	2.97	2.71	3.61
	OR (95% CI)	0.977 (0.946-1.008)		0.973 (0.891-1.063)		0.987 (0.937-1.038)		0.991 (0.966-1.017)	
	p-value	0.148		0.541		0.604		0.488	

Table 30: Association between Age, Predicted methylation age, AMAR and Delta age with the main study outcomes.

As in our previous analysis of mTL, the cohort was divided into quintiles for Age, pMA, AMAR and Delta age. Patients in the top and bottom quintiles were then compared for rates of the primary and secondary endpoints using cross tabulation with significance values derived by Fischer's exact test. The results are shown in Table 31, and demonstrate the same relationships as those derived from analysis of the whole cohort. Again, only pMA was significantly associated with rates of CSA-AKI whilst both Age and pMA were associated with development of the composite outcome. No new relationships were unmasked by this methodology.

		AKI		In-hospital mortality		1-year mortality		Composite outcome	
		Yes	No	Yes	No	Yes	No	Yes	No
Age	Top Quintile	14 (29.2%)	34 (70.8%)	2 (4.2%)	46 (95.8%)	5 (13.2%)	33 (86.8%)	33 (68.8%)	15 (31.3%)
	Bottom Quintile	9 (18.8%)	39 (81.3%)	1 (2.1%)	47 (97.9%)	3 (7.1%)	39 (92.9%)	21 (43.8%)	27 (64.3%)
	p-value	0.339		1.00		0.467		0.023	
pMA	Top Quintile	17 (35.4%)	31 (64.6%)	2 (4.2%)	46 (95.8%)	5 (12.2%)	36 (87.8%)	32 (66.7%)	16 (33.3%)
	Bottom Quintile	6 (12.5%)	42 (87.5%)	1 (2.1%)	47 (97.9%)	3 (7.5%)	37 (92.5%)	18 (37.5%)	30 (62.5%)
	p-value	0.016		1.00		0.712		0.008	
AMAR	Top Quintile	13 (27.1%)	35 (72.9%)	2 (4.2%)	46 (95.8%)	5 (11.6%)	38 (88.4%)	23 (47.9%)	25 (52.1%)
	Bottom Quintile	8 (16.7%)	40 (83.3%)	2 (4.2%)	46 (95.8%)	5 (13.5%)	32 (86.5%)	19 (39.6%)	29 (60.4%)
	p-value	0.324		1		1		0.537	
Delta Age	Top Quintile	8 (16.7%)	40 (83.3%)	2 (4.2%)	46 (95.8%)	5 (13.5%)	32 (86.5%)	19 (39.6%)	29 (60.4%)
	Bottom Quintile	13 (27.1%)	35 (72.9%)	2 (4.2%)	46 (95.8%)	5 (11.6%)	38 (88.4%)	23 (47.9%)	25 (52.1%)
	p-value	0.324		1.00		1.00		0.537	

Table 31: Association of rates of AKI, In-hospital mortality, 1-year mortality, and composite outcome in patients in the top and bottom quintiles of Age, pMA, AMAR, and Delta Age.

6.5 Propensity matched analysis of methylation aging and CSA-AKI

A propensity matched analysis was performed for the 4 markers of aging and the development of CSA-AKI, using the same methodology as previously described in section 5.5. Due to the loss of a proportion of the samples in the sequencing process we were only able to achieve 43 matched pairings. Shapiro-Wilk’s test of normality run on the matched cohort showed that pMA was normally distributed for both cases and controls, but that Age, AMAR, and Delta Age were not. As such, the Wilcoxon Signed Rank test was used as a non-parametric alternative to the Students T-test for paired samples. In this analysis none of the 4 measures of age differed significantly

between the paired populations (*Table 32*). Delta age showed the greatest difference with a value of 1.89 in the AKI cohort compared to 6.12 in the non-AKI cohort ($p=0.07$).

		AKI	Non AKI
Age	Mean +/- SD	66.97+/- 14.31	67.16 +/- 13.6
	p-value	0.975	
Predicted Age	Mean +/- SD	65.09 +/- 14.70	61.04 +/- 12.19
	p-value	0.241	
AMAR	Mean +/- SD	0.986+/- 0.154	0.934 +/- 0.154
	p-value	0.144	
Delta Age	Mean +/- SD	1.89 +/- 9.51	6.12 +/- 11.05
	p-value	0.074	

Table 32: Comparison of Age, pMA, AMAR, and Delta Age in Cases Vs Controls in 43 propensity patched patient pairings.

6.6 Whole population Associations with chronological age, predicted methylation age, AMAR, and Delta age.

The same statistical methodology as previously outlined in section 5.6 was employed to determine whole population associations with pMA, AMAR, and Delta age. A summary of the associations between aging measures and all continuous independent pre-operative and intra-operative variables is shown in *Table 33*. A similar summary for categorical independent variables is shown in *Table 34*.

Variable	Age		pMA		AMAR		Delta Age	
	Corr Coeff	p-value	Corr Coeff	p-value	Corr Coeff	p-value	Corr Coeff	p-value
Length of post-op stay	0.129	0.047	0.168	0.01	0.112	0.084	-0.097	0.135
Age	-	-	0.701	0.000	-0.197	0.002	0.277	0.000
BMI	-0.026	0.690	0.007	0.910	0.024	0.717	-0.020	0.759
Extubation day	0.286	0.000	0.237	0.000	0.020	0.757	0.011	0.872
Vasopressor day	-0.092	0.156	-0.100	0.125	-0.026	0.687	0.005	0.935
Inotrope day	0.056	0.390	0.010	0.876	-0.093	0.154	0.070	0.280
1 st Hb in ITU	-0.247	0.000	-0.171	0.011	0.089	0.191	-0.139	0.039
Urine output 1 st 12 hours	-0.193	0.004	-0.116	0.088	0.048	0.482	-0.071	0.300
Pre WCC	-0.076	0.243	-0.003	0.964	0.110	0.089	-0.101	0.119
Pre INR	0.076	0.245	0.018	0.785	-0.091	0.164	0.092	0.161
Pre APTT	0.018	0.786	0.050	0.450	0.048	0.465	-0.050	0.449
Pre CRP	-0.097	0.475	-0.182	0.181	-0.053	0.696	0.070	0.611
Pre Hb	-0.310	0.000	-0.254	0.000	-0.051	0.427	-0.007	0.909
D1 Hb	-0.155	0.017	-0.094	0.148	-0.030	0.648	-0.020	0.760
Hb Diff	-0.118	0.071	-0.152	0.019	-0.049	0.449	0.047	0.475
Bypass time	0.065	0.331	0.051	0.445	0.107	0.109	-0.077	0.249
Xclamp time	0.081	0.228	0.034	0.606	0.046	0.488	-0.014	0.829
Log EuroSCORE	0.555	0.000	0.371	0.000	-0.090	0.168	0.109	0.094
T/S ratio	-0.237	0.000	-0.227	0.000	-0.073	0.259	0.063	0.329

Table 33: Summary table of Spearman correlations between Age, Predicted age, AMAR, and Delta age and all continuous independent variables. p-values <0.05 shown in bold. Corr Coeff = Spearman correlation coefficient.

	N	Mean Age +/- SD	p-value	pMA +/- SD	p-value	Mean AMAR +/- SD	p-value	Delta age +/- SD	p-value
Gender									
Male	171	63.78 +/- 13.4	0.215	61.22 +/- 14.80	0.890	0.966 +/- 0.167	0.247 (MWU)	2.55 +/- 10.35	0.165
Female	69	65.13 +/- 14.9		60.35 +/- 14.37		0.938 +/- 0.144		4.78 +/- 8.81	
Ethnicity									
White	174	65.29 +/- 13.9	0.150	61.75 +/- 14.67	0.183	0.954 +/- 0.163	0.201 (KW)	3.55 +/- 10.22	0.184
South Asian	43	64.28 +/- 10.3		62.44 +/- 12.67		0.976 +/- 0.151		1.84 +/- 9.27	
Black	12	54.03 +/- 15.7		50.73 +/- 16.22		0.947 +/- 0.178		3.31 +/- 10.77	
Mixed	2	50.50 +/- 34.6		53.44 +/- 27.71		1.138 +/- 0.232		-2.94 +/- 6.94	
Asian	3	65.47 +/- 5.53		53.36 +/- 6.83		0.814 +/- 0.037		12.00 +/- 1.29	
Middle Eastern	2	59.00 +/- 16.97		57.78 +/- 5.96		1.006 +/- 0.189		1.22 +/- 11.01	
Other	4	52.50 +/- 20.27		52.94 +/- 22.72		1.000 +/- 0.137		-0.44 +/- 6.37	
CABG									
No	98	60.14 +/- 16.69	0.004	57.34 +/- 16.60	0.007	0.962 +/- 0.160	0.974	2.80 +/- 8.83	0.751
Yes	142	66.93 +/- 10.68		63.47 +/- 12.61		0.956 +/- 0.162		3.47 +/- 10.70	
Angina Status									
CCS0	53	60.00 +/- 15.23	0.089	57.06 +/- 14.30	0.015	0.967 +/- 0.167	0.607	2.94 +/- 9.53	0.797
CCS1	38	61.06 +/- 16.61		56.68 +/- 17.81		0.927 +/- 0.146		4.38 +/- 7.89	
CCS2	111	66.77 +/- 12.00		63.84 +/- 13.18		0.964 +/- 0.148		2.94 +/- 9.92	
CCS3	23	66.77 +/- 9.12		62.93 +/- 12.20		0.950 +/- 0.185		3.83 +/- 11.90	
CCS4	11	65.26 +/- 12.32		65.65 +/- 11.44		1.030 +/- 0.232		-0.38 +/- 14.09	
Dyspnoea									
NYHA 1	38	60.30 +/- 15.30	0.227	56.66 +/- 15.42	0.256	0.948 +/- 0.180	0.625	3.64 +/- 10.90	0.453
NYHA 2	126	64.24 +/- 13.42		62.01 +/- 14.65		0.970 +/- 0.148		2.23 +/- 9.15	
NYHA 3	63	66.51 +/- 12.62		61.84 +/- 13.23		0.942 +/- 0.156		4.67 +/- 9.92	
NYHA 4	8	65.45 +/- 15.30		60.19 +/- 9.57		0.958 +/- 0.245		5.26 +/- 12.90	
Previous Cardiac Surgery									
No	224	65.12 +/- 12.84	0.004	61.79 +/- 13.61	0.031	0.958 +/- 0.158	0.701	3.33 +/- 10.04	0.488
Yes	16	50.80 +/- 19.93		49.51 +/- 22.75		0.956 +/- 0.210		1.29 +/- 8.91	

Hx of Malignancy									
No	223	63.84 +/- 13.82	0.132	60.66 +/- 14.59	0.336	0.958 +/- 0.162	0.872	3.18 +/- 10.04	0.768
Yes	17	68.39 +/- 13.85		64.99 +/- 15.30		0.958 +/- 0.154		1.29 +/- 8.91	
Diabetes									
No	181	62.99 +/- 14.53	0.102	59.90 +/- 15.20	0.203	0.958 +/- 0.155	0.166	3.08 +/- 9.38	0.273
Diet	4	74.50 +/- 7.51		65.67 +/- 5.89		0.887 +/- 0.102	(KW)	8.83 +/- 8.49	
Oral	45	67.97 +/- 10.26		64.06 +/- 13.37		0.951 +/- 0.194		3.91 +/- 12.62	
Insulin	10	64.16 +/- 13.41		64.49 +/- 10.15		1.020 +/- 0.155		-0.33 +/- 6.45	
Diabetes									
No	181	62.99 +/- 14.53	0.046	55.09 +/- 16.77	0.036	0.958 +/- 0.155	0.927	3.08 +/- 9.38	0.646
Yes	59	67.77 +/- 10.78		63.02 +/- 13.30		0.958 +/- 0.179	(MWU)	3.53 +/- 11.65	
Hypertension									
No	62	57.76 +/- 17.62	0.002	58.72 +/- 16.77	0.003	0.970 +/- 0.188	0.819	2.66 +/- 9.57	0.990
Yes	178	66.39 +/- 11.50		63.02 +/- 13.30		0.954 +/- 0.151		3.38 +/- 10.12	
High cholesterol									
No	127	61.39 +/- 16.01	0.009	58.72 +/- 16.56	0.019	0.966 +/- 0.173	0.868	2.68 +/- 10.16	0.620
Yes	113	67.27 +/- 10.10		63.50 +/- 11.73		0.950 +/- 0.147		3.77 +/- 9.75	
Smoker									
Non-smoker	106	62.16 +/- 16.10	0.007	58.61 +/- 16.54	0.348	0.948 +/- 0.155	0.053	3.55 +/- 9.08	0.068
Ex-smoker	111	67.15 +/- 10.84		63.21 +/- 12.70		0.948 +/- 0.151		3.93 +/- 10.21	
Smoker	23	58.97 +/- 12.80		60.98 +/- 13.02		1.053 +/- 0.207		-2.00 +/- 11.50	
Ex Vs Current		0.007		p = 0.784			P=0.022		p=0.022
Non Vs Current		0.152		p = 0.588			P=0.02		p=0.035
Renal Disease									
No	197	62.59 +/- 14.04	0.000	59.56 +/- 14.92	0.001	0.960 +/- 0.169	0.791	3.03 +/- 10.28	0.542
Yes	43	71.35 +/- 10.29		67.41 +/- 11.47		0.950 +/- 0.121		3.93 +/- 8.41	
Pulmonary Disease									
No	216	63.71 +/- 14.17	0.396	60.21 +/- 14.21	0.066	0.955 +/- 0.158	0.349	3.50 +/- 9.62	0.128
COPD	14	69.06 +/- 10.40		69.99 +/- 16.66		1.016 +/- 0.209		-0.93 +/- 14.01	
Asthma	10	67.00 +/- 9.15		64.71 +/- 17.88		0.951 +/- 0.159		2.29 +/- 10.53	

Neuro disease									
No	213	63.33 +/- 14.05	0.022	60.45 +/- 14.49	0.216	0.963 +/- 0.155	0.334	2.87 +/- 9.34	0.340
TIA/RIND	16	70.20 +/- 10.97		66.39 +/- 13.66		0.944 +/- 0.115		3.81 +/- 8.41	
CVA	11	71.56 +/- 8.89		63.07 +/- 18.54		0.895 +/- 0.295		8.48 +/- 19.52	
PVD									
No	227	63.97 +/- 14.02	0.475	60.85 +/- 14.82	0.545	0.959 +/- 0.161	0.775	3.12 +/- 9.78	0.823
Yes	13	67.54 +/- 9.91		63.08 +/- 11.55		0.947 +/- 0.177		4.46 +/- 13.16	
Previous PCI									
No	203	63.52 +/- 14.25	0.226	60.16 +/- 15.14	0.057	0.954 +/- 0.161	0.503	3.36 +/- 9.95	0.724
Yes	36	67.28 +/- 10.73		65.09 +/- 10.80		0.979 +/- 0.167		2.20 +/- 10.27	
Previous MI									
No	174	63.41 +/- 14.97	0.489	60.05 +/- 15.76	0.157	0.954 +/- 0.160	0.553	3.36 +/- 9.73	0.770
Yes	62	65.91 +/- 10.18		63.38 +/- 11.15		0.973 +/- 0.169		2.53 +/- 10.82	
Previous ACE									
No	144	64.24 +/- 14.61	0.622	61.20 +/- 15.39	0.459	0.960 +/- 0.158	0.627	3.04 +/- 9.57	0.593
Yes	96	64.05 +/- 12.67		60.62 +/- 13.55		0.955 +/- 0.167		3.42 +/- 10.57	
Previous Statin									
No	90	58.98 +/- 17.10	0.000	57.09 +/- 17.65	0.006	0.976 +/- 1.172	0.406	1.89 +/- 9.57	0.158
Yes	150	67.27 +/- 10.33		63.30 +/- 11.99		0.948 +/- 0.154		3.98 +/- 10.14	
LV function									
Good	185	64.00 +/- 14.18	0.900	61.42 +/- 15.49	0.619	0.966 +/- 0.164	0.090	2.58 +/- 10.21	0.180
Fair	46	64.42 +/- 12.94		58.85 +/- 11.47		0.927 +/- 0.148		5.57 +/- 8.57	
Poor	9	66.16 +/- 12.31		62.58 +/- 11.10		0.959 +/- 0.150		3.64 +/- 10.55	
Good Vs fair		0.878		0.348			0.090		0.065
Fair Vs Poor		0.641		0.467			0.400		0.439
Urgency									
Elective	204	64.52 +/- 14.22	0.286	60.96 +/- 15.27	0.893	0.952 +/- 0.160	0.396	3.55 +/- 10.08	0.443
Urgent	34	61.76 +/- 11.62		60.91 +/- 10.81		0.999 +/- 0.169		0.85 +/- 9.21	
Emergency	2	68.50 +/- 4.95		62.88 +/- 12.68		0.914 +/- 0.119		5.62 +/- 7.73	

Reoperation									
No	229	64.37 +/- 13.49	0.926	61.09 +/- 14.47	0.993	0.956 +/- 0.158	0.768	3.28 +/- 10.00	0.955
Yes	10	63.30 +/- 17.24		60.87 +/- 17.74		0.972 +/- 0.199		2.43 +/- 9.00	
Transfused ITU									
No	153	62.74 +/- 13.94	0.029	59.96 +/- 15.07	0.155	0.963 +/- 0.170	0.623	2.78 +/- 10.48	0.379
Yes	87	66.66 +/- 13.38		62.75 +/- 13.80		0.950 +/- 0.146		3.91 +/- 8.98	
Clotting products in ITU									
No	192	63.49 +/- 13.95	0.082	60.41 +/- 14.47	0.362	0.960 +/- 0.162	0.639	3.07 +/- 10.03	0.617
Yes	48	66.86 +/- 13.18		63.19 +/- 15.33		0.952 +/- 0.161		3.67 +/- 9.79	
New AF									
No	170	61.94 +/- 14.02	0.000	59.11 +/- 15.06	0.000	0.962 +/- 0.168	0.801	2.83 +/- 10.35	0.417
Yes	70	69.55 +/- 11.86		65.47 +/- 12.61		0.949 +/- 0.143		4.07 +/- 8.95	

Table 34: Summary of associations of Age, Predicted age, AMAR, and Delta age with independent categorical variables. *p*-values <0.05 shown in bold.

In our study cohort, pMA showed good correlation with chronological age (Spearman correlation coefficient of 0.7; *Figure 26*). Furthermore, pMA and chronological age showed the same patterns of correlation across all pre-operative and intra-operative variables, although the degree of associations varied. However, pMA showed a stronger correlation with length of post-operative stay than chronological age (Spearman correlation coefficient of 0.168 Vs 0.129). The relationship between pMA and length of post-operative stay is shown in *Figure 27*. Both pMA and chronological age were significantly correlated with mTL ($p < 0.001$; *Table 33*).

By comparing the four different aging markers, Age, pMA, AMAR, and Delta age, it is possible to see the individual effects of the independent variables on predicted methylation age in relation to chronological age. Smoking history alone altered the trend in pMA away from that of chronological age. This is demonstrated in *Figure 28*. Current smokers have higher mean predicted methylation ages than their chronological age, whereas the trend is reversed for non-and ex-smokers. This is reflected in a significant difference in both AMAR (predicted age/actual age) and Delta age (Actual age – predicted age) in current smokers. Current smokers had a significantly increased mean AMAR compared to ex-smokers (1.053 Vs 0.948; $p = 0.02$) and non-smokers (1.053 Vs 0.948; $p = 0.022$). The same relationships are seen in Delta age; mean Delta age of -2.0 in smokers compared to 3.93 in ex-smokers ($p = 0.035$), and 3.55 in non-smokers ($p = 0.022$). The increase in mean AMAR and reduction in mean Delta age seen in smokers is the result of higher pMA. As such, smoking appears to be associated with an accelerated methylation aging rate.

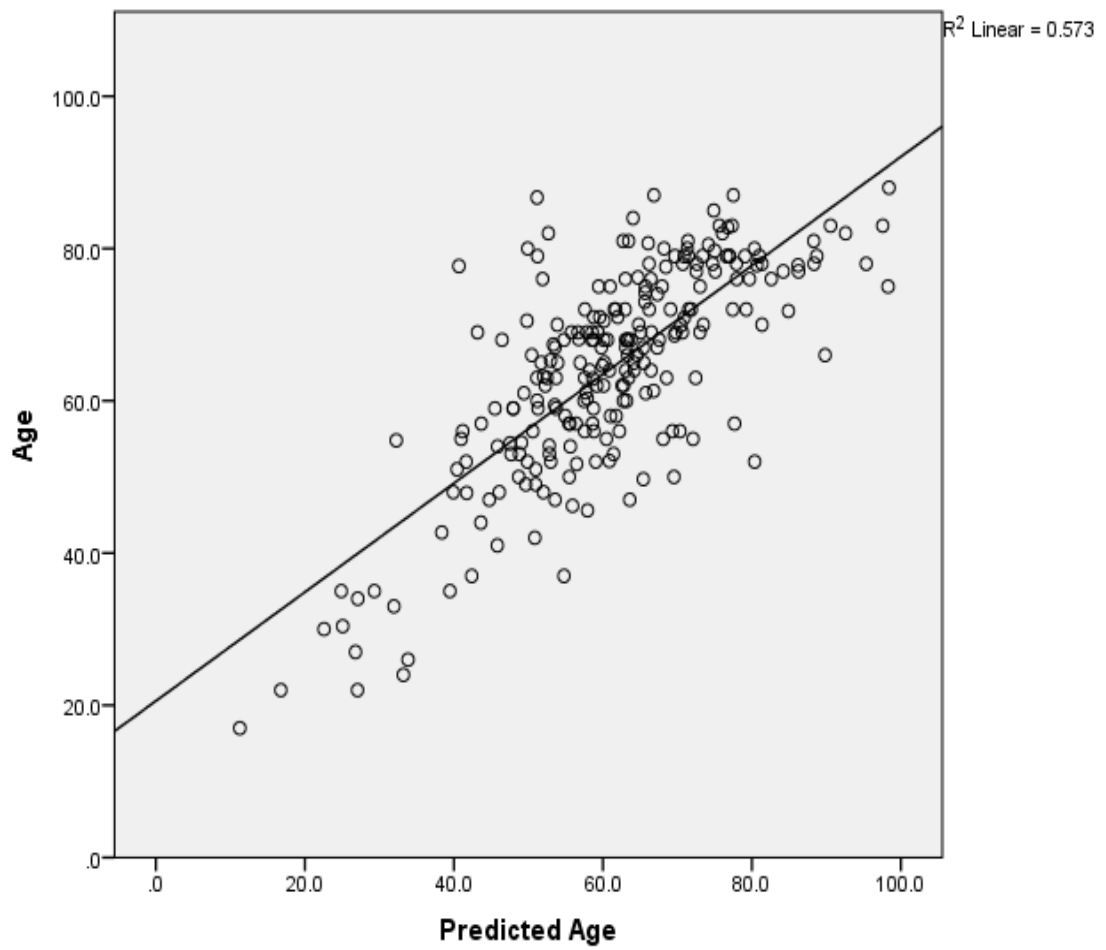


Figure 26: Correlation of Predicated methylation age with chronological age for all subjects (AKI and non-AKI). R2 value of 0.573; Spearman Correlation Coefficient = 0.7. $p < 0.001$

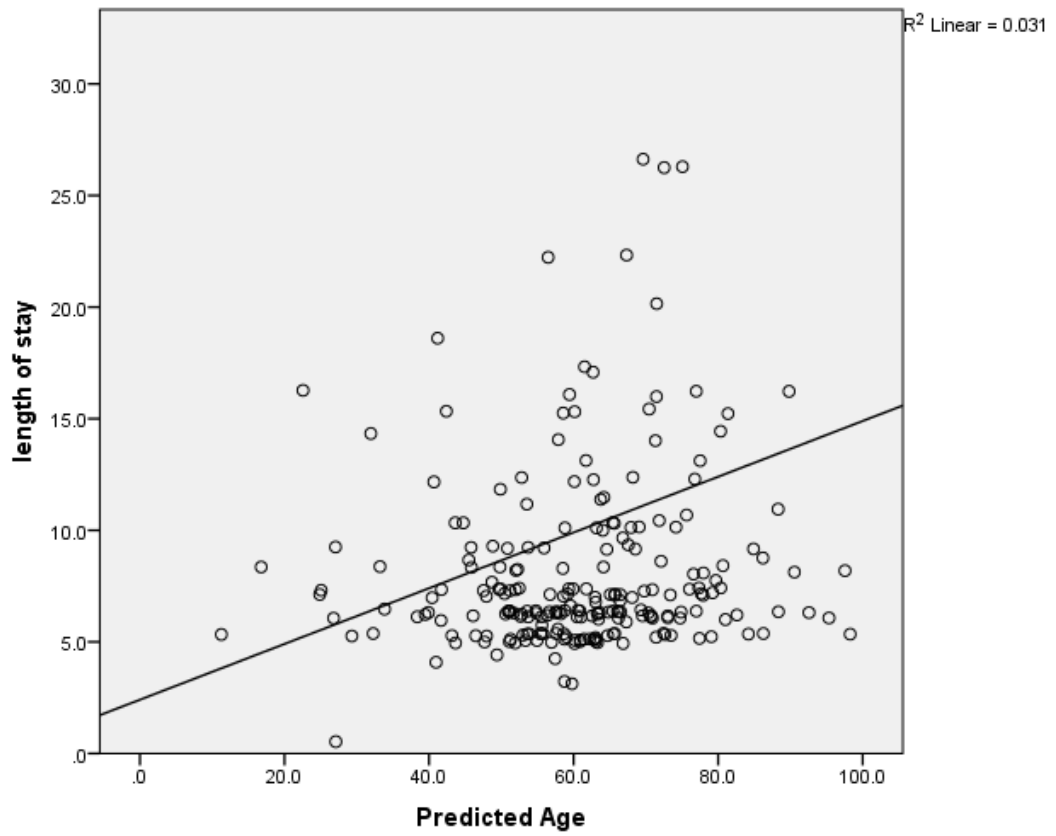


Figure 27: Correlation between predicted methylation age and length of post-operative stay. $R^2 = 0.031$. Spearman Correlation coefficient = 0.168. $p = 0.01$

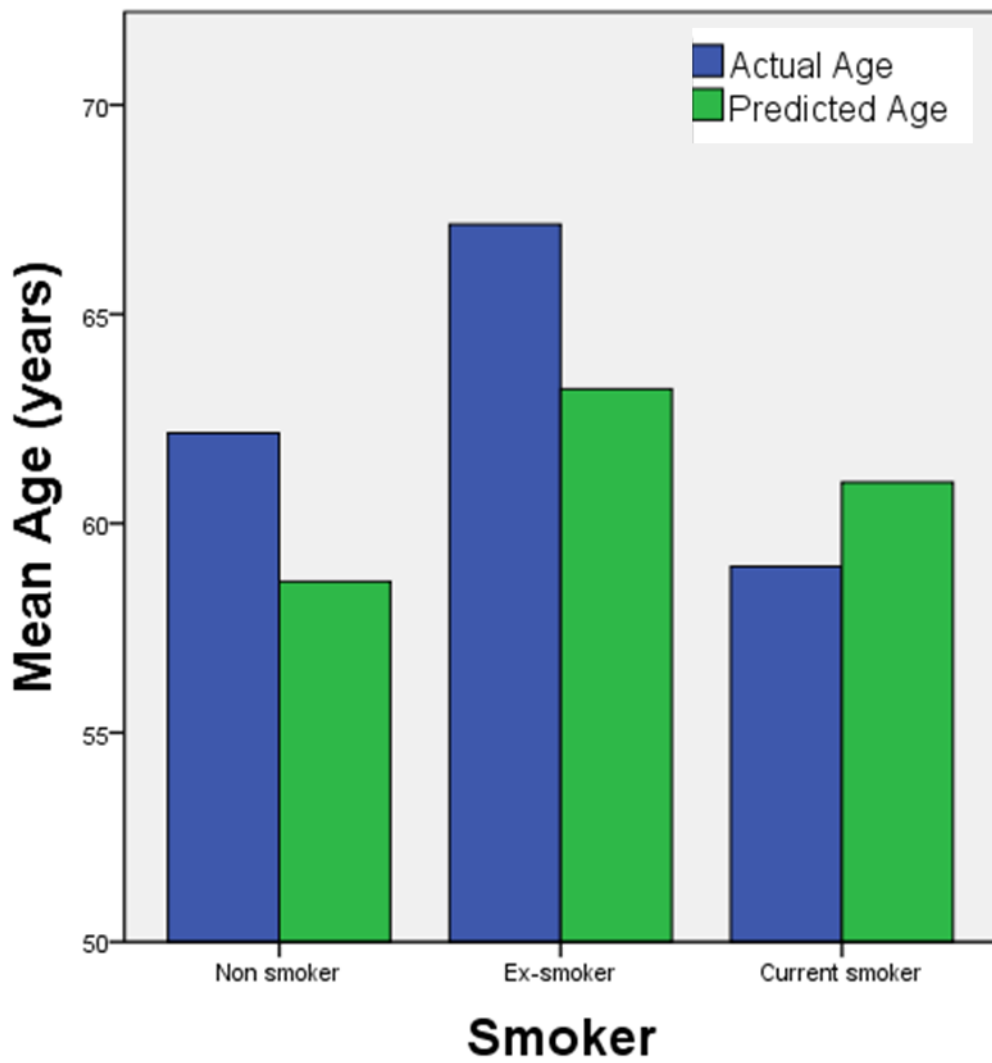


Figure 28: Relationship between smoking history and mean chronological age (blue bars) and predicted age (green bars). Current smokers have a higher mean predicted methylation age than their chronological age, where as in non-smokers and ex-smokers the relationship is reversed.

6.7 Analysis of methylation aging as a predictor of CSA-AKI

6.7.1 Univariate analysis

Due to 14 of the samples failing the sequencing process the final population for analysis of methylation age was reduced from 254 to 240. This necessitated repeating the full analysis for predictors of CSA-AKI using the same methodology as in section 5.7.1. In addition, pMA, AMAR and Delta age were added as independent variables. Results of the univariate binary logistic regression analyses are shown in *Table 35* with the statistically significant predictors summarised in *Table 36*. Of the 4 measures of aging tested, only pMA was significantly associated with the development of CSA-AKI (OR 1.030 (1.006-1.053; $p = 0.013$). As such, it was the only aging marker used in subsequent multivariate analysis.

	OR	95% CI	p-value
Age	1.021	0.996 – 1.046	0.106
Predicted Age	1.030	1.006 - 1.053	0.013
AMAR	5.404	0.812 - 35.97	0.081
Delta Age	0.977	0.946 – 1.008	0.148
Female Gender	1.21	0.620 - 2.386	0.569
Ethnicity (compared to white)			
South Asian	1.594	0.742-3.424	0.232
Black	1.373	0.353-5.344	0.648
Mixed	0.000	NA	0.999
Asian	0.000	NA	0.999
Middle Eastern	0.000	NA	0.999
Other	1.352	0.069-1.091	0.787
BMI	1.049	0.985-1.117	0.136
Cardiac Procedure (compared to CABG)			
CABG + valve	1.350	0.481-3.793	0.569
CABG + valve +other	4.500	0.270-75.03	0.295
CABG + other	1.500	0.148-15.18	0.731
Valve alone	1.340	0.621-2.891	0.455
Valve + other	1.038	0.270-3.988	0.956
Other	1.406	0.461-4.288	0.549
CABG (Yes Vs No)	0.848	0.452-1.592	0.609
Pre-op Angina (compared to stage 0)			
CCS 1	1.500	0.508-4.432	0.463
CCS 2	1.635	0.682-3.919	0.270
CCS 3	1.985	0.600-6.569	0.261
CCS 4	1.250	0.227-6.889	0.798
Pre-op NYHA stage			
NYHA 2	1.320	0.521-3.348	0.577
NYHA 3	1.524	0.591-4.355	0.434
NYHA 4	5.333	0.819-19.30	0.045
Previous Cardiac Surgery (yes Vs No)	1.808	0.598-5.467	0.294
Previous Malignancy	1.648	0.552-4.918	0.370
Diabetes Yes/No	1.430	1.021-2.002	0.037
Hypertension	1.301	0.619-2.732	0.487
Hypercholesterolaemia	2.149	1.134-4.072	0.019
PreviousSmoking			
Ex-smoker	1.495	0.765-2.925	0.240
Current	1.725	0.598-4.980	0.313

Pre-op renal dysfunction (eGFR<60)	1.620	0.762-3.444	0.210
Pre op COPD	1.657	0.495-5.543	0.412
Pre-op Asthma	2.762	0.746-10.228	0.128
Pre-op Neuro disease			
TIA	0.519	0.114-2.364	0.396
CVA	0.807	0.168-3.864	0.788
Previous PVD	1.749	0.516-5.932	0.370
Pre-op ACEI	1.232	0.656-2.312	0.517
Pre-op Statin	0.973	0.512-1.850	0.935
Pre-op LV Function			
Fair	1.875	0.906-3.883	0.091
Poor	0.536	0.065-4.424	0.562
Pre-op Urgency			
Urgent	0.471	0.158-1.408	0.178
Emergency	3.533	0.217-57.61	0.375
1st Hb in ITU	0.982	0.964-1.000	0.050
Pre-op WCC	1.049	0.922-1.193	0.468
Pre-op INR	5.307	0.503-56.03	0.165
Pre-op APTT	1.039	0.967-1.117	0.296
Pre-op CRP	1.007	0.988-1.026	0.495
Pre-op Hb	0.763	0.632-0.922	0.005
Pre-op Cr	1.008	0.996-1.021	0.194
Pre-eGFR	0.993	0.979-1.007	0.323
Bypass time	1.015	1.007-1.022	<0.0001
X-Clamp time	1.015	1.006-1.023	0.001
Logistic EuroSCORE	0.586	0.152-2.258	0.437
T/S Ratio	0.428	0.062-2.943	0.388

Table 35: Univariate analysis of the association of all pre-operative and intra-operative variables with the development of CSA-AKI in the DNA methylation population.

Variable	OR	p-value
Bypass time	1.015	<0.001
X-Clamp time	1.015	0.001
Pre-op Hb	0.763	0.005
Predicted Age	1.030	0.013
Hypercholesterolaemia	2.149	0.019
Diabetes Yes/No	1.430	0.037
Pre-op NYHA stage		
NYHA 2	1.320	0.577
NYHA 3	1.524	0.434
NYHA 4	5.333	0.045
1st Hb in ITU	0.982	0.050

Table 36: Summary of predictors of CSA-AKI on univariate analysis listed by strength of association.

6.7.2 Multivariate analysis

Predictors that were significantly associated with CSA-AKI on univariate analysis were entered into a multivariate model. Cross-clamp time was excluded from the model as it is closely associated with cardiopulmonary bypass time. Similarly, '1st Hb in ITU' was excluded as it is strongly correlated with 'Pre-op Hb' (Spearman Correlation co-efficient of 0.527; p=0.000). Adjusted Odds ratios for the multivariate analysis are shown in *Table 37*. Cardiopulmonary bypass time and pre-operative hypercholesterolaemia were found to be independent predictor of CSA-AKI. After adjustment, predicted methylation age was no longer independently associated with the development of CSA-AKI (p=0.077).

Variable	Adjusted Odds Ratio	95% CI	p-value
Predicted age	1.026	0.997-1.056	0.077
Bypass Time	1.017	1.009-1.026	<0.001
Pre-op Hb	0.806	0.641-1.012	0.064
Hypercholesterolaemia	2.173	1.023-4.615	0.043
Diabetes Yes/No	1.232	0.814-1.865	0.325
NYHA 4	4.274	0.527-34.655	0.174

Table 37: Multivariate model of independent predictors of CSA-AKI. Significant p-values <0.05 shown in bold. Nagelkaerke R square = 0.241. Block 0 predictive value = 78.8%, Block 1 predictive value = 80.2%

6.8 Analysis of methylation age as a predictor of 1-year mortality

A repeat of the analysis of section 5.8. was performed for the secondary outcome of 1-year mortality. Results of the univariate binary logistic regression analyses are shown in *Table 38* with the statistically significant predictors summarised in *Table 39*.

	OR	95% CI	p-value
LOS (increasing LOS a/w AKI)	1.043	1.013-1.074	0.005
Age	1.018	0.977-1.061	0.385
Predicted age	1.022	0.986-1.060	0.239
AMAR	2.611	0.126-54.185	0.535
Delta Age	0.987	0.937-1.038	0.604
Female Gender	1.104	0.367-3.323	0.860
Ethnicity (compared to white)			
South Asian	1.102	0.294-4.132	0.886
Black	0	NA	0.999
Mixed	0	NA	0.999
Asian	0	NA	0.999
Middle Eastern	0	NA	0.999
Other	3.917	0.378-40.605	0.253
BMI	0.977	0.877-1.090	0.680
Cardiac Procedure (compared to CABG)			
CABG + valve	0.578	0.067-4.959	0.617
CABG + valve +other	0	NA	0.999
CABG + other	4.048	0.371-44.209	0.252
Valve alone	1.239	0.373-4.115	0.726
Valve + other	0.934	0.106-8.222	0.951
Other	0.639	0.074-5.506	0.684
CABG (Yes Vs No)	0.938	0.335-2.624	0.903
Pre-op Angina (compared to stage 0)			
CCS 1	1.892	0.395-9.059	0.425
CCS 2	1.380	0.349-5.465	0.646
CCS 3	0.698	0.068-7.122	0.762
CCS 4	0	NA	0.999
Pre-op NYHA stage			
NYHA 2	2.640	0.318-21.901	0.368
NYHA 3	2.640	0.282-24.674	0.368
NYHA 4	24.750	2.053-298.43	0.012
Previous Cardiac Surgery (Yes Vs No)	0.918	0.112-7.504	0.936
Previous Malignancy	2.600	0.518-13.04	0.245
Diabetes Yes/No	1.421	0.833-2.422	0.197
Hypertension	0.839	0.278-2.529	0.755
Hypercholesterolaemia	0.362	0.113-1.163	0.088
Ex-smoker	2.411	0.715-8.123	0.156
Current	3.750	0.772-18.21	0.101
Pre-op renal dysfunction (eGFR<60)	2.662	0.860-8.246	0.090

Pre op COPD	2.247	0.453-11.15	0.322
Pre-op Asthma	0	NA	0.999
Pre-op Neuro disease			
TIA or RIND	1.805	0.798-4.079	0.156
CVA	0.074	NA	0.000
Previous PVD	1.097	0.132-9.082	0.932
Pre-op ACEI	1.966	0.611-6.320	0.257
Pre-op Statin	0.249	0.083-0.747	0.013
Pre-op LV Function			
Fair	0.540	0.117-2.492	0.430
Poor	1.582	0.181-13.870	0.679
Pre-op Urgency			
Urgent	1.587	0.419-6.005	0.497
Emergency	13.75	0.809-233.72	0.070
Extubation Date	1.596	1.142-2.232	0.006
Vasopressor Date	1.096	1.003-1.197	0.042
No. of Inotrope days	1.069	0.982-1.163	0.124
1st Hb in ITU	0.998	0.968-1.027	0.870
UO 1 st 12 hours	0.999	0.998-1.000	0.190
Reoperation	21.25	4.992-90.46	<0.001
Pt transfused in ITU	4.400	1.466-13.20	0.008
Clotting products	0.372	0.127-1.090	0.071
Post-op AF	0.770	0.238-2.488	0.662
Pre-op WCC	1.158	0.954-1.407	0.139
Pre-op INR	10.637	0.601-188.17	0.107
Pre-op APTT	1.045	0.871-1.253	0.635
Pre-op CRP	1.108	1.026-1.195	0.009
Pre-op Hb	0.539	0.386-0.752	<0.001
Pre-op Cr	1.032	1.012-1.052	0.002
Pre-eGFR	0.959	0.929-0.990	0.011
Bypass time	1.009	1.001-1.018	0.033
X-Clamp time	1.010	0.998-1.023	0.108
Logistic EuroSCORE	0.823	0.253-2.677	0.746
T/S Ratio	0.326	0.013-8.035	0.493

Table 38: Univariate analysis of the association of all pre-operative and intra-operative variables with the development of 1-year mortality in the DNA methylation population.

Variable	OR	p-value
Pre-op Hb	0.539	<0.001
Reoperation	21.25	<0.001
Pre-op Cr	1.032	0.002
Extubation Date	1.596	0.006
Pt transfused in ITU	4.400	0.008
Pre-op CRP	1.108	0.009
LOS (increasing LOS a/w AKI)	1.043	0.005
Pre-eGFR	0.959	0.011
Pre-op NYHA stage		
NYHA 2	2.640	0.368
NYHA 3	2.640	0.368
NYHA 4	24.750	0.012
Pre-op Statin	0.249	0.013
Cardiopulmonary Bypass time	1.009	0.033
Vasopressor Date	1.096	0.042

Table 39: Summary of predictors of 1-year mortality on univariate analysis listed by strength of association.

None of the measures of aging were significant predictors of 1-year mortality. As the measure of aging closest to reaching significance, pMA was used in the subsequent multivariate analysis together with the significant predictors listed in *Table 39*. Again, 'patient transfused in ITU' was excluded due to its close relationship with pre-operative haemoglobin level. Pre-operative CRP was also excluded due to 184/240 patients having no pre-operative CRP value recorded, thus potentially biasing the data. Estimated eGFR was excluded as it was neither a linear nor a categorical variable due to the fact that any patient with an eGFR of above 90 has a value of '>90' return by the laboratory. The adjusted odd's ratios of the remaining predictors in the multivariate model are shown in *Table 40*. Only pre-operative haemoglobin level was found to be an independent predictor of 1-year mortality

with reduced haemoglobin level associated with increased risk of death (OR 0.356; $p = 0.006$).

Variable	Adjusted Odds Ratio	95% CI	p-value
Predicted Age	1.020	0.938-1.109	0.638
LOS	0.977	0.872-1.094	0.682
NYHA 4	NA	NA	0.997
Pre-op Statin	0.643	0.085-4.881	0.643
Extubation date	1.637	0.632-4.240	0.310
Vasopressor Date	1.147	0.976-1.348	0.097
Reoperation	0.384	0.000-781.037	0.806
Pre-op Hb	0.356	0.171-0.742	0.006
Pre-op Cr	1.029	1.000-1.059	0.052
Bypass Time	1.020	0.994-1.046	0.135

Table 40: Multivariate model of independent predictors of 1-year mortality. Significant p-values <0.05 shown in bold. Model Nagelkaerke R square = 0.648. Block 0 predictive value = 93%, Block 1 predictive value = 96.8%

6.9 Adjustment for over fitting

As previously described in section 5.9, there is a potential for overfitting in both of the above multivariate analyses due to the limited number of the primary endpoint (AKI, n= 50). As such, the analysis was repeated with just pMA and the 4 most significantly associated predictors on univariate analysis (*Table 41*). The result of this was that pre-operative Hb also became a significant predictor of CSA-AKI in addition to cardiopulmonary bypass time and hypercholesterolaemia.

Variable	Adjusted Odds Ratio	95% CI	p-value
Predicted age	1.025	0.996-1.054	0.087
Bypass Time	1.017	1.009-1.025	<0.001
Pre-op Hb	0.779	0.625-0.971	0.026
Hypercholesterolaemia	2.202	1.042-4.653	0.039
Diabetes Yes/No	1.292	0.863-1.933	0.213

Table 41: Multivariate model of independent predictors of CSA-AKI limited to 5 predictors. Significant p-values <0.05 shown in bold. Model Nagelkaerke R square = 0.233. Block 0 predictive value = 79.2%, Block 1 predictive value = 81.0%

With only 16 endpoints for 1-year mortality, the model for predicting this endpoint was adjusted to include just 2 predictors; pMA and Pre-operative Hb. As expected, the finding that pre-operative Hb but not pMA predicted 1-year mortality was unchanged (Table 42).

Variable	Adjusted Odds Ratio	95% CI	p-value
Predicted age	1.015	0.973-1.058	0.500
Pre-op Hb	0.544	0.389-0.761	<0.001

Table 42: Multivariate model of independent predictors of 1-year mortality limited to 2 predictors. Significant p-values <0.05 shown in bold. Model Nagelkaerke R square = 0.0168. Block 0 predictive value = 92.3%, Block 1 predictive value = 92.8%

6.10 Receiver Operating Characteristic curve analyses of DNA methylation aging measures

6.10.1. Predictors of AKI

The ROC curves for each of the 4 measures of aging are shown in Figure 29 with the corresponding AUC values and significance levels in Table 43. Increasing values of

age, pMA and AMAR were statistically significant predictors of CSA-AKI. Of the three, pMA was the most significantly associated (AUC = 0.615; p= 0,012). The AUC of <0.5 for Delta age indicates that the risk of AKI increases as Delta age falls. As Delta age is a measure of chronological age minus pMA this finding confirms that the risk of AKI increases as pMA increases.

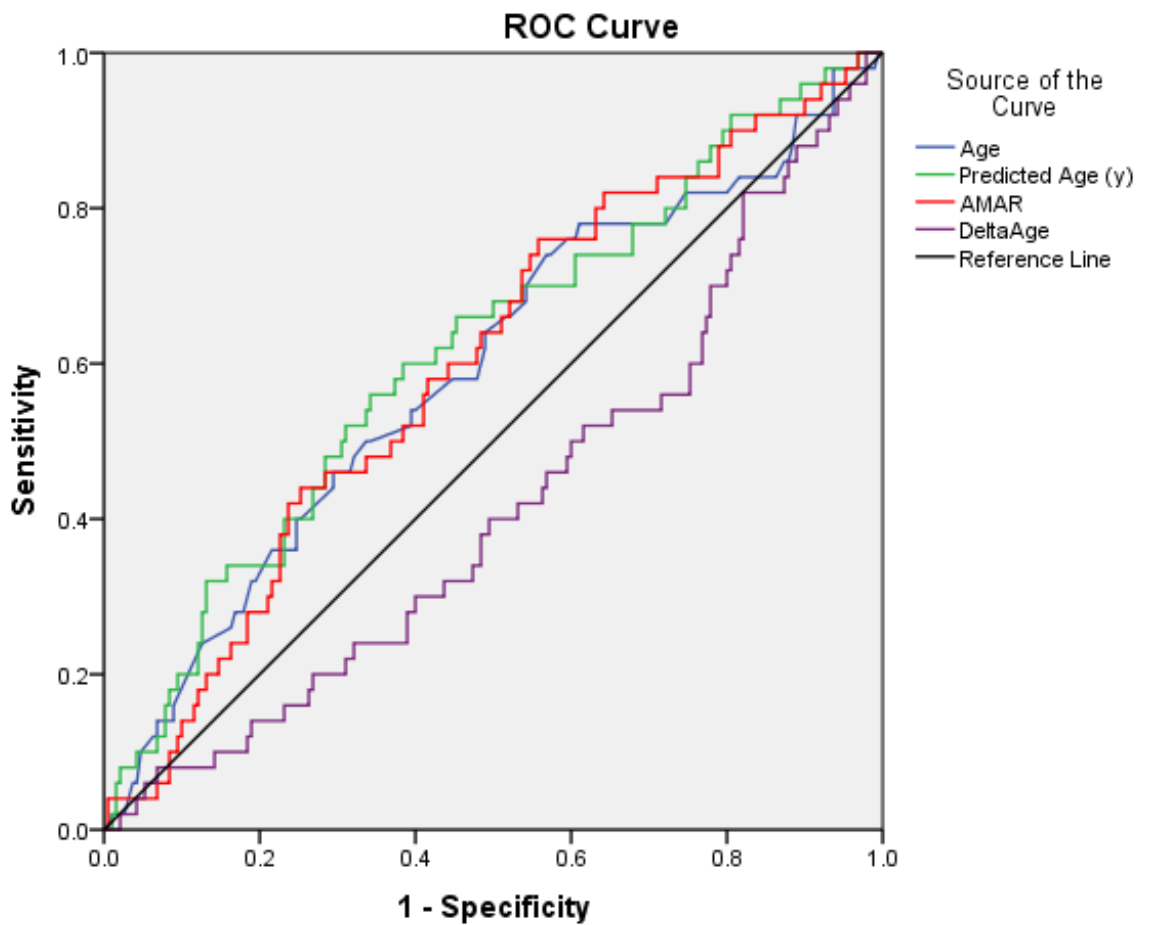


Figure 29: Receiver Operator characteristic (ROC) Curve demonstrating the diagnostic ability for the 4 measured aging measures in predicting CSA-AKI; Age (blue line), predicted methylation age (green line), AMAR (red line), and Delta Age (purple line).

Test Result Variable	Area Under Curve	Std Error	P-value	95% Confidence intervals	
				Lower Bound	Upper Bound
Age	0.591	0.047	0.047	0.500	0.683
Predicted Age	0.615	0.045	0.012	0.526	0.705
AMAR	0.597	0.044	0.034	0.511	0.684
Delta-AGE	0.418	0.045	0.075	0.330	0.507

Table 43: Diagnostic ability of age, predicted methylation age, AMAR, and Delta age for predicting cardiac surgery associated AKI. P-values for statistically significant predictors are shown in bold.

6.10.2 Predictors of 1-year mortality

The same 4 aging measures were correlated with 1-year survival. Logistic EuroSCORE was not included in this analysis as it had previously been run as part of the Telomere Length analysis (see section 5.12). The ROC curves are seen in *Figure 30* with the corresponding AUC and significance values given in *Table 44*. Our results show that none of the four measures of aging were significant predictors of 1-year mortality.

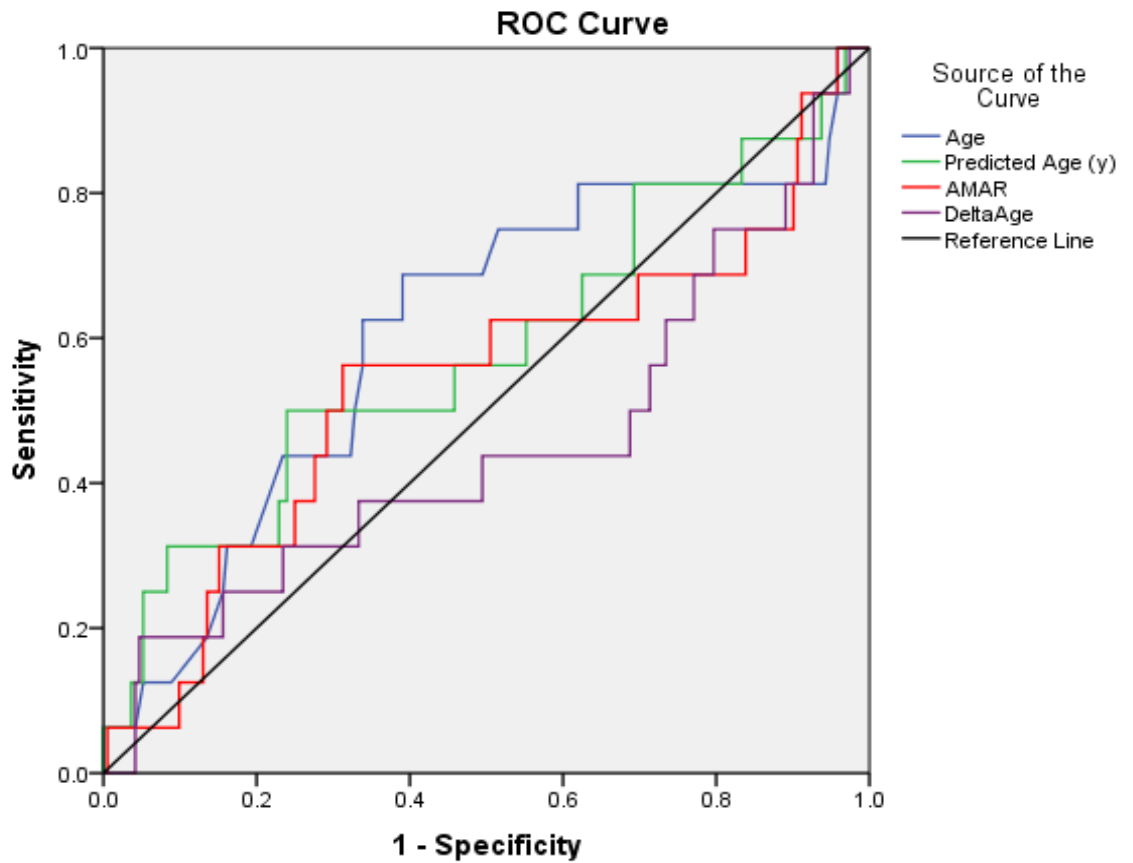


Figure 30: Receiver Operator characteristic (ROC) Curve demonstrating the diagnostic ability for the 4 measured aging measures in predicting 1-year mortality; Age (blue line), predicted methylation age (green line), AMAR (red line), and Delta Age (purple line).

Test Result Variable	Area Under Curve	Std Error	P-value	95% Confidence intervals	
				Lower Bound	Upper Bound
Age	0.609	0.080	0.149	0.452	0.766
Predicted Age	0.582	0.085	0.278	0.416	0.748
AMAR	0.539	0.086	0.601	0.370	0.709
Delta-AGE	0.452	0.087	0.522	0.282	0.622

Table 44: Diagnostic ability of age, predicted methylation age, AMAR, and Delta age for predicting 1-year mortality.

6.11 Additional Analyses of DNA methylation aging

6.11.1 Analysis of effects of fall in serum creatinine level

As previously described in section 5.11.1, analyses were done in which patients with acute falls in serum creatinine post-op (>26mmol/L in 48 hours) were excluded from the 'No AKI' patient group. As a result, 9 patients were excluded from the analysis. The results of the 4 measures of aging against the development of CSA-AKI in this population are shown in Table 45. As for telomere length, the analysis was also repeated with the 9 patients added to the AKI group with the overall effect of mildly reducing the strength of associations between the 4 measures of aging and CSA-AKI (results not shown).

		AKI	
		Yes n = 49	No n= 182
Age	Mean	67.07	63.60
	OR (95% CI)	1.020 (0.995-1.045)	
	p-value	0.122	
Predicted age	Mean	65.66	59.93
	OR (95% CI)	1.029 (1.006 -1.053)	
	p-value	0.016	
AMAR	Mean	0.994	0.950
	OR (95% CI)	5.220 (0.765-35.637)	
	p-value	0.092	
Delta Age	Mean	1.41	3.66
	OR (95% CI)	0.977 (0.947-1.009)	
	p-value	0.163	

Table 45: Association between the 4 measures of aging and development of CSA-AKI in the whole population excluding patients whose serum Cr fell by >26 µmol/l

6.11.2 Investigating the effect of removing patients of South Asian Origin

As previously described for mTL in section 5.11.2, a subgroup analysis was performed on patients of South Asian origin. When these patients were excluded from the population the effect sizes of the aging measures on CSA-AKI were reduced as shown in *Table 46*. There was no longer any significant association between pMA and CSA-AKI (*Figure 31*). When the South Asian population was analysed in isolation, pMA was significantly associated with CSA-AKI despite the reduced sample size (*Table 47 and Figure 32*).

		AKI	
		Yes n = 38	No n= 159
Age	Mean	66.73	63.52
	OR (95% CI)	1.017 (0.990-1.044)	
	p-value	0.221	
Predicted age	Mean	64.31	59.77
	OR (95% CI)	1.021 (0.996-1.047)	
	p-value	0.097	
AMAR	Mean	0.980	0.949
	OR (95% CI)	3.099 (0.376-25.539)	
	p-value	0.293	
Delta Age	Mean	2.42	3.74
	OR (95% CI)	0.987 (0.953-1.022)	
	p-value	0.469	

Table 46: Association between the 4 measures of aging and development of CSA-AKI in the whole population excluding patients of South Asian descent.

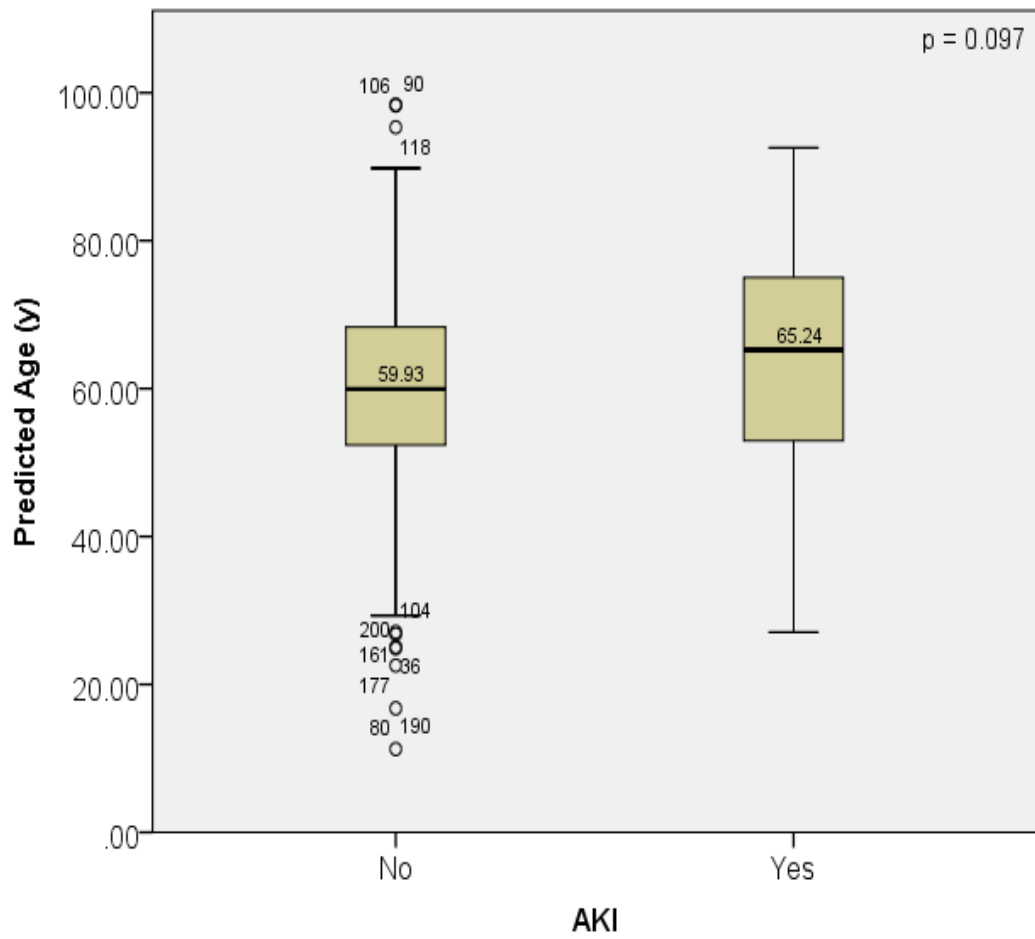


Figure 31: Boxplot of pMA and development of CSA-AKI in the whole population excluding patients of South Asian descent. Black bars represent median values.

		AKI	
		Yes n = 12	No n= 31
Age	Mean	67.82	62.91
	OR (95% CI)	1.050 (0.980-1.124)	
	p-value	0.165	
Predicted age	Mean	69.76	59.61
	OR (95% CI)	1.076 (1.008-1.148)	
	p-value	0.028	
AMAR	Mean	1.039	0.951
	OR (95% CI)	81.026 (0.451-14544.908)	
	p-value	0.097	
Delta Age	Mean	-1.939	3.300
	OR (95% CI)	0.931 (0.855-1.015)	
	p-value	0.105	

Table 47: Association between the 4 measures of aging and development of CSA-AKI in the patients of South Asian descent. Significant values ($p < 0.05$) are shown in bold.

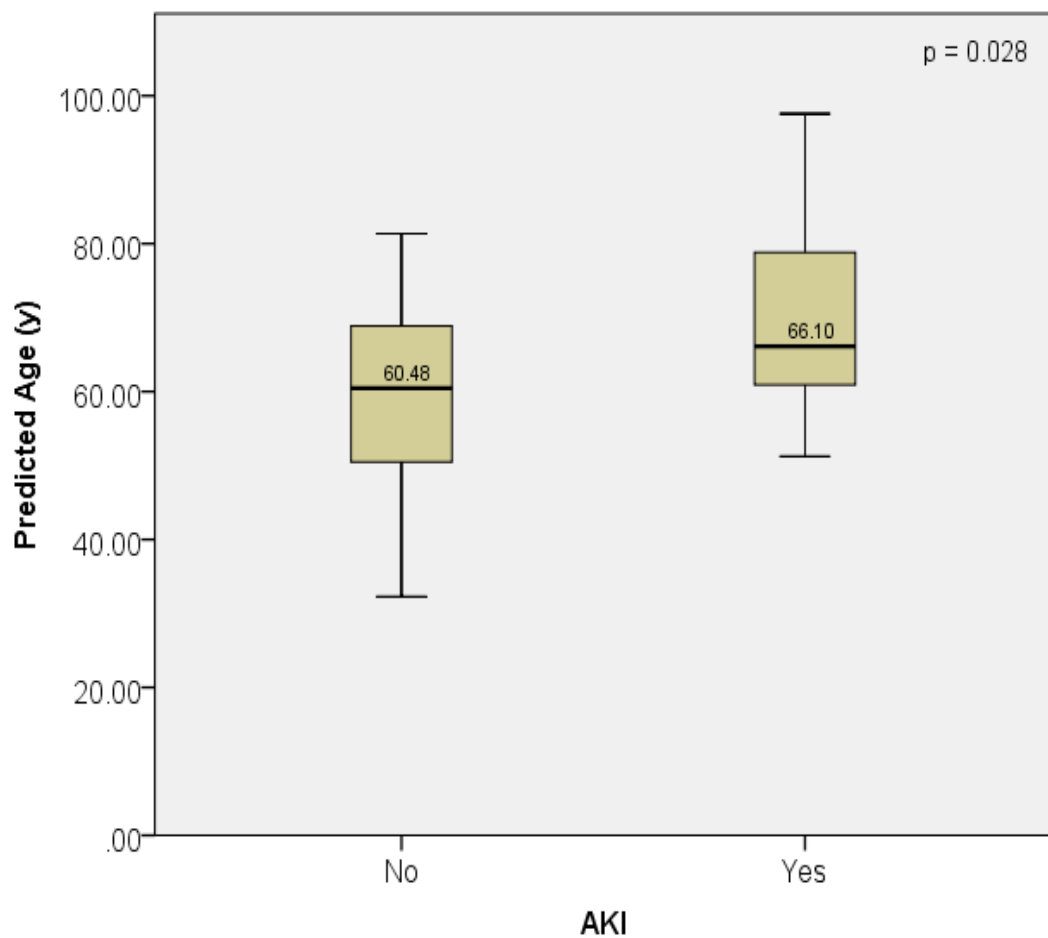


Figure 32: Boxplot of pMA and development of CSA-AKI in the patients of South Asian descent. Black bars represent median values.

6.11.2.1: Univariate analysis of pMA and CSA-AKI in South Asians

A repeat of the univariate analyses outlined in sections 6.7.1 was performed including all the same variables but limited to the South Asian population. Whilst CSA-AKI is significantly associated with pMA in this population ($p = 0.028$, *Table 47*) none of the other variables tested were significantly associated at a p-value of <0.05 (results not shown). As such, no multivariate analysis was performed.

6.11.3 Analysis of DNA methylation aging as a predictor of 1-year mortality in the South Asian population

The analysis of the 4 measures of aging as predictors of 1-year mortality was repeated separately for the Non-South Asian populations and the South Asian population. The results are shown in *Table 48* and *Table 49* respectively. Of note, the number of endpoints in this analysis are much reduced. Of the 35 patients with complete 1-year mortality data, only 3 had died within 12 months of their index operation. (8.6%). No measures of aging were significantly associated with 1-year mortality in either group.

		1 year mortality	
		Yes n = 13	No n= 160
Age	Mean	64.77	63.72
	OR (95% CI)	1.005 (0.965-1.047)	
	p-value	0.799	
Predicted age	Mean	62.31	60.55
	OR (95% CI)	1.008 (0.970-1.048)	
	p-value	0.678	
AMAR	Mean	0.980	0.960
	OR (95% CI)	2.095 (0.072-60.835)	
	p-value	0.667	
Delta Age	Mean	2.45	3.17
	OR (95% CI)	0.993 (0.938-1.051)	
	p-value	0.803	

Table 48: Association between the 4 measures of aging and 1-year mortality in the whole population excluding patients of South Asian descent.

		1-year mortality	
		Yes n = 3	No n= 32
Age	Mean	74.63	62.63
	OR (95% CI)	1.176 (0.976-1.417)	
	p-value	0.087	
Predicted age	Mean	76.58	60.64
	OR (95% CI)	1.101 (0.994-1.219)	
	p-value	0.066	
AMAR	Mean	1.026	0.974
	OR (95% CI)	7.113 (0.004-11814.412)	
	p-value	0.604	
Delta Age	Mean	-1.954	1.986
	OR (95% CI)	0.958 (0.842-1.090)	
	p-value	0.514	

Table 49: Association between the 4 measures of aging and 1-year mortality in patients of South Asian descent.

6.12 DNA methylation markers of senescence and outcomes after cardiac surgery

6.12.1 DNA Methylation senescence markers: Methodology

In addition to the 71 CpG site Aging array, the methylation status of the 6 CpG sites described by Koch *et al* (77) as correlating with cellular senescence were determined. The 6 CpG sites and their genomic sequences are shown in *Table 50*.

Of the 6 CpG sites assayed, 2 failed. One of these (GRM7) failed due to a failure of sequence amplification. The other failed site (PRAMEF-2) did produce reads but these mapped to an incorrect position in the Genome implying that the primer had not correctly amplified the target CpG. That left a total of 4 CpG sites as potential markers of cellular senescence.

CpG site	Genomic Sequence
GRM7	GTGCTGGAGGTGCTCCTGTG CG CGCTGGCGGCGGCGGGCGCGC
CASR	TGGCTGCAGCCAGGAAGGAC CG CACGCCCTTCGCGCAGGAG
PRAMEF2	AGAAGGTGGTGACTTACCAG CG CTGGACTCACTTTGCAGAGT
SELP	ACATAAACTCCATGGCTAT CG CTGTTCTCACTTTCTGAAC
CASP14	CTCTTCTACCTAGGAGATGA CG GGCTGGGGAAGCCATCTCAA
KRTAP13-3	TGACTATGCATGTTGGGTCT CG GGGTTTTGGATCCAATAGCT

Table 50: The 6 CpG sites in the senescence panel and their corresponding genetic sequences.

Developing a measure of cellular senescence in our study population was challenging as there is no direct measure of senescence available on which to base a model. In the aging model of DNA methylation outlined above, a separate population of healthy volunteers of known ages was available which were run on the same array against which a model could be built. In the case of cellular senescence, although the same control group was available, their level of senescence was not known. As the blood samples in this study came from live patients at a single time point it was not possible to know the passage number or population doubling time of the leukocytes from which DNA was extracted. As such, we have utilised the data published from Koch's original paper that described the methylation senescence signature (77). This paper developed models for predicting senescence based on plots of percentage Methylation of the CpG sites against passage number for linear regression analysis. The original plots from Koch *et al* are shown in *Figure 33*. We used these same plots to determine cut off methylation percentages for senescence based on passage numbers. Using the CpG site for SELP as an example, because SELP negatively correlates with passage number, if we define a passage number of 5 as indicating senescence, any sample with a % methylation of less than 71% (see red line, *Figure 33*) can be assumed to have a passage number of greater than 5 and thus be deemed to be senescent. In our routine laboratory work we find that cell lines usually senesce after a passage number of 5. For each of the 4 CpG targets successfully sequenced, this method was used to convert the methylation status to a binary measure of senescence (senescent/non-senescent) and strength of association was measured using the Chi-

squared test. For completeness, further analyses were performed using passage numbers of 10 and 15 as a cut off for defining senescence.

In addition to the above method simple logistic regression analyses were performed for each of the 4 CpG sites with the Beta-values for methylation run against the outcome of CSA-AKI.

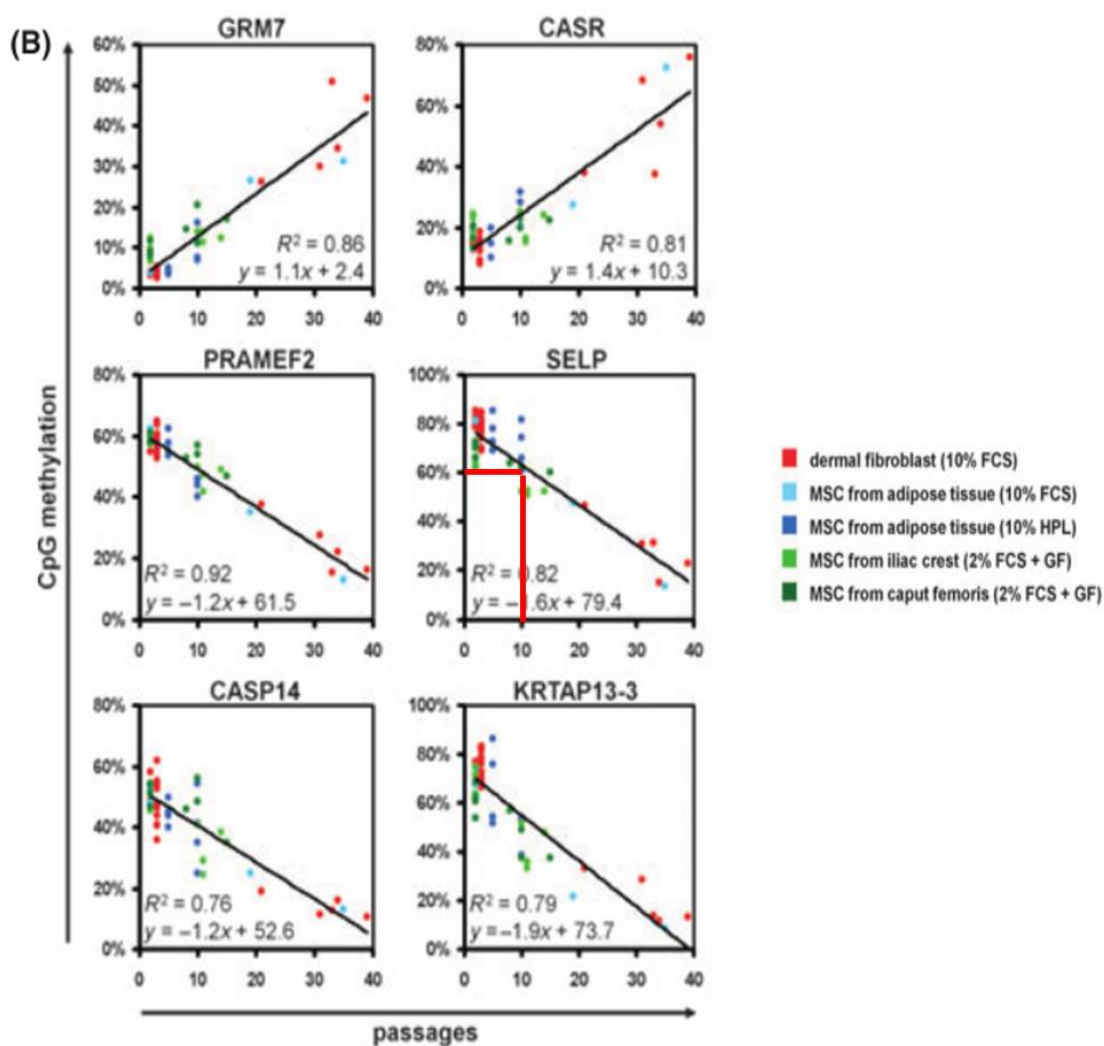


Figure 33: Methylation level of the 6 CpG sites plotted against passage number. The various colours denote the tissue type sampled. The red line demonstrates the determined senescence cut off for SELP. Reprinted from *Aging Cell*, Vol 11 (2), Koch et al, Monitoring of cellular senescence by DNA-methylation at specific CpG sites, Page 368, Copyright (2011), with permission from John Wiley and Sons

6.12.2 DNA Methylation senescence markers: Results

Simple logistical regression analysis of methylation beta values against CSA-AKI showed no significant associations for any of the 4 CpG sites (*Table 51*). Neither were there any significant relationships with either of the 4 sites and CSA-AKI in a multiple logistical regression analysis. The raw data for the Methylation senescence arrays together with the data coded into a binary senescent/non-senescent variable is shown in *Appendix J*. The results of the coded analysis are shown in *Table 52*.

CpG Site	B-value	OR	95% CI	p-value
SELP	-0.016	0.985	0.965-1.004	0.128
CASP14	0.000	1	0.985-1.015	0.990
CASR	-0.001	0.999	0.970-1.038	0.936
KRTAP13-3	-0.016	0.984	0.965-1.003	0.105

Table 51: Results of Binary logistical regression for each of the CpG sites with development of CSA-AKI. None of the relationships reached statistical significance.

CPG Site	Passage No. (Senescent/No n-senescent)	% Senescent AKI	% Non-Senescent AKI	p-value
SELP	5 (154/100)	23.4	18.0	0.306
	10 (107/147)	24.3	19.0	0.312
	15 (57/197)	21.1	21.3	0.965
CASP14	5 (26/228)	19.2	21.5	0.790
	10 (19/235)	21.1	21.3	0.982
	15 (13/241)	23.1	21.2	0.869
CASR	5 (181/73)	22.1	19.2	0.607
	10 (106/148)	19.8	22.3	0.633
	15 (49/205)	22.4	21.0	0.821
KRTAP13-3	5 (77/177)	29.9	17.5	0.027
	10 (31/223)	29.0	20.2	0.259
	15 (13/241)	30.8	20.7	0.390

Table 52: Analysis of CpG sites coded into senescent/Non-senescent based on cut-off values of % methylation approximating to passage numbers of 5, 10 and 15. Statistically significant associations are shown in bold (p<0.05)

The coded senescence variable for KRTAP13-3 (KRTAP133-Senescent at 5%) was entered into a multiple logistical regression together with the other significant predictors of AKI previously demonstrated in this cohort (See section 5.7.2.1; *Table 13*). The results of this are shown in *Table 53* and demonstrate that KRTAP13-3 continues to be an independent predictor of CSA-AKI ($p=0.041$) together with the previously demonstrate significant predictors which were cardiopulmonary bypass time ($p<0.001$), hypercholesterolaemia (0.021), pre-operative asthma ($p= 0.015$), and pre-operative haemoglobin (0.005).

The above analyses, including binary logistical regression, multiple logistical regression and Chi-squared testing of the coded methylation Beta-values were repeated using 1-year mortality as the outcome variable in place of CSA-AKI. No significant associations were found between any of the CpG sites and 1-year mortality across any of these analyses (results not shown).

Variable	Odds Ratio	95% CI	p-value
KRTAP133-Senescent at 5%	2.141	1.031-4.447	0.041
Bypass time	1.016	1.009-1.024	<0.001
Pre-op Hb	0.737	0.596-0.912	0.005
Hypercholesterolaemia	2.374	1.141-4.939	0.021
Diabetes (yes/no)	1.619	0.736-3.566	0.231
Hx of asthma	5.602	1.405-22.335	0.015

Table 53: Multivariate model of independent predictors of CSA-AKI including KRTAP133-Sen. Significant p-values <0.05 shown in bold

6.13 Logistical regression analysis of individual CpG sites and CSA-AKI

Finally, to determine whether any of the 526 CpG sites were individually associated with CSA-AKI we performed logistical regression analysis for each individual CpG with CSA-AKI as a binary outcome. This statistical analysis was performed by Dr Erini Marouli (Lecturer in Computational Biology, WHRI). Out of 526 CpG's, 37 were associated with the development of CSA-AKI at a p-value of <0.05 (results for the top 40 associated CpG's are shown in *Appendix K*). However, with this number of variables being tested the likelihood of observing 'significant' associations increases. The Bonferroni correction is a commonly used method for countering this effect. It alters the p-value to a more stringent value so the chance of introducing a Type 1 error is reduced (i.e. rejecting the null hypothesis when there is not sufficient evidence to). However, it increases the risk of Type 2 error (failing to reject the null hypothesis when you should).

Applying the Bonferroni correction to this dataset produces a corrected significance level of $p < 9.5e^{-5}$. Using this value none of the tested CpG's were significantly associated with CSA-AKI. Adjusting the analyses to correct for differences in gender and age did not significantly alter the associations between CpG methylation and CSA-AKI.

6.14 General Discussion of DNA methylation data

6.14.1 Discussion of significant findings in aging model of DNA Methylation

Primary outcome

For the 4 measures of age analysed, only the predicted DNA methylation age (pMA) was a significant predictor of the development of CSA-AKI on univariate analysis (OR 1.030 p=0.013). The mean pMA in patients who developed AKI was 65.62 years compared to 59.74 in those who did not, a difference of 5.9 years. In comparison the chronological age of patients who developed AKI was 66.99 years compared to 63.41 in those who did not, a difference of 3.6 years. This finding is consistent with our original hypothesis that a patient's 'biological age' may be more important in determining their outcome after cardiac surgery than their chronological age. In this study we have used a previously validated group of 71 CpG sites that have been shown to be highly predictive of age, and built a model of methylation age based on a population of healthy controls. In applying this model to predict the ages of the study population we generated values of predicted methylation (pMA) that varied from the true chronological age. In doing so we have used pMA as a surrogate marker of biological age.

Previous studies into methylation signatures of aging have used measures that incorporate the individual's chronological age either as a ratio (AMAR) or as a difference (Delta age). In the case of our hypothesis that the biological age may be a more accurate predictor of CSA-AKI than chronological age, to use either of these methods seems counter intuitive as the incorporation of the chronological age

might mask any clinically significant associations that exist when the predicted methylation age is considered in isolation. This was found to be the case in the prediction of CSA-AKI with neither AMAR nor Delta age demonstrating a statistically significant association. By running all four markers of aging against all clinical variables it was possible to detect the effects of variables on methylation status that would not have been apparent had only chronological age and pMA been analysed. One example of this is the effect of smoking which is discussed below.

On multivariate analysis, pMA was no longer significantly associated with the development of CSA-AKI. Nearly all of the variables found to be significant predictors of CSA-AKI and included in the multivariate model are themselves affected by chronological age. As such their inclusion in the model reduces the likelihood of aging markers being shown to be independent predictors.

In the propensity score analysis undertaken in this cohort, the propensity score model included chronological age as a variable i.e. cases and controls were age-matched. This had to be the case to ensure that any differences in pMA seen were not simply due to differences in chronological age between the cohorts. As such, the ages of the cases and controls were very well matched (66.97 in AKI group Vs 67.17 in the Non-AKI group; $p = 0.975$). Mean pMA was higher in the AKI group compared to the Non-AKI group (65.09 Vs 61.04), although this did not reach statistical significance ($p = 0.241$). A comparison of Delta-age between the two groups failed to reach statistical significance ($p = 0.07$) using an alpha of <0.05 .

However, this result means that the likelihood of accepting the null hypothesis that there is no difference in Delta age between the two groups, is less than 1 in 10.

In the ROC curve analysis, chronological age, pMA and AMAR all demonstrated p-values of <0.05 , meaning that the area under the curve (AUC) was significantly different from 0.5 and therefore that these measures were able to distinguish between AKI and non-AKI patients to varying degrees. Of the three measures it was pMA that again showed the strongest association (AUC = 0.615; $p=0.012$). As a result of all of the analyses performed, we conclude that increasing pMA is significantly associated with the development of post-operative AKI and that its predictive ability is superior to that of chronological age.

Unlike genetic variations, epigenetic associations with disease can be consequential as well as causal. Distinguishing between the two is not always easy and a key step is determining whether or not the variation was present prior to the onset of the disease process (192). As the blood samples were drawn prior to the onset of CSA-AKI, it seems obvious to conclude that the observed increases in pMA in the AKI group are causal. However, if the higher rates of CSA-AKI are a byproduct of higher cellular age or senescence in the AKI group then the observed methylation changes could also be consequential. Whether the observed association is causal or consequential is not of primary import. If the clinical application is to identify patients at higher risk of post-operative complications, the association alone is sufficient. Unfortunately, as the strength of the association between pMA and CSA-AKI is not strong (AUC of 0.61), the current epigenetic signature for predicting

methylation age is unlikely to be useful in terms of risk stratification for individual patients developing CSA-AKI. As such, the value of this exploratory study is to provide preliminary proof-of-concept validation that targeted methylation signatures are associated with post-operative complications, specifically the development of CSA-AKI. However, by demonstrating that pMA was more closely associated with CSA-AKI than chronological age we provide evidence that epigenetic aging signatures are interesting targets for future studies into the optimisation of cardiovascular risk modification at an individual level.

Secondary outcome

The secondary endpoints for this study included in-hospital mortality and 1-year mortality. Neither pMA, chronological age, AMAR or Delta age were significantly associated with either of these outcomes. Further analysis was not performed for in-hospital mortality due to the low number of cases that died in this period (n=5). However, analyses were run on predictors of 1-year mortality. pMA was not found to be associated with 1-year mortality on either univariate or multivariate analysis. Again, these analyses were limited by the low number of patients reaching this endpoint (n= 16). The study was designed to recruit sufficient numbers for outcome of the primary end-point of CSA-AKI and as such analyses of these secondary endpoints appear underpowered.

As previously described in chapter 5, a composite outcome was created to increase the number of endpoints. This composite outcome was designed as a measure of post-operative morbidity and combined the endpoints of new CSA-AKI, new AF,

stroke and reoperation. We found that predicted methylation age was associated with composite outcome whereas chronological age was not (OR 1.023; p=0.014). However, this trend seems primarily due to the association of pMA with CSA-AKI. If we remove AKI from the composite endpoint (leaving, new AF, stroke and, reoperation) the relationship with predicted age no longer reaches significance (OR = 0.988; p=0.189). In summary, of all of the outcome measures, only CSA-AKI shows a significant association with predicted methylation age on univariate analysis only.

Other significant findings

All 4 measures of age were run against a range of pre-operative, intra-operative and post-operative variables (*Table 33* and *Table 34*). The strength of correlation of pMA with chronological age was seen to be similar in the study subjects (R=0.7) as that seen in the model of healthy controls from which the predicted ages were derived (R=0.75) (*Figure 25* and *Figure 26*). This suggests that the model was applicable to the study subjects. However, the pMA of the study subjects tended to underestimate the chronological age in comparison with the healthy controls. This can be seen in the comparative tables of Age, pMA, AMAR and Delta age shown in *Appendix L*. The average Delta age of the 24 healthy controls was 1.59 compared to -3.8 in the study population, indicating that pMA underestimated age in the study population. This is surprising as we had expected the study patients to have increased pMA in comparison to healthy controls, due to their significant cardiac disease. There are two possible interpretations for this finding. Firstly, that the observation represents a real reduction in pMA in the study patients over the disease state. It is difficult to hypothesise why this might be the case. However, it

might be a result of the patients in the study group having commenced on treatment to correct their underlying disease state such as antihypertensives, lipid lowering medications and smoking cessation. DNA methylation is a dynamic process and changes in risk exposure can be quickly reflected in reversal of methylation changes (148). As such methylation status may represent current risk exposure rather than cumulative lifetime risk exposure. As such, it could be argued that commencement of such therapies may artificially reduce the pMA in the study subjects if DNA methylation is measured at a point at which they have commenced treatment.

The second explanation, is that the population from which the model of pMA was derived differed in some way from the study population so that the model under-predicted methylation age when applied to the study population but not when applied to the healthy control population. We tested whether the ages of the model derivation (model) cohort and the study (test) cohort were well matched and found that they were, both in terms of average age and age range, with the model cohort actually showing a greater age range (*Figure 34*).

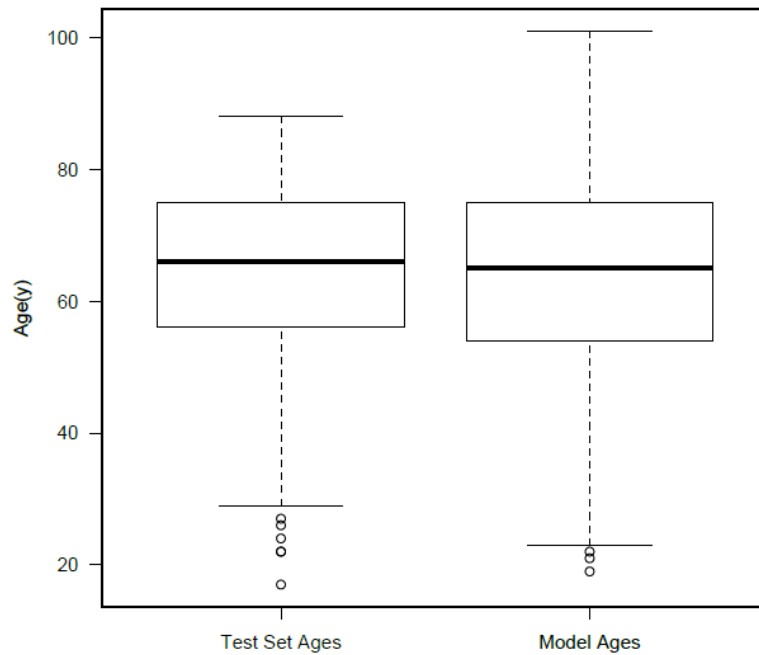


Figure 34: Box plots for age for the study cohort (Test) and the Model derivation cohort (Model). Solid black lines represent mean age with Interquartile range boxes and range (dotted line). Figure provided by Dr Robert Lowe.

An alternative explanation is that the observed reduction in pMA in the study subjects is due to the different tissue handling of the study population to that of the healthy controls which the model for pMA was trained on. The healthy controls from which the model of pMA was derived were provided from a different study with different protocols for tissue storage and DNA extraction. As DNA methylation is highly dependent of the integrity of the extracted DNA it might be that these differences in sample preparation have resulted in slight variations in the predictive model that causes it to underestimate pMA in the study cohort but not in the healthy controls. However, as we are only looking at the relationship of pMA with outcomes within our study population and not across studies, it is the difference in pMA between the two groups rather than the actual values that are of primary interest. The fact that, as a group, the predicted methylation ages of the study

subjects are less than their chronological ages does not invalidate the finding that pMA was significantly greater in the AKI group.

As a result of the close correlation between chronological age and pMA it is not surprising that pMA largely followed chronological age in terms of its associations with pre-operative and intra-operative factors (*see tables 33 and 34*). Factors which associated strongly with age were also found to associate strongly with pMA. For example, length of post-operative stay, pre-op diabetes, hypertension and hypercholesterolaemia were all positively associated with increased age/pMA whilst pre-operative haemoglobin was negatively associated. The only exception to this correlation between age and pMA was seen in smoking status. Whilst a significant difference was seen between the age of ex-smokers and current smokers (67.15 years Vs 58.97 years; $p=0.007$), this trend was not seen in pMA (63.21 years Vs 60.98 years; $p=0.784$). The significant difference seen in Delta age between these two groups (+3.93 years Vs -2.00 years; $p=0.022$) reveals the effect of smoking on methylation age with current smokers showing a marked elevation in pMA when compared with ex-smokers. The same effect is seen when current smokers are compared with lifelong non-smokers ($p=0.035$) but no difference is seen in Delta Age between non-smokers and ex-smokers (3.55 Years Vs 3.93 years; $p=NS$) indicating that once a patient has stopped smoking, their predicted methylation age returned to that of non-smokers. This finding demonstrates the dynamic changes in methylation status that can occur in response to altered environmental stimuli.

6.14.2 Discussion of significant findings in senescence models of DNA Methylation.

Of the 4 successfully assayed CpG sites, none showed any significant correlation with AKI when the % methylation level of the individual samples were run against CSA-AKI using logistical regression. However, when the % methylation values were converted to binary values of senescent or non-senescent, KRTAP13-3 was significantly associated with the development of CSA-AKI. 29.9% of senescent samples developed CSA-AKI compared with 17.5% of non-senescent samples, meaning that rates of senescence were 42.6% in the AKI group compared with 27% in the non-AKI group ($p=0.027$). Similar trends were seen if senescence was defined using passage numbers of 10 or 15, but these analyses did not reach statistical significance due to the reduced proportion of cells coded as senescent with these passage numbers. Multivariate analysis was performed in which the above analysis for KRTAP13-3 at a passage number of 5 was combined with the other factors previously found to be significantly associated with the development of CSA-AKI on univariate analysis (see *Table 53*). In this analysis KRTAP13-3 defined senescence remained as an independent predictor of CSA-AKI ($p=0.041$) together with the previously demonstrate significant predictors which were cardiopulmonary bypass time ($p<0.001$), hypercholesterolaemia (0.021), pre-operative asthma ($p= 0.015$), and pre-operative haemoglobin (0.005).

In the development of the original 6 CpG methylation signature for senescence performed by Koch *et al*, no consideration was given to the functional relevance of the genes corresponding to the 6 markers. Instead the CpG sites were picked solely on their predictive values as epigenetic markers (77). The in-vivo function of

KRTAP13-3 has not been fully elicited but it is thought to code for a Keratin associate protein (KRTAP) within the hair cortex. These proteins form a matrix within which hair keratin intermediate filaments are embedded. They are essential for the formation of a rigid and resistant hair shaft through their extensive disulfide bond cross-linking with abundant cysteine residues of hair keratins (<https://www.uniprot.org/uniprot/Q3SY46>). KRTAP13-3 has not been found to be involved directly in renal function or play a role in cell senescence.

6.14.3 Comparison of results with previous studies

No previous studies have been performed into associations between methylation status and outcome following cardiac surgery. However, several studies have linked methylation status with some of the pre-operative factors investigated in the current study. Firstly, we will look at the association of pMA with chronological age. The various studies outlining epigenetic clocks and their ability to predict chronological age have already been discussed in section 4.2. Hannum *et al* first described the signature of 71 CpG probes associated with aging that we have used for the current study. This model was applied to a validation cohort of 174 samples processed in exactly the same manner as the training set, and achieved a correlation between pMA and age of 0.91 with an RMSE of 4.9 years. It is not stated whether these 174 patients were healthy controls nor is their mean age or age range given, preventing normalisation of the RMSE for direct comparison with the current study. Our aging model was similarly applied to a validation cohort of 24 healthy controls achieving a correlation between pMA and age of 0.75 with an RMSE of 6.89. We have already seen that Horvath's methylation aging signature predicts chronological

age with a mean absolute error (MAE) of 3.6 years and an R correlation of 0.96. This compares with a MAE of 5.5 years in our validation cohort. However, in a further study by Koch *et al*, pMA was determined using an epigenetic-aging signature based on just 5 CpG sites (166). This model achieved a correlation between predicted and chronological age of 0.64 with an average precision of +/- 12.7 years. As such, we feel that our model achieved a good degree of age prediction in the healthy control group given the limited number of CpG's mapped in the current study.

DNA methylation aging and gender. Hannum *et al* found that the methylation aging rate, defined by the authors as AMAR, was 4% quicker in males than in females. We found a similar trend in the current study with AMAR being 3% greater in males than females although this result did not meet statistical significance ($p=0.247$). The non-significant result is likely representative of the study being underpowered to detect a true difference of this size.

DNA methylation aging and smoking. One of the main findings of this study was a significant reduction in Delta age in smokers compared to non-smokers or ex-smokers. Several studies have previously demonstrated changes in methylation status associated with smoking. The study by Tsaprouni *et al* has already been discussed, in which an EWAS was performed on 464 individuals (22 smokers, 263 ex-smokers and 179 non-smokers). They found 53 probes that associated with smoking and were able to replicate 30 of these in an independent cohort of 356 twins (41 current, 104 ex-smokers and 211 non-smokers). All 30 probes were found to exceed the genome wide threshold of significance. All but 1 of these probes

showed a clear trend that smokers have lower methylation levels than non-smokers, and for all 30, methylation levels were at least partially restored in ex-smokers. From this the authors conclude that methylation changes in smoking are at least partially reversible upon cessation.

It should be noted that all of the studies outlined above investigated a direct link between smoking and changes to the methylome. This is different from the current study in which smoking has been found to associate with changes in a predictive model for aging built on 48 methylation probes. One possible explanation is that smoking induces generalised hypomethylation of multiple CpG's and as such results in accelerated aging rates in our model of pMA. This theory is supported by previous studies that have shown that heavy chronic smoking itself has nominally significant effects on methylation status at nearly one quarter of the CpG loci in the genome (193). Beach *et al* (194) investigated the effect of smoking status on aging rate using the same 71 probe epigenetic clock proposed by Hannum *et al* (76). However, as this study was solely based on new analysis of data in publicly available databases, smoking status was defined by demethylation at cg05575921 rather than by determining the smoking status of individuals. Demethylation at cg05575921 has previously been shown to be strongly associated with daily cigarette use (193). Aging rate was determined from an index of the discrepancy between biological and chronological age created by regressing chronological age on biological age and using the residual as the dependent variable. Smoking status was found to be associated with accelerated aging at all levels of smoking exposure. The results of the current study echo these results. In addition, we have demonstrated that the

effect of smoking on aging rate appears to be lost in ex-smokers, supporting the finding of Tsaprouni that smoking related methylation changes are reversible on cessation. This finding is also supported by the findings of a pilot study by Lei *et al*, which demonstrated reduced aging rate in 22 patients following smoking cessation (195). Again, this study utilised the differentially methylated residue (DMR) to determine smoking status.

6.14.4 Discussion of additional analysis of pMA in CSA-AKI

As with the mTL analysis performed in chapter 5, exclusion of patients with acute falls in serum creatinine within the first 48 hours post-operatively did not alter the associations between the 4 measures of aging and CSA-AKI.

In a subgroup analysis of South Asian patients compared with the rest of the population, we found that exclusion of South Asian patients reduced the strength of the association between pMA and CSA-AKI compared with the total population. (OR 1.021; $p = 0.097$ Vs OR 1.030; $p = 0.013$). When patients of South Asian descent were analysed in isolation, the association between pMA and CSA-AKI was increased and remained statistically significant (OR 1.076, $p = 0.028$), despite the reduced sample size. Within this subgroup, pMA was the only significant predictive factor for CSA-AKI ahead of current recognised risk factors such as bypass time ($p=0.508$), Diabetes ($p=0.286$), pre-operative renal disease ($p=0.411$) and pre-operative haemoglobin ($p=0.195$). Unlike the analysis of mTL and CSA-AKI, exclusion of the South Asian population does not appear to eliminate the association between pMA and CSA-AKI in the rest of the population. There is still a trend of increased

pMA in the AKI cohort although this fails to reach statistical significance. Part of the reduction in p-value can be attributed to a reduction in sample size from 240 (total population) to 197 (Non-South Asian population). Furthermore, the association between pMA and AKI remains stronger than that of chronological age supporting our previous conclusion that methylation-based measures of age are interesting targets for future studies into the optimisation of cardiovascular risk stratification. However, we can also conclude that, as with mTL, pMA is much more closely correlated with CSA-AKI in South Asian patients than other ethnicities and further studies are needed to elicit the potential mechanisms underlying this finding.

Analysis of the association of the 4 measures of aging and 1-year mortality was limited due to the small number of endpoints in the mortality group (n=3). Interpretation is also complicated by the fact that the patients who died had increased chronological age. However, if we look at the chronological-age-corrected measures of AMAR and Delta age there are trends towards increased aging rates in the non-survivors (*Table 49*) As such, further follow up is awaited to see if an increased number of endpoints reveals any significant associations.

6.14.5 Strengths and limitations DNA methylation experiments

There are several strengths and limitations to the current study. A significant strength of the study is that it is ambitious in its aim to apply epigenetics in a clinically relevant manner. Several studies into epigenetics have focused on epigenome wide association studies (EWAS) in an attempt to find epigenetic links to disease processes (196-199). The most suitable epigenetic phenomena for EWAS

is DNA methylation due to the development of chips allowing interrogation of several thousand CpG sites. Whilst often successful, the clinical applications of such studies are limited as EWAS is a costly and time intensive technique. The next step in the clinical application of epigenetic data is to demonstrate that targeted epigenetic data can be associated with disease states. This study attempts to do just that by building on previous data acquired from EWAS studies to perform targeted methylation analysis and apply it to a common clinical scenario (CSA-AKI). By mapping just 71 probes instead of the 850,000 mapped in the EPIC methylation array (200) or the 450,000 mapped in the Illumina HumanMethylation450 BeadChip (201), such techniques may form the basis of targeted epigenetic tests for specific clinical conditions. A further strength of the current study is that it was sufficiently powered to detect a significant difference in pMA for the primary outcome of CSA-AKI. It was not expected that there would be a sufficient number of endpoints to detect differences in methylation states between patients grouped by mortality at discharge or at 1-year follow-up. The study also employed a range of statistical methodology to evaluate associations between pMA and the defined endpoints including multivariate modelling with logistic regression and propensity matching.

The current study has several limitations. Firstly, not all 71 of the aging signature CpG's nor all 6 of the senescence signature CpG's were successfully mapped. This was primarily due to a failure to design primers specific enough to amplify the CpG of interest. This is a limitation of determining methylation status via this method rather than using an epigenome wide array. A previous study by Weidner *et al* in which an epigenetic clock was developed to predict chronological age, also

encountered this problem in primer design when trying to perform targeted bisulphite pyrosequencing (167). After identifying 102 age-associated CpG sites based on DNA profiles from 4 studies using the Human-Methylation27 BeadChip platform, the authors attempted to pyrosequence the top 5 most associated sites in a second cohort but were only able to map 3 of the 5 due to failure in primer design for the other 2. As a result of this limitation, only 48 of the 71 CpG's identified by Hannum *et al* were used to generate our model of methylation age. Despite this we were able to generate a model for pMA that correlated well with chronological age in the healthy controls (RMSE 6.89, R=0.75). Therefore, the loss of some of the original CpG's described by Hannum might well not be a limitation but it is important to note that the final model used in our analysis was not the exact same signature as that described in this paper (76). Secondly, as with the Telomere analysis in chapter 3, DNA methylation was performed on DNA extracted from peripheral blood leukocytes. It is not yet known whether DNA methylation age of easily accessible tissues such as blood or saliva can act as surrogate markers for inaccessible tissues such as the kidney (164). As such the aging or senescence signatures from peripheral blood might not be representative of those in the kidney that ultimately determine the propensity to develop CSA-AKI. However, we would defend the use of peripheral blood in this setting by contending that if a test is to be clinically relevant then it must be acceptable to the patient, and obtaining DNA from peripheral blood is much more feasible than obtaining renal tissue.

A third limitation of the study is in the analysis of DNA methylation data for the senescence associated CpG's. Of the 4 CpG's successfully mapped, none correlated

with CSA-AKI on logistic regression analysis. In an attempt to convert the data to a binary output, the original plots from Koch's paper have been used (77). This methodology is open to criticism as these plots were derived from fibroblasts and mesenchymal stem cells growing in vitro and therefore may not be applicable to methylation of DNA extracted from peripheral blood. As there is no possible way of measuring passage number or populations doubling time of leukocytes harvested in this manner there was no alternative way of converting the continuous methylation data to a binary output. Performing such a conversion seems logical as it is not the exact level of methylation that is critical to cellular function but rather whether or not the cell has been triggered to senescence. Because of the inability to validate this conversion against a defined marker of senescence, the association of CSA-AKI with hypo-methylated CpG sites correlating with KRTAP13-3 remains speculative.

CHAPTER 7: Telomerase Activity and outcome after cardiac surgery: Summary of failed optimisation experiments

7.1 Introduction

Prior to starting recruitment, attempts were made to optimise a protocol for measuring the activity of the enzyme Telomerase. Unfortunately, despite a lot of time and effort, we were unable to satisfy ourselves that any of the tests trialled were able to produce results with a level of reproducibility that could be depended on. However, the scientific processes that we undertook in trying to measure telomerase activity taught me many useful lessons and was one of the major learning experiences of my PhD. As such, we have outlined this process in this chapter.

7.2 Isolation of Peripheral Blood Mononuclear Cells

7.2.1 Harvest of Peripheral Blood Mononuclear Cells

Telomerase activity was measured in Peripheral Blood Mononuclear Cells (PBMC). PBMC from healthy volunteers were harvested using the BD Vacutainer Mononuclear Cell Preparation Tube (CPT) (BD Biosciences, San Jose, CA). This system is based on the Ficoll density gradient separation method of PBMC isolation but is more time efficient as blood is not required to be layered onto the Ficoll manually. Comparative studies have shown that vacutainer CPT and Ficoll density gradient separation perform equivalently in terms of maintaining the quality and function of PBMC (203). PBMC were harvested in accordance with the

manufacturer's instructions. In brief, blood is taken by standard venepuncture directly into a BD vacutainer CPT and stored upright at room temperature until processed (within 2 hours of collection). After remixing the blood by inverting 8-10 times, the CPT's were processed by centrifuging the CPT for 15 mins at 1800 RCF at room temperature. Centrifugation caused the blood to separate into constituent layers as shown in *Figure 35*. The Monocyte layer was seen as a whitish layer immediately below the plasma layer. This layer was aspirated off with a Pasteur pipette and transferred to a fresh 15ml conical Eppendorf tube together with Phosphate Buffered Saline (PBS) to a total volume of 15ml. The tube was inverted 15 times to mix the cells before being centrifuged at 300 Relative Centrifugal Force (RCF) for 15 minutes. The supernatant was aspirated and the cell pellet resuspended in a further 10 mls of PBS. A further centrifugation step was performed at 300 RCF for 10 minutes. To reduce the degree of platelet contamination we found that a further centrifugation step at 100RCF for 10 minutes was required. The final cell pellet was diluted in 2mls of PBS.

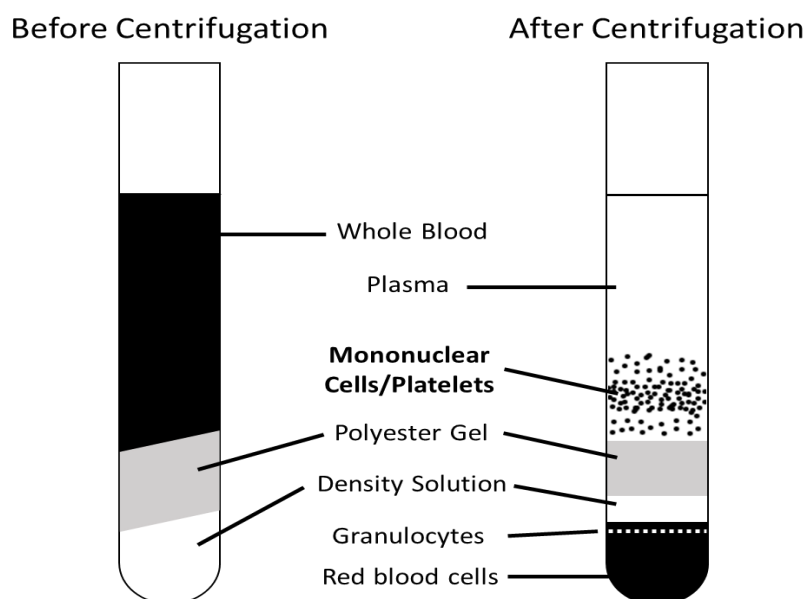


Figure 35: Figure demonstrating the separation of blood in a BD Vacutainer CPT tube after centrifugation.

7.2.2 Quantifying starting amount of PBMC

Accurate comparative quantification of Telomerase activity (TA) is dependent on the same starting quantity of PBMC being used for each sample. Initial optimisation experiments were performed using a set number of cells in each reaction (2×10^5). Cell counts of each sample were determined manually using a haemocytometer. 100 μ L of the final 2ml stock solution obtained from the PBMC harvest was taken and combined with an equal volume of Trypan Blue. The Trypan Blue helps to identify non-viable cells by staining them blue as it is able to permeate their cell membrane. 10 μ L of the mixed solution was loaded onto a disposable haemocytometer which was then visualised using the 10x objective of a standard light microscope. The cell count was obtained by counting the cell number in an area of 16 squares (*Figure 36*). In total 4 areas of 16 squares were counted per sample and the total cell count divided by 4 to give an average value across the 4 areas. This figure was multiplied by 10^4 to give the cell count per ml of solution. Finally, this number was multiplied by two to adjust for the 1:2 dilution of the original stock PBMC when mixed with Trypan Blue. Samples with high cell counts that made counting difficult were subjected to a further 2-4 fold dilution and recounted.

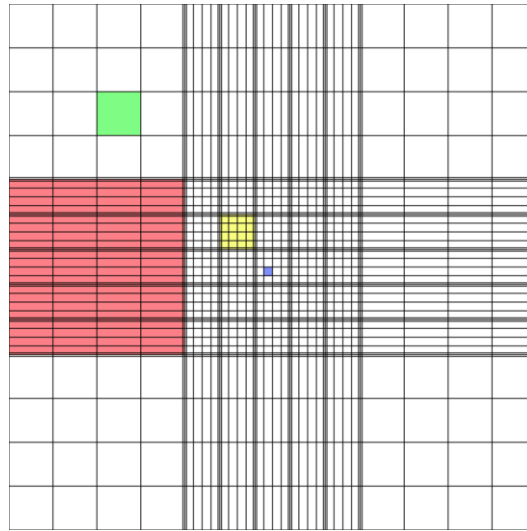


Figure 36: Method of cell counting using a haemocytometer. Number of cells in a peripheral 16-square area (shaded red) were counted. Cells were counted if they were within a square or on the right-hand or bottom boundary line. Image by Zephyris at the English language Wikipedia, CC BY-SA 3.0, [<https://commons.wikimedia.org/w/index.php?curid=10553213>]

7.3 Measuring Telomerase activity: Validation experiments

7.3.1 Telomerase activity: validation experiments 1

TA was measured on a small number of healthy controls from volunteers within our research group (samples D, S, W and J) using the TeloTAGGG Telomerase PCR ELISA (Cat No. 11 854666910 Roche Lifesciences, Pentzberg, Germany). This product combines the Telomerase reverse amplification protocol (TRAP) assay first described by Kim *et al* (204) with an ELISA to detect the amplified product. The steps of this reaction are outlined below.

- Step 1: During the TRAP reaction the native telomerase within the test sample is used to add Telomeric repeats (TTAGGG) to the end of a biotin labelled synthetic primer (P1-TS)

- Step 2: The elongation products are amplified by PCR using the primers P1-TS and P2
- Step 3: An aliquot of the PCR product is denatured and hybridised to a digoxigenin- (DIG) – labelled detection probe specific to the telomeric repeat sequence (P3). Next, the product is immobilised on a streptavidin coated microplate via the biotin labelled primer.
- Step 4: The immobilised PCR product is detected using an anti-DIG antibody conjugated to horseradish peroxidase (anti-DIG-HRP). Finally, the addition of Tetramethylbenzidine (TMB) results in a coloured reaction product as it is metabolised by the peroxidase enzyme. The degree of reaction product is quantified using a microplate reader by measuring the absorbance at 450nm (with a reference wavelength of approximately 690nm).

Unfortunately, difficulties were encountered with this assay in terms of its consistency and reproducibility. Initial validation runs were made in accordance with the manufacturer's instructions. The results of these runs are summarised in *Table 54*. Detailed descriptions and results of each validation experiment are showed in *Appendix M*.

Run 1	Starting amount of PBMC = Large coefficients of variability for duplicate runs (up to 35%)
Run 2	Repeat of run 1: Run failed due to positive control falling below acceptable range.
Run 3	Repeat of run 1: Inter-assay variability of 34.5%. samples also run with citrate CPT tubes rather than Heparin CPT tubes
Run 4	Starting amount of PBMC = 1µg of protein as determined by BCA assay This run produced a much higher TA value for sample D than previously observed (TA = 0.49) but similar values of intra-assay variability with CV values of 20%
Run 5	Repeat of Run 4: Inter-assay variability of 53.3%

Table 54: Summary of TA experiments using TeloTAGGG Telomerase PCR ELISA kit.

7.3.2 Conclusions from validation experiment 1

1. The use of 2×10^5 PBMC as the reaction substrate produced high intra-assay and inter-assay variability ($CV > 20\%$)
2. The use of 1µg Protein content derived from purified PBMC as the reaction substrate did not improve the reproducibility of the assay.
3. The majority of the intra-assay variability comes from the PCR step
4. The likely source of the observed inter-assay variability comes from differences in the starting amount of PBMC, either when using 2×10^5 cells or 1µg of protein.
5. When using 1µg of protein, the difference in starting amount appears to arise prior to the BCA assay, i.e. during the extraction of purified PBMC from whole blood.
6. Both Heparin and Citrate containing PBMC BD Vacutainer tubes have similar degrees of intra-assay variability.

7.3.3: Telomerase activity: Validation experiments 2

In order to overcome the problems of reproducibility with the TeloTAGGG Telomerase PCR ELISA assay, the validation experiments were repeated using the TeloTAGGG Telomerase PCR ELISA Plus assay (Cat No. 12 013 789 001, Roche Lifesciences, Pentzberg, Germany). This assay is a modification on the protocol of the standard TeloTAGG Telomerase PCR ELISA assay to include a 216 base pair internal control that is amplified alongside the telomeric repeats of the TRAP reaction. Both the telomeric and internal control PCR products are then detected by ELISA using identical protocols. As such, the internal control should normalise the measured TA levels between samples, and correct for sample specific differences in PCR (for example; falsely low readings due to the presence of PCR inhibitors in samples). The TeloTAGG Telomerase PCR ELISA Plus assay also includes a Control Sample. This sample is run in every run and allows for standardisation of telomerase activity across samples and across runs. The below validation experiments were run for the same 3 samples as the initial validation experiments (D,S and W) and an additional sample (J). TA was measured with the TeloTAGG Telomerase PCR ELISA Plus as per the manufacturer's instructions (205). A summary of the optimisation experiments performed is outlined in *Table 55*.

All the of the values of Absorbance of Samples (AS) and Relative Telomerase Activity (RTA) for the two samples common to runs 6-12 are shown in *Table 56* together with their coefficient of variance. Runs in which PCR amplification of the internal control appeared to be inhibited are excluded. High CV values are seen for both AS and RTA across both samples. If the RTA results from Run 12 are excluded on the

basis that the Internal Control may not have amplified correctly, the CV values for RTA for samples D and J improve to 35.6% and 73.21% respectively. Both of these results are no improvement on the results that we found with the standard TeloTAGGG PCR ELISA Protocol.

Run 6	Internal control failed to amplify for 3 of the 4 samples
Run 7	Repeat of Run 6.
Run 8	Repeat of run 6 using lysate created from frozen PBMC rather than fresh. Again, internal controls for 3 of the 4 samples failed to amplify.
Run 9	Repeat of run 6 with input amount of PBMC standardised by either cell count (2×10^5 cells) or BCA Assay (3ug Protein). Negative controls out of range so whole run invalid
Run 10	Repeat of run 9 but with just 2 samples to reduce cost of materials for optimisation experiments
Run 11	Repeat of Run 10.
Run 12	Repeat of Run 10. Reduced absorbance seen in internal controls.

Table 55: Summary of TA experiments using TeloTAGGG Telomerase PCR ELISA PLUS kit.

	D		J	
	AS	RTA	AS	RTA
Run 7	0.4027	12.482	0.2688	10.678
Run 7	0.2853	9.3870	0.1927	8.1527
Run 10	0.3623	12.821	0.0078	1.5714
Run 10	0.3942	18.250	0.0904	2.3178
Run 10	0.2025	6.6321	0.0526	0.4968
Run 11	0.0848	7.29	0.12	10.63
Run 11	0.109	10.72	0.0993	8.43
Run 12	0.2389	60.5	0.1864	47.62
Run 12	0.3276	95.4	0.1756	*
Mean	0.267	25.94	0.133	11.24
SD	0.118	30.94	0.081	15.26
CV	44.00	119.3	60.75	135.8

Table 56: Measures of reproducibility in AS and RTA for samples D and J

7.3.4 Conclusions from validation experiment 2

1. The ELISA plus assay does not appear to improve the reproducibility of Telomerase activity quantification which remains poor.
2. The amplification of the internal controls in this assay appear erratic and may represent the presence of PCR inhibitors in the samples. There were no clear differences in the handling of the samples which might have explained the discrepancies in internal control amplification.
3. The repeated finding of valid positive and negative controls in the PCR rings suggest that the PCR reaction was running as it should in these samples.
4. Freezing the lysate for later assaying risks increasing the variability in the input amounts of PBMC added to each TRAP reaction.

Because we were not satisfied with the variability in TA quantification with both TeloTAGGG PCR ELISA assays, we abandoned their use and looked at alternative measures of TA.

7.4 Measuring TERT expression

7.4.1 Introduction

The structure and function of Telomerase were described in section 1.4.2. Telomerase Reverse Transcriptase (TERT) is a DNA polymerase subunit of Telomerase which synthesises Telomeric DNA to the end of chromosomes to

maintain the length of the Telomere. Several studies have demonstrated that the expression of TERT correlates well with Telomerase Activity, so much so that some studies such as Janic *et al*, report measurement of Telomerase Activity where what they have in fact measured is TERT (rather than protein levels of Telomerase) (87). This study had also demonstrated that it was possible to measure TERT in RNA extracted from peripheral blood leukocytes of healthy middle-aged males. As such, we attempted to measure TERT expression in peripheral leukocytes as a surrogate marker of Telomerase Activity.

7.4.2 Methodology

Measuring gene expression requires quantification of mRNA. As such RNA was extracted and quality control performed as previously described in Sections 4.3.5 and 4.3.6. mRNA was quantified by reverse transcription polymerase chain reaction (RT-qPCR). Extracted RNA was reverse transcribed to cDNA using the SuperScript VILO cDNA Synthesis Kit (Invitrogen, Life Technologies, Carlsbad CA, USA) in accordance with the manufacturer's instruction (206). In brief, for each sample 4 μ l Quantity 5X VILO Reaction Mix was combined with 2 μ l of 10X SuperScript Enzyme Mix together with up to 2.5 μ g of RNA made up to a total volume of 20 μ l with DEPC-treated water (components mixed on ice). The components were gently mixed before being run in a PCR machine according to the following protocol: 10 minutes at 25°C (Primer Annealing); 60 minutes at 42°C (Reverse transcription step); 5 minutes at 85°C (Inactivation of enzymes). The TaqMan assay was either carried out immediately or the generated cDNA was stored at -20°C for up to a week or -80°C for longer storage. The cDNA was not quantified with Spectrophotometry as it

contains lots of dNTP's and residual RNA that can invalidate the result. Such a step is unnecessary if a standard amount of RNA is inputted into the Reverse Transcription step and the same protocol used for all cases.

TERT expression was performed using purchased TaqMan[®] Gene Expression Assays and the TaqMan[®] Fast Advanced Master Mix in accordance with the manufacturer's protocols(207). In brief, for each sample 10µl of TaqMan[®] Fast Advanced Master Mix (2X), 1µl of TaqMan[®] Assay (20X) and 7µl of Nuclease free water were combined with 2µl of cDNA template to give a total reaction volume of 20µl. The TaqMan Assay contain a mixture of PCR primers and TaqMan probes with an Applied Biosystems FAM or VIC dye label on the 5' end and minor groove binder and a nonfluorescent quencher on the 3' end (Thermofisher, Germany). Labelling the PCR products with different dyes allows the amplification of separate PCR products in the same reaction tube.

Each reaction was run in a separate well of a 96-well plate and each sample was run in duplicate. qPCR was run according to the following conditions: 2 minutes at 50°C (UNG incubation); 2 minutes at 95°C (Polymerase activation); 40 cycles of 3 seconds at 95°C (denaturing) and 30 seconds at 60°C (anneal/extension step). PCR was run on a Corbett Research Rotorgene 6000 Thermocycler (Qiagen, Manchester, UK) and results interpreted with the use of the Rotor-gene Q series analysis software.

7.4.3 Results

The fundamental problem that we encountered in measuring TERT expression was a failure to achieve amplification of TERT in any of the samples or positive controls that were tested. A summary of the optimisation experiments performed is given in Appendix M.

Following these experiments, expert help was sought from the Genome Centre at Queen Mary University of London. Fresh RNA was extracted to be used in the optimization experiments and its quality checked with the use of an Agilent 2100 Bioanalyzer (Agilent, Santa Clara, CA, USA). The resulting gel electrophoresis of 11 samples tested showed good integrity (*Figure 37*) as did the individual electropherograms for each sample (*Figure 38*). Average RNA Integrity Number (RIN) for all samples was 8.7. RIN is a numerical measure of integrity, and is measured on a scale of 0-10 with 10 representing 100% intact RNA with no degradation. Our results showed a good level of integrity of extracted RNA. The 7 samples with the best integrity were run for TERT expression using a different Thermocycler (Applied Biosystems 7900 HT fast RT PCR machine) in a 384 well plate, using the corresponding Mastermix and the TERT probe HS00972650_m1 (TERT 1). 5-point standard curves were run for both a positive control consisting of XpressRef Total RNA as the sample with best yield and RIN (S1). Unfortunately, this run again showed late amplification for TERT but no amplification for GAPDH.

A further experiment was run on the Genome centre thermocycler which was a repeat of the previous experiments but with a different positive control. A human

breast adenocarcinoma cell line (MCF-7) was used, as in the study by Janic *et al* (87). This run showed some late and discordant amplification for both TERT and GAPDH in the samples, but surprisingly no TERT amplification was seen in the MCF7 positive control. As this cell line had previously been used as a positive control in TERT assays this lack of amplification was surprising and calls into question whether the late amplification seen in previous assays was truly due to amplification of TERT or the result of non-specific amplification.

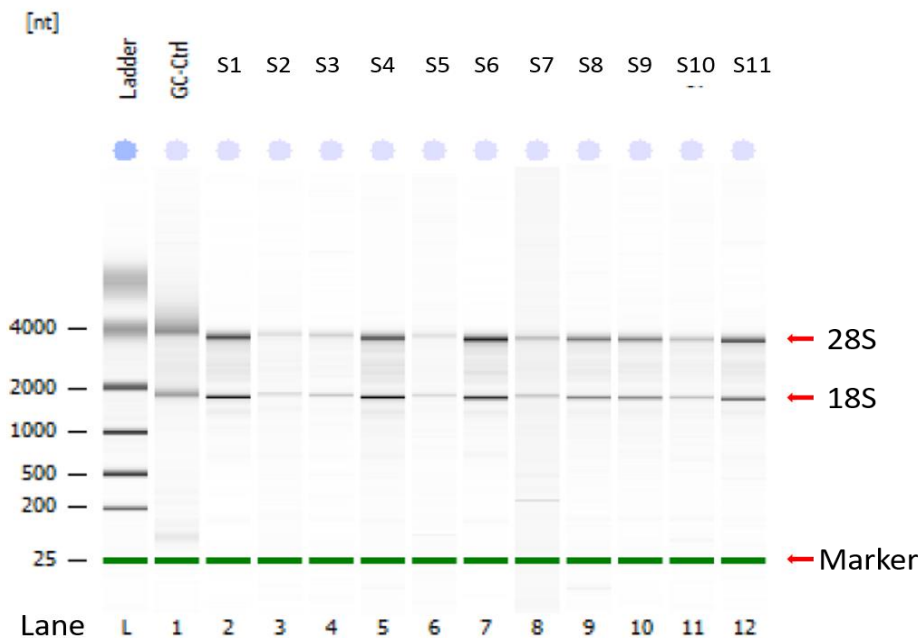


Figure 37: Results of gel electrophoresis of 11 samples extracted RNA plus 1 control sample (GC-Ctrl). The 2 distinct bands represent the ribosomal subunits 28S and 18S. The lack of other bands seem demonstrates the absence of smaller fragments produced by degradation.

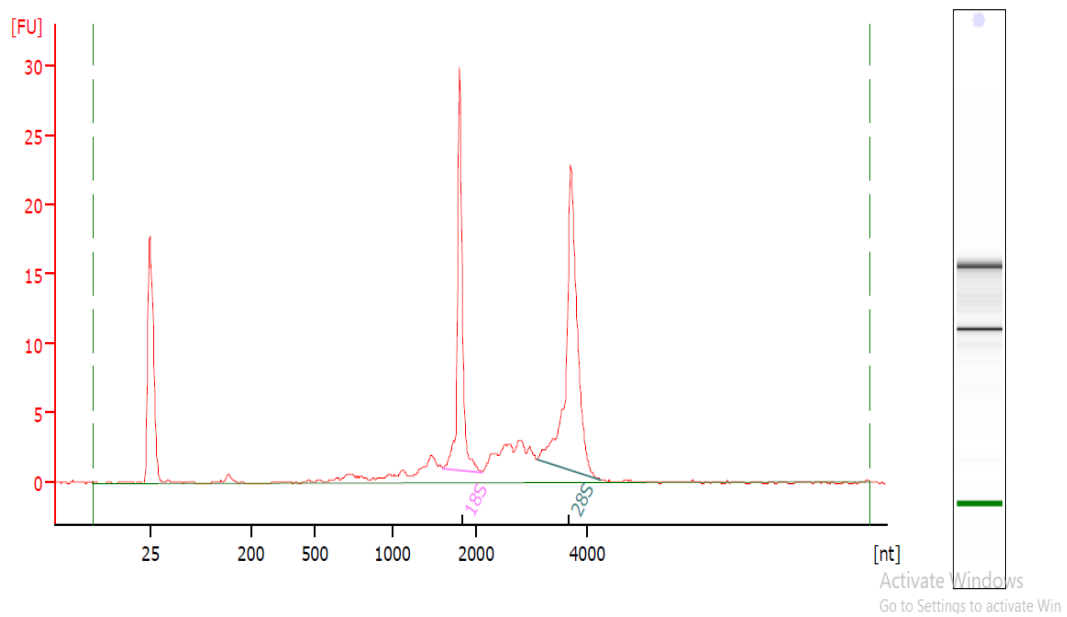


Figure 38: Electrogram for sample S1 (see Figure 37) Two peaks seen corresponding to the two ribosomal subunits and an early peak corresponding to the marker.

7.4.4 Conclusions

- There do not appear to be any issues with the quality or integrity of the extracted RNA using the PAXgene system.
- The excellent amplification results for GAPDH across both samples and XpressRef Total RNA indicates that the reverse transcription reaction is working and that there is no significant PCR inhibition occurring.
- The reason behind the inability to reliably amplify TERT is not clear, even in an MCF7 cell line positive control. Alterations in probes, cycling conditions, Mastermix components and concentration of input RNA all failed to correct the issue.

7.5 Overall Conclusion of Telomerase Experiments

Following nearly 2 months of attempting to optimise both the TeloTAGG PCR-ELISA assays and the TERT PCR , a decision was taken to abandon further experiments. Part of the decision to do this lay in the preliminary results of the mTL analysis. We were primarily interested in measuring Telomerase to support our telomere length analysis. In the event of a significant association between mTL and CSA-AKI it would have been useful to demonstrate a complimentary association between Telomerase activity and CSA-AKI as telomerase acts to increase mTL. By this stage of my thesis, mTL had been measured for the majority of the study cohort and preliminary analysis had shown no significant association between mTL and CSA-AKI. As such, the decision was taken to abandon further work on Telomerase activity in order to dedicate more time to measuring DNA methylation signatures.

CHAPTER 8. Conclusions and Future Work

8.1 Summary of Key Findings

From the results of this study the following conclusions can be drawn:

1. Mean Telomere length was not associated with either the primary outcome of CSA-AKI, or the secondary outcomes of in-hospital or 1-year mortality in the total population.
2. The STELA analysis pilot study did not indicate any significant difference in mTL between patients with or without CSA-AKI.
3. There was little correlation between values of mTL when measured with qPCR or STELA.
4. Increasing pMA is significantly associated with the development of post-operative AKI on univariate analysis and its predictive ability is superior to that of chronological age.
5. In South Asian patients, mTL is significantly associated with CSA-AKI on both univariate and multivariate analysis.
6. In South Asian patients, pMA is significantly associated with CSA-AKI with a stronger association than that demonstrated in the total population.

7. We were able to use targeted bisulphite amplicon sequencing to determine the methylation status at specific CpG sites and correlate them with clinical outcomes.

8.2 Clinical impact of these findings

These results suggest that genetic and epigenetic markers of aging and senescence might be able to more accurately predict long-term outcome after cardiac surgery than chronological age. Such findings could have potential clinical impacts as many decisions in the field of cardiac surgery are determined by age and likely post-operative mortality. The major risk calculators for predicting mortality after cardiac surgery incorporate the patient's age as a major risk factor. These risk calculators, whilst shown to have good predictive ability in the majority of cardiac cases, are not universally applicable. It is possible that personalised measures of epigenetic age such as pMA might provide better predictive powers in such models than the use of chronological age. Further work is required to develop this concept and we are planning for further analysis of this cohort to determine if that is the case. It is likely that further follow up of the cohort out to five years will be required for these analyses as discussed below.

In order for markers of epigenetic aging to be clinically useful, methods are needed to identify and map key CpG sites of interest without the need to sequence the entire methylome for each patient. In the current study we have used a previously validated methylation signature of aging to perform targeted bisulphite amplicon sequencing of individual CpG sites and correlate them with clinical outcome. As

such, we have proved in principal that such targeted sequencing is able to correlate with clinical endpoints even if the associations identified in the present study are not strong enough to evaluate risk on an individual level.

Finally, the novel findings that mTL and pMA are significantly associated with CSA-AKI in South Asian patients provides interesting avenues for investigation into biological aging and senescence in this subgroup.

8.3 Potential future analyses

The main finding of this study is that CSA-AKI is associated with an age-associated signature of methylation (pMA). This raises the possibility that this might also be the case for other post-operative outcomes. No further analyses are planned at the current time. However, such relationships might become apparent with further follow up of this cohort. This cohort will be followed up to 5 and 10 years for mortality and the development of chronic renal impairment. The rationale for this is supported by the trends in Delta-age for both in-hospital mortality observed in this study (0.51yrs Dead Vs 3.25yrs Alive) and 1-year mortality (1.63 years Dead Vs 2.97yrs Alive). Both of these results indicate that pMA was higher with respect to chronological age in patients who died post-operatively, although neither reached statistical significance. The failure to reach statistical significance is likely to be due to a lack of power in the study to detect these rarer endpoints. With further follow up out to 5 years and beyond, increasing mortality might result in relationships with pMA, AMAR, or Delta-age becoming apparent and achieving significance.

Further follow up might also reveal a significant association between mTL and mid or late survival. Whilst no statistical significance was seen in mTL at 1-year follow up, the trend was towards greater mortality in patients with reduced mTL, particularly in the South Asian subgroup. As such, significant differences might become apparent with increased duration of follow up due to an increased number of endpoints.

During the ethical submission and informed consenting process for this study, consent was obtained for future contact with patients or their general practitioner to obtain a latest serum creatinine/eGFR result. This will allow the proportion of patients that progress to chronic renal impairment in the future to be determined. We therefore plan to correlate the development of CKD at 5 and 10 years follow up with the patient's methylation data and mean telomere length.

References

1. Vives M, Wijeyesundera D, Marczin N, Monedero P, Rao V. Cardiac surgery-associated acute kidney injury. *Interact Cardiovasc Thorac Surg*. 2014;18(5):637-45.
2. Bellomo R, Ronco C, Kellum JA, Mehta RL, Palevsky P. Acute renal failure - definition, outcome measures, animal models, fluid therapy and information technology needs: the Second International Consensus Conference of the Acute Dialysis Quality Initiative (ADQI) Group. *Crit Care*. 2004;8(4):R204-12.
3. Kuitunen A, Vento A, Suojaranta-Ylinen R, Pettila V. Acute renal failure after cardiac surgery: evaluation of the RIFLE classification. *Ann Thorac Surg*. 2006;81(2):542-6.
4. Lassnigg A. Minimal Changes of Serum Creatinine Predict Prognosis in Patients after Cardiothoracic Surgery: A Prospective Cohort Study. *J Am Soc Nephrol*. 2004;15(6):1597-605.
5. Mehta RL, Kellum JA, Shah SV, Molitoris BA, Ronco C, Warnock DG, *et al*. Acute Kidney Injury Network: report of an initiative to improve outcomes in acute kidney injury. *Crit Care*. 2007;11(2):R31.
6. Englberger L, Suri RM, Li Z, Casey ET, Daly RC, Dearani JA, *et al*. Clinical accuracy of RIFLE and Acute Kidney Injury Network (AKIN) criteria for acute kidney injury in patients undergoing cardiac surgery. *Crit Care*. 2011;15(1):R16.
7. Haase M, Bellomo R, Matalanis G, Calzavacca P, Dragun D, Haase-Fielitz A. A comparison of the RIFLE and Acute Kidney Injury Network classifications for cardiac surgery-associated acute kidney injury: a prospective cohort study. *J Thorac Cardiovasc Surg*. 2009;138(6):1370-6.
8. Yan X, Jia S, Meng X, Dong P, Jia M, Wan J, *et al*. Acute kidney injury in adult postcardiotomy patients with extracorporeal membrane oxygenation: evaluation of the RIFLE classification and the Acute Kidney Injury Network criteria. *Eur J Cardiothorac Surg*. 2010;37(2):334-8.

9. Bastin AJ, Ostermann M, Slack AJ, Diller GP, Finney SJ, Evans TW. Acute kidney injury after cardiac surgery according to Risk/Injury/Failure/Loss/End-stage, Acute Kidney Injury Network, and Kidney Disease: Improving Global Outcomes classifications. *J Crit Care.* 2013;28(4):389-96.
10. KDIGO clinical practice guideline for acute kidney injury. *Kidney Int Su.* 2012(17):1-138.
11. Luo X, Jiang L, Du B, Wen Y, Wang M, Xi X. A comparison of different diagnostic criteria of acute kidney injury in critically ill patients. *Crit Care.* 2014;18(4):R144.
12. Fuhrman DY, Kellum JA. Epidemiology and pathophysiology of cardiac surgery-associated acute kidney injury. *Curr Opin Anaesthesiol.* 2017;30(1):60-5.
13. McFarlane SI, Winer N, Sowers JR. Role of the natriuretic peptide system in cardiorenal protection. *Arch Intern Med.* 2003;163(22):2696-704.
14. Chou SY, Porush JG, Faubert PF. Renal medullary circulation: hormonal control. *Kidney Int.* 1990;37(1):1-13.
15. Sgouralis I, Evans RG, Layton AT. Renal medullary and urinary oxygen tension during cardiopulmonary bypass in the rat. *Math Med Biol.* 2016.
16. Blauth CI, Cosgrove DM, Webb BW, Ratliff NB, Boylan M, Piedmonte MR, *et al.* Atheroembolism from the ascending aorta. An emerging problem in cardiac surgery. *J Thorac Cardiovasc Surg.* 1992;103(6):1104-11; discussion 11-2.
17. DeFoe GR, Dame NA, Farrell MS, Ross CS, Langner CW, Likosky DS. Embolic activity during in vivo cardiopulmonary bypass. *J Extra Corpor Technol.* 2014;46(2):150-6.
18. Holmes JHt, Connolly NC, Paull DL, Hill ME, Guyton SW, Ziegler SF, *et al.* Magnitude of the inflammatory response to cardiopulmonary bypass and its relation to adverse clinical outcomes. *Inflamm Res.* 2002;51(12):579-86.

19. Kirklin JK, Westaby S, Blackstone EH, Kirklin JW, Chenoweth DE, Pacifico AD. Complement and the damaging effects of cardiopulmonary bypass. *J Thorac Cardiovasc Surg.* 1983;86(6):845-57.
20. Davis CL, Kausz AT, Zager RA, Kharasch ED, Cochran RP. Acute renal failure after cardiopulmonary bypass in related to decreased serum ferritin levels. *J Am Soc Nephrol.* 1999;10(11):2396-402.
21. Seabra VF, Alobaidi S, Balk EM, Poon AH, Jaber BL. Off-pump coronary artery bypass surgery and acute kidney injury: a meta-analysis of randomized controlled trials. *Clin J Am Soc Nephrol.* 2010;5(10):1734-44.
22. Reents W, Hilker M, Borgermann J, Albert M, Plotze K, Zacher M, *et al.* Acute kidney injury after on-pump or off-pump coronary artery bypass grafting in elderly patients. *Ann Thorac Surg.* 2014;98(1):9-14; discussion -5.
23. Lamy A, Devereaux PJ, Prabhakaran D, Taggart DP, Hu S, Paolasso E, *et al.* Off-pump or on-pump coronary-artery bypass grafting at 30 days. *N Engl J Med.* 2012;366(16):1489-97.
24. Yi Q, Li K, Jian Z, Xiao YB, Chen L, Zhang Y, *et al.* Risk Factors for Acute Kidney Injury after Cardiovascular Surgery: Evidence from 2,157 Cases and 49,777 Controls - A Meta-Analysis. *Cardiorenal Med.* 2016;6(3):237-50.
25. Coca SG, Garg AX, Swaminathan M, Garwood S, Hong K, Thiessen-Philbrook H, *et al.* Preoperative angiotensin-converting enzyme inhibitors and angiotensin receptor blocker use and acute kidney injury in patients undergoing cardiac surgery. *Nephrol Dial Transplant.* 2013;28(11):2787-99.
26. Yacoub R, Patel N, Lohr JW, Rajagopalan S, Nader N, Arora P. Acute kidney injury and death associated with renin angiotensin system blockade in cardiothoracic surgery: a meta-analysis of observational studies. *Am J Kidney Dis.* 2013;62(6):1077-86.

27. Ranucci M, Ballotta A, Kunkl A, De Benedetti D, Kandil H, Conti D, *et al.* Influence of the timing of cardiac catheterization and the amount of contrast media on acute renal failure after cardiac surgery. *Am J Cardiol.* 2008;101(8):1112-8.
28. Medalion B, Cohen H, Assali A, Vaknin Assa H, Farkash A, Snir E, *et al.* The effect of cardiac angiography timing, contrast media dose, and preoperative renal function on acute renal failure after coronary artery bypass grafting. *J Thorac Cardiovasc Surg.* 2010;139(6):1539-44.
29. Ozkaynak B, Kayalar N, Gumus F, Yucel C, Mert B, Boyacioglu K, *et al.* Time from cardiac catheterization to cardiac surgery: a risk factor for acute kidney injury? *Interact Cardiovasc Thorac Surg.* 2014;18(6):706-11.
30. Loor G, Rajeswaran J, Li L, Sabik JF, 3rd, Blackstone EH, McCrae KR, *et al.* The least of 3 evils: exposure to red blood cell transfusion, anemia, or both? *J Thorac Cardiovasc Surg.* 2013;146(6):1480-7.e6.
31. Goldberg JB, Shann KG, Fitzgerald D, Fuller J, Paugh TA, Dickinson TA, *et al.* The Relationship between Intra-Operative Transfusions and Nadir Hematocrit on Post-Operative Outcomes after Cardiac Surgery. *J Extra Corpor Technol.* 2016;48(4):188-93.
32. Ranucci M, Baryshnikova E, Castelveccchio S, Pelissero G. Major bleeding, transfusions, and anemia: the deadly triad of cardiac surgery. *Ann Thorac Surg.* 2013;96(2):478-85.
33. Tauriainen T, Koski-Vahala J, Kinnunen EM, Biancari F. The Effect of Preoperative Anemia on the Outcome After Coronary Surgery. *World J Surg.* 2017;41(7):1910-8.
34. Gaudino M, Di Castelnuovo A, Zamparelli R, Andreotti F, Burzotta F, Iacoviello L, *et al.* Genetic control of postoperative systemic inflammatory reaction and pulmonary and renal complications after coronary artery surgery. *J Thorac Cardiovasc Surg.* 2003;126(4):1107-12.

35. MacKensen GB, Swaminathan M, Ti LK, Grocott HP, Phillips-Bute BG, Mathew JP, *et al.* Preliminary report on the interaction of apolipoprotein E polymorphism with aortic atherosclerosis and acute nephropathy after CABG. *The Annals of Thoracic Surgery.* 2004;78(2):520-6.
36. Stafford-Smith M, Podgoreanu M, Swaminathan M, Phillips-Bute B, Mathew JP, Hauser EH, *et al.* Association of genetic polymorphisms with risk of renal injury after coronary bypass graft surgery. *Am J Kidney Dis.* 2005;45(3):519-30.
37. Isbir SC, Tekeli A, Ergen A, Yilmaz H, Ak K, Civelek A, *et al.* Genetic polymorphisms contribute to acute kidney injury after coronary artery bypass grafting. *Heart Surg Forum.* 2007;10(6):E439-44.
38. Jouan J, Golmard L, Benhamouda N, Durrleman N, Golmard JL, Ceccaldi R, *et al.* Gene polymorphisms and cytokine plasma levels as predictive factors of complications after cardiopulmonary bypass. *J Thorac Cardiovasc Surg.* 2012;144(2):467-73, 73.e1-2.
39. Stafford-Smith M, Li YJ, Mathew JP, Li YW, Ji Y, Phillips-Bute BG, *et al.* Genome-wide association study of acute kidney injury after coronary bypass graft surgery identifies susceptibility loci. *Kidney Int.* 2015;88(4):823-32.
40. Huen SC, Parikh CR. Predicting acute kidney injury after cardiac surgery: a systematic review. *Ann Thorac Surg.* 2012;93(1):337-47.
41. Chertow GM, Lazarus JM, Christiansen CL, Cook EF, Hammermeister KE, Grover F, *et al.* Preoperative renal risk stratification. *Circulation.* 1997;95(4):878-84.
42. Fortescue EB, Bates DW, Chertow GM. Predicting acute renal failure after coronary bypass surgery: cross-validation of two risk-stratification algorithms. *Kidney Int.* 2000;57(6):2594-602.
43. Thakar CV, Liangos O, Yared JP, Nelson DA, Hariachar S, Paganini EP. Predicting acute renal failure after cardiac surgery: validation and re-definition of a risk-stratification

- algorithm. Hemodialysis international International Symposium on Home Hemodialysis. 2003;7(2):143-7.
44. Eriksen BO, Hoff KR, Solberg S. Prediction of acute renal failure after cardiac surgery: retrospective cross-validation of a clinical algorithm. *Nephrol Dial Transplant*. 2003;18(1):77-81.
45. Mehta RH, Grab JD, O'Brien SM, Bridges CR, Gammie JS, Haan CK, *et al*. Bedside tool for predicting the risk of postoperative dialysis in patients undergoing cardiac surgery. *Circulation*. 2006;114(21):2208-16; quiz
46. Wijeyesundera DN, Karkouti K, Dupuis JY, Rao V, Chan CT, Granton JT, *et al*. Derivation and validation of a simplified predictive index for renal replacement therapy after cardiac surgery. *JAMA*. 2007;297(16):1801-9.
47. Thakar CV, Arrigain S, Worley S, Yared JP, Paganini EP. A clinical score to predict acute renal failure after cardiac surgery. *J Am Soc Nephrol*. 2005;16(1):162-8.
48. Wong B, St Onge J, Korkola S, Prasad B. Validating a scoring tool to predict acute kidney injury (AKI) following cardiac surgery. *Can J Kidney Health Dis*. 2015;2:3.
49. Vives M, Monedero P, Perez-Valdivieso JR, Garcia-Fernandez N, Lavilla J, Herreros J, *et al*. External validation and comparison of three scores to predict renal replacement therapy after cardiac surgery: a multicenter cohort. *Int J Artif Organs*. 2011;34(4):329-38.
50. Palomba H, de Castro I, Neto AL, Lage S, Yu L. Acute kidney injury prediction following elective cardiac surgery: AKICS Score. *Kidney Int*. 2007;72(5):624-31.
51. Brown JR, Cochran RP, Leavitt BJ, Dacey LJ, Ross CS, MacKenzie TA, *et al*. Multivariable prediction of renal insufficiency developing after cardiac surgery. *Circulation*. 2007;116(11 Suppl):I139-43.
52. STS Online risk calculator. <http://riskcalcsts.org/stswebriskcalc/calculate>.
53. Nashef SA, Roques F, Sharples LD, Nilsson J, Smith C, Goldstone AR, *et al*. EuroSCORE II. *Eur J Cardiothorac Surg*. 2012;41(4):734-44; discussion 44-5.

54. Ad N, Holmes SD, Patel J, Pritchard G, Shuman DJ, Halpin L. Comparison of EuroSCORE II, Original EuroSCORE, and The Society of Thoracic Surgeons Risk Score in Cardiac Surgery Patients. *Ann Thorac Surg.* 2016;102(2):573-9.
55. Pickering JW, James MT, Palmer SC. Acute kidney injury and prognosis after cardiopulmonary bypass: a meta-analysis of cohort studies. *Am J Kidney Dis.* 2015;65(2):283-93.
56. Corredor C, Thomson R, Al-Subaie N. Long-Term Consequences of Acute Kidney Injury After Cardiac Surgery: A Systematic Review and Meta-Analysis. *J Cardiothorac Vasc Anesth.* 2016;30(1):69-75.
57. Liotta M, Olsson D, Sartipy U, Holzmann MJ. Minimal changes in postoperative creatinine values and early and late mortality and cardiovascular events after coronary artery bypass grafting. *Am J Cardiol.* 2014;113(1):70-5.
58. Hobson CE, Yavas S, Segal MS, Schold JD, Tribble CG, Layon AJ, *et al.* Acute kidney injury is associated with increased long-term mortality after cardiothoracic surgery. *Circulation.* 2009;119(18):2444-53.
59. Gallagher S, Jones DA, Lovell MJ, Hassan S, Wragg A, Kapur A, *et al.* The impact of acute kidney injury on midterm outcomes after coronary artery bypass graft surgery: a matched propensity score analysis. *J Thorac Cardiovasc Surg.* 2014;147(3):989-95.
60. Hansen MK, Gammelager H, Jacobsen CJ, Hjortdal VE, Layton JB, Rasmussen BS, *et al.* Acute Kidney Injury and Long-term Risk of Cardiovascular Events After Cardiac Surgery: A Population-Based Cohort Study. *J Cardiothorac Vasc Anesth.* 2015;29(3):617-25.
61. Xu JR, Zhu JM, Jiang J, Ding XQ, Fang Y, Shen B, *et al.* Risk Factors for Long-Term Mortality and Progressive Chronic Kidney Disease Associated With Acute Kidney Injury After Cardiac Surgery. *Medicine (Baltimore).* 2015;94(45):e2025.

62. Ryden L, Sartipy U, Evans M, Holzmann MJ. Acute kidney injury after coronary artery bypass grafting and long-term risk of end-stage renal disease. *Circulation*. 2014;130(23):2005-11.
63. Lim CC, Tan CS, Chia CM, Tan AK, Choo JC, Kaushik M, *et al*. Long-Term Risk of Progressive Chronic Kidney Disease in Patients with Severe Acute Kidney Injury Requiring Dialysis after Coronary Artery Bypass Surgery. *Cardiorenal Med*. 2015;5(3):157-63.
64. Basile DP, Donohoe D, Roethe K, Osborn JL. Renal ischemic injury results in permanent damage to peritubular capillaries and influences long-term function. *Am J Physiol Renal Physiol*. 2001;281(5):F887-99.
65. Basile DP, Fredrich K, Alausa M, Vio CP, Liang M, Rieder MR, *et al*. Identification of persistently altered gene expression in the kidney after functional recovery from ischemic acute renal failure. *Am J Physiol Renal Physiol*. 2005;288(5):F953-63.
66. Garg AX, Devereaux PJ, Yusuf S, Cuerden MS, Parikh CR, Coca SG, *et al*. Kidney function after off-pump or on-pump coronary artery bypass graft surgery: a randomized clinical trial. *JAMA*. 2014;311(21):2191-8.
67. Lopez-Otin C, Blasco MA, Partridge L, Serrano M, Kroemer G. The hallmarks of aging. *Cell*. 2013;153(6):1194-217.
68. Rodier F, Campisi J. Four faces of cellular senescence. *J Cell Biol*. 2011;192(4):547-56.
69. Ziegler DV, Wiley CD, Velarde MC. Mitochondrial effectors of cellular senescence: beyond the free radical theory of aging. *Aging cell*. 2015;14(1):1-7.
70. Lee BY, Han JA, Im JS, Morrone A, Johung K, Goodwin EC, *et al*. Senescence-associated beta-galactosidase is lysosomal beta-galactosidase. *Aging cell*. 2006;5(2):187-95.
71. Bernadotte A, Mikhelson VM, Spivak IM. Markers of cellular senescence. Telomere shortening as a marker of cellular senescence. *Aging (Albany NY)*. 2016;8(1):3-11.

72. de Magalhaes JP, Curado J, Church GM. Meta-analysis of age-related gene expression profiles identifies common signatures of aging. *Bioinformatics*. 2009;25(7):875-81.
73. Keppler D, Zhang J, Bihani T, Lin AW. Novel expression of CST1 as candidate senescence marker. *J Gerontol A Biol Sci Med Sci*. 2011;66(7):723-31.
74. Burzynski SR. Gene silencing--a new theory of aging. *Med Hypotheses*. 2003;60(4):578-83.
75. Boks MP, Derks EM, Weisenberger DJ, Strengman E, Janson E, Sommer IE, *et al*. The relationship of DNA methylation with age, gender and genotype in twins and healthy controls. *PLoS One*. 2009;4(8):e6767.
76. Hannum G, Guinney J, Zhao L, Zhang L, Hughes G, Sada S, *et al*. Genome-wide methylation profiles reveal quantitative views of human aging rates. *Mol Cell*. 2013;49(2):359-67.
77. Koch CM, Jousen S, Schellenberg A, Lin Q, Zenke M, Wagner W. Monitoring of cellular senescence by DNA-methylation at specific CpG sites. *Aging cell*. 2012;11(2):366-9.
78. Moyzis RK, Buckingham JM, Cram LS, Dani M, Deaven LL, Jones MD, *et al*. A highly conserved repetitive DNA sequence, (TTAGGG)_n, present at the telomeres of human chromosomes. *Proc Natl Acad Sci U S A*. 1988;85(18):6622-6.
79. Olovnikov AM. A theory of marginotomy. The incomplete copying of template margin in enzymic synthesis of polynucleotides and biological significance of the phenomenon. *J Theor Biol*. 1973;41(1):181-90.
80. Hayflick L. THE LIMITED IN VITRO LIFETIME OF HUMAN DIPLOID CELL STRAINS. *Exp Cell Res*. 1965;37:614-36.
81. Greider CW. Telomeres do D-loop-T-loop. *Cell*. 1999;97(4):419-22.
82. de Lange T. Shelterin: the protein complex that shapes and safeguards human telomeres. *Genes Dev*. 2005;19(18):2100-10.

83. Greider CW, Blackburn EH. A telomeric sequence in the RNA of Tetrahymena telomerase required for telomere repeat synthesis. *Nature*. 1989;337(6205):331-7.
84. Wojtyla A, Gladych M, Rubis B. Human telomerase activity regulation. *Mol Biol Rep*. 2011;38(5):3339-49.
85. Greenberg RA, Allsopp RC, Chin L, Morin GB, DePinho RA. Expression of mouse telomerase reverse transcriptase during development, differentiation and proliferation. *Oncogene*. 1998;16(13):1723-30.
86. Zurek M, Altschmied J, Kohlgrüber S, Ale-Agha N, Haendeler J. Role of Telomerase in the Cardiovascular System. *Genes*. 2016;7(6):29.
87. Janic M, Lunder M, Cerkovnik P, Prosenc Zmrzljak U, Novakovic S, Sabovic M. Low-dose fluvastatin and valsartan rejuvenate the arterial wall through telomerase activity increase in the middle-aged men. *Rejuvenation Res*. 2015.
88. Gizard F, Heywood EB, Findeisen HM, Zhao Y, Jones KL, Cudejko C, *et al*. Telomerase activation in atherosclerosis and induction of telomerase reverse transcriptase expression by inflammatory stimuli in macrophages. *Arterioscler Thromb Vasc Biol*. 2011;31(2):245-52.
89. Cheng H, Fan X, Lawson WE, Pauksakon P, Harris RC. Telomerase deficiency delays renal recovery in mice after ischemia-reperfusion injury by impairing autophagy. *Kidney Int*. 2015.
90. Leri A, Franco S, Zacheo A, Barlucchi L, Chimenti S, Limana F, *et al*. Ablation of telomerase and telomere loss leads to cardiac dilatation and heart failure associated with p53 upregulation. *EMBO J*. 2003;22(1):131-9.
91. Leri A, Barlucchi L, Limana F, Deptala A, Darzynkiewicz Z, Hintze TH, *et al*. Telomerase expression and activity are coupled with myocyte proliferation and preservation of telomeric length in the failing heart. *Proc Natl Acad Sci U S A*. 2001;98(15):8626-31.

92. Richardson GD, Breault D, Horrocks G, Cormack S, Hole N, Owens WA. Telomerase expression in the mammalian heart. *FASEB J.* 2012;26(12):4832-40.
93. Werner C, Furster T, Widmann T, Poss J, Roggia C, Hanhoun M, *et al.* Physical exercise prevents cellular senescence in circulating leukocytes and in the vessel wall. *Circulation.* 2009;120(24):2438-47.
94. Ornish D, Lin J, Chan JM, Epel E, Kemp C, Weidner G, *et al.* Effect of comprehensive lifestyle changes on telomerase activity and telomere length in men with biopsy-proven low-risk prostate cancer: 5-year follow-up of a descriptive pilot study. *Lancet Oncol.* 2013;14(11):1112-20.
95. Shay JW, Wright WE. Senescence and immortalization: role of telomeres and telomerase. *Carcinogenesis.* 2005;26(5):867-74.
96. Bodnar AG, Ouellette M, Frolkis M, Holt SE, Chiu CP, Morin GB, *et al.* Extension of life-span by introduction of telomerase into normal human cells. *Science.* 1998;279(5349):349-52.
97. Steinert S, Shay JW, Wright WE. Transient expression of human telomerase extends the life span of normal human fibroblasts. *Biochem Biophys Res Commun.* 2000;273(3):1095-8.
98. Denchi EL, de Lange T. Protection of telomeres through independent control of ATM and ATR by TRF2 and POT1. *Nature.* 2007;448(7157):1068-71.
99. d'Adda di Fagagna F, Reaper PM, Clay-Farrace L, Fiegler H, Carr P, Von Zglinicki T, *et al.* A DNA damage checkpoint response in telomere-initiated senescence. *Nature.* 2003;426(6963):194-8.
100. Herbig U, Jobling WA, Chen BP, Chen DJ, Sedivy JM. Telomere shortening triggers senescence of human cells through a pathway involving ATM, p53, and p21(CIP1), but not p16(INK4a). *Mol Cell.* 2004;14(4):501-13.

101. Hemann MT, Strong MA, Hao LY, Greider CW. The shortest telomere, not average telomere length, is critical for cell viability and chromosome stability. *Cell*. 2001;107(1):67-77.
102. Gottschling DE, Aparicio OM, Billington BL, Zakian VA. Position effect at *S. cerevisiae* telomeres: reversible repression of Pol II transcription. *Cell*. 1990;63(4):751-62.
103. Renauld H, Aparicio OM, Zierath PD, Billington BL, Chhablani SK, Gottschling DE. Silent domains are assembled continuously from the telomere and are defined by promoter distance and strength, and by SIR3 dosage. *Genes Dev*. 1993;7(7a):1133-45.
104. Baur JA, Zou Y, Shay JW, Wright WE. Telomere position effect in human cells. *Science*. 2001;292(5524):2075-7.
105. Stewart SA, Ben-Porath I, Carey VJ, O'Connor BF, Hahn WC, Weinberg RA. Erosion of the telomeric single-strand overhang at replicative senescence. *Nat Genet*. 2003;33(4):492-6.
106. Karlseder J, Smogorzewska A, de Lange T. Senescence induced by altered telomere state, not telomere loss. *Science*. 2002;295(5564):2446-9.
107. Prieur A, Peeper DS. Cellular senescence in vivo: a barrier to tumorigenesis. *Curr Opin Cell Biol*. 2008;20(2):150-5.
108. Wang Y, Leung FC. An evaluation of new criteria for CpG islands in the human genome as gene markers. *Bioinformatics*. 2004;20(7):1170-7.
109. Suzuki MM, Bird A. DNA methylation landscapes: provocative insights from epigenomics. *Nature reviews Genetics*. 2008;9(6):465-76.
110. Ehrlich M, Ehrlich KC. Effect of DNA methylation on the binding of vertebrate and plant proteins to DNA. *EXS*. 1993;64:145-68.
111. Nan X, Ng HH, Johnson CA, Laherty CD, Turner BM, Eisenman RN, *et al.* Transcriptional repression by the methyl-CpG-binding protein MeCP2 involves a histone deacetylase complex. *Nature*. 1998;393(6683):386-9.

112. Sharma S, Kelly TK, Jones PA. Epigenetics in cancer. *Carcinogenesis*. 2010;31(1):27-36.
113. Futscher BW, Oshiro MM, Wozniak RJ, Holtan N, Hanigan CL, Duan H, *et al*. Role for DNA methylation in the control of cell type specific maspin expression. *Nat Genet*. 2002;31(2):175-9.
114. Fraga MF, Ballestar E, Paz MF, Ropero S, Setien F, Ballestar ML, *et al*. Epigenetic differences arise during the lifetime of monozygotic twins. *Proc Natl Acad Sci U S A*. 2005;102(30):10604-9.
115. Cruickshanks HA, McBryan T, Nelson DM, Vanderkraats ND, Shah PP, van Tuyn J, *et al*. Senescent cells harbour features of the cancer epigenome. *Nat Cell Biol*. 2013;15(12):1495-506.
116. Zhang Y, Zeng C. Role of DNA methylation in cardiovascular diseases. *Clin Exp Hypertens*. 2016;38(3):261-7.
117. Wagner W, Fernandez-Rebollo E, Frobel J. DNA-methylation changes in replicative senescence and aging: two sides of the same coin? *Epigenomics*. 2016;8(1):1-3.
118. Bork S, Pfister S, Witt H, Horn P, Korn B, Ho AD, *et al*. DNA methylation pattern changes upon long-term culture and aging of human mesenchymal stromal cells. *Aging cell*. 2010;9(1):54-63.
119. Harley CB, Futcher AB, Greider CW. Telomeres shorten during ageing of human fibroblasts. *Nature*. 1990;345(6274):458-60.
120. Cawthon RM, Smith KR, O'Brien E, Sivatchenko A, Kerber RA. Association between telomere length in blood and mortality in people aged 60 years or older. *Lancet*. 2003;361(9355):393-5.
121. Barrett JH, Iles MM, Dunning AM, Pooley KA. Telomere length and common disease: study design and analytical challenges. *Hum Genet*. 2015;134(7):679-89.

122. Haycock PC, Heydon EE, Kaptoge S, Butterworth AS, Thompson A, Willeit P. Leucocyte telomere length and risk of cardiovascular disease: systematic review and meta-analysis. *BMJ*. 2014;349:g4227.
123. Forero DA, Gonzalez-Giraldo Y, Lopez-Quintero C, Castro-Vega LJ, Barreto GE, Perry G. Meta-analysis of Telomere Length in Alzheimer's Disease. *J Gerontol A Biol Sci Med Sci*. 2016.
124. Samani NJ, Boulton R, Butler R, Thompson JR, Goodall AH. Telomere shortening in atherosclerosis. *Lancet*. 2001;358(9280):472-3.
125. Akasheva DU, Plokhova EV, Tkacheva ON, Strazhesko ID, Dudinskaya EN, Kruglikova AS, *et al*. Age-Related Left Ventricular Changes and Their Association with Leukocyte Telomere Length in Healthy People. *PLoS One*. 2015;10(8):e0135883.
126. Hunt SC, Kimura M, Hopkins PN, Carr JJ, Heiss G, Province MA, *et al*. Leukocyte Telomere Length and Coronary Artery Calcium. *Am J Cardiol*. 2015;116(2):214-8.
127. Kurz DJ, Kloeckener-Gruissem B, Akhmedov A, Eberli FR, Buhler I, Berger W, *et al*. Degenerative aortic valve stenosis, but not coronary disease, is associated with shorter telomere length in the elderly. *Arterioscler Thromb Vasc Biol*. 2006;26(6):e114-7.
128. Perez-Rivera JA, Pabon-Osuna P, Cieza-Borrella C, Martin-Herrero F, Gonzalez-Porrás JR, Gonzalez-Sarmiento R. Prognostic value of telomere length in acute coronary syndrome. *Mech Ageing Dev*. 2012;133(11-12):695-7.
129. Brouillette SW, Whittaker A, Stevens SE, van der Harst P, Goodall AH, Samani NJ. Telomere length is shorter in healthy offspring of subjects with coronary artery disease: support for the telomere hypothesis. *Heart*. 2008;94(4):422-5.
130. Matthews C, Gorenne I, Scott S, Figg N, Kirkpatrick P, Ritchie A, *et al*. Vascular smooth muscle cells undergo telomere-based senescence in human atherosclerosis: effects of telomerase and oxidative stress. *Circ Res*. 2006;99(2):156-64.

131. De Meyer T, Rietzschel ER, De Buyzere ML, Langlois MR, De Bacquer D, Segers P, *et al.* Systemic telomere length and preclinical atherosclerosis: the Asklepios Study. *Eur Heart J.* 2009;30(24):3074-81.
132. De Meyer T, Van Daele CM, De Buyzere ML, Denil S, De Bacquer D, Segers P, *et al.* No shorter telomeres in subjects with a family history of cardiovascular disease in the Asklepios study. *Arterioscler Thromb Vasc Biol.* 2012;32(12):3076-81.
133. De Meyer T, Rietzschel ER, De Buyzere ML, Van Criekinge W, Bekaert S. Telomere length and cardiovascular aging: the means to the ends? *Ageing Res Rev.* 2011;10(2):297-303.
134. Valdes AM, Andrew T, Gardner JP, Kimura M, Oelsner E, Cherkas LF, *et al.* Obesity, cigarette smoking, and telomere length in women. *Lancet.* 2005;366(9486):662-4.
135. Fyhrquist F, Saijonmaa O, Strandberg T. The roles of senescence and telomere shortening in cardiovascular disease. *Nat Rev Cardiol.* 2013;10(5):274-83.
136. Benetos A, Okuda K, Lajemi M, Kimura M, Thomas F, Skurnick J, *et al.* Telomere length as an indicator of biological aging: the gender effect and relation with pulse pressure and pulse wave velocity. *Hypertension.* 2001;37(2 Pt 2):381-5.
137. Cherkas LF, Hunkin JL, Kato BS, Richards JB, Gardner JP, Surdulescu GL, *et al.* The association between physical activity in leisure time and leukocyte telomere length. *Arch Intern Med.* 2008;168(2):154-8.
138. von Zglinicki T, Pilger R, Sittler N. Accumulation of single-strand breaks is the major cause of telomere shortening in human fibroblasts. *Free Radic Biol Med.* 2000;28(1):64-74.
139. Hammad M, Al Mheid I, Wilmot K, Ramadan R, Abdelhadi N, Alkholder A, *et al.* Telomere Shortening, Regenerative Capacity, and Cardiovascular Outcomes. *Circ Res.* 2017;120(7):1130-8.

140. Wong LS, Huzen J, van der Harst P, de Boer RA, Codd V, Westenbrink BD, *et al.* Anaemia is associated with shorter leucocyte telomere length in patients with chronic heart failure. *Eur J Heart Fail.* 2010;12(4):348-53.
141. Westhoff JH, Schildhorn C, Jacobi C, Homme M, Hartner A, Braun H, *et al.* Telomere shortening reduces regenerative capacity after acute kidney injury. *J Am Soc Nephrol.* 2010;21(2):327-36.
142. Lund G, Andersson L, Lauria M, Lindholm M, Fraga MF, Villar-Garea A, *et al.* DNA methylation polymorphisms precede any histological sign of atherosclerosis in mice lacking apolipoprotein E. *J Biol Chem.* 2004;279(28):29147-54.
143. Hiltunen MO, Turunen MP, Hakkinen TP, Rutanen J, Hedman M, Makinen K, *et al.* DNA hypomethylation and methyltransferase expression in atherosclerotic lesions. *Vasc Med.* 2002;7(1):5-11.
144. Laukkanen MO, Mannermaa S, Hiltunen MO, Aittomaki S, Airene K, Janne J, *et al.* Local hypomethylation in atherosclerosis found in rabbit *ec-sod* gene. *Arterioscler Thromb Vasc Biol.* 1999;19(9):2171-8.
145. Castro R, Rivera I, Struys EA, Jansen EE, Ravasco P, Camilo ME, *et al.* Increased homocysteine and S-adenosylhomocysteine concentrations and DNA hypomethylation in vascular disease. *Clin Chem.* 2003;49(8):1292-6.
146. Stenvinkel P, Karimi M, Johansson S, Axelsson J, Suliman M, Lindholm B, *et al.* Impact of inflammation on epigenetic DNA methylation - a novel risk factor for cardiovascular disease? *J Intern Med.* 2007;261(5):488-99.
147. Kim M, Long TI, Arakawa K, Wang R, Yu MC, Laird PW. DNA methylation as a biomarker for cardiovascular disease risk. *PLoS One.* 2010;5(3):e9692.
148. Tsaprouni LG, Yang TP, Bell J, Dick KJ, Kanoni S, Nisbet J, *et al.* Cigarette smoking reduces DNA methylation levels at multiple genomic loci but the effect is partially reversible upon cessation. *Epigenetics.* 2014;9(10):1382-96.

149. Pratt JR, Parker MD, Affleck LJ, Corps C, Hostert L, Michalak E, *et al.* Ischemic epigenetics and the transplanted kidney. *Transplant Proc.* 2006;38(10):3344-6.
150. Endo K, Kito N, Fukushima Y, Weng H, Iwai N. A novel biomarker for acute kidney injury using TaqMan-based unmethylated DNA-specific polymerase chain reaction. *Biomed Res.* 2014;35(3):207-13.
151. Huang N, Tan L, Xue Z, Cang J, Wang H. Reduction of DNA hydroxymethylation in the mouse kidney insulted by ischemia reperfusion. *Biochem Biophys Res Commun.* 2012;422(4):697-702.
152. Kang SW, Shih PA, Mathew RO, Mahata M, Biswas N, Rao F, *et al.* Renal kallikrein excretion and epigenetics in human acute kidney injury: expression, mechanisms and consequences. *BMC Nephrol.* 2011;12:27.
153. Aubert G, Hills M, Lansdorp PM. Telomere length measurement—Caveats and a critical assessment of the available technologies and tools. *Mutation Research/Fundamental and Molecular Mechanisms of Mutagenesis.* 2012;730(1–2):59-67.
154. Kimura M, Stone RC, Hunt SC, Skurnick J, Lu X, Cao X, *et al.* Measurement of telomere length by the Southern blot analysis of terminal restriction fragment lengths. *Nat Protoc.* 2010;5(9):1596-607.
155. Cawthon RM. Telomere measurement by quantitative PCR. *Nucleic Acids Res.* 2002;30(10):e47.
156. Montpetit AJ, Alhareeri AA, Montpetit M, Starkweather AR, Elmore LW, Filler K, *et al.* Telomere length: a review of methods for measurement. *Nurs Res.* 2014;63(4):289-99.
157. Cawthon RM. Telomere length measurement by a novel monochrome multiplex quantitative PCR method. *Nucleic Acids Res.* 2009;37(3):e21.
158. O'Callaghan NJ, Fenech M. A quantitative PCR method for measuring absolute telomere length. *Biol Proced Online.* 2011;13:3.

159. Baird DM, Rowson J, Wynford-Thomas D, Kipling D. Extensive allelic variation and ultrashort telomeres in senescent human cells. *Nat Genet.* 2003;33(2):203-7.
160. Britt-Compton B, Rowson J, Locke M, Mackenzie I, Kipling D, Baird DM. Structural stability and chromosome-specific telomere length is governed by cis-acting determinants in humans. *Hum Mol Genet.* 2006;15(5):725-33.
161. Bendix L, Horn PB, Jensen UB, Rubelj I, Kolvraa S. The load of short telomeres, estimated by a new method, Universal STELA, correlates with number of senescent cells. *Aging cell.* 2010;9(3):383-97.
162. Lansdorp PM, Verwoerd NP, van de Rijke FM, Dragowska V, Little MT, Dirks RW, *et al.* Heterogeneity in telomere length of human chromosomes. *Hum Mol Genet.* 1996;5(5):685-91.
163. Zanet DL, Saberi S, Oliveira L, Sattha B, Gadawski I, Cote HC. Blood and dried blood spot telomere length measurement by qPCR: assay considerations. *PLoS One.* 2013;8(2):e57787.
164. Horvath S. DNA methylation age of human tissues and cell types. *Genome Biol.* 2013;14(10):R115.
165. Chen BH, Marioni RE, Colicino E, Peters MJ, Ward-Caviness CK, Tsai P-C, *et al.* DNA methylation-based measures of biological age: meta-analysis predicting time to death. *Aging (Albany NY).* 2016;8(9):1844-59.
166. Koch CM, Wagner W. Epigenetic-aging-signature to determine age in different tissues. *Aging (Albany NY).* 2011;3(10):1018-27.
167. Weidner CI, Lin Q, Koch CM, Eisele L, Beier F, Ziegler P, *et al.* Aging of blood can be tracked by DNA methylation changes at just three CpG sites. *Genome Biol.* 2014;15(2):R24.
168. Levine ME, Lu AT, Quach A, Chen BH, Assimes TL, Bandinelli S, *et al.* An epigenetic biomarker of aging for lifespan and healthspan. *Aging (Albany NY).* 2018;10(4):573-91.
169. PAXgene. Blood RNA kit handbook. 2015;Version 2.

170. Qiagen. EZ1 DNA Handbook. 2010.
171. ThermoScientific. Nanodrop Nucleic Acid Technical Guide. 2010.
172. Anslinger K, Bayer B, Rolf B, Keil W, Eisenmenger W. Application of the BioRobot EZ1 in a forensic laboratory. *Leg Med (Tokyo)*. 2005;7(3):164-8.
173. Sarkar G, Sommer SS. Shedding light on PCR contamination. *Nature*. 1990;343(6253):27.
174. Brouillette SW, Moore JS, McMahon AD, Thompson JR, Ford I, Shepherd J, *et al*. Telomere length, risk of coronary heart disease, and statin treatment in the West of Scotland Primary Prevention Study: a nested case-control study. *Lancet*. 2007;369(9556):107-14.
175. Shapiro R, DiFate V, Welcher M. Deamination of cytosine derivatives by bisulfite. Mechanism of the reaction. *J Am Chem Soc*. 1974;96(3):906-12.
176. Clark SJ, Harrison J, Paul CL, Frommer M. High sensitivity mapping of methylated cytosines. *Nucleic Acids Res*. 1994;22(15):2990-7.
177. Heinze G, Dunkler D. Five myths about variable selection. *Transpl Int*. 2017;30(1):6-10.
178. Vittinghoff E, McCulloch CE. Relaxing the rule of ten events per variable in logistic and Cox regression. *Am J Epidemiol*. 2007;165(6):710-8.
179. Serruys PW, Morice MC, Kappetein AP, Colombo A, Holmes DR, Mack MJ, *et al*. Percutaneous coronary intervention versus coronary-artery bypass grafting for severe coronary artery disease. *N Engl J Med*. 2009;360(10):961-72.
180. Qin J. The Telomere as a Marker for Aging. Applications Laboratory, Qiagen. <https://www.qiagen.com/us/resources/download.aspx?id=0df45038-6076>.
181. Dieleman JM, Peelen LM, Coulson TG, Tran L, Reid CM, Smith JA, *et al*. Age and other perioperative risk factors for postoperative systemic inflammatory response syndrome after cardiac surgery. *Br J Anaesth*. 2017;119(4):637-44.

182. Brault ME, Ohayon SM, Kwan R, Bergman H, Eisenberg MJ, Boivin JF, *et al.* Telomere length and the clinical phenotype of frailty in older adults undergoing cardiac surgery. *J Am Geriatr Soc.* 2014;62(11):2205-7.
183. D'Amario D, Leone AM, Iaconelli A, Luciani N, Gaudino M, Kannappan R, *et al.* Growth properties of cardiac stem cells are a novel biomarker of patients' outcome after coronary bypass surgery. *Circulation.* 2014;129(2):157-72.
184. Roberts JD, Dewland TA, Longoria J, Fitzpatrick AL, Ziv E, Hu D, *et al.* Telomere length and the risk of atrial fibrillation: insights into the role of biological versus chronological aging. *Circulation Arrhythmia and electrophysiology.* 2014;7(6):1026-32.
185. Lin TT, Norris K, Heppel NH, Pratt G, Allan JM, Allsup DJ, *et al.* Telomere dysfunction accurately predicts clinical outcome in chronic lymphocytic leukaemia, even in patients with early stage disease. *Br J Haematol.* 2014;167(2):214-23.
186. Williams J, Heppel NH, Britt-Compton B, Grimstead JW, Jones RE, Tauro S, *et al.* Telomere length is an independent prognostic marker in MDS but not in de novo AML. *Br J Haematol.* 2017.
187. Baird DM, Britt-Compton B, Rowson J, Amso NN, Gregory L, Kipling D. Telomere instability in the male germline. *Hum Mol Genet.* 2006;15(1):45-51.
188. Rizvi S, Raza ST, Mahdi F. Telomere length variations in aging and age-related diseases. *Current aging science.* 2014;7(3):161-7.
189. Dlouha D, Maluskova J, Kralova Lesna I, Lanska V, Hubacek JA. Comparison of the relative telomere length measured in leukocytes and eleven different human tissues. *Physiol Res.* 2014;63 Suppl 3:S343-50.
190. Takubo K, Izumiyama-Shimomura N, Honma N, Sawabe M, Arai T, Kato M, *et al.* Telomere lengths are characteristic in each human individual. *Exp Gerontol.* 2002;37(4):523-31.

191. Friedrich U, Griese E, Schwab M, Fritz P, Thon K, Klotz U. Telomere length in different tissues of elderly patients. *Mech Ageing Dev.* 2000;119(3):89-99.
192. Rakyan VK, Down TA, Balding DJ, Beck S. Epigenome-wide association studies for common human diseases. *Nature reviews Genetics.* 2011;12(8):529-41.
193. Dogan MV, Shields B, Cutrona C, Gao L, Gibbons FX, Simons R, *et al.* The effect of smoking on DNA methylation of peripheral blood mononuclear cells from African American women. *BMC Genomics.* 2014;15:151.
194. Beach SR, Dogan MV, Lei MK, Cutrona CE, Gerrard M, Gibbons FX, *et al.* Methylopic Aging as a Window onto the Influence of Lifestyle: Tobacco and Alcohol Use Alter the Rate of Biological Aging. *J Am Geriatr Soc.* 2015;63(12):2519-25.
195. Lei MK, Beach SR, Dogan MV, Philibert RA. A pilot investigation of the impact of smoking cessation on biological age. *Am J Addict.* 2017;26(2):129-35.
196. Liu Y, Aryee MJ, Padyukov L, Fallin MD, Hesselberg E, Runarsson A, *et al.* Epigenome-wide association data implicate DNA methylation as an intermediary of genetic risk in rheumatoid arthritis. *Nat Biotechnol.* 2013;31(2):142-7.
197. Dick KJ, Nelson CP, Tsaprouni L, Sandling JK, Aissi D, Wahl S, *et al.* DNA methylation and body-mass index: a genome-wide analysis. *Lancet.* 2014;383(9933):1990-8.
198. Rakyan VK, Beyan H, Down TA, Hawa MI, Maslau S, Aden D, *et al.* Identification of type 1 diabetes-associated DNA methylation variable positions that precede disease diagnosis. *PLoS genetics.* 2011;7(9):e1002300.
199. Huynh JL, Garg P, Thin TH, Yoo S, Dutta R, Trapp BD, *et al.* Epigenome-wide differences in pathology-free regions of multiple sclerosis-affected brains. *Nat Neurosci.* 2014;17(1):121-30.
200. Pidsley R, Zotenko E, Peters TJ, Lawrence MG, Risbridger GP, Molloy P, *et al.* Critical evaluation of the Illumina MethylationEPIC BeadChip microarray for whole-genome DNA methylation profiling. *Genome Biol.* 2016;17(1):208.

201. Sandoval J, Heyn H, Moran S, Serra-Musach J, Pujana MA, Bibikova M, *et al.* Validation of a DNA methylation microarray for 450,000 CpG sites in the human genome. *Epigenetics*. 2011;6(6):692-702.
202. Fotino M, Merson EJ, Allen FH, Jr. Micromethod for rapid separation of lymphocytes from peripheral blood. *Ann Clin Lab Sci*. 1971;1(2):131-3.
203. Ruitenbergh JJ, Mulder CB, Maino VC, Landay AL, Ghanekar SA. VACUTAINER CPT and Ficoll density gradient separation perform equivalently in maintaining the quality and function of PBMC from HIV seropositive blood samples. *BMC Immunol*. 2006;7:11.
204. Kim NW, Piatyszek MA, Prowse KR, Harley CB, West MD, Ho PL, *et al.* Specific association of human telomerase activity with immortal cells and cancer. *Science*. 1994;266(5193):2011-5.
205. Roche. TeloTAGG Telomerase PCR ELISA PLUS Protocol. 2015;18.
206. SuperScript VILO cDNA Synthesis Kit. Invitrogen.
207. TaqMan® Fast Advanced Master Mix : For two-step RT-PCR in gene expression experiments or quantitative analysis.

Appendices

Appendix A: Ethical approval and research and development documents



Health Research Authority

**National Research
Ethics Service**

London - Queen Square Research Ethics Committee

HRA NRES Centre Manchester
Barlow House
3rd Floor 4
Minshull Street
Manchester
M1 3DZ

03 November 2015

Professor Magdi Yaqoob
Translational Medicine and Therapeutics
John Vane Science Centre
Queen Mary University of London, Charterhouse Sq
EC1M6BQ

Dear Professor Yaqoob

Study title: **Telomere length and telomerase activity as a predictor of acute kidney injury following cardiac surgery**
REC reference: **15/LO/1741**
IRAS project ID: **181330**

Thank you for your email of 3 November 2015. I can confirm the REC has received the documents listed below and that these comply with the approval conditions detailed in our letter dated 20 October 2015

Documents received

The documents received were as follows:

Document	Version	Date
Other [Email response to REC]		03 November 2015

Approved documents

The final list of approved documentation for the study is therefore as follows:

Document	Version	Date
Evidence of Sponsor insurance or indemnity (non NHS Sponsors only)		16 July 2015
IRAS Checklist XML [Checklist_17092015]		17 September 2015
Letter from sponsor [Sponsor letter]		
Other [Consultee Information Sheet]	1.2	08 September 2015
Other [Consultee declaration form]	1.1	08 September 2015
Other [Email response to REC]		03 November 2015
Participant consent form [ICF]	1.5	08 September 2015
Participant information sheet (PIS) [PIS]	1.4	08 September 2015

REC Application Form [REC_Form_17092015]		17 September 2015
Referee's report or other scientific critique report		04 September 2015
Research protocol or project proposal [Project protocol]	1.4	08 September 2015
Summary CV for Chief Investigator (CI) [CV for CI]		
Summary CV for student [CV for DCB]		
Summary CV for supervisor (student research) [CV for RU]		

You should ensure that the sponsor has a copy of the final documentation for the study. It is the sponsor's responsibility to ensure that the documentation is made available to R&D offices at all participating sites.

15/LO/1741

Please quote this number on all correspondence

Yours sincerely



**Rachel
Heron REC
Manager**

E-mail: nrescommittee.london-queensquare@nhs.net

Copy to: Professor Magdi Yaqoob
Dr Sally Burtles, Barts and the London NHS Trust

Dr. Sally Burtles
Joint Research Management Office
Queen Mary Innovation Centre
5 Walden Street
London
E1 2EF

**Declaration of Sponsorship
(Non-CTIMP)**

16th November 2015

Professor Magdi Yaqoob
William Harvey Research Institute
John Vane Science Centre
Charterhouse Square
EC1M 6BQ

Tel: 020 7882 7250
Email: Sponsorsrep@bartshealth.nhs.uk

Dear Professor Yaqoob

Protocol: Telomere length and telomerase activity as a predictor of acute kidney injury following cardiac surgery

Protocol version: 1.4

Protocol date: 08.09.2015

ReDA Ref: 010706

REC Ref: 15/LO/1741

Chief Investigator: Professor Magdi Yaqoob

This letter is to confirm that **Queen Mary University of London** is willing to act as Sponsor as defined in the Research Governance Framework for Health and Social Care 2005.

Sponsorship will remain in effect until the completion of the project and the ongoing responsibilities of the Chief Investigator as stated in the sponsorship agreement have been met.

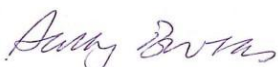
Should the Chief Investigator fail to notify the Joint Research Management Office of a substantial amendment to the project, this may result in inadequate indemnity or sponsorship cover and therefore the project may not be fully insured.

The sponsor may terminate this arrangement with immediate effect if:

- It is reasonably of the opinion that the project should cease in the interests of the safety of participants or staff involved in the project.
- The Chief Investigator is no longer (for whatever reason) able to act as Chief Investigator and no mutually acceptable replacement can be found.
- The Chief Investigator does not adhere to the responsibilities stated in the conditions of sponsorship letter.

Please use page 2 (Conditions of Sponsorship) as a guideline for good research practice and ensure you adhere to any applicable Trust policies and R&D arrangements.

Yours sincerely,



Dr. Sally Burtles
Director of Research Services & Business Development

London - Queen Square Research Ethics Committee

HRA NRES Centre Manchester
Barlow House
3rd Floor
4 Minshull Street
Manchester
M1 3DZ

06 June 2016

Professor Magdi Yaqoob
Translational Medicine and Therapeutics John
Vane Science Centre
Queen Mary University of London, Charterhouse Sq EC1M6BQ

Dear Professor Yaqoob

Study title: Telomere length and telomerase activity as a predictor of acute kidney injury following cardiac surgery
REC reference: 15/LO/1741
Amendment number: 1
Amendment date: 29 March 2016
IRAS project ID: 181330

1. Addition of a blood test on day 3 or 4 post operatively.
2. Removal of remove the tests for blood and urine at 4 hours from the protocol.
3. Amended protocol that blood and urine for renal biomarker analysis will not be taken on every patient.

The above amendment was reviewed by the Sub-Committee in correspondence.

Ethical opinion

The members of the Committee taking part in the review gave a favourable ethical opinion of the amendment on the basis described in the notice of amendment form and supporting documentation.

The Sub-Committee identified no ethical issues.

Approved documents

The documents reviewed and approved at the meeting were:

Document	Version	Date
Notice of Substantial Amendment (non-CTIMP)		29 March 2016
Participant consent form [ICF main Telomere Ver 1.6 clean]	1.6	29 March 2016
Participant consent form [ICF main Telomere Ver 1.6 tracked]	1.6 (tracked)	29 March 2016
Participant information sheet (PIS) [PIS main Telomere Ver 1.5]	1.5	29 March 2016

clean]		
Participant information sheet (PIS) [PIS main Telomere Ver 1.5 clean]	1.5 (tracked)	29 March 2016
Research protocol or project proposal [QMUL Main Trial Protocol Ver 1.5 clean]	1.5	29 March 2016
Research protocol or project proposal [QMUL Main Trial Protocol Ver 1.5 tracked]	1.5 (tracked)	29 March 2016

Membership of the Committee

The members of the Committee who took part in the review are listed on the attached sheet.

R&D approval

All investigators and research collaborators in the NHS should notify the R&D office for the relevant NHS care organisation of this amendment and check whether it affects R&D approval of the research.

Statement of compliance

The Committee is constituted in accordance with the Governance Arrangements for Research Ethics Committees and complies fully with the Standard Operating Procedures for Research Ethics Committees in the UK.

We are pleased to welcome researchers and R & D staff at our NRES committee members' training days – see details at <http://www.hra.nhs.uk/hra-training/>

15/LO/1741:	Please quote this number on all correspondence
--------------------	---

Yours sincerely



Signed on behalf of
Dr Eamonn Walsh
Chair

E-mail: nrescommittee.london-queenssquare@nhs.net

Enclosures: List of names and professions of members who took part in the review

Copy to: Dr Sally Burtles, Barts Health NHS Trust

London - Queen Square Research Ethics Committee

Attendance at Sub-Committee of the REC meeting

Committee Members:

Name	Profession	Present	Notes
Dr Ciaran Scott Hill	Neurosurgery Speciality Registrar	Yes	
Dr Eamonn Walsh	Lecturer	Yes	

Also in attendance:

Name	Position (or reason for attending)
Ms Rachel Heron	REC Manager

Participation Information Sheet (PIS)

Study Title: Telomere length and telomerase activity as a predictor of acute kidney injury following cardiac surgery

Invitation to participate in the above study

We would like to invite you to participate in a research study during your upcoming hospital stay. Before you decide, we would like to explain why the research is being done and what it would involve for you. Please take time to read the information in this sheet carefully and discuss it with family and friends if you wish. **You will have the opportunity to go through the information sheet in detail with a member of the research team and ask questions prior to deciding whether to participate.**

What is the purpose of the study?

Following cardiac surgery, a proportion of patients will develop acute kidney failure. This is usually temporary and treatment is focused on supporting the kidneys and allowing them time to recover. At present it is difficult to predict who might develop acute kidney failure post-operatively. Whilst those with pre-existing kidney problems are at higher risk, patients with normal pre-operative kidney function can also suffer this complication.

The primary aim of this study will be to run DNA tests on blood samples to determine if we can identify patients at greater risk of developing acute kidney injury following cardiac surgery. As a secondary aim we are hoping to identify new tests for detecting kidney failure earlier than those currently in clinical use..

Why have I been invited to participate?

All patients undergoing cardiac surgery in the Barts Heart Centre will be considered for inclusion in this trial. In addition, a smaller group of patients having thoracic surgery will also be invited to participate. This will provide a comparison of our findings in patients not having cardiac surgery.

Do I have to take part?

It is entirely up to you whether or not to take part. If you decide to take part you will be given this information sheet and a member of the research team will address any questions or concerns you may have. If you decide to participate you will be asked to sign a consent form. If you chose not to take part in the study, this decision will not affect in any way the normal care you are entitled to receive from your doctor.

What will happen to me if I take part?

This research project does not alter the normal hospital care that you will receive whilst undergoing your surgery. If you decide to participate, you will have additional blood tests taken. These will be performed on the day of admission and on the third or fourth day after your operation. Wherever possible, the blood tests will be coordinated to coincide with those that would need to be taken as part of your routine care. We will

simply take a few more millilitres of blood to perform the additional research related tests. Where additional blood tests are required, we will try to use existing access points such as the central venous line (required for all cardiac surgical operations) to minimise the need for additional venepuncture (taking blood from vein with a needle).

In addition, you will be asked to provide a urine sample pre-operatively. You may also be asked to provide a urine sample on the 1st post-operative day. Where possible, samples will be taken from a urinary catheter (a tube placed into the bladder routinely after all cardiac operations). If you are asked to provide urine sample on the 1st post-operative day, you will have a further blood test on the 1st post-operative day also. This will be taken from a central venous line. These blood and urine samples are collected in a subgroup of patients (i.e. not all patients) to test for early biomarkers for post-operative acute kidney injury.

In addition, any waste tissue generated from your surgery may be sampled and stored for later analysis. We will only sample tissue that would otherwise be disposed of following your surgery and will not take any additional material for the purpose of this research study.

Following cardiac surgery it is expected that you will be unconscious for a period. During this period we will continue to take samples at the time points outlined above. Following cardiac surgery, it is not uncommon that you may experience a period of temporary confusion. If this is the case, or if you are unable to consent to ongoing testing yourself for any reason once your anaesthetic has worn off, we will ask a person close to you to advise on whether you should remain in the study. If no such person is available we shall ask an impartial member of the medical team to offer this advice.

What are the potential disadvantages and risks of taking part?

The only disadvantage to participating in the study is the potential need for 1 or 2 additional blood tests over and above that required for your routine care. The exact number will depend on how frequently the surgical team decides to test your blood for clinical reasons. You will also have the minor inconvenience of having to provide additional urine samples.

No harm will come to you from participating in this study. Nor will the quality of your medical care be compromised in anyway. The amount of additional blood you will be required to give above that given for your routine care is not clinically significant. The genetic tests that will be performed will have no effect on your clinical care and all data will be anonymised. However, if at any point you do not feel that you are able to continue in the trial you are free to withdraw your consent at any time.

What are the possible benefits of taking part?

It is unlikely that taking part in this study will be of significant benefit to you. However, by participating in this research, you will help to increase our understanding in this area and hopefully improve our ability to more accurately predict acute kidney injury following cardiac surgery.

What if there is a problem?

If you have concerns about any aspect of this study, you should ask to speak with a member of the research team who will do their best to answer your questions. If you are not satisfied by this and wish to complain formally, this can be done through the NHS Complaints Procedure or Private Institution. The contact details for the Patient Advice and Liaison Service (PALS) at St Bartholomew's Hospital are:

PALS Helpline: Open Monday to Friday, 9.30am – 4.30pm.
Tel: 02035942040
pals@bartshealth.nhs.uk

Will my taking part in the study be kept confidential?

Yes. We will follow standard ethical and legal guidelines for good clinical practice. Any personal identifiable data will be anonymised. All data will be kept on secure hospital databases.

What will happen if I no longer want to participate in the study?

You will be free to withdraw from participation in the study at anytime. You will not have to give any justification and your medical care will not be affected in anyway.

What will happen to the results of the research study?

We will aim to present the results of this study at conferences at a national or international level, and publish them in scientific journals. You will not be identifiable in any report/publication. It will be possible to view a copy of the published research upon request to the researcher.

Who is organising the research?

The study is part of the ongoing research programme in the Cardiothoracic Department at St Bartholomew's Hospital and is organised by Queen Mary University of London. None of the researchers have any conflicts of interest to declare.

Who has reviewed the study?

All research in the NHS is reviewed at by an independent panel, called a Research Ethics Committee, to protect your safety, rights, wellbeing and dignity. This study has been reviewed and given favourable opinion by London - Queen Square Research Ethics Committee.

What do I do now?

If you would like any further information or have any questions, the members of the research team will be happy to help you. Please feel free to discuss this information with your family, friends or GP if you wish. If you decide to participate in the study you will be asked to sign a consent form. You will be given a copy of the consent form to keep.

Contact Details

Please direct all enquiries that you may have about this research study to:
Mr Damian Balmforth

Honorary Specialist Registrar in Cardiothoracic Surgery
The Barts Heart Centre
St Bartholomew's Hospital
Email: damiancharles.balmforth@bartshealth.nhs.uk

Thank you for taking time to read this information and for considering whether to participate in the study. Please ask a member of the research team if there is anything that is not clear.

REC Reference Number:

Patient Identification Number:

PATIENT CONSENT FORM

Study Title: Telomere length and telomerase activity as a predictor of acute kidney injury following cardiac surgery

Contact Details of Researcher:

Mr Damian Balmforth
Specialist Registrar in Cardiothoracic Surgery
Queen Mary, University of London
Tel:
Email: hhx313@qmul.ac.uk

Please
initial box

1. I confirm that I have read and understood the patient information sheet dated 29/3/16 (Version 1.5) for the above study and have had the opportunity to consider the information, ask questions and have these answered satisfactorily.
2. I understand that my participation is voluntary and that I am free to withdraw at any time, without my medical care or legal rights being affected.
3. I understand that relevant sections of any of my medical notes and data collected during the study may be looked at by responsible individuals from Queen Mary University of London (QMUL) and Barts Health NHS Trust (BHNT) or from regulatory authorities involved in auditing the study. I give permission for these individuals to have access to my records.
4. I understand that following my operation it is expected that I will lose capacity to consent to further tissue sample collection for a period. If this is the case, I consent for my blood and urine to be tested for research purposes at the times stipulated in the information sheet dated 8/9/15 (Version 1.4). I understand that venepuncture will not be attempted if I am unable to give implied or explicit consent.

5. Following analysis, I consent for my tissues to be placed in long-term storage for use in future research.

6. I consent to being contacted in the future to enquire about my last known renal function test result and general health enquiries.

7. I consent to being contacted in the future for other ethically approved related research projects.

8. I consent for my GP to be contacted in the future to obtain my latest renal function result.

9. I agree to take part in the above study.

10. I would/would not like to be contacted with information regarding the future publication of this research.

Contact email

Name of Patient

Date

Signature

Name of person taking consent

Date

Signature

2 copies to be made once completed: 1 for patient; 1 for researcher's records; and original to be retained in the hospital notes.

Appendix B: DNA Methylation Methodology

Bisulphite conversion protocol

Bisulphite conversion was performed with the EZ-96 DNA methylation kit (Zymo Research, Cambridge Bioscience, Cambridge UK). For each sample, 500ng of stock DNA was added to 5µL of M-Dilution buffer and made up to a final volume of 50µL with nuclease free water (NFW) in a 96 well plate. This solution was incubated at 37 °Celsius for 15 minutes. 100µL of CT Conversion reagent was then added and the samples incubated for 15 hours (overnight) in the dark, before being cooled on ice. During this incubation the denaturation, sulphonation and deamination steps of the conversion took place. Samples were then transferred to the Zymo-Spin™ I-96 Plate (Catalogue number: 5004) containing 400 µl of M-Binding Buffer. The plate was centrifuged at full speed (>10,000 x g) for 30 seconds and the follow-through discarded. 100 µl of M-Wash Buffer was added to the spin columns and the plate centrifuged for a further 30 seconds. The plate was then incubated with 200 µl of M-Desulphonation Buffer at room temperature for 15 minutes. During this stage, Desulphonation occurred to convert Uracil-SO₃⁻ to Uracil. After incubation, two further washes with 200 µl of M-Wash Buffer were performed. The final Bisulphite-converted DNA (BC-DNA) was eluted by adding 10 µl of M-Elution Buffer directly to the column matrix and centrifuging for 30 seconds at full speed.

Typical yields of BC-DNA were approximately 50ng/µL in 20µl volume. This quantification was performed by Spectrophotometry (Nanodrop). Each sample was

diluted to a concentration of 50ng/ μ L with TE buffer prior to proceeding to Bisulphite PCR.

Bisulphite PCR

Region specific PCR was performed with the Fluidigm 48:48 Access Array (Fluidigm, San Francisco, US). Before proceeding with the Bisulphite PCR, the Fluidigm Access Array was primed to ensure all of its channels were cleared. 0.7ml of Control Line Fluid were instilled into the 'Accumulators' of the array and 500 μ l of 1x Access Array Harvest Solution were loaded into the H1, H2, H3, and H4 wells of the Access Array (both solutions provided by Fluidigm). The array was then placed onto the Pre-PCR Fluidigm IFC Controller AX for priming. Once priming was complete, the Access array was prepared by loading the Primer solution into the Primer inlets and the Sample reaction mixtures into the Sample inlets.

Primer Solution Preparation

The designed primers were provided by Fluidigm in Singleplex form in 96 well plates. Each well contained a single primer pair at a concentration of 60 μ M. Stock multiplex primer mix was made by combining 2-4 primer pairs per well and diluting to a final concentration of 5 μ M. The final primer solution was made up according to *Table 1* by dilution of the stock Multiplex primer mix in a separate 96 well plate. 4 μ L of the final pooled primer solutions were added to the 48 primer inlets.

The exact sequences for CS1 and CS2 used in our primer set were ACACTGACGACATGGTTCTACA and TACGGTAGCAGAGACTTGGTCT respectively

Component	Volume (μL)	Final Concentration
Stock Primer mix (5 μM): CS1-Forward Primers CS2-Reverse Primers	2 per primer 2 per primer	1 μM per primer 1 μM per primer
20X Access Array Loading Buffer	5	1X
DNA suspension buffer	Make up to 100 total	

Table 1: Composition of the primer dilution for one well of the stock Multiplex primer mix plate.

Sample reaction mix preparation

A PCR master mix was created for a total of 60 reactions by combining the components listed in *Table 2*. The function of Dimethyl Sulphoxide (DMSO) in the mix was to alter the structure of cytosine residues from 3 hydrogen bonds to 2 hydrogen bonds to facilitate the PCR.

Component	Volume per reaction (μL)	Volume for 60 reactions
10X FastStart High Fidelity Reaction Buffer without MgCl_2 (Roche)	0.5	30
25mM MgCl_2 (Roche)	0.9	54
DMSO (Roche)	0.25	15
10mM PCR Grade Nucleotide Mix (Roche)	0.1	6
5 U/ μL FastStart High Fidelity Enzyme Blend (Roche)	0.05	3
20X Access Array Loading Reagent (Fluidigm)	0.25	15
PCR Certified Water (TEKnova)	1.95	117
Total	4	240

Table 2: Constituents of PCR mastermix for the 48:48 Access Array

4 μL of master mix was combined with 1 μL of BS-DNA (50ng/ μL) for each sample to give a total volume of 5 μL of sample mix solution. This step was performed in a plane 96-well plate. 4 μL of the resulting sample mix solution was then loaded into each of the sample inlets of the 48.48 Access Array using a hand-held multichannel pipette. Once both the primer mix and sample mix solutions had been manually loaded, the Access Array was placed in the primed Pre-PCR IFC Controller AX for the samples and primers to be automatically combined (1.5 hours duration). The Array was then transferred to the Fluidigm FC1™ Cycler for target amplification by PCR.

Touch down polymerase chain reaction

The cycling conditions for this PCR are given in *Table 3*.

Step Temperature (°C)	Step Duration	Number of cycles
50	2 mins	1
70	20 mins	1
95	10 mins	1
95	15 secs	10
60	30 secs	
72	1 min	1
95	15 secs	2
80	30 secs	
60	30 secs	
95	15 secs	8
60	30 secs	
72	1 min	1
95	15 secs	5
80	30 secs	
60	30 secs	
72	1 min	1
72	3 min	1
4	Hold	

Table 3. Thermocycling conditions for the 48:48 Access Array PCR

The total duration of the PCR was 2 hours and 10 minutes, following which the PCR products were harvested. After removing residual fluid from the H1-4 wells of the 48.48 Access Array, 600µL of Access Array Harvest Solution was instilled into the same wells. A further 2µL of Harvest Solution was added to each sample inlet and the Array placed into the Post-PCR IFC Controller AX. The harvesting script duration was 1.5 hours and resulted in approximately 10µL of harvested PCR product solution being drawn back into each of the 96 sample inlets. These were then transferred to a 96 well plate. Quality control was performed on a random selection of the harvested

PCR products using an Aligent 2200 TapeStation System and D1000 ScreenTape (Aligent technologies) to determine the quantity and integrity of the PCR product.

Barcoding

Barcoding was performed using the Access Array Barcode Library for Illumina Sequencers - 384 (Single Direction) (Fluidigm, PN 100-4876) with a different 10 base pair sequence used for each sample. Firstly, the harvested PCR products were diluted 100-fold by adding 1 μ L of PCR product from each sample with 99 μ L of water in a fresh 96 well plate. For each sample, 1 μ L of diluted PCR product was combined with 4 μ L of sample specific barcode and 15 μ L of master mix to give a final volume of 20 μ L per sample mix. The constituents of the mastermix are shown in *Table 4*. The final concentration of barcode primer mix was 400nM per well. Barcoding of the Access Array PCR product was performed with a further PCR, the conditions of which are given in *Table 5*.

Component	Volume per reaction (μ L)	Volume for 60 reactions
10X FastStart High Fidelity Reaction Buffer without MgCl ₂ (Roche)	2	120
25mM MgCl ₂ (Roche)	3.6	216
DMSO (Roche)	1	60
10mM PCR Grade Nucleotide Mix (Roche)	0.4	24
5 U/ μ L FastStart High Fidelity Enzyme Blend (Roche)	0.2	12
PCR Certified Water (TEKnova)	7.8	469
Total	15	900

Table 4: Sample pre- mix constituents for barcoding PCR

Step Temperature (°C)	Step Duration	Cycles
95	10 mins	1
95	15 s	15
60	30 s	
72	1 min	
72	3 mins	1

Table5: Thermocycling conditions for Barcoding PCR.

Finally, Quality Control was performed on the barcoded PCR products for the same samples that were tested after Bisulphite PCR using the Aligent 2200 TapeStation. Successful barcoding was indicated by a barcoded PCR product that was 59 base pairs larger than the original PCR product (*Figure 1*)

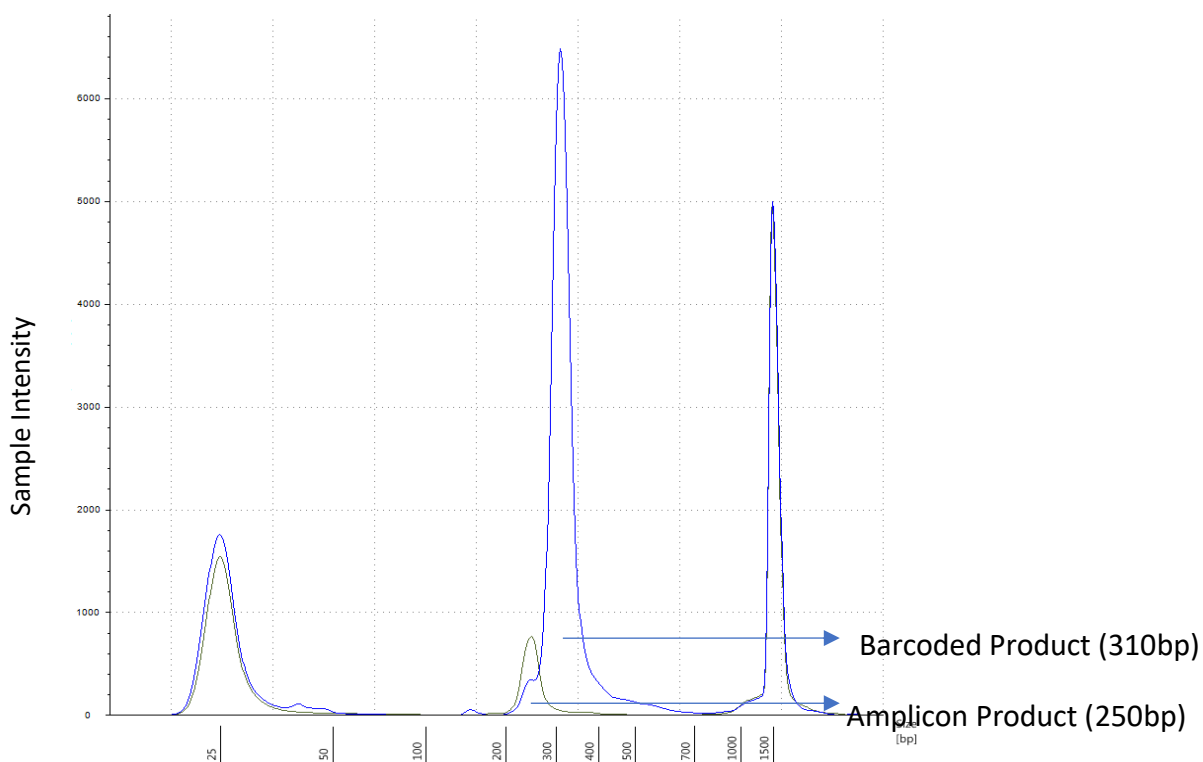


Figure 1: Library quality control to check barcoded product using the Agilent TapeStation. A successful barcoding reaction will produce a product approximately 60 base pairs longer than the original PCR product.

Once the PCR products had been successfully barcoded they could then be pooled for sequencing using the Illumina MiSeq platform (Illumina, California, USA). Samples were pooled by combining 2 μ L of each barcoded product.

Sequencing

The final constructs produced after barcoding were sequenced using the Illumina MiSeq Sequencing system. Sequencing was performed using the 'Sequencing by Synthesis' (SBS) method in which the library fragments are amplified and read simultaneously. SBS is comprised of four main stages; library preparation, cluster generation, sequencing and data analysis.

1. Library Preparation

Pooled PCR products were cleaned using the Agencourt AMPure XP PCR Purification system (Beckman Coulter, Massachusetts, USA). This system uses magnetic bead technology to selectively bind PCR amplicons greater than 100bp, allowing smaller fragments as well as excess primers, nucleotides, salts and enzymes to be washed away. In brief, 12 μ l of pooled PCR products were added to 24 μ l of Tris-EDTA (TE) Buffer and 36 μ l of AMPure XP magnetic beads. The beads covalently bond to fragments >100 base pairs and magnetically separated from the supernatant which is discarded. The beads were then washed with 70% ethanol and the purified PCR product eluted from the beads with TE buffer. Finally, the unbound beads were magnetically separated leaving only purified PCR product. The purified PCR product was run on the Aligent 2200 TapeStation to check that fragments <100 base pairs had

been removed and to check the concentration. This concentration was then diluted to a concentration of 4nM.

5 μ l of pooled PCR product (sequencing library) at a concentration of 4nM was combined with 5 μ l of 0.2M Sodium hydroxide and incubated for 5 minutes to denature the DNA. 990 μ l of pre-chilled MiSeq HTI buffer (Illumina) was then added to stop the denaturation process and produce a final concentration of 20pM. 120 μ l of this solution was then added to a further 480 μ l of HT1 buffer to produce a final running concentration of 5pM.

To 600 μ l of the 5pM library we added the Fluidigm custom sequencing primers, FL1 and FL2. FL1 contains 50 μ M of CS1 and CS2 primers and equimolar concentrations of indexing primers. FL2 contains 50 μ M of CS1 reverse complement and CS2 reverse complement and equimolar concentrations of indexing primers.

2. Cluster generation.

The prepared library is loaded onto a Flow-cell (Illumina) consisting of a lawn of membrane bound oligonucleotide sequences. There are two types of oligonucleotide sequence, complementary to either the P5 or P7 adaptors within the library. As such, the DNA fragment strands within the library bind to the oligonucleotide sequences on the Flow-cell lawn via one of their adaptors. Next, a DNA polymerase synthesises a strand complementary to the hybridized fragment. The resulting double stranded structure is denatured and the original non-membrane bound fragment is washed away. The remaining fragment is then clonally amplified by bridge amplification. The

newly formed membrane bound strand loops over so that the adapter at its free end is able to bind to the second type of oligonucleotide on the flow cell membrane. Again, DNA polymerases generate the complimentary strand, forming a double stranded bridge. This double stranded bridge is denatured, resulting in two DNA fragments that are tethered to the Flow-cell. These fragments undergo separate bridge amplification so that the DNA fragment is amplified exponentially. This process occurs simultaneously for all DNA fragments within the library resulting in clusters of the same DNA fragment grouped together on the Flow cell surface. Following bridge amplification, the reverse strands are cleaved and washed away leaving only the forward strands. The 3' ends of these strands are then blocked to prevent unwanted priming. These clusters are then sequenced simultaneously.

3. Sequencing by synthesis

Sequencing by synthesis (SBS) refers to a process whereby the sequence of a single-stranded DNA fragment is determined as its complimentary chain is formed. It employs a technique termed cyclic reversible termination (CRT). In this process DNA polymerization is performed with reversible terminators. These are deoxynucleotides with an attached fluorophore and blocking group. After the binding of a sequence primer, a complimentary deoxynucleotide binds to the first nucleotide of the template strand. The attached blocking agent terminates further DNA synthesis and unbound nucleotides are washed away. The incorporated nucleotide is imaged and identified from the wavelength of fluorescent signal emitted. In this way the sequence is determined, one base at a time. With each cycle, the 3 deoxynucleotides (Bisulphite converted DNA is a 3 base-pair code) compete with

each other for addition to the chain. Finally, the blocking group and fluorophore are then cleaved, and the process repeats with the addition of the next deoxynucleotide. Sequencing occurs for all DNA fragments within a cluster and for multiple clusters simultaneously. In 'Read 1' the sequences of the membrane bound forward fragments are determined by the synthesis of complimentary strands. This read product is then washed away and the barcode or 'index' read primer hybridizes to the template fragment. The index portion of the fragment is then read by the same CRT process (Index read). This allows the source of the DNA fragment to be determined. The index read product is removed and the original bound fragment is again used as a template to generate a complimentary reverse strand. This is done by removing the blocking cap of the 3' end of the forward fragment, allowing the 3' end to bridge to a complimentary oligonucleotide sequence on the flow-cell surface. The reverse strand is then produced by DNA polymerase and unlabeled nucleotides. The double stranded bridge is denatured and the bound forward strand is cleaved and washed away. Read 2 is now undertaken in which the reverse strand is sequenced by CRT.

4.Data Analysis

The sequencing process generates millions of reads in total representing all of the DNA fragments. Sequences within the pooled DNA library are separated into individual samples based on the unique sample specific barcodes attached to each fragment during preparation of the library. Within fragments from the sample, reads with similar base sequences are clustered and grouped by forward and reverse reads. Any discrepancies are resolved by comparison within these grouped reads. Finally,

the percentage of methylated cytosine residues is calculated for each CpG site for all fragments generated from a single sample.

Appendix C: Sample log of patients included in mTL and Methylation analyses

	Sample Number	Appearance of Buffy	Extraction vol	Nanodrop performed	DNA Conc (ng/μl)	260/280	260/230	Amount needed for DNAm (ng)	Volume needed for DNAm (μl)	Number of 20uL Aliquots	Single band on gel
1	1	1R	300	Yes	65.3	1.84	1.54	500	7.65696784	1	Yes
2	2	1S	300	Yes	89.7	1.86	1.44	500	5.57413601	1	Yes
3	3	1S	300	Yes	28.4	1.91	2.31	500	17.6056338	1	Yes
4	4	1S	300	Yes	99.2	1.84	1.3	500	5.04032258	1	Yes
5	5	1R	300	Yes	84.3	1.88	2.33	500	5.9311981	1	Yes
6	6	1R	300	Yes	89.8	1.86	1.2	500	5.56792873	1	Yes
7	7	1S	300	Yes	96.7	1.86	1.53	500	5.17063082	1	Yes
8	8	0	300	Yes	94.2	1.9	2.11	500	5.30785563	1	Yes
9	9	1R	300	Yes	116.1	1.86	1.75	500	4.30663221	1	Yes
10	10	1R	300	Yes	19.9	1.94	0.7	500	25.1256281	2	x
11	11	1S	300	Yes	38.1	1.88	1.9	500	13.1233596	1	Yes
12	12	1R	300	Yes	64.6	1.87	2.16	500	7.73993808	1	Yes
13	13	1S	300	Yes	93.9	1.89	2.4	500	5.32481363	1	Yes
14	14	1R	300	Yes	32.7	1.94	2.45	500	15.2905199	2	Yes
15	15	1R	300	Yes	101.9	1.9	2.37	500	4.90677134	1	Yes
16	16	1R	300	Yes	85	1.89	2.36	500	5.88235294	1	Yes
17	17	1R	300	Yes	71.7	1.85	0.21	500	6.9735007	1	Yes
18	18	1R	300	Yes	57.9	1.87	1.65	500	8.63557858	1	Yes
19	19	1R	300	Yes	105.8	1.9	2.04	500	4.72589792	1	Yes
20	20	1R	300	Yes	35.9	1.89	2.07	500	13.9275766	1	Yes
21	21	1R	300	Yes	74.2	1.88	2.24	500	6.73854447	1	Yes

22	22	1R	300	Yes	152.3	1.88	1.88	500	3.28299409	1	Yes
23	23	2R	300	Yes	126.1	1.88	2.18	500	3.96510706	1	Yes
24	24	1R	300	Yes	91	1.91	1.62	500	5.49450549	1	Yes
25	25	2R	300	Yes	36.7	1.93	1.95	500	13.6239782	1	Yes
26	26	2R	300	Yes	91.2	1.86	0.56	500	5.48245614	1	Yes
27	27	1R	300	Yes	76.4	1.88	0.99	500	6.54450262	1	Yes
28	28	2R	150	Yes	47	1.89	1.98	500	10.6382979	1	Yes
29	29	2R	150	Yes	77	1.87	1.53	500	6.49350649	1	Yes
30	30	3R	150	Yes	72.6	1.87	2.01	500	6.88705234	1	Yes
31	31	3R	150	Yes	40.9	1.88	1.98	500	12.2249389	1	Yes
32	32	3R	150	Yes	32.8	1.89	1.94	500	15.2439024	1	Yes
33	33	2R	150	Yes	29.5	1.9	1.84	500	16.9491525	1	Yes
34	35	3R	150	Yes	41.6	1.89	1.71	500	12.0192308	1	Yes
35	36	2R	150	Yes	61.4	1.91	2.33	500	8.14332248	1	Yes
36	37	2R	150	Yes	62.6	1.91	2.31	500	7.98722045	1	Yes
37	38	2R	150	Yes	34.3	1.89	2.64	500	14.5772595	1	Yes
38	39	2R	150	Yes	36.5	1.93	1.17	500	13.6986301	1	Yes
39	40	2R	150	Yes	31.3	1.82	1.43	500	15.9744409	1	Yes
40	41	1R	75	Yes	85	1.87	2.08	500	5.88235294	1	Yes
41	42	1S	75	Yes	90.1	1.87	2.12	500	5.54938957	1	Yes
42	43	2S	150	Yes	67.5	1.9	1.61	500	7.40740741	1	Yes
43	44	1R	150	Yes	58.4	1.84	1.89	500	8.56164384	1	Yes
44	45	2R	150	Yes	94.1	1.83	1.98	500	5.31349628	1	Yes
45	46	2S	75	Yes	41.4	1.87	0.58	500	12.0772947	1	Yes
46	47	2R	150	Yes	54.7	1.87	0.96	500	9.14076782	1	Yes
47	48	2R	150	Yes	73.7	1.89	1.83	500	6.78426052	1	Yes
48	49	2S	150	Yes	36.4	1.8	1.7	500	13.7362637	1	Yes

49	50	2S	150	Yes	16.2	1.9	1.34	500	30.8641975	2	Yes
50	51	2S	150	Yes	41.4	1.83	1.45	500	12.0772947	1	Yes
51	52	1S	75	Yes	45.4	1.86	1.45	500	11.0132159	1	Yes
52	53	2S	75	Yes	79	1.89	1.98	500	6.32911392	1	Yes
53	54	2S	150	Yes	76.3	1.87	1.89	500	6.55307995	1	Yes
54	55	2S	75	Yes	60.2	1.87	1.65	500	8.30564784	1	Yes
55	56	2S	150	Yes	40.5	1.83	1.44	500	12.345679	1	Yes
56	57	1S	150	Yes	70	1.85	1.66	500	7.14285714	1	Yes
57	58	2R	150	Yes	51.3	1.86	1.66	500	9.74658869	1	Yes
58	59	2R	150	Yes	93.3	1.86	1.01	500	5.35905681	1	Yes
59	60	2S	150	Yes	93.3	1.85	2.11	500	5.35905681	1	Yes
60	61	2S	150	Yes	86.1	1.87	1.86	500	5.80720093	1	Yes
61	62	2R	150	Yes	79.8	1.9	1.46	500	6.26566416	1	Yes
62	63	2R	150	Yes	23.5	1.97	1.25	500	21.2765957	2	Yes
63	64	2R	150	Yes	74.2	1.86	1.88	500	6.73854447	1	Yes
64	65	2R	150	Yes	18.1	1.96	1.24	500	27.6243094	2	Yes
65	66	2R	150	Yes	33.4	1.81	1.23	500	14.9700599	1	Yes
66	67	2R	150	Yes	68.7	1.88	1.92	500	7.27802038	1	Yes
67	68	2R	150	Yes	74.8	1.88	1.61	500	6.68449198	1	Yes
68	69	2R	150	Yes	59	1.89	0.88	500	8.47457627	1	Yes
69	70	2R	150	Yes	55.5	1.87	1.53	500	9.00900901	1	Yes
70	71	2R	150	Yes	54.4	1.87	1.81	500	9.19117647	1	Yes
71	72	1S	150	Yes	12.3	1.96	0.42	500	40.6504065	3	Yes
72	73	1S	150	Yes	71.7	1.89	1.8	500	6.9735007	1	Yes
73	74	1S1C	150	Yes	79	1.88	2.12	500	6.32911392	1	Yes
74	75	2S	150	Yes	70.7	1.88	2.06	500	7.07213579	1	Yes
75	76	2C	150	Yes	82.2	1.88	1.08	500	6.08272506	1	Yes

76	77	2S	150	Yes	33.1	1.87	0.95	500	15.1057402	1	Yes
77	78	1S1C	150	Yes	26.2	1.44	0.66	500	19.0839695	2	Yes
78	87	1R1S	300	Yes	90.9	1.83	2.09	500	5.50055006	1	Yes
79	90	2R	300	Yes	82.7	1.84	1.98	500	6.04594921	1	Yes
80	91	2S	300	Yes	44.2	1.83	0.47	500	11.3122172	1	Yes
81	92	1S1C	300	Yes	51.3	1.8	0.56	500	9.74658869	1	Yes
82	93	2S	300	Yes	36.2	1.85	0.72	500	13.8121547	1	Yes
83	94	2C	300	Yes	38.6	1.81	1.66	500	12.9533679	1	Yes
84	95	1S1C	300	Yes	83.9	1.85	2.09	500	5.95947557	1	Yes
85	96	1S1C	300	Yes	37.6	1.8	1.71	500	13.2978723	1	Yes
86	98	2C	300	Yes	37.3	1.95	1.8	500	13.4048257	1	x
87	100	2S	300	Yes	79.9	1.83	2.02	500	6.25782228	1	Yes
88	103	1S1C	300	Yes	11	1.89	0.54	500	45.4545455	3	Yes
89	104	1S1C	300	Yes	36.7	1.79	1.4	500	13.6239782	1	Yes
90	108	2C	300	Yes	12.7	1.7	1.13	500	39.3700787	3	x
91	109	1S1C	300	Yes	21.2	1.82	1	500	23.5849057	1	Yes
92	110	1S1C	300	Yes	14.8	1.81	1.11	500	33.7837838	2	Yes
93	113	2C	300	Yes	16.4	2.05	1.34	500	30.4878049	2	x
94	114	2C	300	Yes	16.1	1.73	1.19	500	31.0559006	2	Yes
95	117	2R	300	Yes	78.8	1.83	1.74	500	6.34517766	1	Yes
96	118	2R	300	Yes	87.1	1.81	2.01	500	5.74052813	1	Yes
97	119	2R	300	Yes	59.5	1.82	1.6	500	8.40336134	1	Yes
98	120	2R	300	Yes	53	1.84	1.21	500	9.43396226	1	Yes
99	121	2R	300	Yes	43.3	1.84	1.92	500	11.5473441	1	Yes
100	122	1S1C	300	Yes	39.9	1.78	1.83	500	12.5313283	1	Yes
101	123	1S1C	300	Yes	48.4	1.82	1.86	500	10.3305785	1	Yes
102	124	2S	300	Yes	68.1	1.82	1.88	500	7.34214391	1	Yes

103	125	2S	300	Yes	58.8	1.84	1.44	500	8.50340136	1	Yes
104	126	2S	300	Yes	50.2	1.81	1.93	500	9.96015936	1	Yes
105	127	1S1C	300	Yes	43	1.85	1.78	500	11.627907	1	Yes
106	129	2R	300	Yes	30.3	1.86	1.44	500	16.5016502	2	Yes
107	130	2R	300	Yes	38.6	1.86	1.55	500	12.9533679	1	Yes
108	131	2R	300	Yes	13.7	1.99	0.69	500	36.4963504	1	Yes
109	132	2R	300	Yes	74.7	1.85	1.32	500	6.69344043	1	Yes
110	133	1S1C	300	Yes	35	1.89	1.98	500	14.2857143	1	Yes
111	134	2R	300	Yes	23.1	1.88	1.12	500	21.6450216	2	Yes
112	135	2R	300	Yes	27.8	1.91	1.5	500	17.9856115	2	Yes
113	136	2R	300	Yes	37.2	1.86	0.63	500	13.4408602	1	Yes
114	137	2S	300	Yes	38.7	1.89	1.71	500	12.9198966	1	Yes
115	138	2S	300	Yes	46	1.84	1.46	500	10.8695652	1	Yes
116	139	2R	300	Yes	17.1	1.85	1.08	500	29.2397661	2	Yes
117	140	2R	300	Yes	10.7	1.84	0.85	500	46.728972	3	Yes
118	141	2R	300	Yes	146.7	1.85	2.03	500	3.40831629	1	Yes
119	142	2C	300	Yes	34.7	1.89	1.69	500	14.4092219	1	x
120	143	2R	300	Yes	19.5	1.91	1.21	500	25.6410256	2	Yes
121	144	2R	300	Yes	87.5	1.87	1.63	500	5.71428571	1	Yes
122	145	2S	300	Yes	45.8	1.82	1.48	500	10.9170306	1	Yes
123	146	2S	300	Yes	22.9	1.95	1.68	500	21.8340611	2	Yes
124	147	2S	300	Yes	36.3	1.88	1.82	500	13.7741047	1	Yes
125	148	1S1C	300	Yes	18.2	1.85	1.42	500	27.4725275	2	Yes
126	150	2R	300	Yes	78	1.85	1.1	500	6.41025641	1	Yes
127	151	2S	300	Yes	41.8	1.93	1.87	500	11.9617225	1	Yes
128	152	2S	300	Yes	29.9	1.92	1.74	500	16.722408	2	Yes
129	153	2S	300	Yes	41.5	1.85	1.74	500	12.0481928	1	Yes

130	154	1S	300	Yes	39.2	1.87	0.51	500	12.755102	1	Yes
131	155	2S	300	Yes	48.3	1.89	1.67	500	10.3519669	1	Yes
132	156	2S	300	Yes	12	1.88	1.12	500	41.6666667	3	Yes
133	157	2S	300	Yes	37.6	1.94	2.2	500	13.2978723	1	Yes
134	158	2R	300	Yes	57.6	1.81	2.13	500	8.68055556	1	Yes
135	159	2S	300	Yes	72.6	1.88	2.09	500	6.88705234	1	Yes
136	160	2C	300	Yes	67.5	1.91	2.14	500	7.40740741	1	x
137	161	2R	300	Yes	39.3	1.9	1.69	500	12.7226463	1	Yes
138	162	2R	300	Yes	72.7	1.89	1.94	500	6.87757909	1	Yes
139	163	2R	300	Yes	83.2	1.87	2.18	500	6.00961538	1	Yes
140	164	2R	300	Yes	63.4	1.86	1.6	500	7.88643533	1	Yes
141	165	2R	300	Yes	68.1	1.87	0.96	500	7.34214391	1	Yes
142	166	2R	300	Yes	109	1.86	2.15	500	4.58715596	1	Yes
143	167	2R	300	Yes	101.2	1.88	1.93	500	4.94071146	1	Yes
144	168	2R	300	Yes	65.1	1.89	2.05	500	7.68049155	1	Yes
145	169	2R	300	Yes	48.9	1.9	1.76	500	10.2249489	1	Yes
146	171	2R	300	Yes	87.7	1.92	1.32	500	5.70125428	1	Yes
147	172	2R	300	Yes	67	1.9	2.05	500	7.46268657	1	Yes
148	173	2R	300	Yes	96.8	1.87	1.34	500	5.16528926	1	Yes
149	174	2R	300	Yes	80.2	1.89	1.7	500	6.23441397	1	Yes
150	175	2R	300	Yes	63.4	1.87	1.66	500	7.88643533	1	Yes
151	176	2R	300	Yes	84.9	1.88	1.72	500	5.88928151	1	Yes
152	178	2R	300	Yes	103	1.77	1.01	500	4.85436893	1	Yes
153	179	2R	300	Yes	116	1.89	1.26	500	4.31034483	1	Yes
154	180	2S	300	Yes	104.4	1.87	0.73	500	4.78927203	1	Yes
155	181	2R	300	Yes	78.6	1.88	2.27	500	6.36132316	1	Yes
156	182	2R	300	Yes	73.5	1.89	2.38	500	6.80272109	1	Yes

157	183	2R	300	Yes	49.5	1.92	1.11	500	10.1010101	1	Yes
158	184	2S	300	Yes	82.5	1.89	2.01	500	6.06060606	1	Yes
159	185	2R	300	Yes	88.2	1.89	2.31	500	5.66893424	1	Yes
160	186	2R	300	Yes	113.5	1.89	1.98	500	4.40528634	1	Yes
161	187	2R	300	Yes	82.3	1.88	1.69	500	6.07533414	1	Yes
162	188	2R	300	Yes	107.6	1.87	2.2	500	4.64684015	1	Yes
163	189	2R	300	Yes	77	1.89	1.48	500	6.49350649	1	Yes
164	190	2R	300	Yes	40.9	1.89	1.42	500	12.2249389	1	Yes
165	191	2R	300	Yes	62.9	1.75	2.17	500	7.9491256	1	Yes
166	192	2C	300	Yes	93.8	1.89	2.08	500	5.33049041	1	x
167	193	2S	300	Yes	143.8	1.88	1.12	500	3.47705146	1	Yes
168	194	2R	300	Yes	98	1.86	2.14	500	5.10204082	1	Yes
169	195	2R	300	Yes	97.6	1.86	1.92	500	5.12295082	1	Yes
170	196	2R	300	Yes	94.3	1.86	1.97	500	5.30222694	1	Yes
171	197	2R	300	Yes	134.9	1.86	1.88	500	3.70644922	1	Yes
172	198	2S	300	Yes	61.2	1.9	1.36	500	8.16993464	1	Yes
173	200	2S	300	Yes	47.1	1.86	1.92	500	10.6157113	1	Yes
174	201	2S	300	Yes	72.3	1.86	1.92	500	6.91562932	1	Yes
175	202	2S	300	Yes	69.3	1.86	1.4	500	7.21500722	1	Yes
176	203	R2	300	Yes	105.6	1.86	2.08	500	4.73484848	1	Yes
177	204	C2	300	Yes	24.9	1.83	0.15	500	20.0803213	2	Yes
178	205	R2	300	Yes	90.2	1.86	1.82	500	5.54323725	1	Yes
179	206	R2	300	Yes	76.7	1.85	1.64	500	6.51890482	1	Yes
180	207	R2	300	Yes	69.7	1.87	2.03	500	7.17360115	1	Yes
181	208	R1S1	300	Yes	83.6	1.87	2	500	5.98086124	1	Yes
182	209	2S	300	Yes	34.3	1.88	1.73	500	14.5772595	1	Yes
183	210	2S	300	Yes	35.9	1.91	1.57	500	13.9275766	1	Yes

184	211	2S	300	Yes	38.8	1.91	1.7	500	12.8865979	1	Yes
185	212	2S	300	Yes	42.8	1.85	1.84	500	11.682243	1	Yes
186	213	2S	300	Yes	64.7	1.89	1.95	500	7.72797527	1	Yes
187	214	2S	300	Yes	71.2	1.87	1.8	500	7.02247191	1	Yes
188	215	R2	300	Yes	82	1.87	1.38	500	6.09756098	1	Yes
189	216	2S	300	Yes	84.3	1.87	1.56	500	5.9311981	1	Yes
190	217	2S	300	Yes	80	1.86	1.58	500	6.25	1	Yes
191	218	2S	300	Yes	50.8	1.91	1.86	500	9.84251969	1	Yes
192	219	2S	300	Yes	38.6	1.91	2	500	12.9533679	1	Yes
193	220	2S	300	Yes	49.8	1.87	1.74	500	10.0401606	1	Yes
194	221	2S	300	Yes	59.2	1.87	2.02	500	8.44594595	1	Yes
195	222	2S	300	Yes	55.1	1.88	2.05	500	9.07441016	1	Yes
196	223	2S	300	Yes	51.2	1.89	1.93	500	9.765625	1	Yes
197	224	2S	300	Yes	76.2	1.88	2.03	500	6.56167979	1	Yes
198	225	2S	300	Yes	85	1.84	1.86	500	5.88235294	1	Yes
199	226	2S	300	Yes	94.7	1.86	2.04	500	5.27983105	1	Yes
200	227	2S	300	Yes	99.5	1.87	2.04	500	5.02512563	1	Yes
201	228	2S	300	Yes	26.9	1.94	1.54	500	18.5873606	2	Yes
202	229	2S	300	Yes	60	1.88	1.8	500	8.33333333	1	Yes
203	230	2S	300	Yes	91.2	1.86	2.02	500	5.48245614	1	x
204	231	2S	300	Yes	97.7	1.85	1.55	500	5.11770727	1	x
205	232	2S	300	Yes	78.1	1.87	1.99	500	6.40204866	1	x
206	233	2S	300	Yes	86.3	1.85	1.88	500	5.79374276	1	x
207	234	2S	300	Yes	76.6	1.85	1.88	500	6.52741514	1	x
208	235	2S	300	Yes	78	1.86	1.95	500	6.41025641	1	x
209	236	2S	300	Yes	110.4	1.86	1.56	500	4.52898551	1	x
210	237	2S	300	Yes	99.4	1.86	1.56	500	5.03018109	1	x

211	238	2S	300	Yes	77.2	1.85	1.17	500	6.47668394	1	x
212	239	2S	300	Yes	48.6	1.86	1.9	500	10.2880658	1	x
213	240	2S	300	Yes	73.9	1.87	1.98	500	6.76589986	1	x
214	241	2S	300	Yes	98.5	1.85	1.81	500	5.07614213	1	x
215	242	2S	300	Yes	92.2	1.86	2.1	500	5.42299349	1	x
216	243	2S	300	Yes	113.7	1.86	2.03	500	4.39753738	1	x
217	244	2S	300	Yes	86	1.85	1.17	500	5.81395349	1	x
218	245	2S	300	Yes	87	1.86	1.83	500	5.74712644	1	x
219	246	2S	300	Yes	43	1.88	1.65	500	11.627907	1	x
220	247	2S	300	Yes	39.4	1.84	1.25	500	12.6903553	1	x
221	248	2S	300	Yes	126.2	1.86	1.38	500	3.96196513	1	x
222	249	2S	300	Yes	95.7	1.87	1.79	500	5.2246604	1	x
223	250	2S	300	Yes	68.8	1.88	1.85	500	7.26744186	1	x
224	251	2S	300	Yes	48.4	1.87	1.78	500	10.3305785	1	x
225	252	2S	300	Yes	76.4	1.86	0.69	500	6.54450262	1	x
226	253	2S	300	Yes	71.8	1.87	1.97	500	6.9637883	1	x
227	254	2S	300	Yes	83.2	1.85	1.71	500	6.00961538	1	x
228	255	2S	300	Yes	117.9	1.89	2.02	500	4.2408821	1	x
229	256	2S	300	Yes	118.5	1.89	0.87	500	4.21940928	1	x
230	257	2S	300	Yes	99.2	1.91	1.23	500	5.04032258	1	x
231	258	2S	300	Yes	113.7	1.89	2.1	500	4.39753738	1	x
232	259	2S	300	Yes	94.4	1.82	1.79	500	5.29661017	1	x
233	260	2S	300	Yes	116.5	1.59	0.89	500	4.29184549	1	x
234	261	2S	300	Yes	109	1.83	1.91	500	4.58715596	1	x
235	262	2S	300	Yes	119.5	1.87	1.48	500	4.18410042	1	x
236	263	2S	300	Yes	120.9	1.86	1.72	500	4.1356493	1	x
237	264	2S	300	Yes	140.7	1.87	1.21	500	3.55366027	1	x

238	265	2S	300	Yes	93.1	1.88	2.01	500	5.37056928	1	x
239	266	2S	300	Yes	120.1	1.85	1.83	500	4.16319734	1	x
240	267	2S	300	Yes	143.4	1.88	0.79	500	3.48675035	1	x
241	268	2S	300	Yes	76.7	1.87	1.44	500	6.51890482	1	x
242	269	2S	300	Yes	120.5	1.93	1.78	500	4.14937759	1	x
243	270	2S	300	Yes	133	1.85	0.95	500	3.7593985	1	x
244	271	2S	300	Yes	101.3	1.86	1.85	500	4.93583416	1	x
245	272	2S	300	Yes	106.8	1.85	1.75	500	4.68164794	1	x
246	273	2S	300	Yes	127.1	1.85	1.58	500	3.93391031	1	x
247	274	2S	300	Yes	130.2	1.86	1.58	500	3.84024578	1	x
248	275	2S	300	Yes	17	2.05	0.25	500	29.4117647	1	x
249	276	2S	300	Yes	25.9	1.89	0.3	500	19.3050193	2	x
250	277	2S	300	Yes	28	1.9	0.36	500	17.8571429	2	x
251	278	2S	300	Yes	65.6	1.85	0.58	500	7.62195122	1	x
252	279	2S	300	Yes	64	1.82	0.59	500	7.8125	1	x
253	280	2S	300	Yes	38.1	1.82	0.59	500	13.1233596	1	x
254	281	2S	300	Yes	40.4	1.81	1.56	500	12.3762376	1	x

Key: Appearance: Format = Number of cryovials:Appearance e.g. 1R = 1 cryovial of red buffy. 2S = 2 cryovials of blood stained buffy

Appendix D: Summary of Raw Mean Telomere Length Data

Study ID	T/S 1	T/S 2	T/S 3	T/S Final	Study ID	T/S 1	T/S 2	T/S 3	T/S Final	Study ID	T/S 1	T/S 2	T/S 3	T/S Final
1	0.7691			0.7691181	31	0.77505			0.775052	62	0.572797			0.572797
2	0.7353	0.7731	0.7775	0.777452	32	0.8176			0.817601	63	0.843467			0.843467
3	0.755			0.7550166	33	0.83377			0.833773	64	0.876335	1.012587		1.012587
4	0.5314			0.5313573	35	0.95093			0.95093	65	0.545709			0.545709
5	0.4964			0.4963898	36	0.84777			0.847767	66	0.92244			0.92244
6	0.596			0.5959936	37	1.21238	0.65946	0.60286	0.602862	67	0.53386	0.591867		0.591867
7	0.7534			0.7533878	38	1.0206			1.020601	68	0.525219			0.525219
8	0.6927	0.6465		0.646453	39	0.8536			0.853603	69	0.621405	0.569191		0.569191
9	0.6854			0.6854182	40	0.55171			0.551708	70	0.74712			0.74712
10	0.6608	0.4541	0.4926	0.4925825	41	0.94481			0.944814	71	0.735724	0.5572		0.5572
11	0.5281			0.5280941	42	2.65827	0.60166		0.601658	72	0.805654			0.805654
12	0.7383			0.7383283	43	0.83412			0.834118	73	0.464579	0.692081		0.692081
13	0.6171			0.6170906	44	0.90013			0.900134	74	0.96183	0.814369	0.610074	0.610074
14	0.6799			0.6799047	45	2.20697	0.60463		0.604626	75	0.558867			0.558867
15	0.6939			0.6938865	46	0.8877			0.887697	76	0.990751			0.990751
16	0.5953			0.595271	47	0.93901			0.939009	77	0.903326			0.903326
17	0.5241			0.5240863	48	1.01484			1.014844	78	0.831409			0.831409
18	0.6693			0.6693325	49	5.08813	0.96225		0.962251	87	0.541213			0.541213
19	0.6762	0.6493		0.6492813	50	1.35521	1.0179		1.017899	90	0.771617			0.771617
20	0.8847			0.884704	51	4.02558	0.74267	0.6389	0.638898	91	0.558571	0.486162	0.471453	0.471453
21	0.7532			0.7531748	52	0.88504			0.885039	92	0.556429	0.538087		0.538087
22	0.9372			0.9371509	53	0.83957			0.839568	93	0.618705	0.859502		0.859502
23	0.8881			0.8880516	54	0.88377			0.88377	94	0.620535			0.620535

24	0.9879			0.9878738	55	0.85145			0.851446	95	0.583098			0.583098
Study ID	T/S 1	T/S 2	T/S 3	T/S Final	Study ID	T/S 1	T/S 2	T/S 3	T/S Final	Study ID	T/S 1	T/S 2	T/S 3	T/S Final
25	0.9195			0.9194587	56	0.96062			0.960616	96	0.487092			0.487092
26	0.9534			0.9534402	57	5.06702	0.69446	0.6207	0.620699	98	1.084802	0.96483		0.96483
27	1.0182			1.0182439	58	0.9173			0.917295	100	0.755722			0.755722
28	0.7274			0.7273931	59	0.58734	0.71574		0.715742	103	0.870569			0.870569
29	0.6859	0.8436		0.8436333	60	0.69213			0.692129	104	0.68793			0.68793
30	0.8443			0.8443377	61	0.84752			0.847515	108	0.891704			0.891704
109	0.933			0.9329684	144	0.56884			0.568841	176	0.799795			0.799795
110	0.819			0.8189537	145	0.39369			0.393685	178	0.709387	0.595625		0.595625
113	0.9246			0.9246041	146	0.5371	0.52133		0.521331	179	0.989579			0.989579
114	0.938			0.9380321	147	0.48966			0.489664	180	0.975856			0.975856
117	0.8762			0.8761916	148	0.85887	0.70357		0.703573	181	0.591518	0.484642		0.484642
118	0.9648			0.9647781	150	0.68832			0.688322	182	0.829818	0.580417		0.580417
119	0.8489			0.8488622	151	0.52327			0.523268	183	0.859469	0.614647		0.614647
120	0.8038			0.8037888	152	0.74808			0.748082	184	0.653424			0.653424
121	0.8866			0.8865818	153	0.81981			0.819806	185	0.929291			0.929291
122	0.8257			0.8257062	154	0.71099			0.710991	186	0.888071			0.888071
123	1.0196			1.0196224	155	0.65525			0.655254	187	1.027417			1.027417
124	0.5435			0.5434836	156	0.54753			0.547532	188	0.904107			0.904107
125	0.928			0.9279616	157	0.59265			0.592645	189	0.865072			0.865072
126	0.5762			0.5762443	158	0.82503			0.82503	190	1.022295			1.022295
127	0.6042			0.6042463	159	0.75849			0.758493	191	0.695009	0.546966		0.546966
129	0.7965			0.7964663	160	0.75785			0.757853	192	0.646575			0.646575
130	0.9405			0.9404829	161	0.8515			0.851502	193	0.595057			0.595057
131	0.9765			0.9764963	162	0.70676			0.706758	194	0.96992			0.96992
132	0.6201			0.6200614	163	0.78096			0.780959	195	0.907453			0.907453

133	0.6084			0.6083699	164	0.73251			0.732513	196	1.081752			1.081752
134	0.614			0.614015	165	0.89135			0.89135	197	0.619257			0.619257
135	0.588			0.5880364	166	0.97347			0.973469	198	0.768462	0.819108		0.768462
Study ID	T/S 1	T/S 2	T/S 3	T/S Final	Study ID	T/S 1	T/S 2	T/S 3	T/S Final	Study ID	T/S 1	T/S 2	T/S 3	T/S Final
136	0.6437			0.6437223	167	0.79319	0.8802		0.880203	200	0.559602			0.559602
137	0.6332	0.5247		0.524704	168	0.8025	1.19741	0.78346	0.783458	201	0.637447			0.637447
138	0.5754	0.5811		0.5811403	169	0.93537			0.935372	202	0.723327	0.801839		0.801839
139	1.1509			1.1508512	171	0.89661			0.896613	203	0.584141			0.584141
140	0.8932			0.8931637	172	0.86841			0.868407	204	0.655748			0.655748
141	0.573			0.5729943	173	0.76692			0.766916	205	0.77831	0.805584		0.805584
142	0.7258			0.7258374	174	0.89595			0.895949	206	0.916677			0.916677
143	0.6015	0.6309		0.6309174	175	0.77152			0.771518	207	0.929516			0.929516
208	0.7509	0.8488		0.8488464	238	0.588			0.587996	268	2.168728	0.799132		0.799132
209	0.5776			0.5776419	239	0.44473			0.444728	269	0.705047	0.941194		0.941194
210	0.5954			0.5953521	240	1.05692			1.056923	270	0.19577	0.519971		0.519971
211	0.9256			0.9255678	241	0.73184			0.731837	271	0.552628			0.552628
212	0.6297			0.629707	242	0.90851			0.908506	272	0.557005			0.557005
213	0.7586	0.5802		0.5802039	243	0.75732			0.757324	273	0.575372			0.575372
214	0.6547			0.6547161	244	0.66278			0.662779	274	0.513386			0.513386
215	0.8577			0.8577077	245	0.70833	0.56284		0.562842	275	1.079305	0.837042		0.837042
216	1.1725			1.1725016	246	0.65333			0.65333	276	0.999177			0.999177
217	0.6584			0.6583899	247	0.62025			0.620253	277	0.924364			0.924364
218	0.5047			0.5046734	248	0.83117			0.831175	278	0.921899	0.73712		0.73712
219	0.9889			0.9889018	249	0.60759			0.607591	279	0.782866			0.782866
220	0.5443			0.5443161	250	0.60771			0.607706	280	0.961422			0.961422
221	0.7435	0.7923		0.7922687	251	0.90143			0.901434	281	0.886769			0.886769
222	1.0125	0.8676		0.8676324	252	0.72831	0.82189		0.821888					

223	0.541			0.5409983	253	0.75994			0.75994					
224	0.5953			0.5952591	254	0.85033			0.850331					
225	0.7417	0.8655		0.865525	255	0.58038			0.580379					
226	0.9007			0.9007206	256	0.5649			0.564905					
227	0.738	0.8536		0.853584	257	0.86641			0.866412					
Study ID	T/S 1	T/S 2	T/S 3	T/S Final	Study ID	T/S 1	T/S 2	T/S 3	T/S Final	Study ID	T/S 1	T/S 2	T/S 3	T/S Final
228	0.6923	0.7541		0.7540571	258	0.89701			0.897008					
229	0.6196			0.619586	259	0.69665	0.76769		0.767695					
230	1.0062			1.0062014	260	0.96706			0.967065					
231	0.6151			0.6150693	261	0.66882	0.54039		0.540391					
232	0.6304			0.6303584	262	0.62681			0.626811					
233	0.5942			0.59423	263	1.06672	0.89773		0.897726					
234	0.5979			0.5979346	264	0.5424			0.542397					
235	0.5955			0.5954693	265	0.89936			0.899359					
236	0.6188	0.7447		0.7447205	266	0.85785			0.857855					
237	0.8373			0.8372643	267	0.90342	0.93363		0.933635					

Table 1: Summary of raw data for mTL measurement. Red values indicate a failed measurement where by the Intra-assay coefficient of variation for duplicate samples was >10%. Such failed measurements were repeated. T/S = Telomere/Standard Ratio. 'T/S Final' represents the final value of T/S ratio (also known as mean telomere length) used in subsequent analysis.

Run	Tel R ²	Tel Efficiency	Std R ²	Std Efficiency	Std TS T/S	Std A T/S	Std B T/S	Std C T/S	Std D T/S		
0-19	0.998	0.99	0.991	1.14	0.995208	1.076866	0.941808	0.920313	1.076531		
20-39	0.998	1.06	0.999	1.17	0.991289	1.022454	0.972661	1.024108	0.990489		
40-57	0.999	1.05	0.998	1.17	0.998978	0.990347	1.026843	0.980404	1.004031		
58-76	0.995	1.01	0.998	1.17	1.037844	0.977785	0.960402	0.986258	1.026444		
77-114	0.998	1.09	0.997	1.17	1.036938	0.954739	0.974334	1.046933	0.990229		
117-136	0.998	1.05	0.998	1.15	1.004375	0.983261	1.006525	1.020377	0.985939		
137-156	0.994	1.14	0.999	1.14	0.948342	1.069402	1.010353	0.990307	0.985487		
157-176	0.991	0.95	0.997	1.11	0.975089	1.038772	1.026315	0.936916	1.026725		
178-196	0.999	1.04	0.994	1.04	1.050179	0.953885	0.989916	0.966631	1.043233		
197-216	0.999	1.04	0.999	1.04	1.031062	0.987239	0.973101	0.971135	1.039576		
217-235	0.999	1.05	0.999	1.14	0.982381	1.0201	1.000259	1.010944	0.98682		
236-254	0.994	1.07	0.999	1.15	0.967439	1.090629	0.945079	0.985232	1.017872		
255-273	0.999	1.03	0.998	1.19	0.977376	1.046748	0.986409	0.982004	1.009081		
274-281	0.999	1.05	0.999	1.16	1.013186	0.998758	0.963761	1.025474	0.9999		
Repeat 1	0.997	1.12	0.999	1.2	0.967511	1.012821	1.031828	1.061084	0.945251		
Repeat 2	0.999	1.06	0.999	1.14	1.012162	1.002702	0.964848	1.015235	1.005894		
Repeat 3	0.998	1.06	0.998	1.14	1.009873	0.996318	1.022004	0.996458	0.992727		
Repeat 4	0.998	1.09	0.998	1.16	1.042169	0.961994	0.968281	1.017465	1.012438		
Repeat 5	0.999	1.08	0.999	1.15	1.006242	1.003559	0.980015	1.004836	1.005602		
Repeat 6	0.995	1.02	0.998	1.16	0.981617	1.056847	0.9646	0.980621	1.019055		
Average	0.997263	1.055789474	0.998158	1.144736842	1.001792	1.008861	0.987765	1.000127	1.004568	Average	1.000623
										CV	0.029097

Table 2: Summary of the T/S ratio values for all of the standards in each run of the mTL and CSA-AKI experiment. All standards should have a value of 1.0 measured with 100% accuracy. The Average overall inter-assay CV value of all of the standards in all of the runs was 2.91%.

Appendix E: Normality test results

	Normally distributed		Combined
	AKI	No AKI	
Length of post-op stay	Not normal	Not normal	Not normal
Age	Not normal	Not normal	Not normal
BMI	Normal	Not normal	Not normal
Extubation day	Not normal	Not normal	Not normal
Vasopressor day	Not normal	Not normal	Not normal
Inotrope day	Not normal	Not normal	Not normal
1 st Hb in ITU	Normal	Normal	Normal
UO 1 st 12 hours	Normal	Not normal	Not normal
Pre WCC	Normal	Not normal	Not normal
Pre INR	Not normal	Not normal	Not normal
Pre APTT	Not normal	Not normal	Not normal
Pre CRP	Not normal	Not normal	Not normal
D1 CRP	Not normal	Not normal	Not normal
D2 CRP	Normal	Not normal	Not normal
D3 CRP	Normal	Normal	Not normal
Pre Hb	Normal	Not normal	Not normal
D1 Hb	Normal	Not normal	Not normal
Hb Diff	Normal	Not normal	Not normal
Bypass time	Not normal	Not normal	Not normal
Xclamp time	Not normal	Not normal	Not normal
Euroscore 2	Not normal	Not normal	Not normal
Log EuroSCORE	Not normal	Not normal	Not normal
T/S ratio	Normal	Not normal	Not normal

Table 1: Summary of Normality tests for continuous variables for population used in Telomere length experiment (N=254). Shapiro-Wilks normality tests were calculated for the dataset as a whole and separately for the two cohorts; AKI and No-AKI.

	Normally distributed		Combined
	AKI	No AKI	
Age	Not normal	Not normal	Not normal
Predicted age	Normal	Not normal	Not normal
AMAR	Normal	Not normal	Not normal
Delta Age	Normal	Not normal	Not normal

Table 2: Additional normality tests for the DNAm cohort. Shapiro-Wilks normality tests were calculated for the dataset as a whole and separately for the two cohorts; AKI and No-AKI.

Appendix F: Propensity matched analysis of mTL and CSA-AKI

Pair	Study No.	PODDAYS	AGE	GENDER	ETHNIC	OP	DM	LVEF	AF	sCR-PRE	AKI	BYPASS TIME	EUSCORE	BMI	SCORE
1	73	11.24	61	1	1	1	0	1	0	88	1	72	2	30.8113	0.06584381
1	58	6.78	68	1	1	2	0	1	0	84	0	96	4	29.9836	0.06682701
2	191	10.1	56	1	2	5	0	1	0	60	1	76	2	21.304	0.08283217
2	193	10.31	73	2	1	6	0	1	0	47	0	141	9	25.7778	0.08250884
3	147	6.29	56	1	1	5	0	1	0	44	1	89	2	30.0947	0.08667486
3	253	6.99	55	1	1	1	0	1	0	82	0	99	2	29.8028	0.08645776
4	202	8	79	2	1	2	0	1	0	83	1	105	7	33.3109	0.08726834
4	184	6.21	76	1	1	5	0	1	0	83	0	62	6	26.6749	0.08728066
5	197	6.06	78	1	1	1	0	1	0	84	1	80	4	26.8544	0.09473302
5	241	5.38	57	2	1	1	0	3	0	54	0	71	2	26.8977	0.0942969
6	234	6.34	69	1	1	2	0	1	1	82	1	80	4	32.6048	0.1021873
6	248	6.22	35	1	6	5	0	1	0	72	0	127	5	22.2222	0.1009649
7	21	9.17	71.8	1	2	1	0	1	0	94	1	90	3	27.7634	0.1121
7	156	6.17	78	1	1	1	0	2	1	95	0	38	6	31.6032	0.1127396
8	220	6.31	48	1	1	1	0	1	0	79	1	126	0	36.5714	0.1260039
8	96	6.17	48	1	1	1	1	1	0	90	0	78	1	26.2917	0.1265762
9	158	60.42	79	2	1	6	0	1	0	69	1	156	8	29.4078	0.1495878
9	37	6.35	86.7	2	1	5	0	1	0	77	0	97	10	32.6531	0.1493701

10	242	9.25	22	2	1	8	0	1	0	74	1	151	3	19.6506	0.1589347
10	100	4.42	61	1	1	1	1	2	0	74	0	68	1	37.2907	0.1584779
11	125	7.33	48	1	3	5	0	1	1	104	1	74	2	26.8817	0.173779
11	178	20.15	72	2	2	1	1	1	0	98	0	75	6	19.9219	0.1722029
12	145	8.08	76	1	2	1	1	1	0	100	1	91	8	31.6406	0.1749929
12	70	6.12	69	1	2	4	1	1	0	65	0	91	4	22.9854	0.1752035
13	187	15.33	37	2	1	6	0	2	0	87	1	187	4	38.2934	0.1838453
13	18	6.16	75	2	4	1	1	2	0	74	0	63	4	30.4076	0.1846173
14	252	13.13	72	1	2	2	1	1	0	80	1	117	5	32.7449	0.1852779
14	54	5.38	81	2	1	1	1	1	0	60	0	88	6	30.5469	0.1850721
15	155	7.29	79	1	2	1	0	2	0	94	1	106	5	25.2174	0.1910897
15	238	6.13	55	1	2	1	1	1	0	93	0	91	0	29.4029	0.1940985
16	192	8.19	83	1	2	4	1	1	0	65	1	99	8	19.433	0.2014911
16	110	6.38	67	2	1	1	0	1	1	53	0	151	3	164	0.2004985
17	228	13.12	87	1	1	5	0	1	1	104	1	62	8	26.5338	0.2126732
17	40	72.01	77.6	2	1	5	0	1	1	126	0	55	7	35.4917	0.2098464
18	45	7.09	74.2	2	1	5	0	1	1	74	1	76	6	23.2434	0.2157771
18	134	15.25	69	2	1	5	1	1	0	60	0	86	5	31.1634	0.2194067
19	262	7.19	66	1	2	1	1	1	0	94	1	93	2	26.6436	0.2214391
19	55	15.16	77	1	2	1	0	1	0	103	0	134	5	29.7143	0.2222452
20	140	7.17	66	1	1	1	0	2	1	68	1	96	2	28.2828	0.2382479
20	189	5.11	71	1	1	1	0	1	1	67	0	109	3	22.8571	0.236327
21	168	9.15	66	1	6	1	1	1	0	98	1	97	2	27.1416	0.2395645

21	59	11.38	68	1	6	1	0	2	1	88	0	99	5	30.4705	0.2365149
22	165	6.29	37	1	1	5	0	1	0	90	1	174	5	22.2041	0.24338
22	103	7.41	63	1	1	6	0	1	1	60	0	170	6	26.7299	0.2406059
23	257	7.12	64	1	2	1	0	1	1	108	1	100	2	25.9645	0.2476401
23	175	4.99	53	1	1	1	0	2	0	98	0	137	0	27.4286	0.2528579
24	274	8.13	83	1	1	1	0	1	1	112	1	90	5	31.25	0.2547375
24	169	7	72	1	2	2	1	2	0	109	0	112	6	27.7551	0.2537259
25	136	7.2	72	1	6	5	1	1	0	86	1	102	7	31.2213	0.2679744
25	109	8.35	65	2	2	5	1	1	0	117	0	87	6	34.9277	0.2691322
26	104	6	68	2	1	5	1	2	0	92	1	73	5	31.139	0.277572
26	264	37.94	70	1	1	1	1	3	0	74	0	109	8	27.4286	0.281325
27	94	6.29	61	1	2	1	1	1	0	130	1	103	2	24.977	0.2894116
27	150	5.19	76	2	1	1	1	2	0	146	0	74	6	37.3333	0.2907817
28	243	12.18	62	1	2	1	1	2	1	105	1	80	6	25.7117	0.3145462
28	277	5.57	69	1	5	1	0	1	1	81	0	123	2	26.7299	0.3118661
29	269	6.33	70	1	1	1	0	1	1	111	1	119	3	25.344	0.3379006
29	131	5.21	81	2	1	5	1	1	0	90	0	112	10	30.8185	0.3353188
30	171	6.38	49	1	1	1	1	3	1	82	1	90	3	38.4243	0.3496264
30	114	10.08	62	1	1	6	0	2	1	98	0	185	10	30.6689	0.3413568
31	196	22.33	74	1	6	1	1	2	0	74	1	121	4	26.7949	0.3605377
31	142	6.35	51	1	1	5	1	2	1	63	0	87	3	31.4627	0.359803
32	132	7.14	61	2	2	1	1	2	0	78	1	136	4	32.4444	0.3783121
32	118	8.38	24	2	1	5	0	2	1	61	0	195	9	32.4219	0.371208

33	35	8.2	63.2	1	3	2	0	2	0	83	1	204	4	27.9904	0.3822599
33	225	10.15	72	2	1	4	0	2	1	73	0	151	10	24.3418	0.3886476
34	93	9.35	68	1	1	1	1	2	1	74	1	96	4	30.9917	0.390415
34	6	12.17	77.7	1	1	1	1	1	0	101	0	130	4	31.7901	0.3921399
35	46	68.92	79.7	1	1	1	1	2	1	66	1	87	4	32.9287	0.4041749
35	255	5.9	67	1	2	1	1	1	0	116	0	129	2	25.4028	0.4037426
36	117	8.29	63	1	1	5	0	1	1	66	1	140	3	26.0617	0.4083235
36	216	16.23	79	1	1	3	0	1	1	77	0	127	9	25.7276	0.4108442
37	129	26.25	77	1	1	1	1	2	1	94	1	80	4	22.3863	0.4284192
37	173	8.29	68	2	1	5	0	1	0	85	0	171	5	30.4878	0.4129123
38	31	27.29	68.6	2	1	2	0	1	1	43	1	203	5	34.7078	0.4426372
38	41	17.32	72	1	1	6	0	2	1	77	0	177	6	24.6755	0.4187496
39	146	9.23	41	2	1	5	0	1	0	57	1	225	4	32.05	0.4474889
39	275	10	84	2	1	2	1	2	0	69	0	165	10	23.7812	0.419258
40	198	34.35	63	2	2	5	1	1	1	123	1	93	7	27.1809	0.4576877
40	63	11.36	29	1	1	5	1	1	0	60	0	190	3	23.2317	0.4224392
41	265	17.08	81	1	1	5	1	1	0	197	1	95	9	29.7578	0.4596599
41	270	7.42	83	1	2	2	1	1	1	75	0	136	7	31.2452	0.4252106
42	261	6.31	82	1	1	2	0	1	1	141	1	163	7	36.3636	0.4652047
42	176	5.01	64	1	1	1	1	1	1	83	0	109	1	26.4721	0.4361532
43	113	6.36	63	1	1	6	0	2	0	98	1	241	7	34.5581	0.4661489
43	205	7.1	79	1	1	5	0	1	1	98	0	129	6	32.7449	0.4482423
44	11	8.42	77.8	2	1	5	0	1	1	64	1	153	8	30.0781	0.4746976

44	71	5.27	62	1	1	5	0	1	1	84	0	145	3	31.6735	0.4516594
45	8	8.35	70.5	2	1	1	1	2	1	71	1	130	5	20.3428	0.5816468
45	60	7.36	80	1	1	2	0	1	1	91	0	191	7	27.0416	0.4921081
46	76	38.75	53	1	3	8	0	1	0	122	1	220	5	36.2902	0.5867481
46	120	15.99	79	1	1	2	0	3	1	88	0	173	9	23.8624	0.5149401
47	181	26.29	77	1	1	3	0	1	1	110	1	155	9	26.7698	0.5891558
47	137	14.33	33	1	1	8	0	1	0	71	0	254	5	24.9308	0.5281161
48	39	10.14	80.5	2	1	5	1	1	1	113	1	115	8	20.5761	0.6338254
48	2	15.43	69.9	1	2	1	1	2	0	188	0	120	4	27.7671	0.5573435
49	17	42.92	65.3	1	1	8	0	1	0	73	1	329	12	26.8274	0.8437236
49	278	5.08	75	1	1	5	1	1	1	128	0	112	6	24.281	0.620265
50	162	17	65	1	1	8	0	1	0	107	1	314	12	23.2203	0.8464461
50	151	11.47	64	1	1	1	1	1	1	94	0	150	1	31.1419	0.633777
51	163	68.33	79	2	1	8	0	1	1	53	1	301	10	29.6427	0.9185391
51	244	15.23	78	1	2	1	0	1	1	144	0	187	4	22.0386	0.7250457

Table 1: Summary of data used to develop Propensity score and matched cohorts. PODAYS = Number of post-operative days; Op = type of operation performed (e.g. CABG or valve); DM = Diabetes Mellitus; LVEF = Left Ventricular Ejection Fraction; sCr-PRE = Pre-operative serum creatinine; AKI = acute kidney injury; Bypass Time = total time spent on cardiopulmonary bypass; EUSCORE = Logistic EuroSCORE; BMI = Body Mass Index.

Appendix G: Raw data values for STELA Analysis

Study ID	Number of values	Minimum	25% Percentile	Median	75% Percentile	Maximum	Mean	Std. Deviation	Std. Error of Mean	Lower 95% CI of mean	Upper 95% CI of mean	Sum
58	52	0.529	3.586	6.421	9.165	15.6	6.62	3.454	0.479	5.658	7.582	344.2
73	24	1.976	3.151	3.539	4.179	5.323	3.605	0.7798	0.1592	3.275	3.934	86.51
193	10	2.918	3.126	4.687	5.93	8.511	4.899	1.81	0.5722	3.604	6.193	48.99
191	33	1.209	4.048	5.89	6.811	8.687	5.303	2.023	0.3522	4.585	6.02	175
253	41	1.257	3.761	4.858	6.174	8.641	4.959	1.743	0.2722	4.409	5.509	203.3
147	21	1.847	5.123	6.594	7.424	12.34	6.311	2.115	0.4616	5.348	7.273	132.5
241	37	1.505	3.679	5.341	6.894	11.36	5.445	2.207	0.3628	4.709	6.18	201.5
197	48	1.466	3.371	4.284	5.952	8.714	4.644	1.621	0.2339	4.173	5.115	222.9
248	36	2.732	5.011	6.402	7.852	10.43	6.497	2.063	0.3438	5.799	7.195	233.9
234	32	0.204	3.174	4.408	5.907	8.927	4.701	2.107	0.3724	3.941	5.46	150.4
100	54	2.376	3.409	4.811	6.861	9.965	5.247	2.112	0.2874	4.671	5.824	283.4
242	53	1.371	3.517	5.104	6.354	10.09	5.075	1.976	0.2715	4.53	5.62	269
184	40	1.932	3.198	4.421	5.607	10.27	4.734	2.007	0.3174	4.092	5.376	189.4
202	30	2.378	3.696	4.429	5.516	6.566	4.555	1.119	0.2043	4.137	4.973	136.7
71	30	3.009	4.208	5.595	6.943	10.69	5.808	1.951	0.3562	5.079	6.536	174.2
11	34	1.405	2.864	3.538	4.508	5.855	3.693	1.116	0.1914	3.304	4.083	125.6
2	19	1.016	3.733	4.664	7.361	10.53	5.037	2.386	0.5474	3.887	6.187	95.7
39	47	1.747	3.707	5.207	6.693	14.17	5.708	2.67	0.3894	4.925	6.492	268.3
134	115	1.805	3.767	4.902	6.027	9.789	4.975	1.565	0.1459	4.686	5.264	572.1
45	71	2.004	3.8	5.22	7.148	15.27	5.837	2.596	0.3081	5.223	6.452	414.4
244												
163	98	1.247	3.829	4.716	5.886	11.59	4.959	1.878	0.1897	4.583	5.336	486

103	67	1.079	3.205	4.37	5.503	13.69	4.589	2.265	0.2768	4.036	5.141	307.4
175	56	0.886	3.098	4.26	5.854	9.16	4.479	1.918	0.2564	3.965	4.993	250.8
165	83	1.588	4.529	5.902	7.985	15.79	6.375	2.758	0.3027	5.773	6.978	529.2

Appendix H: Qiagen experiment into mTL measurement and association with age

The Telomere as a Marker for Aging



James Qin, Applications Laboratory, QIAGEN Sciences, Inc., Germantown, MD
Rodrigo Calado, NHLBI, NIH, Bethesda, MD

The following presentation describes applications that are currently under development and are not commercially available. Therefore, they are presented here only for research purposes. They are not intended for diagnostic use.

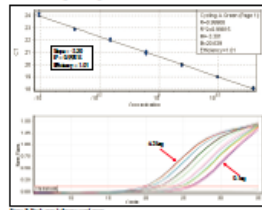
Introduction

Telomeres are the ends of linear chromosomes and are composed of tandem hexameric nucleotide repeats of the six-nucleotide sequence, 5'-TTAGGG-3', coated by several proteins, which are collectively termed shelterin. The main function of telomeres is to protect the natural ends of chromosomes from being recognized as damaged DNA, hence contributing to chromosomal stability. Due to DNA polymerase's inability to fully duplicate the DNA strands at their extremities, telomeres shorten with each cell division and as a consequence telomeres shorten with aging. To maintain telomeres, cells with highly proliferative capacity express telomerase, a reverse transcriptase enzyme that uses RNA template to elongate the 3' end of the leading strand of telomeres, thus maintaining their length. Some genetic diseases are caused by deficient telomerase function in which mutations in the telomerase complex are etiologic. In these diseases, telomeres are extremely short and patients present the clinical manifestations of cell senescence and chromosomal instability. Patients with telomerase mutations usually present bone marrow failure and an increased propensity for leukemia development.

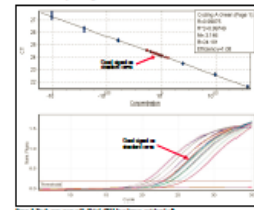
Thus, precise, reproducible, and simple methods aiming to measure telomere length are highly desired both in the laboratory and in clinical practice. Three major methods are available today in the laboratory: Southern blot, which is the gold standard method, but is labor intensive, time consuming, and requires large DNA quantities; flow-FISH, which combines flow cytometry and fluorescence in situ hybridization, but is labor intensive and requires intact cells for analysis; and quantitative PCR (qPCR), which requires low quantities of DNA, but the method until today requires several reagents to stabilize the reaction in a "laboratory-developed" mastermix. Here we describe a simplified and automated qPCR method to measure telomere length using standardized, commercially available chemistry. The method is demonstrated to be highly reproducible and accurate for human peripheral cells.

Method Part II – Reference Assay

Method Design – Single Gene Standard Curve



Human Samples Against a Standard Curve



Normal Population Data: Linear Regression between Age and Telomere Length

Telomere Length in Healthy Individuals

Data was obtained by quantitative PCR using a Rotor-Gene® Q real-time instrument. Signals from the telomere assay were normalized to a single gene reference (T/S ratio) before comparing to age information. Data shows good linear regression with $R^2=0.4642$ and p-value <0.0001 suggesting there is broad variation around the mean but telomere length is still highly age-dependent.

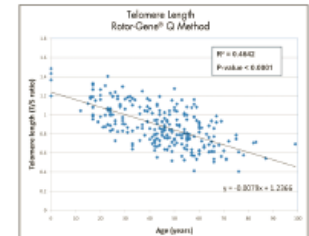
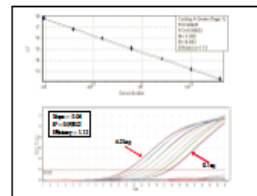


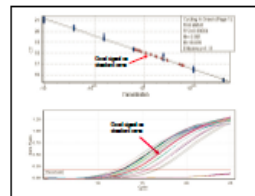
Figure 3. Telomere length of healthy individuals as a function of age. The data shows a good linear regression between telomere length and age. The telomere length is still highly age-dependent.

Method Part I – Telomere Assay

Method Design – Telomere Assay Standard Curve



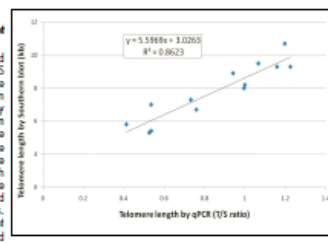
Human Samples Against a Standard Curve



Method Validation

Telomere Length Correlation between Southern Blot and qPCR

C_t values from the telomere assay were normalized to the single gene reference assay using the T/S ratio to determine telomere length. The telomere length (T/S ratio) from real-time PCR was then correlated against telomere length as determined by Southern Blot analysis. The telomere length (x) from each sample was based on the telomere to single copy gene ratio (T/S ratio) and was based on the calculation of the ΔC_t [$C_t(\text{telomere}) - C_t(\text{reference})$]. Telomere length was expressed as a relative T/S ratio, which was normalized to the average T/S ratio of the reference sample [$2^{(C_{t,ref} - C_{t,sample})}$] for all standard curves, reference samples, and validation samples. In order to make results comparable from different assay runs, the results of each run were approved only if the relative T/S ratio of the validation reference sample fell within a 3% variation.



Summary

This quantitative PCR method was demonstrated to be highly accurate, reproducible, and simple for human peripheral cells. The assay has enhanced sensitivity using a reaction volume of 25 µl with DNA at 1 ng/ assay, and has a good correlation of $R^2 = 0.99064$, slope = -3.081 and amplification efficiency at 100%. Furthermore, the real-time PCR assay takes only 47 min for up to 100 telomere targets.

We evaluated this assay with 299 healthy human subjects of varying ages ranging from 0 (cord blood) to 99 years old. The results are positive with an inverse correlation between telomere length and age. The telomere length was measured in 13 samples using the gold standard Southern Blot method and the new quantitative PCR method (correlation of $R^2=0.8623$), which is a significantly higher correlation than was previously described (Cawthon NAG 2002).

Descriptor	qPCR	Southern Blot
No. samples tested	299	13
Total time per process Analyzed	90 min	7 days
Quantity: Sample (DNA) required	1 ng	200 ng

This method has potential applications in a clinical setting for the diagnosis of age-related telomere diseases and conditions such as: muscular degeneration (vision loss), atherosclerosis (hardening of arteries by plaque), impaired wound healing, heart disease, gray hair, and wrinkles.

It provides investigators with an easy-to-use technique for addressing the full extent and significance of telomere shortening in age-related telomere conditions, diseases and in the tumorigenic process. This fast, sensitive method is a powerful tool to study genomic instability, heart disease, cancer progression, and cancer therapy.

Qiagen, Rotor-Gene, and the logo are trademarks of Qiagen. All other trademarks are the property of their respective owners.

Activate Windows
Go to Settings to activate Windows.

Reproduced with permission from Qiagen

Appendix I: CpG probes used in DNAm aging model

450K ProbeID

cg22512670	cg24079702
cg01789150	cg26344233
cg08169949	cg06907053
cg25410668	cg22016779
cg04400972	Cg20787219
cg13898106	cg18448426
cg25256723	cg08415592
cg16054275	cg03607117
cg22796704	cg05121480
cg19935065	cg00481951
cg23744638	cg00457403
cg04940570	cg02650266
cg11067179	cg08234504
cg22213242	cg22736354
cg06419846	cg26718511
cg05496363	cg06493994
cg09843573	cg05675331
cg02046143	cg16806794
cg03032497	cg08540945
cg14692377	cg16219603
cg06874016	cg16419235
cg14556683	cg16072688
cg02085953	cg11610346
cg06639320	
cg22454769	

Appendix J: DNA methylation senescence markers: beta values and coded data

Study ID	SELP	CASP14	CASR	KRTAP13_3	SELP Passage No.			CASP Passage No.			CASR Passage No.			KRTAP13 Passage No.			Composite Passage No.		
					5	10	15	5	10	15	5	10	15	5	10	15	5	10	15
1	88.2883	82.6087	12.9181	81.9672	0	0	0	0	0	0	0	0	0	0	0	0	0	0	0
2	59.5420	75.0000	24.6879	71.4286	1	1	0	0	0	0	1	1	0	0	0	0	2	2	0
3	42.3841	70.0000	31.3090	30.5709	1	1	1	0	0	0	1	1	1	1	1	1	3	3	3
4	37.0909	91.6667	28.2716	87.8151	1	1	1	0	0	0	1	1	0	0	0	2	2	1	
5	86.4000	64.2857	22.4764	75.3769	0	0	0	0	0	0	1	0	0	0	0	1	0	0	
6	70.9677	80.0000	17.9520	74.9077	1	0	0	0	0	0	1	0	0	0	0	2	0	0	
7	56.0000	60.0000	15.9292	80.8081	1	1	0	0	0	0	0	0	0	0	0	1	1	0	
8	74.9263	89.2857	24.8563	60.6965	0	0	0	0	0	0	1	1	0	1	0	2	1	0	
9	42.0195	87.3239	9.7525	86.4583	1	1	1	0	0	0	0	0	0	0	0	1	1	1	
10	84.6154	75.0000	24.5122	69.9605	0	0	0	0	0	0	1	1	0	0	0	1	1	0	
11	57.1930	88.8889	20.6385	54.0107	1	1	0	0	0	0	1	0	0	1	1	3	2	0	
12	50.1873	81.8182	18.5539	83.7662	1	1	1	0	0	0	1	0	0	0	0	2	1	1	
13	71.4286	55.5556	32.2745	71.3693	0	0	0	0	0	0	1	1	1	0	0	1	1	1	
14	69.4656	72.2222	21.0775	84.7584	1	0	0	0	0	0	1	0	0	0	0	2	0	0	
15	70.1149	77.1429	19.2797	66.4234	1	0	0	0	0	0	1	0	0	0	0	2	0	0	
16	72.4566	82.6087	13.3261	91.1032	0	0	0	0	0	0	0	0	0	0	0	0	0	0	

17	77.0950	85.7143	11.7647	87.4074	0	0	0	0	0	0	0	0	0	0	0	0	0	0	0
18	54.5741	85.4167	20.0201	47.3333	1	1	1	0	0	0	1	0	0	1	1	0	3	2	1
19	75.5952	43.4783	20.1780	35.2542	0	0	0	1	0	0	1	0	0	1	1	1	3	1	1
20	71.5789	53.8462	20.3065	85.9091	0	0	0	0	0	0	1	0	0	0	0	0	1	0	0
21	58.3942	81.8182	17.6172	72.3636	1	1	0	0	0	0	1	0	0	0	0	0	2	1	0
22	60.9677	79.3103	22.6501	34.5455	1	1	0	0	0	0	1	0	0	1	1	1	3	2	1
23	83.0588	94.4444	13.4454	57.3460	0	0	0	0	0	0	0	0	0	1	0	0	1	0	0
24	35.8255	93.9394	25.4144	78.7097	1	1	1	0	0	0	1	1	0	0	0	0	2	2	1
25	85.2713	68.2927	24.9400	85.5670	0	0	0	0	0	0	1	1	0	0	0	0	1	1	0
26	94.9555	60.0000	17.3913	74.4444	0	0	0	0	0	0	1	0	0	0	0	0	1	0	0
27	63.6628	53.8462	9.7649	70.8223	1	0	0	0	0	0	0	0	0	0	0	0	1	0	0
28	50.5848	66.6667	17.4283	65.3137	1	1	1	0	0	0	1	0	0	0	0	0	2	1	1
29	66.1184	37.5000	28.2609	86.1190	1	0	0	1	1	0	1	1	0	0	0	0	3	2	0
30	58.6667	62.5000	15.4856	75.2212	1	1	0	0	0	0	0	0	0	0	0	0	1	1	0
31	70.2174	55.0000	15.1461	49.3197	1	0	0	0	0	0	0	0	0	1	1	0	2	1	0
32	41.4110	93.7500	21.6279	93.0514	1	1	1	0	0	0	1	0	0	0	0	0	2	1	1
33	67.5841	68.7500	24.1119	61.1111	1	0	0	0	0	0	1	1	0	1	0	0	3	1	0
35	58.9251	65.5172	21.6073	57.4132	1	1	0	0	0	0	1	0	0	1	0	0	3	1	0
36	79.4964	83.3333	7.7766	71.0526	0	0	0	0	0	0	0	0	0	0	0	0	0	0	0
37	65.6371	91.3043	22.2343	83.8951	1	0	0	0	0	0	1	0	0	0	0	0	2	0	0

38	77.6860	69.2308	27.5613	84.4371	0	0	0	0	0	0	1	1	0	0	0	0	1	1	0
39	50.1639	66.6667	31.6779	82.9630	1	1	1	0	0	0	1	1	1	0	0	0	2	2	2
40	72.6073	71.8750	24.5192	70.7904	0	0	0	0	0	0	1	1	0	0	0	0	1	1	0
41	49.0463	60.0000	24.9677	75.7143	1	1	1	0	0	0	1	1	0	0	0	0	2	2	1
42	75.0769	79.3103	32.4427	76.2918	0	0	0	0	0	0	1	1	1	0	0	0	1	1	1
43	51.1706	80.0000	18.5430	90.0568	1	1	1	0	0	0	1	0	0	0	0	0	2	1	1
44	65.3386	80.0000	47.8426	59.4737	1	0	0	0	0	0	1	1	1	1	0	0	3	1	1
45	86.2295	65.3846	21.4470	73.0519	0	0	0	0	0	0	1	0	0	0	0	0	1	0	0
46	48.1343	81.2500	23.7515	87.2404	1	1	1	0	0	0	1	0	0	0	0	0	2	1	1
47	85.0000	72.0930	26.3499	36.7698	0	0	0	0	0	0	1	1	0	1	1	1	2	2	1
48	63.0137	81.2500	29.5724	63.0037	1	0	0	0	0	0	1	1	0	1	0	0	3	1	0
49	57.5843	77.2727	13.8232	55.4545	1	1	0	0	0	0	0	0	0	1	0	0	2	1	0
50	84.2491	75.0000	39.6783	40.4332	0	0	0	0	0	0	1	1	1	1	1	1	2	2	2
51	56.9930	45.0000	11.7073	73.4375	1	1	0	1	0	0	0	0	0	0	0	0	2	1	0
52	74.9333	72.7273	28.2332	68.7285	0	0	0	0	0	0	1	1	0	0	0	0	1	1	0
53	40.5512	100.0000	18.8082	59.6026	1	1	1	0	0	0	1	0	0	1	0	0	3	1	1
54	45.2282	100.0000	32.0755	81.1475	1	1	1	0	0	0	1	1	1	0	0	0	2	2	2
55	85.0515	50.0000	5.8989	55.0926	0	0	0	0	0	0	0	0	0	1	0	0	1	0	0
56	66.6667	100.0000	16.1220	69.9115	1	0	0	0	0	0	0	0	0	0	0	0	1	0	0
57	72.2449	33.3333	20.8437	92.5926	0	0	0	1	1	1	1	0	0	0	0	0	2	1	1

58	70.2509	41.1765	26.7267	55.5102	1	0	0	1	0	0	1	1	0	1	0	0	4	1	0
59	84.4920	54.5455	10.0000	66.0819	0	0	0	0	0	0	0	0	0	0	0	0	0	0	0
60	88.4170	71.4286	22.6064	70.2128	0	0	0	0	0	0	1	0	0	0	0	0	1	0	0
61	51.5152	100.0000	24.4681	66.1130	1	1	1	0	0	0	1	1	0	0	0	0	2	2	1
62	57.7143	50.0000	37.4286	87.4419	1	1	0	0	0	0	1	1	1	0	0	0	2	2	1
63	88.5714	80.0000	21.7172	71.3636	0	0	0	0	0	0	1	0	0	0	0	0	1	0	0
64	92.6108	NA	17.9558	77.9762	0	0	0	0	0	0	1	0	0	0	0	0	1	0	0
65	71.1656	75.0000	30.9406	87.6667	0	0	0	0	0	0	1	1	0	0	0	0	1	1	0
66	71.2919	90.0000	17.2840	56.2738	0	0	0	0	0	0	1	0	0	1	0	0	2	0	0
67	85.8896	66.6667	44.8505	79.9331	0	0	0	0	0	0	1	1	1	0	0	0	1	1	1
68	64.2857	100.0000	5.4348	75.5725	1	0	0	0	0	0	0	0	0	0	0	0	1	0	0
69	72.0000	40.0000	3.5047	75.9690	0	0	0	1	1	0	0	0	0	0	0	0	1	1	0
70	58.6826	100.0000	39.2097	58.7234	1	1	0	0	0	0	1	1	1	1	0	0	3	2	1
71	90.4255	100.0000	8.4433	77.9783	0	0	0	0	0	0	0	0	0	0	0	0	0	0	0
72	61.1940	25.0000	29.9401	56.2500	1	1	0	1	1	1	1	1	0	1	0	0	4	3	1
73	23.3010	100.0000	3.5370	62.7551	1	1	1	0	0	0	0	0	0	1	0	0	2	1	1
74	46.5306	72.7273	23.4637	89.2593	1	1	1	0	0	0	1	0	0	0	0	0	2	1	1
75	82.0513	100.0000	16.6667	56.8000	0	0	0	0	0	0	0	0	0	1	0	0	1	0	0
76	81.5094	75.0000	32.1875	66.3462	0	0	0	0	0	0	1	1	1	0	0	0	1	1	1
77	74.0741	66.6667	23.4940	52.0161	0	0	0	0	0	0	1	0	0	1	1	0	2	1	0

78	49.7382	100.0000	39.8625	91.6667	1	1	1	0	0	0	1	1	1	0	0	0	2	2	2
87	61.7021	100.0000	24.5614	62.3853	1	1	0	0	0	0	1	1	0	1	0	0	3	2	0
90	55.5102	NA	41.7755	58.2569	1	1	0	0	0	0	1	1	1	1	0	0	3	2	1
91	39.0681	41.6667	28.1095	97.5845	1	1	1	1	0	0	1	1	0	0	0	0	3	2	1
92	53.9007	83.3333	13.5135	84.3602	1	1	1	0	0	0	0	0	0	0	0	0	1	1	1
93	81.2903	66.6667	24.3827	46.1165	0	0	0	0	0	0	1	1	0	1	1	0	2	2	0
94	57.2917	50.0000	19.6552	82.8571	1	1	0	0	0	0	1	0	0	0	0	0	2	1	0
95	59.8870	11.1111	23.9264	68.0180	1	1	0	1	1	1	1	0	0	0	0	0	3	2	1
96	88.7255	100.0000	34.7985	70.5882	0	0	0	0	0	0	1	1	1	0	0	0	1	1	1
98	70.1657	100.0000	12.4646	77.2894	1	0	0	0	0	0	0	0	0	0	0	0	1	0	0
100	50.0000	50.0000	21.0654	65.9389	1	1	1	0	0	0	1	0	0	0	0	0	2	1	1
103	77.6892	100.0000	42.7807	74.1803	0	0	0	0	0	0	1	1	1	0	0	0	1	1	1
104	75.2988	100.0000	17.0792	66.3830	0	0	0	0	0	0	1	0	0	0	0	0	1	0	0
108	67.0391	88.8889	10.0000	77.8210	1	0	0	0	0	0	0	0	0	0	0	0	1	0	0
109	66.6667	100.0000	29.4118	56.5421	1	0	0	0	0	0	1	1	0	1	0	0	3	1	0
110	83.6735	100.0000	9.1873	84.7973	0	0	0	0	0	0	0	0	0	0	0	0	0	0	0
113	62.5806	100.0000	15.2727	72.9858	1	1	0	0	0	0	0	0	0	0	0	0	1	1	0
114	64.8649	100.0000	26.5116	75.3012	1	0	0	0	0	0	1	1	0	0	0	0	2	1	0
117	85.7143	0.0000	15.6069	61.3527	0	0	0	1	1	1	0	0	0	1	0	0	2	1	1
118	60.7477	77.7778	16.7123	52.2388	1	1	0	0	0	0	0	0	0	1	1	0	2	2	0

119	76.9634	66.9903	15.3094	89.1608	0	0	0	0	0	0	0	0	0	0	0	0	0	0	
120	68.6411	49.2308	26.1538	69.9115	1	0	0	0	0	0	1	1	0	0	0	0	2	1	0
121	51.7007	74.3590	5.4487	81.9188	1	1	1	0	0	0	0	0	0	0	0	0	1	1	1
122	76.3265	64.2857	34.1176	53.2468	0	0	0	0	0	0	1	1	1	1	1	0	2	2	1
123	81.3008	77.5000	38.7812	89.2241	0	0	0	0	0	0	1	1	1	0	0	0	1	1	1
124	62.4561	85.7143	21.9298	53.9171	1	1	0	0	0	0	1	0	0	1	1	0	3	2	0
125	42.2500	74.5763	44.6224	58.3596	1	1	1	0	0	0	1	1	1	1	0	0	3	2	2
126	95.7020	80.0000	28.0423	81.4672	0	0	0	0	0	0	1	1	0	0	0	0	1	1	0
127	49.6732	81.8182	20.1863	76.7857	1	1	1	0	0	0	1	0	0	0	0	0	2	1	1
129	58.8235	84.6154	29.4294	76.5125	1	1	0	0	0	0	1	1	0	0	0	0	2	2	0
130	90.4000	86.8852	17.7083	68.1159	0	0	0	0	0	0	1	0	0	0	0	0	1	0	0
131	63.8095	71.4286	20.4301	53.8136	1	0	0	0	0	0	1	0	0	1	1	0	3	1	0
132	64.6209	85.7143	19.2802	55.7994	1	0	0	0	0	0	1	0	0	1	0	0	3	0	0
133	79.8587	23.4375	35.9621	62.5954	0	0	0	1	1	1	1	1	1	1	0	0	3	2	2
134	67.2269	59.1837	24.8538	58.9041	1	0	0	0	0	0	1	1	0	1	0	0	3	1	0
135	46.6667	87.8049	43.4426	46.9880	1	1	1	0	0	0	1	1	1	1	1	0	3	3	2
136	24.3446	77.7778	8.3333	74.4337	1	1	1	0	0	0	0	0	0	0	0	0	1	1	1
137	65.9919	63.6364	15.4839	79.5539	1	0	0	0	0	0	0	0	0	0	0	0	1	0	0
138	71.0084	73.6842	17.8182	74.0947	0	0	0	0	0	0	1	0	0	0	0	0	1	0	0
139	65.0980	79.1667	16.9675	34.8837	1	0	0	0	0	0	0	0	0	1	1	1	2	1	1

140	70.4319	95.1220	17.7596	74.7082	1	0	0	0	0	0	1	0	0	0	0	0	2	0	0
141	75.3333	60.0000	17.4377	76.2712	0	0	0	0	0	0	1	0	0	0	0	0	1	0	0
142	78.1350	81.2500	13.9818	57.2000	0	0	0	0	0	0	0	0	0	1	0	0	1	0	0
143	67.0695	65.3846	22.7723	77.2989	1	0	0	0	0	0	1	0	0	0	0	0	2	0	0
144	83.8150	27.2727	47.3193	69.1304	0	0	0	1	1	1	1	1	1	0	0	0	2	2	2
145	69.5341	73.1707	19.5846	83.4615	1	0	0	0	0	0	1	0	0	0	0	0	2	0	0
146	60.9756	50.0000	18.4466	89.6104	1	1	0	0	0	0	1	0	0	0	0	0	2	1	0
147	64.9123	33.3333	15.2104	65.1741	1	0	0	1	1	1	0	0	0	0	0	0	2	1	1
148	69.5652	56.2500	57.7406	62.6866	1	0	0	0	0	0	1	1	1	1	0	0	3	1	1
150	56.5371	63.6364	33.5347	65.5797	1	1	0	0	0	0	1	1	1	0	0	0	2	2	1
151	56.5625	68.8889	23.9875	64.6377	1	1	0	0	0	0	1	0	0	1	0	0	3	1	0
152	68.0653	79.4118	24.1192	84.0000	1	0	0	0	0	0	1	1	0	0	0	0	2	1	0
153	75.7669	89.7436	23.0198	58.4677	0	0	0	0	0	0	1	0	0	1	0	0	2	0	0
154	67.5595	89.8305	27.2973	87.3077	1	0	0	0	0	0	1	1	0	0	0	0	2	1	0
155	59.4262	64.2857	38.2671	57.9310	1	1	0	0	0	0	1	1	1	1	0	0	3	2	1
156	62.4434	50.0000	45.1178	74.2105	1	1	0	0	0	0	1	1	1	0	0	0	2	2	1
157	62.6959	72.4138	21.2465	92.4419	1	1	0	0	0	0	1	0	0	0	0	0	2	1	0
158	30.6383	100.0000	37.1094	73.0000	1	1	1	0	0	0	1	1	1	0	0	0	2	2	2
159	29.6758	40.5405	26.2530	46.1538	1	1	1	1	1	0	1	1	0	1	1	0	4	4	1
160	65.0442	75.0000	20.3085	40.6091	1	0	0	0	0	0	1	0	0	1	1	1	3	1	1

161	69.8630	77.2152	20.1893	75.9162	1	0	0	0	0	0	1	0	0	0	0	0	2	0	0
162	59.3137	77.5000	27.6119	91.5789	1	1	0	0	0	0	1	1	0	0	0	0	2	2	0
163	52.7363	64.7059	47.9554	65.6805	1	1	1	0	0	0	1	1	1	0	0	0	2	2	2
164	64.1350	0.0000	16.9492	81.1927	1	0	0	1	1	1	0	0	0	0	0	0	2	1	1
165	72.3333	43.5897	28.3133	82.7381	0	0	0	1	0	0	1	1	0	0	0	0	2	1	0
166	90.8257	45.9459	9.1216	86.4754	0	0	0	1	0	0	0	0	0	0	0	0	1	0	0
167	62.7063	90.1961	3.4946	82.9268	1	1	0	0	0	0	0	0	0	0	0	0	1	1	0
168	67.3653	63.2911	16.9014	59.1928	1	0	0	0	0	0	0	0	0	1	0	0	2	0	0
169	84.9162	73.4266	18.4290	91.6667	0	0	0	0	0	0	1	0	0	0	0	0	1	0	0
171	46.4789	78.7879	19.1729	11.2903	1	1	1	0	0	0	1	0	0	1	1	1	3	2	2
172	77.8169	64.2857	50.7331	90.9483	0	0	0	0	0	0	1	1	1	0	0	0	1	1	1
173	76.4151	62.5000	33.6735	46.9484	0	0	0	0	0	0	1	1	1	1	1	0	2	2	1
174	50.8772	68.9655	29.8611	71.3080	1	1	1	0	0	0	1	1	0	0	0	0	2	2	1
175	90.2913	60.9756	13.8462	75.6458	0	0	0	0	0	0	0	0	0	0	0	0	0	0	0
176	79.4702	35.8974	40.0662	64.8148	0	0	0	1	1	0	1	1	1	1	0	0	3	2	1
178	66.5722	78.0488	27.7778	82.2314	1	0	0	0	0	0	1	1	0	0	0	0	2	1	0
179	48.2353	82.1918	5.5703	94.0000	1	1	1	0	0	0	0	0	0	0	0	0	1	1	1
180	42.3729	80.3279	14.4295	89.7196	1	1	1	0	0	0	0	0	0	0	0	0	1	1	1
181	56.5217	90.6250	22.6190	43.4343	1	1	0	0	0	0	1	0	0	1	1	1	3	2	1
182	55.2870	37.5000	25.2226	80.4255	1	1	0	1	1	0	1	1	0	0	0	0	3	3	0

183	72.2930	83.3333	27.4566	90.2778	0	0	0	0	0	0	1	1	0	0	0	0	1	1	0
184	61.2903	77.7778	10.5572	55.5970	1	1	0	0	0	0	0	0	0	1	0	0	2	1	0
185	81.8182	90.0000	12.8205	53.8860	0	0	0	0	0	0	0	0	0	1	1	0	1	1	0
186	72.5212	76.4706	17.9054	82.9670	0	0	0	0	0	0	1	0	0	0	0	0	1	0	0
187	55.0523	86.1538	12.8713	60.0000	1	1	0	0	0	0	0	0	0	1	0	0	2	1	0
188	32.0132	87.0130	32.1799	82.2967	1	1	1	0	0	0	1	1	1	0	0	0	2	2	2
189	84.8837	44.4444	12.5000	75.5725	0	0	0	1	0	0	0	0	0	0	0	0	1	0	0
190	52.3659	80.8511	21.2418	72.5490	1	1	1	0	0	0	1	0	0	0	0	0	2	1	1
191	41.2844	57.4468	19.5187	53.1250	1	1	1	0	0	0	1	0	0	1	1	0	3	2	1
192	73.1861	80.4878	13.2258	81.3131	0	0	0	0	0	0	0	0	0	0	0	0	0	0	0
193	93.6963	96.0000	14.4118	37.3333	0	0	0	0	0	0	0	0	0	1	1	1	1	1	1
194	76.4557	88.3333	13.7313	84.4106	0	0	0	0	0	0	0	0	0	0	0	0	0	0	0
195	72.8261	80.0000	26.4624	55.0000	0	0	0	0	0	0	1	1	0	1	0	0	2	1	0
196	55.0314	73.3333	12.8358	64.1026	1	1	0	0	0	0	0	0	0	1	0	0	2	1	0
197	71.9008	80.7692	26.9531	77.0898	0	0	0	0	0	0	1	1	0	0	0	0	1	1	0
198	53.3632	31.5789	6.2731	87.5380	1	1	1	1	1	1	0	0	0	0	0	0	2	2	2
200	50.3356	70.2128	30.3226	68.3616	1	1	1	0	0	0	1	1	0	0	0	0	2	2	1
201	59.7173	85.7143	13.8408	85.7616	1	1	0	0	0	0	0	0	0	0	0	0	1	1	0
202	65.2482	71.4286	35.7341	85.2459	1	0	0	0	0	0	1	1	1	0	0	0	2	1	1
203	64.1161	66.6667	17.6282	79.8193	1	0	0	0	0	0	1	0	0	0	0	0	2	0	0

204	62.6214	67.3267	25.6198	71.7791	1	1	0	0	0	0	1	1	0	0	0	0	2	2	0
205	50.1385	77.1429	26.3014	57.8512	1	1	1	0	0	0	1	1	0	1	0	0	3	2	1
206	75.7098	80.0000	29.6296	83.9286	0	0	0	0	0	0	1	1	0	0	0	0	1	1	0
207	62.9032	83.3333	18.5759	88.3333	1	1	0	0	0	0	1	0	0	0	0	0	2	1	0
208	74.8521	86.4865	13.5870	80.6061	0	0	0	0	0	0	0	0	0	0	0	0	0	0	0
209	78.7546	72.0000	40.2439	91.9003	0	0	0	0	0	0	1	1	1	0	0	0	1	1	1
210	56.2500	82.2222	30.8943	67.1554	1	1	0	0	0	0	1	1	0	0	0	0	2	2	0
211	41.7840	50.0000	27.4286	82.6531	1	1	1	0	0	0	1	1	0	0	0	0	2	2	1
212	41.6667	50.0000	30.5842	70.5686	1	1	1	0	0	0	1	1	0	0	0	0	2	2	1
213	61.9048	55.5556	41.9142	67.9245	1	1	0	0	0	0	1	1	1	0	0	0	2	2	1
214	54.9180	95.5556	53.0249	88.8889	1	1	1	0	0	0	1	1	1	0	0	0	2	2	2
215	32.2709	88.8889	8.0128	84.9206	1	1	1	0	0	0	0	0	0	0	0	0	1	1	1
216	60.0000	72.7273	24.0000	75.5656	1	1	0	0	0	0	1	0	0	0	0	0	2	1	0
217	91.5385	64.2857	11.4583	84.4262	0	0	0	0	0	0	0	0	0	0	0	0	0	0	0
218	86.5828	82.1429	17.2577	41.1765	0	0	0	0	0	0	1	0	0	1	1	1	2	1	1
219	80.1386	60.9524	10.1235	93.1880	0	0	0	0	0	0	0	0	0	0	0	0	0	0	0
220	73.7931	68.4211	20.0000	82.5203	0	0	0	0	0	0	1	0	0	0	0	0	1	0	0
221	53.5452	95.9459	18.4080	85.0427	1	1	1	0	0	0	1	0	0	0	0	0	2	1	1
222	62.3482	81.8182	12.4242	75.0000	1	1	0	0	0	0	0	0	0	0	0	0	1	1	0
223	78.2427	22.8571	42.6966	69.2308	0	0	0	1	1	1	1	1	1	0	0	0	2	2	2

224	76.9231	51.6129	40.8935	66.6667	0	0	0	0	0	0	1	1	1	0	0	0	1	1	1
225	50.9434	85.7143	18.9873	46.4516	1	1	1	0	0	0	1	0	0	1	1	0	3	2	1
226	82.3362	71.4286	11.9891	75.4098	0	0	0	0	0	0	0	0	0	0	0	0	0	0	0
227	60.9418	64.8148	6.2500	70.2265	1	1	0	0	0	0	0	0	0	0	0	0	1	1	0
228	60.6272	78.1250	28.2443	58.1498	1	1	0	0	0	0	1	1	0	1	0	0	3	2	0
229	51.9337	94.4444	25.5132	91.7582	1	1	1	0	0	0	1	1	0	0	0	0	2	2	1
230	85.2590	57.5000	5.5556	52.9617	0	0	0	0	0	0	0	0	1	1	0	1	1	0	
231	72.1569	80.0000	18.0000	91.1111	0	0	0	0	0	0	1	0	0	0	0	0	1	0	0
232	49.5677	50.9091	9.0625	54.7120	1	1	1	0	0	0	0	0	1	1	0	2	2	1	
233	43.5556	81.8182	20.5656	76.9022	1	1	1	0	0	0	1	0	0	0	0	0	2	1	1
234	87.1345	47.6190	31.6384	89.4161	0	0	0	0	0	0	1	1	1	0	0	0	1	1	1
235	89.8010	82.6531	25.4808	66.6667	0	0	0	0	0	0	1	1	0	0	0	0	1	1	0
236	76.0116	56.9767	21.4815	70.1754	0	0	0	0	0	0	1	0	0	0	0	0	1	0	0
237	85.0980	92.1053	33.0544	85.6383	0	0	0	0	0	0	1	1	1	0	0	0	1	1	1
238	79.7665	88.8889	27.8884	57.9832	0	0	0	0	0	0	1	1	0	1	0	0	2	1	0
239	55.7078	62.5000	32.9167	84.5890	1	1	0	0	0	0	1	1	1	0	0	0	2	2	1
240	82.7815	54.2857	23.8390	75.6944	0	0	0	0	0	0	1	0	0	0	0	0	1	0	0
241	71.3793	86.6667	27.8810	81.6860	0	0	0	0	0	0	1	1	0	0	0	0	1	1	0
242	75.7106	61.8182	25.4717	83.6120	0	0	0	0	0	0	1	1	0	0	0	0	1	1	0
243	65.7576	80.7692	20.0000	64.1844	1	0	0	0	0	0	1	0	0	1	0	0	3	0	0

244	73.9496	88.1356	22.4490	46.2406	0	0	0	0	0	0	1	0	0	1	1	0	2	1	0
245	71.6475	83.3333	24.6637	55.9028	0	0	0	0	0	0	1	1	0	1	0	0	2	1	0
246	88.7097	77.7778	15.2672	91.0615	0	0	0	0	0	0	0	0	0	0	0	0	0	0	0
247	65.4008	84.6154	18.8596	67.0068	1	0	0	0	0	0	1	0	0	0	0	0	2	0	0
248	63.0996	90.9091	12.1771	94.1176	1	0	0	0	0	0	0	0	0	0	0	0	1	0	0
249	47.3545	86.4865	24.1888	87.0130	1	1	1	0	0	0	1	1	0	0	0	0	2	2	1
250	57.5540	50.0000	21.6216	79.8283	1	1	0	0	0	0	1	0	0	0	0	0	2	1	0
251	83.4951	58.8235	18.1467	64.4068	0	0	0	0	0	0	1	0	0	1	0	0	2	0	0
252	59.4366	85.5556	31.2500	43.4307	1	1	0	0	0	0	1	1	1	1	1	1	3	3	2
253	65.0735	94.4444	15.6716	31.3846	1	0	0	0	0	0	0	0	0	1	1	1	2	1	1
254	78.8194	91.4286	7.6923	67.5000	0	0	0	0	0	0	0	0	0	0	0	0	0	0	0
255	84.1176	63.6364	43.6667	72.2222	0	0	0	0	0	0	1	1	1	0	0	0	1	1	1
256	63.0094	80.4878	18.7500	78.7500	1	0	0	0	0	0	1	0	0	0	0	0	2	0	0
257	74.6429	62.7119	41.4179	82.8313	0	0	0	0	0	0	1	1	1	0	0	0	1	1	1
258	51.6035	85.7143	27.5204	62.3053	1	1	1	0	0	0	1	1	0	1	0	0	3	2	1
259	58.8595	62.0370	48.1675	88.9590	1	1	0	0	0	0	1	1	1	0	0	0	2	2	1
260	70.0000	50.0000	11.6732	79.0476	1	0	0	0	0	0	0	0	0	0	0	0	1	0	0
261	73.7410	62.5000	5.7348	69.8997	0	0	0	0	0	0	0	0	0	0	0	0	0	0	0
262	64.5161	76.4706	22.3629	87.6289	1	0	0	0	0	0	1	0	0	0	0	0	2	0	0
263	51.2739	76.5957	17.0833	69.2098	1	1	1	0	0	0	1	0	0	0	0	0	2	1	1

264	59.4156	90.4762	16.3043	83.1804	1	1	0	0	0	0	0	0	0	0	0	0	1	1	0
265	48.4321	74.5098	19.8556	60.6870	1	1	1	0	0	0	1	0	0	1	0	0	3	1	1
266	68.7285	58.8235	8.4942	96.0432	1	0	0	0	0	0	0	0	0	0	0	0	1	0	0
267	53.8983	60.5769	32.3077	79.8851	1	1	1	0	0	0	1	1	1	0	0	0	2	2	2
268	80.4348	25.9259	32.8125	80.1587	0	0	0	1	1	1	1	1	1	0	0	0	2	2	2
269	69.7674	64.7059	27.6018	59.0625	1	0	0	0	0	0	1	1	0	1	0	0	3	1	0
270	70.8333	61.5385	9.1623	58.1081	1	0	0	0	0	0	0	0	0	1	0	0	2	0	0
271	33.3333	76.6667	34.8730	77.2595	1	1	1	0	0	0	1	1	1	0	0	0	2	2	2
272	61.9048	76.6667	22.4537	79.8780	1	1	0	0	0	0	1	0	0	0	0	0	2	1	0
273	87.5000	33.3333	9.1644	63.4703	0	0	0	1	1	1	0	0	0	1	0	0	2	1	1
274	82.2581	66.6667	42.6901	86.4151	0	0	0	0	0	0	1	1	1	0	0	0	1	1	1
275	59.1837	58.3333	4.8276	74.9206	1	1	0	0	0	0	0	0	0	0	0	0	1	1	0
276	51.0638	86.0000	18.6207	76.4350	1	1	1	0	0	0	1	0	0	0	0	0	2	1	1
277	91.3043	88.8889	14.7392	78.0928	0	0	0	0	0	0	0	0	0	0	0	0	0	0	0
278	30.0000	38.8889	38.0734	69.4639	1	1	1	1	1	0	1	1	1	0	0	0	3	3	2
279	32.0000	25.0000	28.7726	89.7163	1	1	1	1	1	1	1	1	0	0	0	0	3	3	2
280	75.8621	60.0000	12.1693	67.9310	0	0	0	0	0	0	0	0	0	0	0	0	0	0	0
281	62.9630	78.9474	27.0886	64.5985	1	1	0	0	0	0	1	1	0	1	0	0	3	2	0

Table 1: Raw data for the Methylation senescence arrays (beta values) together with the data coded into a binary senescent/non-senescent variable. The composite variable is the sum of the 4 individually coded variables.

Appendix K: Logistical regression of individual CpG sites and CSA-AKI.

CpG	BETA	SE	p-value	MEAN	SD
cg20426994.130418314	0.440034	0.123791	0.000462	NA	27.23802
cg07082267.85429007	0.006084	0.001775	0.000717	61.19293	14.65783
cg04940570.12696785	0.01022	0.003095	0.00111	11.92806	8.412798
cg25410668.28241509	-0.0256	0.008517	0.002932	3.06599	3.053487
cg07927379.156433095	0.009404	0.003349	0.0054	16.50134	8.388309
cg22016779.230452310	-0.00993	0.003662	0.007175	10.45489	7.450601
cg14556683.15343076	0.0132	0.004919	0.007809	5.440351	5.383566
cg06419846.66083692	0.01032	0.003958	0.009708	87.77388	6.661769
cg02046143.133797845	0.044956	0.017999	0.013184	0.971557	1.456574
cg07927379.156433107	0.012396	0.005093	0.015687	6.742099	5.238876
cg20426994.130418334	0.006551	0.002701	0.01605	5.136551	9.780799
cg07927379.156433032	0.013628	0.005624	0.016143	7.007173	4.748746
cg22736354.18122787	0.009627	0.004058	0.018476	4.678866	6.43849
cg21296230.33010576	-0.03286	0.013935	0.019183	2.106596	1.870578
cg16419235.57360555	0.006217	0.002669	0.020707	16.58626	9.754482
cg03032497.61108129	0.00972	0.004204	0.021633	10.28029	6.208008
cg07553761.160168094	-0.00419	0.001822	0.022211	31.55684	14.68951
cg16419235.57360787	0.01507	0.006617	0.023645	2.709226	3.942149
cg16419235.57360585	0.007835	0.003454	0.024196	10.90825	7.561611
cg03607117.53080379	0.027211	0.012096	0.025399	1.162378	2.187365
cg07927379.156433089	0.007067	0.003177	0.02709	20.85563	9.03587
cg04940570.12696803	0.011328	0.005095	0.027127	3.833572	5.149851
cg04940570.12696790	0.009297	0.004196	0.02766	5.581383	6.282213
cg21139312.55663255	-0.93101	0.372194	0.029433	NA	20.83531
cg20426994.130418178	-0.00223	0.001032	0.031667	35.56238	25.58058
ch.2.30415474F.30561912	0.011906	0.005544	0.032771	93.25296	4.744738
cg04474832.52008445	0.862896	0.403454	0.033787	NA	5.979224
cg03607117.53080360	-0.0079	0.003733	0.035486	8.601068	7.150859
cg07927379.156433098	0.010125	0.004844	0.037661	8.207077	5.587723
cg24079702.106015796	-0.00771	0.003715	0.039029	11.73526	7.04264
cg04940570.12696797	0.006726	0.003301	0.042683	7.715209	8.04156
cg09651136.72525221	0.009523	0.004706	0.044134	92.48852	5.603714
cg23744638.10323908	-0.00316	0.001581	0.04652	72.74258	17.04779
cg20426994.130418099	0.003427	0.001731	0.048907	28.28284	15.18891
cg20426994.130418325	0.79323	0.401799	0.049634	NA	17.75618
cg07927379.156433011	0.780782	0.402418	0.053564	NA	5.09947
cg22454769.106015770	0.004837	0.002557	0.059784	33.06222	10.73505
cg20426994.130418149	0.806874	0.437078	0.067755	NA	25.43262
cg04940570.12696853	0.017774	0.009809	0.071243	1.139446	2.723113

Table 1: Logistical regression analysis of individual CpG sites and CSA-AKI. Results of top 40 associated probes shown. Highlighted p-values = significant at <0.05.

Appendix L: Comparison between measures of DNAm age: Raw data

Study ID	Age	Predicted Age (y)	Delta Age	AMAR	Study ID	Age	Predicted Age (y)	Delta Age	AMAR
1	54.0	45.9	8.146	0.849	52	52.0	49.9	2.134	0.959
2	69.9	70.5	-0.551	1.008	53	66.0	63.3	2.700	0.959
3	54.8	32.3	22.534	0.589	56	75.0	65.7	9.299	0.876
4	70.9	70.9	0.001	1.000	57	59.0	45.5	13.496	0.771
5	61.3	66.8	-5.504	1.090	58	68.0	63.0	4.952	0.927
6	77.7	40.7	37.021	0.524	59	68.0	63.8	4.241	0.938
7	45.6	57.9	-12.330	1.270	60	80.0	49.9	30.095	0.624
8	70.5	49.8	20.694	0.707	62	59.0	51.3	7.721	0.869
9	59.0	53.7	5.291	0.910	64	63.0	72.4	-9.440	1.150
10	46.2	55.9	-9.713	1.210	65	71.0	59.6	11.421	0.839
11	77.8	80.7	-2.855	1.037	66	68.0	60.6	7.382	0.891
12	59.0	58.7	0.265	0.996	67	75.0	59.4	15.569	0.792
13	54.4	47.5	6.863	0.874	69	81.0	88.3	-7.295	1.090
14	54.1	52.8	1.296	0.976	70	69.0	70.7	-1.667	1.024
15	60.3	57.9	2.419	0.960	72	80.0	68.2	11.798	0.853
16	59.4	53.5	5.872	0.901	74	67.0	63.1	3.938	0.941
17	65.3	53.0	12.338	0.811	75	77.0	84.2	-7.199	1.093
18	75.0	73.0	1.962	0.974	76	53.0	61.4	-8.425	1.159
19	62.9	58.6	4.260	0.932	77	35.0	29.3	5.681	0.838
20	80.7	66.1	14.620	0.819	78	59.0	48.0	11.028	0.813
21	71.8	84.9	-13.089	1.182	87	72.0	77.4	-5.411	1.075
22	64.0	63.1	0.938	0.985	90	69.0	69.8	-0.774	1.011
23	51.7	56.5	-4.777	1.092	91	69.0	43.2	25.836	0.626
24	77.8	86.2	-8.396	1.108	93	68.0	67.6	0.433	0.994
25	80.0	80.3	-0.336	1.004	95	56.0	69.3	-13.318	1.238
26	42.7	38.4	4.335	0.899	96	48.0	46.1	1.909	0.960
27	47.9	41.7	6.188	0.871	98	69.0	59.3	9.660	0.860
28	69.0	65.1	3.916	0.943	100	61.0	49.4	11.607	0.810
29	52.1	60.9	-8.765	1.168	103	63.0	52.5	10.504	0.833
30	49.7	65.4	-15.719	1.316	104	68.0	63.3	4.733	0.930
31	68.6	69.6	-1.013	1.015	108	22.0	16.8	5.232	0.762
32	67.4	53.3	14.052	0.792	109	65.0	64.1	0.868	0.987
35	63.2	52.0	11.184	0.823	110	67.0	65.4	1.557	0.977
36	70.5	60.1	10.362	0.853	113	63.0	57.6	5.437	0.914
37	86.7	51.2	35.548	0.590	118	24.0	33.2	-9.216	1.384
38	30.4	25.1	5.329	0.825	119	58.0	54.9	3.070	0.947
39	80.5	74.2	6.335	0.921	120	79.0	71.5	7.532	0.905
40	77.6	68.4	9.156	0.882	121	69.0	55.8	13.234	0.808

41	72.0	61.5	10.484	0.854	122	78.0	88.3	-10.337	1.133
42	76.2	64.7	11.490	0.849	123	60.0	51.2	8.825	0.853
43	64.6	59.9	4.673	0.928	124	88.0	98.4	-10.400	1.118
44	82.8	76.8	6.040	0.927	125	48.0	52.0	-4.007	1.083
45	74.2	65.7	8.531	0.885	126	62.0	59.2	2.821	0.955
46	79.7	75.0	4.693	0.941	127	82.0	52.7	29.324	0.642
47	54.5	49.1	5.434	0.900	129	77.0	72.5	4.469	0.942
48	68.1	56.7	11.350	0.833	130	49.0	49.6	-0.643	1.013
49	68.0	63.4	4.617	0.932	131	81.0	71.4	9.581	0.882
50	52.0	80.4	-28.366	1.546	132	61.0	65.8	-4.754	1.078
51	58.0	61.8	-3.760	1.065	133	58.0	61.0	-3.021	1.052
Study ID	Age	Predicted Age (y)	Delta Age	AMAR	Study ID	Age	Predicted Age (y)	Delta Age	AMAR
134	69.0	58.6	10.443	0.849	188	53.0	48.8	4.190	0.921
135	60.0	63.2	-3.168	1.053	189	71.0	58.8	12.239	0.828
136	72.0	79.2	-7.233	1.101	190	62.0	62.6	-0.561	1.009
137	33.0	31.9	1.055	0.968	191	56.0	58.8	-2.792	1.050
138	50.0	48.7	1.303	0.974	192	83.0	97.5	-14.548	1.175
139	27.0	26.8	0.215	0.992	193	73.0	65.6	7.378	0.899
140	66.0	50.5	15.546	0.764	194	63.0	68.5	-5.546	1.088
141	75.0	98.3	-23.275	1.310	195	52.0	53.0	-0.996	1.019
142	51.0	51.0	0.022	1.000	196	74.0	67.3	6.673	0.910
143	83.0	75.6	7.370	0.911	197	78.0	74.7	3.265	0.958
144	56.0	62.2	-6.209	1.111	198	63.0	63.4	-0.435	1.007
145	76.0	78.0	-1.955	1.026	200	70.0	73.5	-3.481	1.050
146	41.0	45.8	-4.822	1.118	201	34.0	27.1	6.902	0.797
147	56.0	57.6	-1.554	1.028	202	79.0	76.6	2.414	0.969
148	72.0	66.2	5.786	0.920	203	76.0	66.4	9.566	0.874
150	76.0	63.0	12.979	0.829	204	53.0	52.8	0.186	0.996
151	64.0	64.2	-0.190	1.003	205	79.0	73.4	5.628	0.929
152	69.0	56.6	12.359	0.821	206	65.0	60.2	4.797	0.926
153	62.0	62.8	-0.792	1.013	207	57.0	77.7	-20.660	1.362
154	78.0	95.3	-17.334	1.222	208	47.0	53.6	-6.567	1.140
155	79.0	51.2	27.778	0.648	209	63.0	53.7	9.283	0.853
156	79.0	51.2	27.778	0.648	210	70.0	53.9	16.126	0.770
157	68.0	60.1	7.864	0.884	211	60.0	62.8	-2.753	1.046
158	79.0	69.7	9.329	0.882	212	55.0	72.1	-17.096	1.311
159	82.0	76.0	5.971	0.927	213	68.0	46.5	21.539	0.683
160	79.0	70.9	8.086	0.898	214	47.0	44.7	2.259	0.952
161	80.0	71.3	8.682	0.892	215	67.0	59.8	7.219	0.892
162	65.0	53.9	11.086	0.829	216	79.0	77.0	2.029	0.974
163	79.0	88.7	-9.700	1.123	217	30.0	22.6	7.434	0.752
164	72.0	71.8	0.152	0.998	218	76.0	79.7	-3.678	1.048

165	37.0	54.8	-17.777	1.481	219	26.0	33.8	-7.846	1.302
166	50.0	55.5	-5.494	1.110	220	48.0	39.9	8.083	0.832
167	68.0	54.8	13.222	0.806	221	54.0	55.6	-1.618	1.030
168	66.0	64.6	1.414	0.979	222	47.0	63.6	-16.607	1.353
169	72.0	63.0	9.025	0.875	223	79.0	81.0	-2.001	1.025
171	49.0	51.0	-1.986	1.041	224	56.0	70.3	-14.346	1.256
172	68.0	58.8	9.235	0.864	225	72.0	69.1	2.927	0.959
173	68.0	58.5	9.486	0.861	226	52.0	41.7	10.347	0.801
174	61.1	57.7	3.382	0.945	227	56.0	50.6	5.408	0.903
175	53.0	47.7	5.312	0.900	228	87.0	77.5	9.492	0.891
176	64.0	60.9	3.116	0.951	229	79.0	77.0	2.019	0.974
178	72.0	71.5	0.505	0.993	230	17.0	11.3	5.738	0.662
179	44.0	43.6	0.378	0.991	231	65.0	65.5	-0.496	1.008
180	75.0	67.9	7.065	0.906	232	57.0	58.6	-1.599	1.028
181	77.0	75.1	1.934	0.975	233	69.0	73.0	-4.035	1.058
182	78.0	66.2	11.803	0.849	234	69.0	66.5	2.498	0.964
183	85.0	74.9	10.131	0.881	235	56.0	41.2	14.819	0.735
184	76.0	82.6	-6.592	1.087	236	64.0	58.2	5.779	0.910
186	65.0	51.7	13.291	0.796	237	57.0	55.6	1.423	0.975
187	37.0	42.4	-5.390	1.146	238	55.0	60.5	-5.476	1.100
Study ID	Age	Predicted Age (y)	Delta Age	AMAR	Study ID	Age	Predicted Age (y)	Delta Age	AMAR
239	71.0	62.0	9.010	0.873	260	72.0	57.6	14.423	0.800
240	35.0	24.9	10.121	0.711	261	82.0	92.6	-10.568	1.129
241	57.0	55.4	1.575	0.972	263	51.0	40.4	10.582	0.793
242	22.0	27.1	-5.059	1.230	264	70.0	81.3	-11.349	1.162
243	62.0	60.1	1.896	0.969	265	81.0	62.7	18.302	0.774
244	78.0	81.4	-3.354	1.043	266	67.0	53.6	13.430	0.800
245	62.0	52.3	9.745	0.843	267	65.0	56.9	8.057	0.876
246	50.0	69.5	-19.535	1.391	268	42.0	50.9	-8.857	1.211
247	52.0	59.0	-7.026	1.135	269	70.0	64.8	5.193	0.926
248	35.0	39.5	-4.461	1.128	270	83.0	77.3	5.654	0.932
249	66.0	89.8	-23.814	1.361	271	81.0	63.5	17.547	0.783
250	55.0	41.0	14.032	0.745	272	78.0	72.6	5.373	0.931
251	57.0	43.7	13.336	0.766	273	76.0	51.9	24.099	0.683
252	72.0	61.7	10.285	0.857	274	83.0	90.6	-7.555	1.091
253	55.0	68.1	-13.091	1.238	275	84.0	64.0	19.959	0.762
254	63.0	51.1	11.872	0.812	276	60.0	57.5	2.545	0.958
255	67.0	67.3	-0.286	1.004	277	69.0	57.8	11.169	0.838
256	79.0	79.1	-0.062	1.001	278	75.0	61.0	14.029	0.813
257	64.0	66.4	-2.446	1.038	279	87.0	66.8	20.153	0.768
258	57.0	56.4	0.603	0.989	280	59.0	47.9	11.067	0.812
259	77.0	86.3	-9.260	1.120	281	78.0	77.9	0.078	0.999

Appendix M: Results of TA Validation Experiments

Results of Validation Experiment 1: TeloTAGGG PCR ELISA Protocol

Runs 1-3 were performed on cells derived from a single PBMC collection tube for each sample.

Run 1: Run with Heparin CPT tubes Run with 2x10 ⁵ cell count								
Sample	PCR 1	PCR 2	PCR 3	Average	CV	Negative control	Av - control	TA +ve ?
D	0.267	0.2248	0.0824*	0.2459	12.13498	0.1174	0.1285	No
S	0.2246	0.1089	0.1745	0.169333	34.26542	0.0973	0.0720	No
W	0.0969	0.0987	0.0762*	0.0978	1.301424	0.1181	-0.0203	No
Positive control	2.4889							

*Table 1: Results of Run 1 TRAP Assay. *. Some degree of evaporation of PCR product so result excluded from analysis*

Run 2 Run with Heparin CPT tubes Run with 2x10 ⁵ cell count								
Sample	PCR 1	PCR 2	PCR 3	Average	CV	Negative control	Av - control	TA +ve?
D	0.0879	0.0904	0.0769	0.0851	8.442971	0.0521	0.0330	No
S	0.0723	0.0702	0.0894	0.0773	13.62404	0.0806	-0.0033	No
W	0.0723	0.0867	0.0783	0.0791	9.144446	0.0701	0.009	No
Positive control	0.5629							

Table 2: Results of Run 2 TRAP Assay. Run failed. Positive control below threshold.

Run 3: Run with Citrate CPT tubes (except DH sample run in Heparin CPT for comparison) Run with 2×10^5 cell count									
	PCR 1		PCR 2		Av.	CV	Negative control	Av – control	TA +ve?
	Hyb a	Hyb b	Hyb a	Hyb b					
D	0.1861	0.1871	0.1795	0.1622	0.1788	6.446	0.1055	0.073	No
S	0.127	0.1272	0.1623	0.1503	0.1417	12.390	0.1221	0.020	No
W	0.2532	0.2462	0.1617	0.1722	0.2083	23.066	0.1068	0.102	No
DH	0.1625	0.1279	0.1485	0.1583	0.1493	10.332	0.1112	0.038	No
P	3.1727								

Table 3: Results of Run 3 TRAP Assay.

It was felt that the observed issues with repeatability were most likely due to variability in the starting amount of PBMC that was being included in each reaction. As such an alternative method of standardising input amount of PBMC was adopted. This involved lysing the pellet from 1ml of final PBMC solution and then performing a Bichinchoninic (BCA) assay to measure the protein concentration of the sample. Assuming a pure sample of PBMC with minimal platelet contamination, protein concentration should be proportional to total quantity of PBMC cell lysate. However, making this assumption is a potential source of error as levels of contamination may differ between samples thus altering the proportion of PBMC entering the TRAP assay. To help reduce protein contamination an additional washing step was included in the PBMC harvest (centrifuging at 100 RCF for 10 minutes).

Run 4 was a repeat of run 3 but with $1 \mu\text{g}$ of protein used as a starting amount for each sample (*Table 4*). This run produced a much higher TA value for sample D than previously observed (TA = 0.49) but similar values of intra-assay variability with CV values of 20%. As such this sample was run again in Run 5, using a second extracted PBMC pellet (*Table 5*). Repeat BCA assays were performed on pellets from 0.5mls

PBMC and 1ml PBMC for comparison (both derived from a single purification). This run produced similar TA values for sample D as runs 1 and 3 but greatly different from that of run 4 (0.493 Vs 0.223; inter-assay CV of 53.3%). There was relative consistency in TA activity across samples derived from 0.5mls and 1ml of PBMC (CV of 13.9 across 10 valid samples).

Run 4: Run with Citrate CPT tubes Run with 1 ug Protein									
Sample	PCR 1		PCR 2		Av.	CV	Negative control	Av - control	TA +ve?
	Hyb a	Hyb b	Hyb a	Hyb b					
D	0.6027	0.5346	0.4681	0.368	0.493	20.273	0.1023	0.391	Yes
S	0.1234	0.0892	0.1376	0.1509	0.125	21.187	0.1232	0.002	No
W	0.2512	0.2272	0.2799	0.2696	0.257	9.000	0.1081	0.149	No
P	3.1727								

Table 4: Results of Run 4.

Run 5: Run with Citrate CPT tubes Run with 1 ug Protein											
	PCR 1		PCR 2		PCR 3		Av	CV	-ve control	Av - control	TA +ve?
	Hyb a	Hyb b	Hyb a	Hyb b	Hyb a	Hyb b					
D1: 0.5ml	0.089 *	0.099 *	0.281	0.25	0.185	0.177	0.2 23	22. 62	0.0881	0.135	No
D2: 1ml	0.220	0.219	0.198	0.220	0.210	0.225	0.2 15	4.5 71	0.0967	0.118	No
P	2.826										

Table 5: Results of Run 5. *. Some degree of evaporation of PCR product so result excluded from analysis

Results of Validation Experiment 2: TeloTAGGG PCR ELISA PLUS Protocol

TA was measured with the TeloTAGG Telomerase PCR ELISA Plus as per the manufacturer's instructions (205). For Run 6, the internal control failed to amplify for 3 of the 4 samples (Table 6)

Sample	AS	AS-AS,0	AS,0 x2	Telomerase positive?	AS-IS	RTA high
D1	0.0771	0.0394	0.0754	No	0.0300	72.5482
D2	0.0812	0.0435	0.0754	No	0.0300	80.0977
S1	0.1305	0.0952	0.0706	Yes	0.0358	146.8946
S2	0.0998	0.0645	0.0706	No	0.0326	109.2934
W1	0.1835	0.1463	0.0744	Yes	0.4596	17.5839
W2	0.2005	0.1633	0.0744	Yes	0.4875	18.5039
J1	0.1331	0.0955	0.0752	Yes	0.0822	64.1776
J2	0.1288	0.0912	0.0752	Yes	0.0617	81.6510

Table 6: Run 6. Note that the internal standards (IS) of samples D, S and J have not amplified resulting in spuriously high RTA readings.

Sample	AS	AS-AS,0	AS,0 x2	Telomerase positive?	AS-IS	RTA high
D1	0.4027	0.3678	0.0698	Y	1.0529	12.4824
D2	0.2853	0.2504	0.0698	Y	0.9532	9.3870
S1	0.1720	0.1306	0.0828	Y	0.9637	4.8426
S2	0.1801	0.1387	0.0828	Y	1.3084	3.7880
W1	0.2154	0.1743	0.0822	Y	1.5145	4.1125
W2	0.2262	0.1851	0.0822	Y	1.4736	4.4885
J1	0.2688	0.2278	0.0820	Y	0.7623	10.6783
J2	0.1927	0.1517	0.0820	Y	0.6649	8.1527

Table 7: Run 7. All internal controls produced higher readings than in the previous run.

As such, Run 7 was repeated with all conditions the same except that the PMBC lysate was generated from stored lysate generated in Run 6 (*Table 7*). All of these lysates had been diluted to a concentration of 0.33µg/µl prior to freezing. On defrosting, repeat BCA assay run in triplicate showed that there was some variation in the concentration of the lysates on thawing (*Table 8*). This may be due to clumping of protein upon thawing and non-homogenous distribution throughout the lysate. Irrespective of the cause, it creates a potential source of error in achieving uniformity

in terms of PBMC added to the TRAP assay for each sample. 1µg of protein was added for each of the thawed samples and the TRAP reaction performed (Run 8, *Table 9*).

Sample	1	2	3	Average (µg/ml)
DF	493.437	289.767	275.004	352.736
JF	331.862	314.973	466.048	370.961
SF	461.088	236.497	562.379	419.988
WF	320.673	293.105	239.29	284.356

Table 8: BCA assay of thawed PBMC lysate. Lysate diluted to conc of 333 µg/ml prior to freezing

Sample	AS	AS-AS,0	AS,0 x2	Telomerase positive?	AS-IS	RTA high
DF1	0.0690	0.0286	0.0808	No	0.0352	29.0334
DF2	0.1199	0.0795	0.0808	No	0.0359	79.1311
SF1	0.1234	0.0811	0.0846	No	0.0381	76.0618
SF2	0.1278	0.0855	0.0846	Yes	0.0373	81.9083
WF1	0.1890	0.1454	0.0872	Yes	0.3478	14.9384
WF2	0.2580	0.2144	0.0872	Yes	0.5642	13.5788
JF1	0.1249	0.0832	0.0834	No	0.0596	49.8829
JF2	0.1740	0.1323	0.0834	Yes	0.0629	75.1595

Table 9: Run 8. As in run 6, the internal controls of samples D,S and J failed.

A further repeat of this experiment (Run 9) was performed in which samples D, S, W and J were run in duplicate with freshly extracted PBMC. In this run, two methods were used to standardise the amount of input PBMC. Firstly, PBMC was extracted from whole blood and a volume of 200,000 cells was obtained for each using the haemocytometer. This was done in duplicate for each sample (e.g D1 and D2). The volumes of 200,000 cells was lysed and frozen at -80°C. After 24 hours, the lysate was defrosted and a BCA assay performed at 1:5 dilution of the stock lysate to determine protein concentration. The results of this BCA assay are shown in *Table 10*.

Sample	Reading 1	Reading 2	Average reading
D1	279.818	293.747	286.78
D2	290.554	334.528	312.541
S1	305.478	317.212	311.345
S2	312.371	317.180	314.76
W1	289.611	301.666	295.64
W2	358.810	360.710	359.76
J1	306.897	312.750	309.823
J2	290.632	294.487	292.56

Table 10: Results of BCA assay for samples in Run 9

They show that the process of extracting approximately 200,000 cells has yielded approximately equal concentrations of protein across all 4 samples (approx. 300µg/ml), with good consistency between samples drawn from the same individual (e.g. D1 and D2) and between individuals (e.g. D1 and W1). Because of the consistency of these results, we were satisfied that approximately equal quantities of PBMC were being added to the TRAP reaction between samples. For each sample, i.e. both D1 and D2, 3µl of the stock lysate was added to the TRAP reaction (i.e for D1: 3µl of (5x286.78)/1000 = 4.3 µg protein). In addition, one of the samples for each individual were normalised for protein content by correcting the volume added to the TRAP reaction to contain a total of 3µg of protein. As such, three runs per sample were performed. Unfortunately, the negative controls for this PCR fell outside the acceptable range rendering the whole run invalid (results not shown). The cause for this failure was not apparent.

Further repeats of the assay were performed with just two samples D and S, in order to reduce the number of kits required for the optimisation experiments (*Table 11*). The two samples were prepared as for the failed Run 9 with both samples being run in triplicate (2 standardised by input volume of stock lysate, and 1 standardised by input protein content). The results of this run are shown in *Table 11*. Results were relatively stable between the samples standardised by input volume (e.g. D1 and D2) most likely reflecting the previously proven similarities in quantity of PBMC inputted to the TRAP reaction. The samples standardised by protein content (D2P and J2P) showed reduced TA but this is expected given the reduced quantity of input PBMC by this method (1µg).

Sample	AS	AS-AS,0	AS,0 x2	Telomerase positive?	AS-IS	RTA high
D1	0.3623	0.321	0.0826	Yes	0.8951	12.8217
D2	0.3942	0.3414	0.1056	Yes	0.6688	18.2508
D2P	0.2025	0.1425	0.12	Yes	0.7682	6.6321
J1	0.0078	0.0356	0.085	No	0.81	1.5714
J2	0.0904	0.0515	0.0778	No	0.7944	2.3178
J2P	0.0526	0.0128	0.0796	No	0.9212	0.4968

Table 11: Results of Run 10 TeloTAGGG Telomerase PCR ELISA Plus assay. D1, D2, J1 and J2 standardised by input volume of cell lysate (3 µl). D2P and J2P = extracts of D2 and J2 standardised by input amount of protein (1 µg).

A further 2 runs, Run 11 and 12, were performed for samples D and J in repeats of Run 10 but using 3µg of input PBMC (*Tables 12 and 13*). The results of both the absolute TA and the RTA differ between the 2 runs and between Run 10. Run 12 resulted in significantly higher values of RTA due to the reduction in absorbance of the internal control again suggesting the possibility of PCR inhibition in these reactions.

Sample	AS	AS-AS,0	AS,0 x2	Telomerase positive	AS-IS	RTA High
D1	0.0848	0.0559	0.0588	N	0.5045	7.29
D2	0.109	0.0801	0.0588	Y	0.4918	10.72
J1	0.12	0.0908	0.0584	Y	0.5619	10.63
J2	0.0993	0.0701	0.0584	Y	0.547	8.43

Table 12: Results of Run 11. TeloTAGGG Telomerase PCR ELISA Plus assay.

	AS	AS-AS,0	AS,0 x2	Telomerase positive	AS-IS	RTA High
D1	0.2389	0.2078	0.062	Y	0.1041	60.5
D2	0.3276	0.2965	0.0622	Y	0.0943	95.4
J1	0.1864	0.1556	0.0616	Y	0.0991	47.62
J2	0.1756	0.1448	0.0616	Y	0.0067*	655.5

Table 13: Results of Run 12. TeloTAGGG Telomerase PCR ELISA Plus assay

Measuring TERT expression - Results

A fundamental problem that we encountered in measuring TERT expression was a failure to achieve amplification of TERT in any of the samples or positives controls that were tested. A summary of the initial 9 optimisation experiments performed is given in Table 14.

Experiment	Summary
1	<p>Conditions</p> <p>TERT 1 Probe: HS0097265Qm_1 (recommended TERT TaqMan probe by Thermofisher)</p> <p>GAPDH Probe: Hs02786624_g1</p> <p>6 samples (10ng RNA)</p> <p>Positive control = Total RNA (XpressRef universal Total RNA – QIAGEN)</p> <p>1x No Reverse Transcription control (NRTC)</p> <p>1x Negative Control (NC)</p>

	<p>3 point standard curve (SC) (10, 5, 2.5 ng RNA)</p> <p>Results GAPDH: Amplification with CT values ~15. Standard Curve R=0.94</p> <p>TERT: Late amplification. Poor concordance between duplicates. Standard Curve R= 0.61 Samples amplifying earlier for TERT than Total RNA positive control Poor concordance of duplicates: possible pipetting error Samples not all falling within range of standard curve</p> <p>Recommendations Increase pipetting volumes of RNA into mastermix by diluting cDNA and pipetting large volumes (reduce water content of mastermix to compensate) Increase the number of points in the standard curve Trial of using samples as positive control. It may be that PBMC RNA is more TERT positive than pooled RNA from several body tissues. May need to increase the input amount of RNA/cDNA</p>
2	<p>Conditions Same probes as Expt 1 2 samples 2x NRTC and 2xNC Sample X used as positive control – 5-point standard curve (10,5,2.5,1.25,0.625ng RNA)</p> <p>Results GAPDH: Good amplification: CT value of top standard (TS) ~16. R = 0.995, Efficiency 1.05 TERT: Unreliable amplification. Poor standard curve and high CT values >30</p> <p>Recommendations Need to increase in input amount of RNA/cDNA. Even GAPDH CT values too high for such a ubiquitous marker. Need to increase range of standard curve</p>
3	<p>Conditions Probes as per previous. 8 point standard curve only run (80, 40, 20, 10, 5, 2.5, 1.25, 0.625ng)</p> <p>Results GAPDH amplification still excellent. Standard Curve: R = 0.999, Efficiency= 0.93. But Ct values still high. TERT: Late amplification with extremely poor standard curve and poor concordance between duplicates.</p> <p>Recommendations The excellent GAPDH result indicates that the RNA extraction and reverse transcription steps are OK. Also linear standard curve for GAPDH suggests that PCR itself is working efficiently and not inhibited.</p>

	<p>Cause of poor TERT amplification could be a probe issue or that TERT is in very low abundance and thus difficult to amplify Try alternate TERT TaqMan probes such as Hs00972656_m1 (same as used by Janic <i>et al</i> (87). May need to increase input RNA further. Janic <i>et al</i> used 200ng RNA as their starting amount in their successful TERT TaqMan Assays(87).</p>
4	<p>Conditions TERT 2 probe = Hs00972656_m1 (same as used by Janic <i>et al</i> (87)). GAPDH probe as per previous. Same 8-point Standard Curve as Experiment 3 (80, 40, 20, 10, 5, 2.5, 1.25, 0.625ng).</p> <p>Results GAPDH: Excellent amplification. Standard Curve: R = 0.998, Efficiency= 0.96 TERT: Ongoing Late and erratic amplification. Worse than previous probe.</p> <p>Recommendations Increase input RNA Use previous Probe (HS00972650_m1 – recommended by Thermofischer)</p>
5	<p>Conditions Two TERT probes used; TERT1 (HS00972650_m1) and new probe – TERT 3 (Hs00972648_g1) 7-point standard curve run: 400, 200, 100, 50, 25, 12.5, 6.25ng</p> <p>Results GAPDH: Excellent amplification. Standard Curve: R = 0.999, Efficiency = 0.99. TERT 1(HS00972650_m1): Standard curve looks better at these higher concentrations but still late amplification and poor concordance between duplicates. TERT 3(Hs00972648_g1). Worse amplification than TERT 1 probes</p> <p>Recommendations As neither changing probes or increasing RNA input amount have resulted in successful amplification, need to try other strategies.</p>
6	<p>Conditions An attempt was made to try different PCR conditions to try to prolong amplification in the hope of increasing TERT amplification. New PCR conditions were taken from the standard TaqMan® Gene Expression Assays protocol consisting of: 2 minutes at 50°C (UNG incubation); 10 minutes at 95°C (Polymerase activation); 40 cycles of 15 seconds at 95°C (denaturing) and 60 seconds at 60°C (anneal/extension step). TERT 1 probes and TERT 2 probe used. 6-point standard curve (100, 50, 25, 12.5, 6.25, 3.125ng).</p> <p>Results GAPDH: Reasonable amplification. No reduction in CT threshold values. Standard Curve: R=0.998, Efficiency = 0.87</p>

	<p>TERT 1 and TERT 2: Inconsistent amplification with many samples not amplifying at all.</p> <p>Recommendations No improvement in TERT amplification with amended PCR protocol.</p>
7	<p>Conditions As per experiment 6 but with a 20-second-long 95°C denaturing step. Only TERT 1 probes used. 5-point standard curve run (100,50,25,12.5,6.25ng).</p> <p>Results Worsening of amplification for both TERT and GAPDH.</p> <p>Recommendations Alter Mastermix in addition to altering PCR Protocol.</p>
8	<p>Conditions As per Experiment 6 but new Masttermix (TaqMan® Gene Expression Mastermix) used. Additional TERT reaction run with Qiagen TERT Assay (TERT 4) and the corresponding recommended mastermix (SYBRgreen ROX fast mastermix solution).</p> <p>Results GAPDH: No amplification seen. Both TERT runs (TERT 1 and TERT 4 Assays) gave unreliable and late amplification.</p> <p>Recommendations Since neither changing the input amount of RNA or changing the probes, mastermix and PCR conditions have improved TERT amplification, suggest seeking expert help.</p>

Table 14: Summary of Optimisation Experiments for TERT measurement.